Merozoite Surface Protein – 7

A Novel Protein On The Surface of

Plasmodium falciparum Merozoites

Justin Alexander Pachebat

A thesis submitted in partial fulfilment of

the requirements of University College London

for the degree of Doctor of Philosophy

Division of Parasitology,

National Institute for Medical Research

Mill Hill, London, U.K.

January 2002

ProQuest Number: U643941

All rights reserved

INFORMATION TO ALL USERS
The quality of this reproduction is dependent upon the quality of the copy submitted.

In the unlikely event that the author did not send a complete manuscript
and there are missing pages, these will be noted. Also, if material had to be removed,
a note will indicate the deletion.

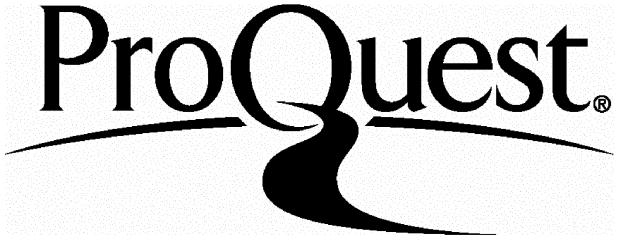

ProQuest U643941

Published by ProQuest LLC(2016). Copyright of the Dissertation is held by the Author.

All rights reserved.
This work is protected against unauthorized copying under Title 17, United States Code.
Microform Edition © ProQuest LLC.

ProQuest LLC
789 East Eisenhower Parkway
P.O. Box 1346
Ann Arbor, MI 48106-1346

Acknowledgements

Many thanks to everybody past and present in the lab for support, humour and friendship. Especial thanks to Irene Ling, Sola Ogun, Carlotta Trucco, Muni Grainger, Tony O'Connor, Simon Wilkins, Barbara Clough, Katherine Ellis, G'bemiro O'Sodiende, Terry Scott-Finnigan, Helen Taylor, Kaveri Rangachari, Mike Blackman and Malika Kaviratine, for advice and help. Special thanks to Chairat Uthaipibull for friendship and long conversations on MSP-1 and MSP-7, and to Rosangela Nwuba for bringing life and humour to our bench just when I needed it. Special thanks also to my supervisor, Tony Holder, for advice and proof reading. Thanks to the LMB and NIMR Visual Aids Departments for the work they did, and to Kate Sullivan of the Image Analysis Laboratory for help with the DeltaVision image analysis. Thanks also to Phil and Dimi for showing me how to keep smiling. Thanks to everybody in the HAPPY Mapping Lab for the daily questions: "How's the thesis?" and "Haven't you finished it yet?" Especial thanks to Paul Dear for his support, and deadlines, during the writing of this thesis. Thank you to my Father and Mother both of whom supported me in their ways and helped me get this far.

Most of all I want to thank my beautiful wife, Leslie, for her love and continuous support, despite long hours, my moaning and general reluctance to write. Finally I wish to thank our son James, who was born during the writing of the thesis, for not screaming too much when I was writing, and for missing the laptop whilst wetting my notes.

This PhD was funded by a Medical Research Council studentship.

This thesis is dedicated to Leslie and our son James with my everlasting love.

INDEX OF CONTENTS

INDEX OF FIGURES

ABBREVIATIONS

Ab	Antibody
ABRA	Acidic Basic Repeat Antigen
ACN	Acetonitrile
Ag	Antigen
AMA-1	Apical Merozoite Antigen-1
AP	Alkaline Phosphatase
bp	Base pairs
BCA	Bicinchoninic acid
BCIP	5-Bromo-4-Chloro-3-Indoyl Phosphate
β-ME	β-Mercaptoethanol
BFA	Brefeldin A
BSA	Bovine Serum Albumin
DAPI	4,6-Diamidino-2-phenylindole
DMF	Dimethylformamide
DTT	Dithiothreitol
EBA	Erythrocyte Binding Antigen
ECL	Enhanced Chemo-Luminescence
EDTA	Ethylene diamine tetra acetic acid
EGTA	Ethylene glycol-bis[β-aminoethylether]-N,N'N'N'tetraacetic acid
ELISA	Enzyme Linked ImmunoSorbant Assay
ER	Endoplasmic Reticulum
FA	Freund's Adjuvant
FCS	Foetal Calf Serum

FITC	Fluorescein-isothiocyanate
g	acceleration due to gravity
GST	Glutathione S-Transferase
HAT	Hypoxanthine Aminopterin Thymidine
6*His	6*Histidine N-terminal fusion tag
HT	Hypoxanthine Thymidine
HRP	Horse Radish Peroxidase
hr / hrs	hour / hours
IAA	Isoamyl Alcohol
IEM	ImmunoElectron Microscopy
IFAT	Indirect Immunofluorescence Antibody Test
IgA	Immunoglobulin Alpha
IgG	Immunoglobulin Gamma
IMAC	Immobilised Metal Affinity Chromatography
IP	Immunoprecipitation
IPTG	Isopropyl-β-D-ThioGalactoside
IPWB I	Immunoprecipitation Wash Buffer I
IPWB II	Immunoprecipitation Wash Buffer II
KAHRP	Knob-Associated Histidine Rich Protein
kb	Kilobase pairs
kDa	Kilo Daltons
LB	Luria-Bertani Medium
MCS	Multiple Cloning Site
MESA	Mature-parasite-infected Erythrocyte Membrane Antigen
min	minutes

MSP	Merozoite Surface Protein
NBT	Nitro Blue Tetrazolium
NP40	Nonidet P40
O/N	Overnight
OPD	O-Phenylenediamine Dihydrochloride
P.	*Plasmodium*
PAGE	Poly-Acrylamide Gel Electrophoresis
PBS	Phosphate Buffered Saline
Pc	*Plasmodium chabaudi*
PCR	Polymerase Chain Reaction
PEG	Polyethylene Glycol
Pf	*Plasmodium falciparum*
PMSF	Phenylmethyl-Sulphonyl Fluoride
Pv	*Plasmodium vivax*
Py	*Plasmodium yoelii*
RAP	Rhoptry-Associated Protein
rbc	Red Blood Cell
RESA	Ring-infected Erythrocyte Surface Antigen
RhopH	High Molecular Weight Rhoptry Protein
rpm	revolutions per minute
rt	reverse transcription
RT	Room Temperature
SDS	Sodium Dodecyl Sulphate
sdw	Sterile Distilled Water

S/N	Supernatant
TAE	Tris Acetate EDTA
TB	Terrific broth
TBE	Tris Borate EDTA
TE	Tris EDTA
TLC	Thin Layer Chromatography
Tm	Temperature, melting
TRITC	Tetramethylrhodamine B isothiocyanate
TuRNER	Tubular reticular network of the ER
Tween 20	Polyoxyethylene-Sorbitan Monolaurate
X-Gal	5-Bromo-4-Chloro-3-Indolyl-β-D-Galactoside

Abstract

During the erythrocytic cycle of human malaria caused by *Plasmodium falciparum,* merozoites released from mature schizonts attach to and invade red blood cells. Understanding this invasion process may identify suitable chemotherapy or vaccine targets with which to combat malaria. On the merozoite surface is a complex of polypeptides derived by proteolytic cleavage from merozoite surface protein-1 (MSP-1), and two unrelated 36kDa and 22kDa polypeptides derived from MSP-6 and MSP-7 respectively. On erythrocyte invasion the majority of the MSP-1 complex is shed into the blood stream. This shed complex contains MSP-6_{36}, MSP-7_{22}, and a 19kDa polypeptide (MSP-7_{19}) proposed to be the product of N-terminal cleavage of MSP-7_{22}. MSP-1 is a major vaccine candidate, hence any proteins complexed to it, such as MSP-7_{22}, are potential vaccine targets and warrant further research.

To study MSP-7_{22} and its relationship with MSP-1, it was necessary to clone the *msp-7* gene. A combination of genome database searches and Vectorette PCR steps were used to obtain the gene coding for MSP-7, and confirmed that MSP-7_{19} is related to MSP-7_{22}. RT-PCR was used to examine *msp-7* for the presence of introns, and the precursor's 351 amino acid sequence analysed using structure and function prediction programmes. The *msp-7* gene was cloned and sequenced from several lines of *P. falciparum* and found to be highly conserved.

To obtain antibodies with which to study MSP-7 biosynthesis, GST-fusion proteins were produced using bacterial expression systems, and used to immunise mice, producing anti-sera and a specific monoclonal antibody. The pattern of MSP-7 transcription throughout the erythrocytic cycle was analysed by Northern blotting. The translation of 48 kDa MSP-7 precursor and subsequent processing events were determined by western blotting, immunofluorescence and immunoprecipitation techniques. These suggested that the MSP-7 precursor associated with the MSP-1 precursor in schizonts and subsequently underwent three proteolytic processing steps. The time and kinetics of MSP-1 and MSP-7 precursor complex formation, and processing events, were analysed by immunoprecipitation, pulse chase and sensitivity to Brefeldin A. Preliminary experiments were performed to determine the relationship between MSP-1 and MSP-7 processing in merozoites.

CHAPTER ONE : INTRODUCTION

1.0 Human Malaria

Malaria is the most important parasitic disease of mankind. It is endemic in 110 countries, with over 40% of the world's population at risk.

Malaria is the disease caused when a protozoan parasite of the *Plasmodium* genus infects a host. Humans are infected by four species of *Plasmodium,* these are: *Plasmodium falciparum, Plasmodium malariae, Plasmodium ovale* and *Plasmodium vivax.* Of these *falciparum* malaria is the most important, as it is prevalent in 92 countries and has a characteristically high morbidity and mortality (WHO 1999d).

Malaria is transmitted between human hosts by female anopheline mosquitoes. The life cycle of the malaria parasite has four distinct stages: in the mosquito vector the parasite undergoes the sexual replication stages of fertilisation and sporogony; whilst in the human host the parasite undergoes asexual replication in the hepatic and erythrocytic schizogony stages (See Figure 1.0 for an overview of the *Plasmodium* life cycle).

The pathogenic effects that characterise malaria are caused during the erythrocytic cycle. Symptoms can range from those seen in mild malaria, with flu-like chills, fever and headaches, to those in severe malaria, with hypoglycaemia, metabolic acidosis, renal failure, non-cardiac pulmonary oedema, severe anaemia, cerebral malaria (encephalopathy) and death (Miller *et al.* 1994; Miller *et al.* 2002).

Each year there are an estimated 300 - 500 million cases of clinical malaria, and up to two million deaths (WHO 1999b; WHO 1999d). Malaria disproportionately affects

children under five years of age, pregnant women, and immunologically naive hosts. Over 700,000 children under five years old die of malaria annually, and malaria is predicted to be the cause of one in five childhood deaths in Africa (WHO 1999d).

Malaria adversely affects the poorest people, in underdeveloped countries that can ill-afford the increasing healthcare costs due to malaria, tuberculosis and AIDS. The situation is worsened by the economic burden that malaria places on the output of a country: reducing the potential gross national product (GNP) of a country by over 1 % each year (WHO 1998). In addition, malaria places an economic burden on the individual: with 25% of a household's annual income being lost due to the costs of treatment, prevention, and lost income due to illness (WHO 1999a). As a result malaria hinders long term economic growth and associated benefits of economic growth such as public health infrastructure (Sachs and Malaney 2002).

The malaria parasite has developed resistance to many previously effective anti-malarial drugs. The increasingly global prevalence of this drug resistance, especially in *P. falciparum*, compromises the control and treatment of malaria. In addition, the spread of insecticide resistant mosquitoes, in conjunction with the collapse of *Anopheles* control programs, has lead to the return of malaria, often with increased severity, to areas from which it had been previously eradicated.

1.1 Malaria Control Or Lack Of It

In the absence of an effective vaccine to malaria, an integrated programme of vector control, rapid malaria diagnosis and effective chemotherapy is the best method of controlling malaria (Alles *et al.* 1998).

The environmental suitability of breeding sites for the anopheline malaria vector determines the distribution of malaria in a geographical region (WHO 1999b). Over 90% of the world's malaria cases occur in sub-Saharan Africa, due to the presence of the highly anthropophilic and behaviourally adaptable malaria vectors: *Anopheles arabiensis*, *A. funestus* and *A. gambiae* (Collins and Besanky 1994). Mosquito control methods aim to reduce vector-host contact, and hence the malaria transmission rate. Methods such as larviciding and environmental management target anopheline breeding sites. Spraying the interiors of houses with residual insecticides to kill resting mosquitoes, and the use of insecticide-treated bed nets, reduce vector-host contact, the number of infective bites received and hence the malaria transmission rate (Curtis 1992; Collins and Besanky 1994). In addition, primary healthcare systems with facilities for rapid diagnosis and effective treatment of infection, reduce both morbidity and mortality and decrease the reservoir of infected individuals.

In the 1940's to 1950's national malaria control campaigns were initiated. These used a combination of vector control methods especially house spraying with DDT, and chemotherapy (chloroquine) to reduce the malaria transmission rate. The campaigns were successful and resulted in the eradication of malaria from large regions of the world (WHO 1999d). However, from the 1960's inappropriate use of anti-malarial drugs in South-East Asia resulted in the selection of chloroquine and multi-drug resistant *P. falciparum* parasites. This drug resistance became increasingly prevalent on a global scale and combined with the emergence of insecticide-resistant mosquitoes, has severely compromised the treatment and control of malaria. The global prevalence of anti-malarial and insecticide resistance in conjunction with other factors such as: population movements due to civil unrest, drought and economic migration; the decay of healthcare

infrastructures; and man-made environmental changes e.g. deforestation, has led to the re-emergence of *P. falciparum* malaria, often with increased severity, in regions from which it had been previously eradicated, was in remission or had never existed (WHO 1999d; Snow *et al.* 2001).

Anti-malarial drugs are commonly used inefficiently, with self administration and poverty often resulting in premature termination of treatment. This has lead to the development of resistance in *P. falciparum,* to many cheap and previously effective drugs such as chloroquine, sulfadoxine and pyrimethamine (Fairlamb 1996). Multi-drug resistant parasites are becoming ubiquitous in Africa, South-America and South-East Asia. This necessitates the use of more expensive drugs such as mefloquine, artemisinin or artemisinin derivatives, the high costs of which result in under use and further selection of drug resistant phenotypes (Congpuong *et al.* 1998).

Pharmaceutical companies show little interest in the development of new anti-malarial drug classes, as target verification and drug development costs are high, and the potential financial returns from Third World diseases far lower than those for drugs targeted at the lucrative healthcare systems of First World economies (Macreadie *et al.* 2000). As a result, no new classes of anti-malarial drugs have been commercially developed over the last 20 years, and the repertoire of drugs available to treat multi-drug resistant parasites is rapidly decreasing.

In the past, anti-malarial drugs were discovered by serendipity. In the future, it is essential that as well as optimising known classes of drugs, novel chemotherapy targets are identified (Fairlamb 1996). This requires basic research into the biology of the malaria parasite, identification of targets that are either novel or analogous to drug targets identified in other organisms, e.g. N-myristoyl-transferase (NMT), and understanding and

optimisation of the mechanisms of inhibition (Bell 1998; Gunaratne *et al.* 2000; Macreadie *et al.* 2000).

1.2 The Need for a Vaccine

To control and eventually eradicate malaria, a vaccine against malaria would be an ideal tool. This vaccine should be used as part of an integrated programme of vector control, personal protection and education, malaria diagnosis, chemotherapy, and the establishment and maintenance of a permanent healthcare system (WHO 1999c; WHO 1999d). The vaccine would ideally be cheap to produce, easy to store and administer in Third World countries, and result in life long protection against infection by the human *Plasmodium* species.

Much of the evidence for the effectiveness of a malaria vaccine comes from epidemiological studies of human populations in malaria infected regions. In regions of endemic malaria, children develop immunity to severe non-cerebral malaria by five years of age, and immunity to mild malaria by adolescence (Miller *et al.* 1994; Gupta *et al.* 1999). In regions of high endemicity children develop immunity to severe disease at an earlier age than those from regions of low endemicity (Gupta *et al.* 1999). Thus continuous pre-munition of the immune response with the malaria parasite is correlated to the development of immunity to severe non-cerebral malaria, suggesting that in theory a vaccine could mimic this effect (Druilhe and Perignon 1999). Cerebral malaria is common in three to four year old children from regions of low endemicity, and rare in children from regions of high endemicity, and appears to be the result of strain dependent pathogenic effects (Miller *et al.* 1994; Gupta *et al.* 1999). In regions of seasonal or

epidemic malaria the majority of the population has no immunity to malaria, resulting in severe life-threatening disease throughout the population (Miller *et al.* 1994). This suggests that a vaccine which imparts only partial immunity may lead to a reduction in the transmission rate in holo-endemic regions, but an increase in the proportion of severe disease cases (Bojang *et al.* 1997; Druilhe and Perignon 1999). Hence any potential vaccine must provide complete immunity. In theory this could be achieved using multiple antigens that cover a variety of targets, hence providing an overlapping system of protection.

Immunisation of humans with irradiated *Plasmodium falciparum* sporozoites induces an immune response that protects against subsequent experimental challenge with infective mosquitoes (Clyde 1973). Severe malaria is generally associated with a high blood stage parasitemia, whilst mild or asymptomatic malaria is associated with a low parasitemia (Miller *et al.* 1994). Passive transfer of antibodies from naturally immune individuals into children protects against malaria (Cohen *et al.* 1961). This suggests that naturally acquired immunity to malaria is mediated by antibodies that suppress or regulate the malaria parasite during the erythrocytic cycle. In animal malaria models, immunisation with a variety of *P. falciparum* protein homologues, protects against subsequent parasite challenge, suggesting that immunity to malaria is achievable through vaccination (Holder and Freeman 1981; Ridley *et al.* 1990 ; Hirunpetcharat *et al.* 1997; Tian *et al.* 1997). However the human - parasite relationship is very complex, as the parasite exhibits clonal antigenic variation and utilises alternate erythrocyte invasion pathways, whilst the human immune response is highly heterogeneous (Kyes *et al.* 1999; Preiser *et al.* 1999; Snounou *et al.* 2000; Miller *et al.* 2002; Richie and Saul 2002). Hence further elucidation and

evaluation of the interaction of potential vaccine candidates with the immune response is required.

There are currently four potential vaccine concepts, these are listed below with examples of potential candidates. (Reviewed by Targett 1995; Holder 1996; Engers and Godal 1998; Miller and Hoffman 1998; James and Miller 2000; Tsuji and Zavala 2001; Richie and Saul 2002) .

- **anti-pre-erythrocytic stage:** the aim is to raise antibodies against sporozoites, and a cell mediated immune response to hepatic schizonts. Candidate antigens include circumsporozoite protein (CSP), liver stage antigen-1 (LSA-1), and thrombospondin-related anonymous protein (TRAP).
- **anti-erythrocytic stage:** the aim is to raise antibodies against merozoite proteins or against proteins expressed on the surface of parasitised red blood cells. Candidates include: apical membrane antigen-1 (AMA-1), erythrocyte binding antigen-175 (EBA-175), merozoite surface protein-1 (MSP-1), merozoite surface protein-2 (MSP-2), rhoptry associated protein-1 (RAP-1) and serine repeat antigen (SERA).
- **anti-disease:** the aim is to raise antibodies against antigens involved in cytoadherance and rosetting of late erythrocytic stages, and against malaria toxins. Candidates include: cytoadherence-linked asexual gene protein (CLAG), erythrocyte membrane protein family (EMP), glycosyl-phosphatidylinositol (GPI), knob-associated histidine-rich protein (KAHRP), and RIFINs.
- **anti-transmission:** the aim is to raise antibodies against proteins expressed by sexual stages taken up by mosquitoes. Candidates include: gametocyte 27kDa antigen (Pfg27), and 25kDa ookinete antigen (Pfs25).

Clinical trials with a variety of vaccine candidates have been performed in humans, many result in high antibody titres against the immunogen, but most do not transfer long-lasting or complete protection against subsequent parasite challenge, and in the case of the SPf66 vaccine actually increased morbidity in the vaccinated group (Bojang *et al.* 1997; Anders and Saul 2000; Bojang *et al.* 2001). Any potential vaccine is likely to consist of a multi-valent, multi-stage antigen preparation, that is administered either singly or as a combination of peptide, attenuated virus or DNA vaccine approaches (Tine *et al.* 1996; Holder 1999).

The information released by sequencing of the *P. falciparum* genome is leading to the discovery of a large number of potential drug and vaccine targets (Hoffman *et al.* 2002). Their identification will enable further understanding of the complex interaction between the parasite and its human host. This, in conjunction with advances in DNA and peptide vaccinology, will hopefully result in the future development of an effective vaccine against human malaria.

1.3 A New Age of Malaria Research

Understanding the biology of the parasite-host relationship, and determining the structure and function of *Plasmodium* proteins expressed during the life cycle, may help identify novel chemotherapeutic or vaccine targets. To aid in this the 30 Mb *P. falciparum* genome is being sequenced by an international sequencing consortium (Gardner *et al.* 1998; Gardner 1999). The aim of sequencing the genome is to define every gene in the organism (Wirth 1998). The information is being used to understand the molecular details of the complex interaction between the *Plasmodium* parasite and its

hosts, with the aim of identifying potential targets for drug and vaccine development (Wirth 1998; Gardner 1999; Hoffman *et al.* 2002).

The availability of the *P. falciparum* genome sequence data enables researchers to rapidly identify genes of interest and determine their role in the parasite. Knowledge of the genome sequence has also led to the development of genetic tools for the functional analysis of genes in *Plasmodia.* These include the development of oligo-nucleotide and DNA micro-arrays for expression profiling and comparative genome analysis (Carucci 2000; Carucci and Hoffman 2000); and most importantly, the development of techniques for the stable transfection of the haploid erythrocytic stage of *P. falciparum* (Crabb *et al.* 1997; Tomas *et al.* 1998; Waterkeyn *et al.* 1999; de Koning-Ward *et al.* 2000). Stable transfection enables researchers to elucidate the function of proteins by disrupting, modifying or replacing the genes encoding them (Craig *et al.* 1999; Cowman 2000). This functional analysis is a powerful tool with which the role of merozoite proteins in the erythrocyte invasion process can be characterised, and putative chemotherapy and vaccine targets identified (Cowman 2000).

1.4 Erythrocytic life cycle

The 48-hour erythrocytic cycle of *P. falciparum* has been well characterised (see Figure 1.1). Most of the pathogenic effects of malaria occur during this cycle. The stages of the *P. falciparum* erythrocytic life cycle have been reviewed by several researchers (Bannister and Dluzewski 1990; Wilson 1990; Bannister *et al.* 2000; Pinder *et al.* 2000).

On schizont rupture, released merozoites are briefly exposed in the plasma before binding to and invading an erythrocyte. Sera from immune individuals contain antibodies targeted against merozoites that prevent erythrocyte invasion. This suggests that components on the merozoite surface are potential vaccine candidates, which should induce an antibody response that mimics natural immunity to malaria. Understanding the mechanism of red blood cell invasion and development of erythrocytic stages will identify potential drug and vaccine targets. (See Figure 1.2 for a diagramatic representation of erythrocyte invasion).

Merozoites are 1.5 - 3μm long, (depending on the *Plasmodium* sp.), shaped like lemons, have a low negative charge, and a spatially ordered bristly coat of filaments (15-20nm long and 2-3nm wide) anchored to the plasma membrane. These filaments are predicted to include the merozoite surface protein-1 (MSP-1) complex (see sections 1.5 and 1.6). Merozoites have a cluster of secretory organelles at their apex. These consist of two bulbous rhoptries (650nm long by 300nm wide), and several elongated flask-like micronemes (120nm long by 40nm wide). Both the rhoptries and micronemes have ducts that converge at the apex of the merozoite. It is postulated that the microneme ducts exit into the rhoptry ducts. These membranous organelles contain an electron-dense mix of proteins that are located in specific regions of the structures (see section 1.5). Also present in the cytoplasm at the merozoite apex, are numerous microspheres or dense granules (80nm diameter), each containing specific proteins (see section 1.5).

When a merozoite comes into initial contact with the erythrocyte surface, there is an initial electrostatic attraction, followed by reversible adhesion at a distance of 20-40nm between the filament coat on the merozoite and receptors on the red blood cell surface. After the initial contact with the erythrocyte, the merozoite moves or glides along the red

cell surface, re-orientating so that its apical region is in apposition to the erythrocyte membrane. This leads to the irreversible formation of a tight junctional zone (4nm), thought to involve multiple receptor-ligand interactions between the apical end of the merozoite and the erythrocyte membrane. Apical contact triggers exocytosis of the rhoptry and microneme contents from the apex of the merozoite. The membranous rhoptry contents fuse with the erythrocyte membrane, inducing localised dissociation and disaggregation of the erythrocyte cytoskeleton, and invagination of the erythrocyte membrane resulting in the formation of an invasion pit.

It is uncertain which red blood cell ligands are involved in either of these adhesion steps, although sialic acid residues on glycophorins have been implicated in binding of MSP-1, whilst EBA-140 and EBA-175 bind to sialic acid receptors on the erythrocyte surface (Perkins and Rocco 1988; Holder and Blackman 1994; Thompson *et al.* 2001).

The merozoite then enters the invasion pit, with the region of apical attachment changing from a cone to an annulus, through which the merozoite passes. It is postulated that a linear actin-myosin motor drives entry of the merozoite into the invasion pit (Pinder *et al.* 2000). It is suggested that at the tight junction, red blood cell receptors bind to trans-membrane merozoite proteins which are in turn bound to myosin tails beneath the merozoite's plasma membrane, with the myosin heads bound to actin filaments that are anchored to a microtubule or other cytoskeletal structure of the merozoite (Pinder *et al.* 2000; Fowler *et al.* 2001). As the merozoite enters the invasion pit, surface proteins are lost from the point of contact with the annulus and shed from the invasion pit into the extracellular matrix. The exact mechanism by which the surface proteins are stripped off is unknown, but is probably due to the action of proteases released from the apical organelles into the incipient invasion pit.

As the merozoite is internalised the invasion pit closes by annular membrane fusion to form a parasitophorous vacuole, and dense granules are exported to the merozoite surface and their contents discharged into the parasitophorous vacuole. The time between initial contact and entry of the merozoite into the erythrocyte is 20 - 30 seconds. Erythrocyte surface proteins are excluded from the parasitophorous vacuole membrane (PVM) which is probably a mixture of erythrocyte membrane and membranes discharged from the apical organelles (Ward *et al.* 1993; Bannister *et al.* 2000). The PVM increases in surface area, organelles specific to merozoites disappear, and the parasite elongates and flattens, developing into a ring stage trophozoite.

The ring stage trophozoite is contained within the parasitophorous vacuole, and has a flattened ring of cytoplasm that holds all the major organelles. The parasite feeds on the erythrocyte cytoplasm, through a small dense ring on the parasite surface called the cytostome. The waste products of haemoglobin digestion accumulate as brown crystals of haemozoin in the food vacuole. These crystals are visible by 15 hours post-invasion. As the ring stage feeds on its host, it enlarges, developing into a trophozoite by 20 hours post-invasion. The trophozoite undergoes an increase in protein synthesis with an associated increase in free ribosomes, endoplasmic reticulum (ER) and the development of a Golgi complex close to the nucleus. The surface area of the trophozoite enlarges considerably suggesting the parasite is trafficking substances to and from the PVM. By 27 hours post-invasion, the trophozoite has greatly increased the quantity of rough ER and Golgi complex, and is exporting proteins into the erythrocyte, forming electron-dense knobs on the red blood cell surface. These consist of a complex of proteins: EMP-1, EMP-3, MESA and KAHRP, which are anchored by KAHRP to the cytoskeleton of the

infected erythrocyte (Waller *et al.* 1999). These knobs mediate the cytoadherance to the vascular endothelium seen in sequestration of late stages of the erythrocytic cycle.

The parasite is able to sort proteins targeted to a variety of destinations within the infected erythrocyte i.e. within the parasite plasma membrane, to the parasitophorous vacoule, and to the erythrocyte membrane. Proteins targeted to locations within the parasite plasma membrane are transported from the Golgi via a classical secretory pathway, that is inhibited by Brefeldin A (Dooren *et al.* 2000). Brefeldin A is postulated to inhibit either vesicular trafficking between the ER and the *cis*-Golgi, or trafficking between the Golgi and the *trans*-Golgi secretory system (Crary and Haldar 1992; Haldar and Holder 1993; Ogun and Holder 1994; Dooren *et al.* 2000).

Plasmodium parasites have two protein transport pathways, one for proteins transported within the boundaries of the parasite membrane, and the other for export of proteins targeted to the parasitophorous vacuole or to the erythrocyte. Wiser *et al* have shown that proteins exported past the parasite membrane accumulate in a compartment at the parasite periphery, whilst proteins transported within the parasite boundaries accumulate in the ER (Wiser *et al.* 1997). In most mammalian cells the classical secretory mechanism of protein transport involves the cycling of coated vesicles from the plasma membrane to the trans-Golgi via early endosomes, and subsequent vesicular export of proteins to the membrane surface. The trafficking of parasite proteins to the erythrocyte membrane induces the formation of caveolae-vesicle complexes and Maurer's clefts in the erythrocyte, suggesting that the parasite may be utilising a modification of the classical-secretory mechanism of protein transport to export proteins from the parasite periphery to the erythrocyte surface (Aikawa 1988; Crary and Haldar 1992; Dooren *et al.* 2000).

At around 30 hours post-invasion the trophozoite starts to undergo nuclear division and turns into a schizont. The schizont nucleus divides endomitotically, with the segregating chromosomes and spindle apparatus remaining within the nuclear envelope.* Following nuclear replication a mitotic spindle forms in the nucleus and elongates, pinching the two sets of chromosomes apart in the nucleus. New spindles then form at each set of chromosomes and the process of nuclear division is repeated several times resulting in between 16 to 32 chromosome sets. At the same time as nuclear division the schizont undergoes a large increase in rough ER and free ribosomes, multiplication of mitochondria and plastids and the creation of lipid vacuoles. At the 8-nucleus stage of nuclear division, the individual nuclei move towards the surface of the parasite as a precursor for the formation of individual merozoites. During the last nuclear division, centres of merozoite formation develop at the ends of each mitotic spindle, these are spaced at regular intervals in the schizont. The merozoites then develop in a highly ordered sequence of events. At each spindle pole body, coated vesicles bud off from the nuclear envelope to form a single cisterna Golgi body. Secretory vesicles bud from the newly formed Golgi to create the apical organelles (Bannister *et al.* 2000). Ribosomes attached to the nuclear envelope and rough ER synthesise proteins that are transported via coated vesicles from the nuclear envelope to the Golgi. At the *cis*-Golgi, Golgi-transport complexes sort proteins according to their targeting signals, to vesicles budding from the *trans*-Golgi. These vesicles are subsequently transported to the appropriate organellar destination in the merozoite.

The merozoite cytoskeleton assembles around each nascent merozoite, forming a cleavage furrow that defines the merozoite shape. The nucleus, mitochondrion and plastid move into the developing merozoite, and a coat of proteins is exported to the merozoite

* (Reviewed by Bannister *et al.* 2000)

surface. As the merozoite matures it is separated from the schizont via a constriction ring, and is released into the parasitophorous vacuole. At 48 hours post invasion, the mature merozoites exit the host erythrocyte in a two step process. This process, that is probably mediated by secretions from the rhoptry or microneme ducts of merozoites, involves the initial rupture of the host erythrocyte, followed by rupture of the parasitophorous vacuole membrane (Salmon *et al.* 2000).

1.5 Apical Organelle, Parasitophorous Vacuole and Merozoite Surface Proteins

Several proteins have been identified in the apical organelles, parasitophorous vacuole and on the surface of released merozoites (see Figure 1.3). These proteins are of interest as they have a potential role in the initial recognition and attachment of merozoites to the erythrocyte surface, many are recognised by human immune sera and are as a result potential vaccine targets (Holder 1994). Several of these proteins either undergo proteolytic cleavage or are putative proteases, suggesting that they may also be potential chemotherapy targets (Blackman 2000). There is considerable interest in identifying proteins in *P. falciparum* that show homology to proteins from other *Plasmodium* species, as this suggests that they share a conserved function. Hence studying these homologues in animal-malaria models may help to elucidate their function in erythrocyte invasion, and to identify chemotherapy and vaccine targets for use in humans.

Proteins in the apical organelles are predicted to have several functions, these include: promoting exit from the host red blood cell, adhesion to the erythrocyte; uncoupling of the host cytoskeleton, and entry into the invasion pit (Preiser *et al.* 2000; Blackman and Bannister 2001).

1.5.0 Rhoptry Proteins

The rhoptries are highly membranous pear-shaped structures, with a narrow duct at the merozoite apex, widening to a basal body in the apical cytoplasm. Rhoptries contain at least between 9 – 15 polypeptides. These proteins are present in a highly developed order in the structure, with their location in the rhoptry dictated by differential expression times during merogony. So proteins located in the rhoptry duct are synthesised before those located in the basal body (Jaikaria *et al.* 1993). Once synthesised these proteins are transported through the Golgi to the developing rhoptry organelle (Howard and Schmidt 1995). Several rhoptry proteins either bind to or may be inserted into red cell membranes, suggesting that they are involved in adhesion.

Proteins present in the rhoptry duct of *P. faciparum* merozoites include, AMA-1; the RhopH-1, RhopH-2, and RhopH-3 complex of 140, 130, and 110 kDa polypeptides; and the 225 kDa rhoptry protein (p225) (Jaikaria *et al.* 1993; Narum and Thomas 1994). The 110 kDa RhopH-3 is found in the parasitophorous vacuole during invasion and on the surface of newly invaded red blood cells.

In the basal region of the rhoptries is located the RAP-1, RAP-2, RAP-3 complex of 82, 42 and 37 kDa polypeptides (Howard and Reese 1990). The RAP complex is transported to the rhoptries after the RhopH complex, and by the 8 nuclei stage of merogony both the RAP and RhopH complexes are present in the rhoptries (Jaikaria *et al.* 1993). Disruption of the RAP-1 gene, which has no effect on the invasion phenotype, results in retention of RAP-2 in the lumen of the ER, suggesting that RAP-1 and RAP-2 are co-translationally expressed, and that RAP-2 needs to form a complex with RAP-1 to be transported to the rhoptry (Baldi *et al.* 2000). RAP-3 joins the RAP-1 - RAP-2 complex at some point during vesicular transport from the ER to the Golgi. RAP-1 is

processed during schizont maturation and merozoite development, in the rhoptries, the function of which is unknown (Howard *et al.* 1998). Antibodies to RAP-1 block *in vitro* merozoite invasion, are present in humans exposed to malaria, and partially protect monkeys against parasite challenge (Ridley *et al.* 1990 ; Jakobsen *et al.* 1997).

Additional proteins that have been identified in the rhoptries of *P. falciparum* include the 60 kDa polypeptide (p60), and a serine protease (*Pf*p76). *Pf*p76 has a GPI anchor and acts like a serine protease once this is cleaved off.

A number of rhoptry proteins have also been identified in other *Plasmodium* species. This includes the *P. yoelii* 235 kDa rhoptry protein, which is encoded by a gene family of over 35 copies, is related to the *P. vivax* reticulocyte binding proteins (*Pv*RBP-1, *Pv*RBP-2), and is predicted to be one of the components involved in formation of the tight-junctional zone during erythrocyte invasion (Preiser *et al.* 2000; Khan *et al.* 2001) . Also present in the rhoptries of both *P. yoelii* and *P. berghei* rodent malaria parasites is the MAEBL protein family that is a paralogue of *Pf*AMA-1 and the *P. vivax* Duffy binding protein (DBP) (Kappe *et al.* 1998; Noe and Adams 1998). MAEBL is expressed early in schizont development and appears on the merozoite surface after the formation of individual merozoites during merogony.

1.5.1 Microneme Proteins

The micronemes are small flask-like structures, with ducts that secrete their contents into the rhoptry ducts. Microneme proteins include AMA-1 and erythrocyte binding antigens (EBA-140 and EBA-175), and are predicted to be involved in the initial interaction with the red blood cell during invasion (Blackman and Bannister 2001).

The 83kDa AMA-1 is transcribed 3 hours later than RAP-1 and RAP-2, and appears to be initially located in the micronemes, and is then secreted into the rhoptry duct (Jaikaria *et al.* 1993). On schizont rupture the 83 kDa AMA-1 polypeptide undergoes N-terminal cleavage into a 66 kDa protein that is initially detected at the apical end of the merozoite, and then relocates to the entire merozoite surface (Narum and Thomas 1994; Howell *et al.* 2001). On relocation to the merozoite membrane the 66 kDa protein then undergoes further processing at either of two sites, to give either a 44 or a 48 kDa polypeptide, which is then shed from the merozoite surface (Howell *et al.* 2001). The role of AMA-1 is currently unknown, however vaccine trials in animal models with homologues to *Pf* AMA-1 result in protection against subsequent parasite challenge, suggesting that it is involved in merozoite attachment to or entry into erythrocytes (Reviewed by Preiser et al. 2000).

A family of related erythrocyte binding proteins present in merozoite micronemes are thought to be released after initial contact of the merozoite with the erythrocyte. In *P. vivax* and *P. knowlesi* they are 135 kDa proteins which bind to the Duffy blood group antigen, a prerequisite for junction formation and invasion, while in *P. falciparum* they are the 140 and 175 kDa erythrocyte binding antigens (EBA-140 and EBA-175) which bind to sialic acid residues on the erythrocyte surface (Reviewed by Holder 1994). EBA-175 is predicted to bind to sialic residues on glycophorin A, whilst EBA-140 does not appear to bind to glycophorin A, B or C (Thompson *et al.* 2001). Some parasite lines lack *eba-140*, whilst disruption of EBA-175 results in a switch to a sialic-acid independent invasion pathway, suggesting that neither are essential and that erythrocyte invasion can follow alternative paths (Reed *et al.* 2000; Thompson *et al.* 2001).

1.5.2 Dense Granule Proteins

During erythrocyte invasion, dense granules or microspheres move to the merozoite surface, passing through pellicular membranes, to release their contents by exocytosis into the parasitophorous vacuole. The release of these vesicles and of the other apical organelles leads to the further expansion of the PVM. Several proteins have been identified in the dense granules of *P. falciparum*, including: ring-infected erythrocyte surface antigen (RESA) which either crosses the PVM to interact with the erythrocyte cytoskeleton or accumulates in the newly formed parasitophorous vacuole; ring membrane antigen (RIMA); and two membrane-bound subtilisin-like serine proteases (*Pf*Sub-1, *Pf*Sub-2) (Aikawa *et al.* 1990; Blackman *et al.* 1998; Blackman and Bannister 2001). Both the PfSub-1 and PfSub-2 precursors undergo processing reactions which are believed to be essential for exposure of the active site (Barale *et al.* 1999; Hackett *et al.* 1999; Sajid *et al.* 2000). A number of other proteins are likely to be located to dense granules and these may include proteases responsible for a number of the cleavage events seen with proteins involved in erythrocyte invasion i.e. MSP-1, AMA-1, and RAP-1.

1.5.3 Parasitophorous Vacuole Proteins

The acidic basic repeat antigen (ABRA) and serine repeat antigen (SERA) are major antigens in the parasitophorous vacuole of *P. falciparum* schizonts, and are peripherally associated with the schizont and merozoite surface. ABRA is a 101 kDa protein released from the parasitophorous vacuole on schizont rupture. ABRA may be a serine protease with chymotrypsin-like activity, and antibodies targeted to it can inhibit erythrocyte invasion (Blackman 2000). On merozoite release the 126 kDa SERA is processed into three fragments of 18, 47 and 50 kDa, and is the target of antibodies that inhibit merozoite dispersal (Debrabant and Delplace 1989; Pang *et al.* 1999). A number of

homologues to SERA have been identified, and can divided into two classes of SERA and SERA homologue (SERPH) proteins. The SERPH proteins show significant homology to the papain family of cysteine proteases, and may mediate primary processing of MSP-1 and other processing events on the merozoite surface (Blackman 2000).

1.5.4 Proteins on the Surface of *P. falciparum* Merozoites

Proteins such as AMA-1 and EBA-175, that are secreted onto the merozoite surface from the apical organelles, are class I membrane proteins with trans-membrane domains (Narum and Thomas 1994). Several other proteins have been identified on the surface of *P. falciparum* merozoites. These are the merozoite surface proteins (designated MSP-1, -2, -3, -4, -5, -6, -7 and -8) which are ubiquitous on the merozoite surface, as well as parasitophorous vacuole proteins such as SERPH which are peripherally associated with the nascent merozoite surface. At least four of these, MSP-1, -2, -4, -5, and -8 are linked to the plasma membrane via GPI anchors, whilst MSP-3 is partially soluble in the parasitophorous vacuole, and MSP-1, -4, -5 and -8, contain epidermal growth factor (EGF)-like domains (Gerold *et al.* 1996; Marshall *et al.* 1997; Marshall *et al.* 1998; Black *et al.* 2001). EGF-like domains contain six cysteine residues and are implicated in mediating protein-protein recognition, and hence may be involved in erythrocyte invasion. Several MSPs are recognised by human immune sera, suggesting they are potential vaccine targets (Holder 1994; Wang *et al.* 1999). During the process of merozoite release and erythrocyte invasion several of these proteins undergo proteolytic processing events which may be chemotherapy targets (Blackman 2000).

MSP-1 is a major component of the merozoite surface, in the form of a complex with proteins derived from MSP-6 and MSP-7, and is implicated in erythrocyte

recognition and invasion (Holder and Blackman 1994) (See Sections 1.6-7 for more details on MSP-1, -6 and -7).

1.6 Merozoite Surface Protein –1

Relatively few proteins are associated with the merozoite surface, and of these Merozoite Surface Protein-1 (MSP-1) has been extensively studied. MSP-1 is a ubiquitous component of the merozoite surface in all *Plasmodium* species, which is predicted to be involved in the initial stages of merozoite invasion. The 15 - 20 nm protein spikes seen on the merozoite surface by EM are postulated to be the MSP-1 complex (Bannister and Dluzewski 1990). Sialic acid residues on glycophorins have been implicated with binding of MSP-1 in *P. falciparum* (Perkins and Rocco 1988; Holder and Blackman 1994). Antibodies to MSP-1 have been identified in immune individuals, and are correlated with low parasitemia and protection against severe disease, whilst vaccine trials with MSP-1 in animals and humans, have resulted in protection against subsequent parasite challenge (Hirunpetcharat *et al.* 1997; Lyon *et al.* 1997; Egan *et al.* 1999; O'Donnell *et al.* 2001; Stowers *et al.* 2001).

1.6.0 The MSP-1 Gene and Protein

P. falciparum MSP-1 is coded by a single copy gene of approximately 5kb on Chromosome 9. Homologues to MSP-1 have been identified in all species of *Plasmodium.* The *P. falciparum* MSP-1 amino acid sequence can be divided into 17 blocks that are either highly conserved, moderately conserved, or highly diverse (Tanabe *et al.* 1987). This sequence variation falls into two distinct types, suggesting that *Pf*MSP-

1 is dimorphic (Tanabe *et al.* 1987). These two allelic types of *Pf*MSP-1 are designated as MAD20 and Wellcome / K1 type alleles (Holder *et al.* 1985; Tanabe *et al.* 1987). Attempts to create a *Pfmsp-1* knockout in the erythrocytic stage parasites have failed, suggesting that *msp-1* is an essential gene (O'Donnell *et al.* 2000).

P. falciparum msp-1 is transcribed in schizonts at 36 to 46 hours post invasion, and expressed as a 195 kDa precursor (Myler 1990; Stafford *et al.* 1996b). The MSP-1 precursor has an N-terminal signal sequence of 19 amino acids that targets the MSP-1 precursor for transport to the merozoite surface via the Golgi cisterna. The transport of MSP-1 to the developing merozoite surface is BFA sensitive, treatment with which results in accumulation of MSP-1 in an ER like compartment (Wiser *et al.* 1997). This confirms that the MSP-1 precursor is transported via the Golgi in the normal intra-parasitic transport system. The MSP-1 precursor undergoes several post-translational modifications including the addition of a GPI anchor to its C-terminus and two proteolytic processing steps.

1.6.1 The Processing Events of MSP-1

The MSP-1 precursor undergoes two proteolytic processing steps throughout the genus (Holder *et al.* 1987; Blackman *et al.* 1991a; Blackman *et al.* 1991b; Holder *et al.* 1992; Holder and Blackman 1994; Blackman *et al.* 1996). These processing steps occur after addition of the GPI anchor, and after translocation of the precursor from the *trans*-Golgi to the developing merozoite surface (See Figure 1.4 for a schematic of MSP-1 processing events).

The first MSP-1 processing step occurs on the merozoite surface around the time of merozoite release. The 195 kDa MSP-1 precursor is cleaved into a complex of 83, 42 ,

38, and 30 kDa polypeptides (respectively designated MSP-1_{83}, MSP-1_{42}, MSP-1_{38}, and MSP-1_{30}). The cysteine protease SERPH has been suggested as being responsible for primary processing of MSP-1, but this remains to be shown experimentally (Blackman 2000). These primary processed MSP-1 polypeptides form a non-covalently bound complex on the merozoite surface. This primary processed MSP-1 complex contains the four 83, 42, 38 and 30 kDa MSP-1-derived polypeptides, and two non-MSP-1 derived polypeptides of 22 kDa (MSP-7_{22}) and 36 kDa (MSP-6_{36}) (McBride and Heidrich 1987; Stafford *et al.* 1996a; Trucco *et al.* 2001) (See section 1.7 for further details).

The second MSP-1 processing event occurs at or just prior to erythrocyte invasion. MSP-1_{42} is cleaved into a N-terminal 33 kDa polypeptide (MSP-1_{33}) and a C-terminal 19 kDa polypeptide (MSP-1_{19}). After cleavage MSP-1_{19} remains bound to the merozoite membrane via the GPI anchor, whilst MSP-1_{33} is shed from the merozoite surface with the remainder of the MSP-1 complex (Blackman *et al.* 1991a; Blackman *et al.* 1991b) (See section 1.7 for further details).

The second MSP-1 cleavage step is an essential prerequisite for erythrocyte invasion. Processing of MSP-1_{42} and erythrocyte invasion is inhibited in the presence serine protease inhibitors (e.g. PMSF), and calcium chelators (e.g. EDTA) (Blackman and Holder 1992; Blackman *et al.* 1993). As these have no effect on primary processing of MSP-1, nor on release of merozoites, this suggests that different classes of protease are responsible for the two MSP-1 processing steps (Blackman *et al.* 1991b; Blackman and Holder 1992). The protease responsible for cleavage of MSP-1_{42} has been characterised as a membrane-bound calcium-dependent serine protease (Blackman and Holder 1992; Blackman *et al.* 1993). The subtilisin-like serine proteases (*Pf*Sub-1 and *Pf*Sub-2) were initially candidates for processing of MSP-1_{42}, however evidence of their ability to cleave

MSP-1_{42} has yet to be produced (Blackman *et al.* 1998; Hackett *et al.* 1999; Sajid *et al.* 2000).

MSP-1_{19} is taken into the invaded red blood cell with the merozoite (Blackman *et al.* 1990). MSP-1_{19} is in block 17 of the amino acid sequence, which is highly conserved in both allelic types of *Pf*MSP-1 (Tanabe *et al.* 1987). The MSP-1_{19} structure has been recently determined and consists of two EGF-like domains (Blackman *et al.* 1991a; Morgan *et al.* 1999). The MSP-1_{19} structure is remarkably conserved between *P. falciparum* and the simian malaria *P. cynomolgi*, despite differences in the number of disulphide bonds (Blackman *et al.* 1991a; Morgan *et al.* 1999). Functional complementation of the *Pf*MSP-1_{19} C-terminus with the highly divergent C-terminal sequence of *P. chabaudi* MSP-1_{19}, does not result in any differences in the processing of MSP-1_{42} nor in the invasion phenotype with human erythrocytes (O'Donnell *et al.* 2000). This indicates that the role of MSP-1_{19} in erythrocyte invasion is functionally conserved in these *Plasmodium* species despite sequence divergence, and hence that MSP-1_{19} is a good chemotherapy and vaccine target.

Antibodies against MSP-1_{19} have been shown to inhibit parasite growth, erythrocyte invasion and secondary processing of MSP-1 (reviewed by Holder and Blackman 1994). Several of these antibodies recognise conformation dependent epitopes, and their binding can be annulled by reduction of the disulphide bonds in the EGF-like domains of MSP-1_{19} (Blackman *et al.* 1990; Chappel and Holder 1993). *In vitro* MSP-1 secondary processing assays have shown that antibodies against MSP-1_{19} have three possible effects on processing of MSP-1_{42} (Blackman *et al.* 1990; Chappel and Holder 1993; Blackman *et al.* 1994; Guevara Patino *et al.* 1997).

Inhibitory antibodies - prevent secondary processing of MSP-1 and hence erythrocyte invasion, either by directly blocking access by the protease to its cleavage site, or indirectly changing the quaternary structure of MSP-1_{19} and hence the protease binding sites.

Blocking antibodies – prevent the binding of inhibitory antibodies by sterically blocking access to the binding epitopes of inhibitory antibody, allowing secondary processing of MSP-1_{42} to occur.

Neutral antibodies - have no effect on either processing, invasion or on the binding of inhibitory antibody.

The raising of blocking antibodies is presumably a form of immune evasion by the parasite, as these blocking antibodies would prevent binding of inhibitory antibodies to MSP-1_{42}, allowing secondary processing and hence erythrocyte invasion to occur. It is unknown whether the immune response gradually matures with exposure to the parasite, developing more inhibitory antibodies whilst decreasing the titre of blocking antibodies.

The binding of known inhibitory and blocking mouse monoclonal anti-MSP-1_{19} antibodies can be specifically annulled by the insertion of mutations into the amino acid sequence of an MSP-1_{19} recombinant fusion protein (Uthaipibull *et al.* 2001). This suggests that a mutant MSP-1_{19} polypeptide can be engineered to selectively bind only inhibitory antibodies (Uthaipibull *et al.* 2001). This mutant MSP-1_{19} could be used in a vaccine to raise inhibitory antibodies that prevent MSP-1_{42} processing and erythrocyte invasion. The same concept could also be used to raise additional inhibitory antibodies against epitopes to the N-terminal side of the MSP-1_{19} – MSP-1_{33} cleavage site, again with the aim of blocking access to the protease. The apparent success of MSP-1_{42} as a

major vaccine candidate in human trials (showing approximately 50% protection against severe disease), compared to the failure of wild-type MSP-1_{19} based vaccines, suggests that antibodies to the MSP-1_{33} region of MSP-1_{42} also play an important role in protection (Bojang *et al.* 2001; Stowers *et al.* 2001).

1.7 Proteins Complexed With MSP-1

On the merozoite surface, the primary processed 83, 42, 38 and 30 kDa MSP-1 polypeptides are in a non-covalently bound complex with two additional polypeptides of 22 kDa (MSP-7_{22}) and 36 kDa (MSP-6_{36}) (McBride and Heidrich 1987; Stafford *et al.* 1996a; Trucco *et al.* 2001). These two proteins are not derived from MSP-1, as determined by N-terminal amino acid sequencing and antibody affinity-select experiments (Stafford *et al.* 1994).

The shed MSP-1 complex, released after secondary MSP-1 processing, has been immuno-affinity purified using an anti-MSP-1_{33} antibody (X509) (see Figure 1.5). Analysis of the purified complex suggested that a 19kDa protein (MSP-7_{19}), the 22 kDa MSP-7_{22} polypeptide, and a 36kDa polypeptide (MSP-6_{36}) are part of the shed MSP-1 complex (Stafford *et al.* 1994; Stafford 1996). N-terminal sequencing of the 19, 22 and 36 kDa and MSP-1 polypeptides purified from the shed complex showed that MSP-7_{19}, MSP-7_{22}, and MSP-6_{36} are distinct from the MSP-1 products of secondary processing (Stafford *et al.* 1994; Stafford *et al.* 1996a). Two dimensional peptide mapping and antibody affinity select experiments suggested that MSP-7_{19} and MSP-7_{22} were closely related to each other but not to MSP-6_{36} (Stafford *et al.* 1996a).

The gene coding for *Pf*MSP-6 has been identified (Trucco *et al.* 2001). The *msp-6* gene shows no sequence diversity, and codes for a 371-residue MSP-6 precursor (Trucco *et al.* 2001). The amino acid sequence of MSP-6 shows similarity at the N-terminus and C-terminus to that of MSP-3 (Trucco *et al.* 2001). The MSP-6 precursor undergoes N-terminal cleavage to give the 211-residue, MSP-6_{36}, that is associated with the MSP-1 complex. MSP-6_{36} is a highly hydrophilic, negatively-charged protein, that contains a glutamic acid-rich region and two hydrophobic amino acid clusters that may form part of its binding site with MSP-1 (Trucco *et al.* 2001). The cellular location of the MSP-6 cleavage is unknown, as is the fate of the N-terminal cleavage product. The lack of sequence diversity exhibited by MSP-6 may be due to structural and hence functional constraints in its interactions with the MSP-1 complex. This suggests that MSP-6 is an optimal drug and vaccine target, as it may prove to be an essential component in the MSP-1 complex and hence in erythrocyte invasion.

Cell surface radio-iodination and immunofluorescence experiments suggest that MSP-7_{22} is present on the surface of released merozoites (McBride and Heidrich 1987; Stafford *et al.* 1996a). MSP-7_{22} is non-covalently bound to the primary processed MSP-1 complex of both MAD20 and Wellcome allellic types (McBride and Heidrich 1987; Stafford *et al.* 1996a). In the shed MSP-1 complex, MSP-7_{22} is partially cleaved at the N-terminus into a 19 kDa (MSP-7_{19}) protein, with MSP-7_{19} present in the shed complex at an estimated 2:1 molar ratio with MSP-7_{22} (Stafford *et al.* 1996a). The cleavage of MSP-7_{22} into MSP-7_{19} appears to occur at the same time as secondary processing of MSP-1_{42}, since MSP-7_{19} was detected in the shed MSP-1 complex, but not in primary processed MSP-1 complex isolated from the merozoite surface (Stafford *et al.* 1996a).

As MSP-7_{22} appears to undergo cleavage to MSP-7_{19} at a similar time as MSP-1 undergoes secondary processing, it is possible that the same protease is responsible for both events. Hence MSP-7_{22} may be a putative chemotherapy target. As MSP-7_{22} is closely associated with MSP-1 on the merozoite surface it may also be the target of antibodies that inhibit erythrocyte invasion. Hence the biological significance of MSP-7, in particular in its interaction with the MSP-1 complex requires determination.

1.8 Aims

In order to study the function of MSP-7_{22}, in particular its interaction with MSP-1 and its location on the merozoite, the initial aim for my project was to identify and clone the *msp-7* gene. The partial malaria genome sequence databases were to be searched using the MSP-7_{22} and MSP-7_{19} N-terminal amino acid sequences. To obtain the whole *msp-7* gene, primers were to be designed using retrieved sequences, for use in vectorette PCR, a form of one-sided PCR. The *msp-7* gene would be cloned and sequenced from several *P. falciparum* lines, and analysed by DNA and protein structure programmes.

Regions of the MSP-7 protein would be expressed as GST or 6*His tagged fusion proteins in pGEX-3X or pTrcHisC inducible bacterial expression systems. These fusion proteins would be used to raise specific antibodies against parts of MSP-7, by immunisation into mice, and production of hybridomas expressing monoclonal antibodies. Antibody specificity would be determined by IFAT on parasitised erythrocytes, and by immuno-precipitation of labelled protein.

The time of *msp-7* transcription would be determined by Northern blot analysis. MSP-7 translation and its association with MSP-1 would be studied by western blot

analysis, and by immuno-precipitation from lysates of radiolabelled parasites using detergents that either disrupt or preserve the MSP-1 complex. The timing and location of the association between MSP-1 and MSP-7 would be further studied by dual-immuno-fluorescence assays, and by immunoprecipitation from lysates of synchronised parasites pulse-chased with radiolabelled amino acid precursor. The effect of Brefeldin A on MSP-7 transport and its association with MSP-1 would be studied

To determine the functional activity of antibodies to MSP-7, assays would be performed to determine their effect on MSP-1 secondary processing, and on processing of the MSP-7 precursor.

Figure 1.0 The *Plasmodium* Life Cycle in Humans

A schematic of the life cycle of *Plasmodium* species that infect humans. Taken from a diagram by the Wellcome Trust. The life cycle can be separated into 4 distinct stages: (Knell 1991)

1. Fertilisation A female anopheline mosquito takes a blood meal containing male and female gametocytes from an infected human. (1) The male gametocyte exflagellates, producing up to 8 motile microgametes. (2) These fuse with female macrogametes forming a zygote, which develops into a motile ookinete. (3) The ookinete penetrates the peritrophic membrane and then the midgut wall, and lodges between the outer membrane of the midgut and the midgut epithelial cells where it develops into an oocyst.

2. Sporogony (1 - 2) The oocyst undergoes asexual division developing several thousands of motile sporozoites. (3) After 7 to 20 days the oocyst ruptures and the released sporozoites migrate to the salivary glands where they undergo a brief period of maturation, before entering the salivary ducts.

3. Hepatic Schizogony When the mosquito takes a blood meal sporozoites are injected with saliva into the blood. (1) Sporozoites are transported via the blood stream to the liver where they invade parenchymal cells and develop into pre-erythrocytic schizonts. (2–3) In these the parasite undergoes asexual division into thousands of invasive merozoites, which after 7 to 20 days are released when the hepatic schizont bursts. (4) The released merozoites enter red blood cells within the hepatic sinusoids to start the asexual intraerythrocytic cycle. (5) Some *P. vivax* and *P. ovale* sporozoites develop into hypnozoites, which remain dormant for months or years before undergoing schizogony, resulting in relapsing malaria.

4. Erythrocytic Schizogony (1) Merozoites invade red blood cells, developing into ring stages, and then into trophozoites. (2 – 3) Ring and early trophozoites stages are present in the peripheral circulation. (4 – 5) Trophozoites undergo asexual division (schizogony) developing into schizonts that contain 16 merozoites. Late trophozoites and schizonts of *P. falciparum* mature in capillaries of internal organs. (6 - 7) On schizont rupture the released merozoites reinvade red blood cells continuing the intra-erythrocytic cycle. This cyclical amplification in red blood cells takes 48 hours. (8 - 9) Some merozoites develop into gametocytes, which mature if taken up by a feeding *Anopheline* mosquito.

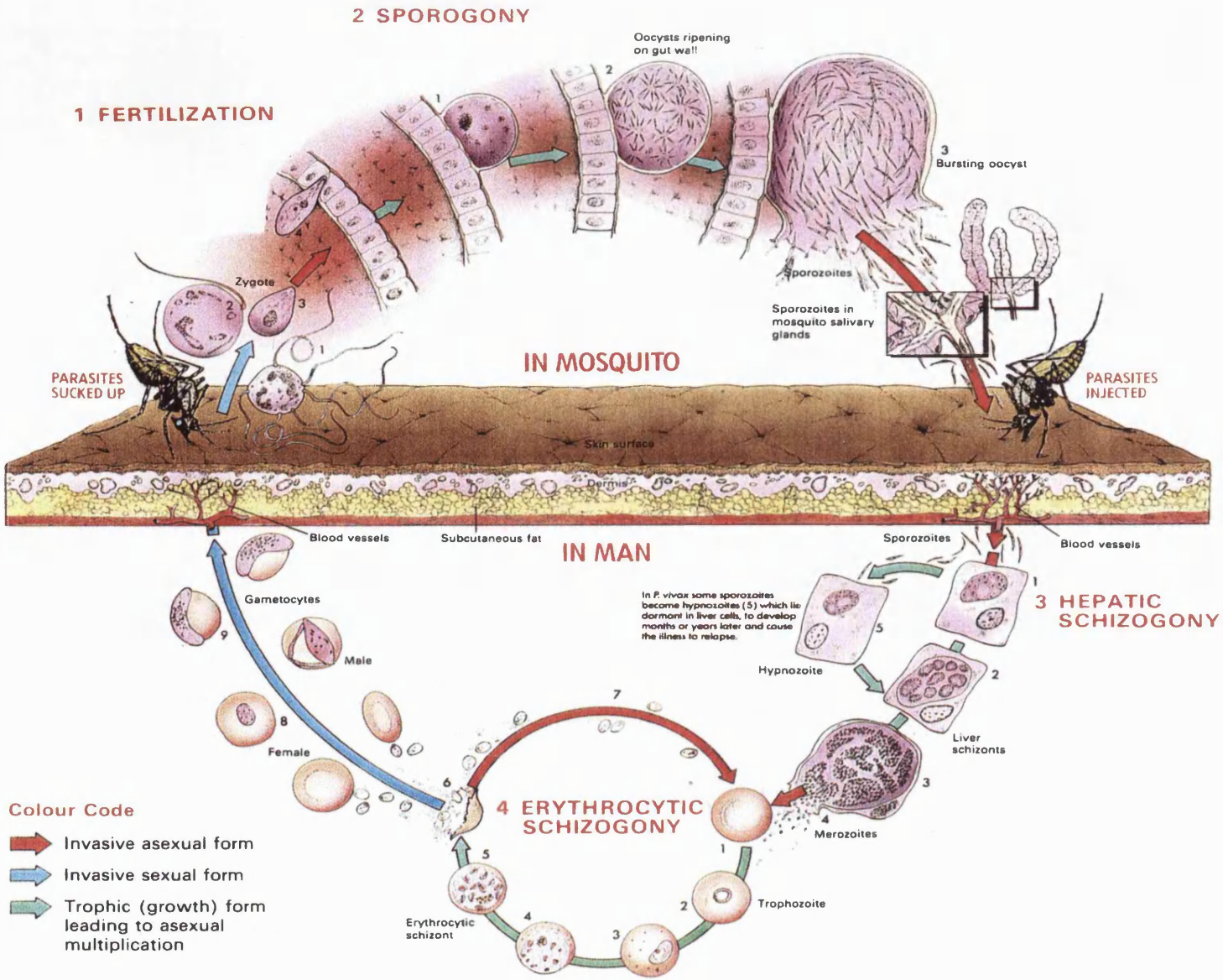
2 SPOROGONY
Oocysts ripening on gut wall
1 FERTILIZATION
3 Bursting oocyst
Zygote
Sporozoites
Sporozoites in mosquito salivary glands
IN MOSQUITO
PARASITES SUCKED UP
PARASITES INJECTED
Skin surface
Dermis
Blood vessels
Subcutaneous fat
IN MAN
Sporozoites
Blood vessels
Gametocytes
Male
Female
In P. vivax some sporozoites become hypnozoites (5) which lie dormant in liver cells, to develop months or years later and cause the illness to relapse.
Hypnozoite
3 HEPATIC SCHIZOGONY
Liver schizonts
4 ERYTHROCYTIC SCHIZOGONY
Merozoites
Trophozoite
Erythrocytic schizont
Colour Code
Invasive asexual form
Invasive sexual form
Trophic (growth) form leading to asexual multiplication

Figure 1.1 The 48 Hour Erythrocyte Cycle

Photographs of Giemsa stained parasites taken at three hour intervals showing the development of the malaria parasite in a newly invaded red blood cell to a mature schizont over the 48 hour erythrocytic cycle (From (Freeman and Holder 1983).

Merozoites bind to and invade erythrocytes, forming a parasitophorous vacuole in which the parasite develops into a ring stage trophozoite. The ring stage digests the host cell haemoglobin and stores the waste products as brown haemozoin crystals, that are visible by 15 hours post-invasion. Haemoglobin digestion continues throughout the cycle.

By 20 hours post invasion the trophozoite starts expanding and building the cellular framework for later schizogony. At about 30 hours post invasion, the trophozoite begins schizogony (asexual replication), developing into a schizont. At the 8 nuclei stage of replication (36-39 hours post invasion), progeny nuclei move apart from each other, towards the surface of the schizont where a final nuclear division occurs.

The merozoite forms around each nucleus in a highly ordered fashion. A single Golgi cisternae forms first, followed by formation of apical organelles, and then the merozoite cytoskeleton. Once fully developed, merozoites bud out of the schizont into the parasitophorous vacuole. Mature schizonts contains between 16 to 32 progeny merozoites.

At 48 hours post invasion, merozoites are released in a two step process. The erythrocyte membrane ruptures first, followed by protease-mediated rupture of the parasitophorous vacuole membrane. Released merozoites then reinvade more red blood cells, continuing the erythrocytic cycle.

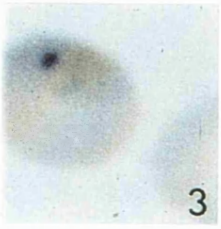
3

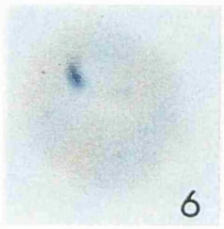
6

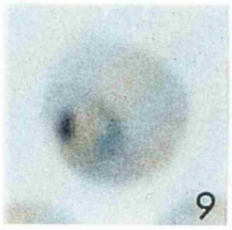
9

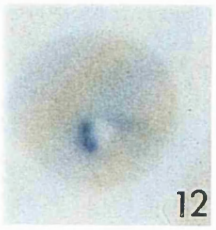
12

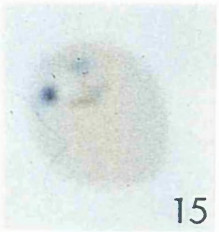
15

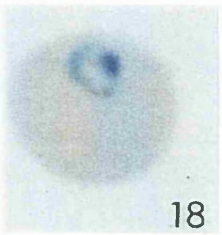
18

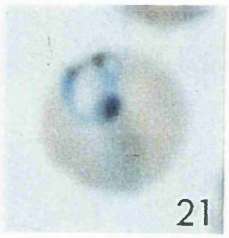
21

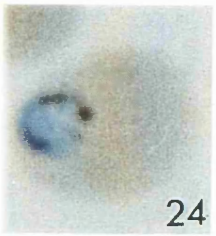
24

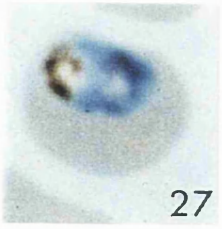
27

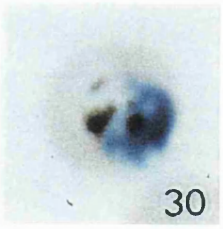
30

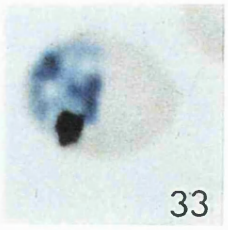
33


36


39

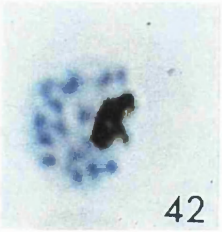
42

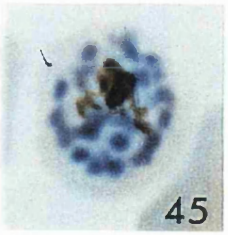
45


48

Figure 1.2 The Major Stages of Erythrocyte Invasion

Schematic showing the major stages of erythrocyte invasion by the *P. falciparum* merozoite. Adapted from diagram by (Bannister *et al.* 1975).

The merozoite undergoes initial and reversible attachment with the red blood cell, mediated by the merozoite's coat of surface proteins. The merozoite reorientates so that its apical end containing the rhoptries and micronemes is in aposition with the erythrocyte membrane. Irreversible binding then occurs with the formation of a tight junction probably via proteins localised at the merozoite's apex from the micronemes or the rhoptries. On formation of the tight junction the erythrocyte cytoskeleton loses rigidity and the erythrocyte membrane invaginates forming an invasion pit into which the merozoite secretes additional rhoptry and microneme contents. The merozoite is drawn into the invasion pit via an actin-myosin motor located at the tight junction. As the merozoite enters the invasion pit its coat of surface proteins including MSP-1 is expelled from the invasion pit. Once the merozoite has entered the invasion pit or parasitophorous vacuole it elongates and flattens into the ring stage trophozoite.

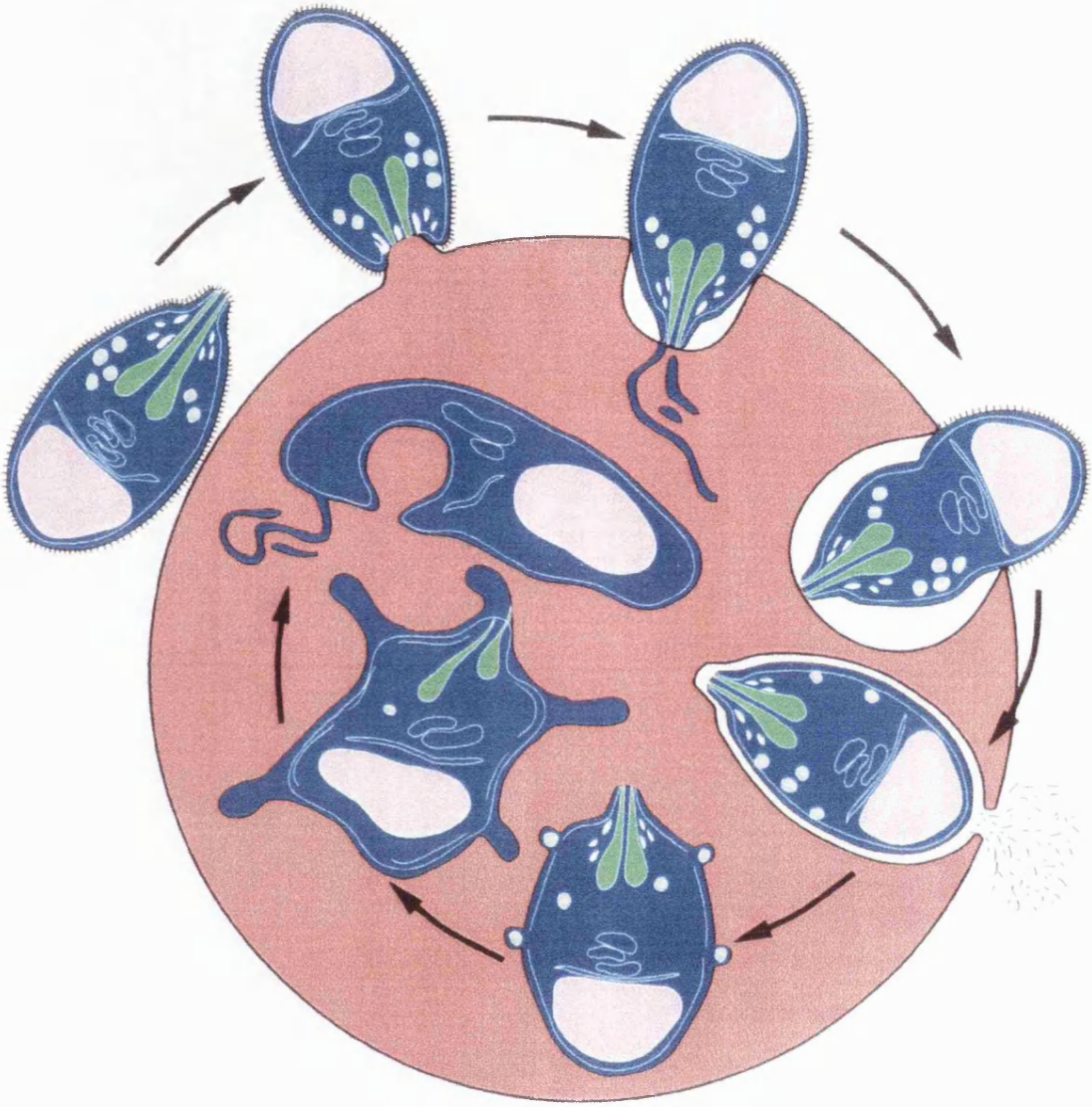

Figure 1.3 The *Plasmodium falciparum* Merozoite

Diagramatic representation of the *P. falciparum* merozoite, showing important structural features and locations of some merozoite proteins. Adapted from diagram by (Cowman 2000).

Structural abbreviations: AP, apical end; DG, dense granules; Im, inner membrane; M, microtubules; Mn, micronemes; Mt, mitochondria; N, nucleus; Pl, plastid; Pr, polar rings; Rh, rhoptries.

Protein abbreviations: ABRA, acid basic rich antigen; AMA-1, apical membrane antigen 1; EBA-140/175, erythrocyte binding antigens 140 and 175; MSP 1-8, merozoite surface proteins 1 - 8; p60, 60 kDa polypeptide; p76, 76 kDa serine protease; p225, 225 kDa rhoptry protein; RAP 1-3, rhoptry-associated proteins 1 - 3; RESA; RhopH1-3, high molecular weight rhoptry proteins 1-3; RIMA, ring membrane antigen; S-Antigen; Sub-1,2, subtilisin-like serine proteases 1 - 2.

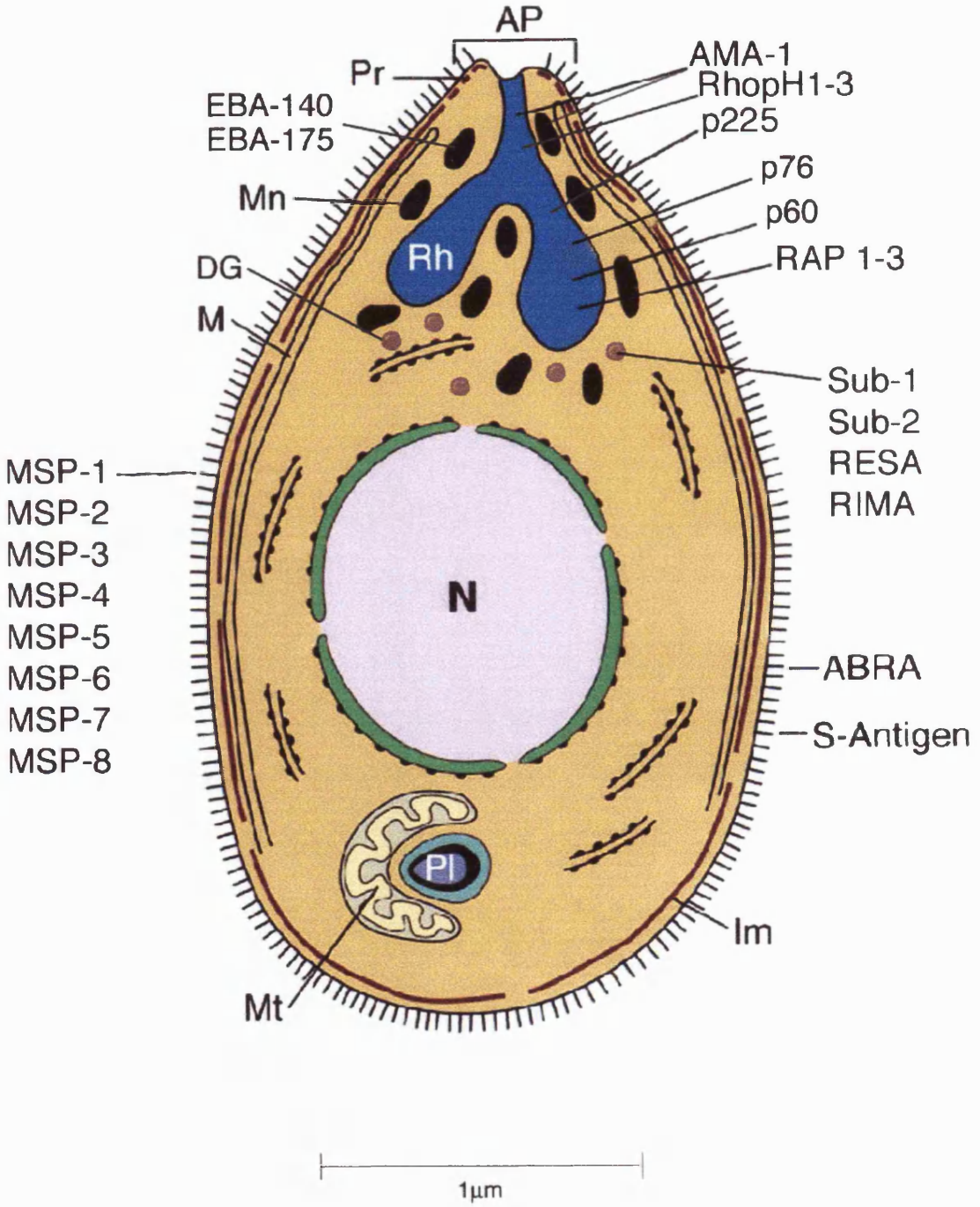
AP
Pr
AMA-1
RhopH1-3
EBA-140
EBA-175
p225
p76
Mn
p60
Rh
RAP 1-3
DG
M
Sub-1
Sub-2
RESA
RIMA
MSP-1
MSP-2
MSP-3
MSP-4
MSP-5
MSP-6
MSP-7
MSP-8
N
ABRA
S-Antigen
Pl
Im
Mt
1µm

Figure 1.4 Merozoite Surface Protein-1 Processing

In the mature schizont, the 195 kDa MSP-1 precursor is attached to the merozoite membrane surface via a C-terminal GPI anchor.

On schizont rupture and merozoite release, the 195 kDa MSP-1 precursor undergoes primary processing into 4 polypeptides of 83, 42, 38 and 30 kDa (**MSP-$1_{83, 42, 38, 30}$**). These primary processed MSP-1 polypeptides remain attached to the merozoite surface via the GPI anchor on MSP-1_{42}, in the form of a non-covalently bound complex with two additional but unrelated proteins of 22 kDa (**MSP-7_{22}**) and 36 kDa (**MSP-6_{36}**).

The second MSP-1 processing step occurs during erythrocyte invasion. This cleaves MSP-1_{42} into two fragments: a C-terminal 19 kDa polypeptide (**MSP-1_{19}**), and an N-terminal 33 kDa polypeptide (**MSP-1_{33}**). MSP-1_{19} remains anchored to the merozoite membrane via the GPI anchor, and is taken into the invaded red blood cell with the merozoite. MSP-1_{33} is shed with the remaining MSP-1 complex into the extracellular environment. The shed MSP-1 complex is soluble and contains the MSP-1-derived polypeptides MSP-1_{83}, MSP-1_{38}, MSP-1_{33} and MSP-1_{30}, and three non-MSP-1 derived polypeptides. These polypeptides are the 36 kDa (**MSP-6_{36}**), the 22 kDa (**MSP-7_{22}**), and a 19 kDa polypeptide (**MSP-7_{19}**) predicted to be derived from partial N-terminal cleavage of MSP-7_{22}.

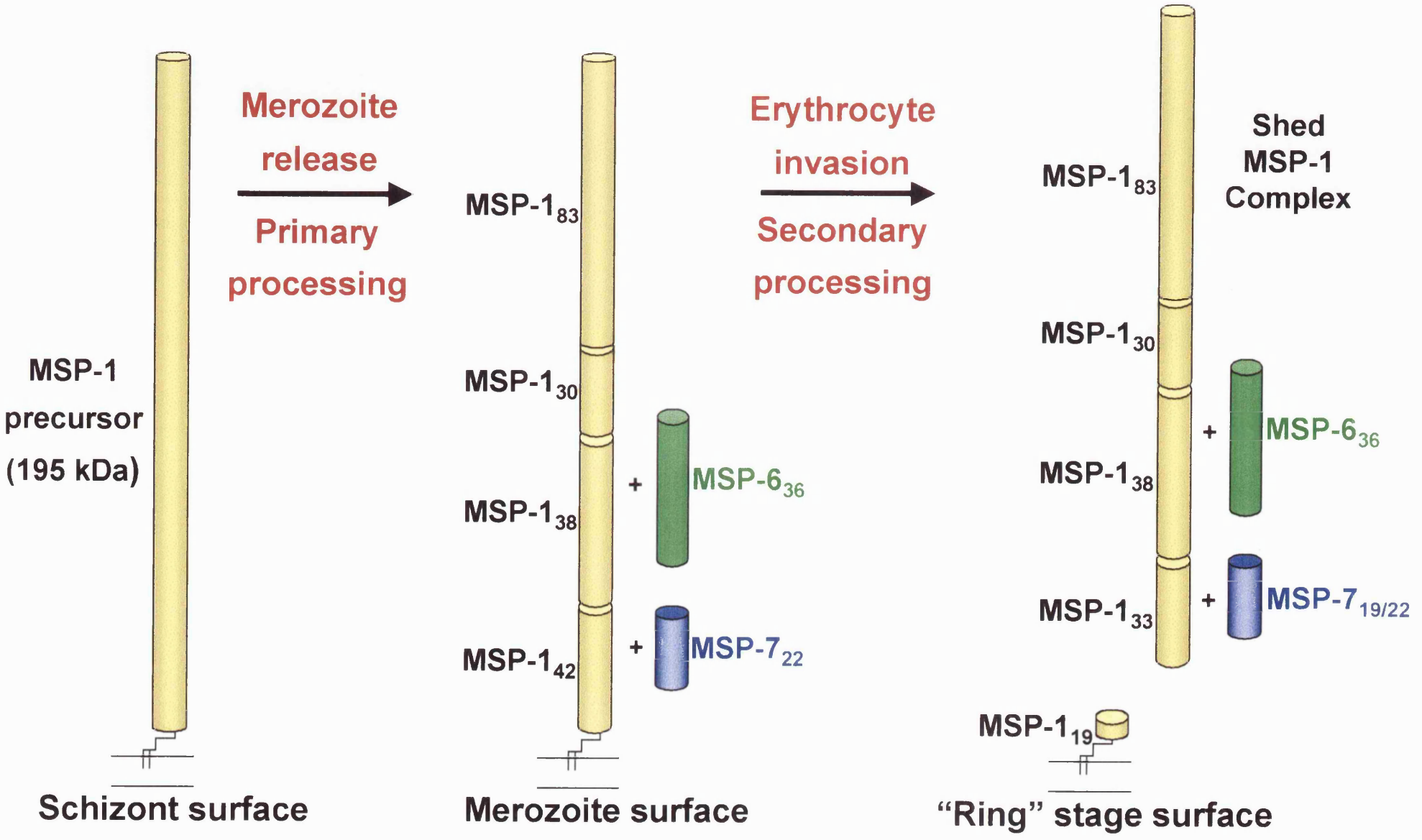
MSP-1
precursor
(195 kDa)
Merozoite
release
Primary
processing
MSP-1 83
MSP-1 30
MSP-1 38
MSP-1 42
+ MSP-6 36
+ MSP-7 22
Erythrocyte
invasion
Secondary
processing
Shed
MSP-1
Complex
MSP-1 83
MSP-1 30
MSP-1 38
MSP-1 33
+ MSP-6 36
+ MSP-7 19/22
MSP-1 19
Schizont surface
Merozoite surface
"Ring" stage surface

Figure 1.5 The Shed MSP-1 Complex

Schematic of the shed MSP-1 complex released on erythrocyte invasion from the merozoite surface by secondary processing of MSP-1_{42}.

Silver-stained SDS-PAGE gel showing the polypeptide components of the T9/96 *P. falciparum* shed MSP-1 complex, purified from culture supernatant by antibody-affinity chromatography. The three non-MSP-1 polypeptides of 19 (**MSP-7_{19}**), 22 (**MSP-7_{22}**) and 36 (**MSP-6_{36}**) kDa were N-terminal amino acid sequenced, and the first 10 N-terminal residues are indicated. The entire N-terminal sequences obtained from both FCB-1 and T9/96 parasite lines are shown below. Adapted from (Stafford *et al.* 1996).

Protein	Parasite Line	N- terminal sequence
MSP-6_{36}	T9/96	^{1}SETNK ^{6}NPTSH ^{11}SN-TN ^{16}TQLNN ^{21}Q
MSP-7_{22}	FCB1	^{1}SETDK ^{6}QSK
	T9/96	^{1}SETDT ^{6}QSKNE ^{11}QEPST ^{16}QGGEE ^{21}INPQP
MSP-7_{19}	T9/96	^{1}EVQKP ^{6}AQGGE ^{11}STFQK ^{16}-LN-- ^{21}LYN

Failure to detect a peak at a particular cycle is designated by a hyphen (-).

Shed MSP-1 Complex

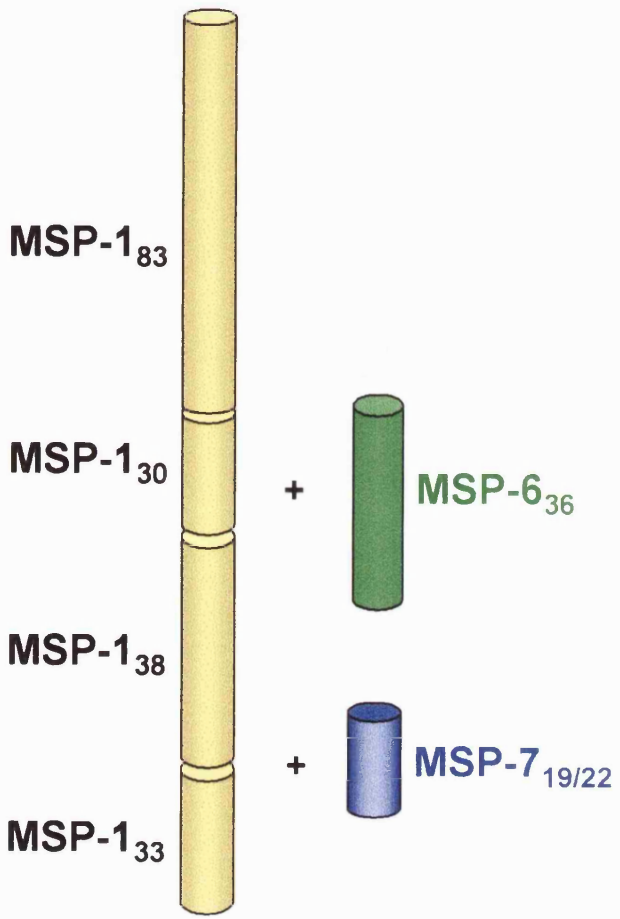

SDS-PAGE of Soluble Shed MSP-1 complex

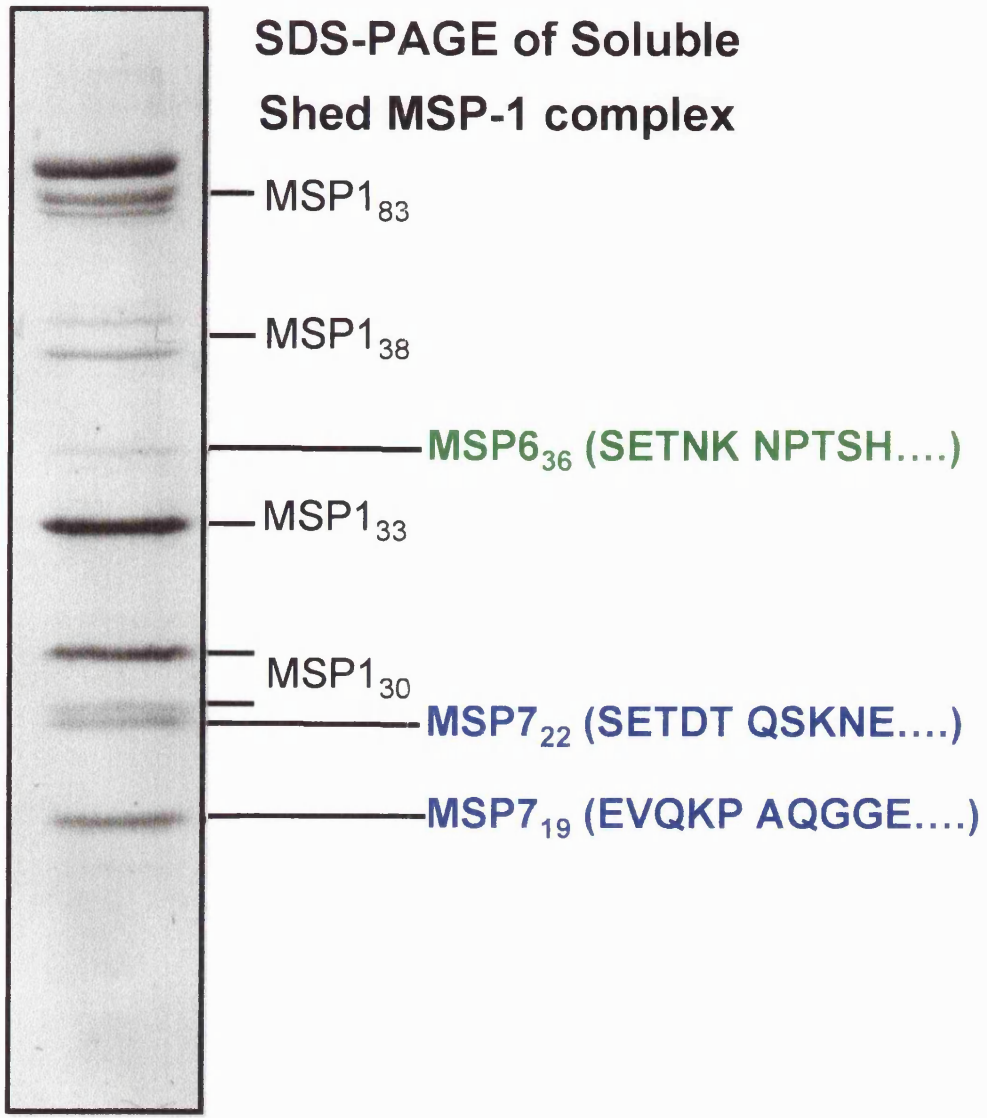

CHAPTER TWO : METHODS

METHOD SECTION ONE : BASIC METHODS

2.0 *In Vitro* Culture of *Plasmodium falciparum*

The NIMR Code of Practice for Work Involving *P. falciparum* was followed for all manipulations involving the parasite. Blood stages of *P. falciparum* were cultured *in vitro* in human red blood cells by Muni Grainger and Terry Scott-Finnigan (Division of Parasitology, NIMR) or by the author as follows.

2.0.0 Erythrocyte Stage Culture of *Plasmodium falciparum*

Asexual blood stages of lines 3D7, FCB1 and T9/96 were maintained at 5 - 10 % parasitaemia in O^+ erythrocytes, in complete RPMI 1640 medium supplemented with 0.5 % w/v AlbuMAX™ and 1 % L-glutamine. Medium was aspirated daily, replaced with an equal volume of medium pre-warmed to 37 °C, washed erythrocytes added to maintain a 1 % haematocrit, and cultures gassed with 7 % CO_2, 5 % O_2, 88 % N_2, before incubation at 37 °C (Blackman *et al.* 1990; Guevara Patino *et al.* 1997).

Parasitaemia and stage of cultured cells were determined by thin blood smears. Cells in a small sample of culture were pelleted by pulsing on a microfuge, most of the supernatant aspirated, the pellet was resuspended in the remaining supernatant and a drop smeared over a glass microscope slide. The slides were air dried, briefly fixed in methanol, stained for 10 min in 10 % Giemsa stain and analysed by light microscopy.

Erythrocytes were washed by resuspending in an equal volume of RPMI 1640 without AlbuMAX, then pelleted by centrifugation for 10 min at 400 x *g*, and the

supernatant removed. This wash was repeated, finally resuspending the erythrocytes in an equal volume of RPMI with AlbuMAX and 1 % glutamine. Parasites were frozen and thawed when required as previously described (Phillips *et al.* 1975).

2.0.1 Synchronisation of Erythrocytic Stages

Schizonts were isolated from other stages of the erythrocytic cycle by Percoll separation, which separates parasite stages by density, and Plasmagel treatment, which is dependent on the presence of knobs at the erythrocyte surface. Following isolation the quality and maturity of schizonts were determined by viewing a Giemsa-stained smear prior to any further manipulations. Cultures were further synchronised by allowing enriched schizonts to release merozoites and undergo erythrocyte invasion, followed by lysis of any remaining schizonts with sorbitol.

2.0.1.0 Plasmagel Schizont Enrichment

FCB-1 and 3D7 (knobbed) parasite cultures were pelleted, the cells washed in RPMI 1640, 1 % glutamine pre-warmed to 37 °C, and the pellet resuspended in 2.4 x pellet volume of RPMI with AlbuMAX, 1 % glutamine; the suspension was then gently mixed with an equal volume of pre-warmed Plasmagel and incubated at 37 °C for 30 min, allowing the cells to settle. The top layer was mixed with an equal volume of pre-warmed RPMI 1640, pelleted at 200 x *g*, 5 min, the supernatant aspirated, and washed enriched schizonts were then ready for further parasite synchronisation by Percoll and / or sorbitol treatment.

2.0.1.1 Percoll Schizont Enrichment

Mature 3D7, FCB-1, and T9/96 schizonts were fractionated from other erythrocytic stages by centrifugation over a layer of 70 % isotonic Percoll (Dluzewski *et*

al. 1984). Isotonic Percoll was made by adding 9 volumes of neat Percoll to 1 volume of 10 x PBS A, 70 % isotonic percoll was made by mixing 7 volumes of isotonic percoll with 3 volumes of RPMI 1640.

Schizonts were washed by centrifugation 3 times in pre-warmed RPMI 1640, and the schizont pellet resuspended to a 10 % haematocrit in pre-warmed RPMI. This was layered onto 2 volumes of 70 % isotonic Percoll pre-warmed to 37 °C in a 50 ml Corning centrifuge tube, and centrifuged at 400 x *g* for 11 min. The schizont layer was removed and washed in 50 volumes of RPMI, spun at 300 x *g* for 3 min, and the washed enriched schizonts were ready for further manipulation.

Ring stages are also separated by the procedure and after washing, can be sorbitol treated as described below to lyse any mature asexual stages.

2.0.1.2 Sorbitol Induced Lysis of Schizonts Following Merozoite Release

To further synchronise parasites, merozoites from enriched schizonts were allowed to re-invade red blood cells for a specific time window, followed by lysis of any remaining schizonts by incubation with 5 % sorbitol, which leaves only early ring stages viable for further culture (Lambros and Vanderberg 1979).

Enriched mature schizonts were cultured at 37 °C as before with fresh erythrocytes for 10 min to 6 hours (depending on required synchronicity of culture), pelleted at 200 x *g* for 5 min, then gently resuspended in a 10 x pellet volume of 5 % sorbitol and incubated at 37 °C for 10 min. Parasites were resuspended, pelleted at 300 x *g*, 10 min and washed with RPMI, 1 % glutamine. The surviving highly synchronous ring forms were cultured as before.

2.0.2 Merozoite Collection

Merozoites were collected by Chairat Uthaipibull, in the presence of calcium chelators to prevent secondary processing of MSP-1, as follows: mature schizonts enriched by percoll or plasmagel treatment were resuspended in RPMI 1640, 10 % human serum, 5 mM EGTA, 1 % glutamine and incubated at 37 °C for 30 min to 60 min. The schizonts were resuspended and pelleted by centrifugation at 200 x *g*, 5 min, and supernatant containing released merozoites filtered through a 3 μm filter, followed by a 1.2 μm filter. Merozoites were pelleted by centrifuging the resulting filtrate at 800 x *g* for 10 min at 4 °C. From this point samples were kept on ice and manipulated in a 4 °C cold room. The supernatant was aspirated and the merozoite pellet resuspended in PBS, 2 mM EGTA, transferred to a microfuge tube and pelleted at 13,000 x *g* for 10 min. The supernatant was aspirated and the merozoite pellets stored at –70 °C until required.

2.1 Genomic DNA Extraction from *P. falciparum*

Three different methods were used to isolate genomic DNA (gDNA) from *Plasmodium falciparum* asexual blood stage cultures. After isolation the gDNA was analysed by agarose-TBE gel electrophoresis (Section 2.3) and spectrophotometry to confirm it met the criteria of being over 100 kb in size, and having an Absorbance 260 / 280 nm ratio of between 1.7 and 1.8.

2.1.0 Genomic DNA Isolation Method One

Asexual blood stage cultures of clones 3D7 and T9/96 at 10 % parasitaemia were resuspended in their culture medium and pelleted by centrifugation at 2000 x *g*, 5 min at 4 °C. To remove excess medium, the supernatant was aspirated, then the cell pellet was

resuspended in PBS, and centrifuged as before. Red blood cells (rbc) were lysed by resuspending the pellet in 1 - 2 x pellet volume of ice cold 1 % acetic acid, followed by the addition of 5 x pellet volume of ice-cold PBS. Parasites were pelleted by centrifugation at 5000 x *g* for 5 min at 4 °C, the supernatant aspirated, and washes in ice cold PBS were performed until excess haemoglobin was removed. The pelleted parasites were stored at –70 °C prior to DNA extraction. Genomic DNA was extracted as described in the method for a Qiagen Blood and Cell Culture DNA kit. Briefly, parasites were lysed in cell lysis buffer C1, centrifuged at 1300 x *g* for 15 min at 4 °C, nuclei lysed and nuclear proteins denatured in general lysis buffer G2. Denatured nuclear proteins were digested with 0.4 mg ml^{-1} Qiagen serine protease at 50 °C. Extracted DNA was isolated using Qiagen Genomic Maxi tips, dissolved in TE buffer, and stored at 4 °C.

2.1.1 Genomic DNA Isolation Method Two

Cultures were pelleted and rbc lysed in 1 % acetic acid as described in Section 2.1.0. Parasites were lysed by resuspending the pellet in one quarter of the original pellet volume of ice cold lysis buffer (40 mM Tris-HCl pH 8.0, 80 mM EDTA, 2 % SDS), followed by the addition of Pronase E to 2 mg ml^{-1}, the mixture vortexed and incubated at 37 °C overnight on a rotating wheel. The lysed cells were mixed with 3 volumes of sterile distilled water (sdw) and vortexed at room temperature (RT), then an equal volume of phenol was added, the sample vortexed, centrifuged at 13000 x *g*, 10 min at RT, and the aqueous phase transferred to a new tube. To this was added an equal volume of phenol / chloroform / isoamyl alcohol (IAA) (50 : 48 : 2 ratio), centrifugation was repeated and the aqueous phase transferred to a fresh tube. This step was repeated with chloroform / IAA (24 : 1 ratio), and the aqueous phase transferred to a new tube. To this was added 0.1 x volume 3 M potassium acetate and 2 volumes of ice-cold 99 % ethanol;

the mix was vortexed, and stored at –20 °C overnight. The DNA was pelleted by centrifugation at 13000 x *g* for 10 min, the supernatant aspirated, and the pellet washed in 1 ml of 80 % ice cold ethanol, spun at 13000 x *g* for 10 min, the supernatant aspirated, and the DNA pellet air dried at RT before resuspending in 100 µl of TE buffer (10 mM Tris HCl pH 7.2, 1 mM EDTA) and storage at 4 °C.

2.1.2 Genomic DNA Isolation Method Three

Parasite DNA suitable for PCR was extracted from frozen schizonts using a method derived from Wooden (Wooden *et al.* 1992). Pellets of enriched schizonts were defrosted and resuspended gently into a 10 x volume of PBS A at RT. Samples were pelleted by centrifugation at 15,000 x *g*, 1 min, supernatants discarded, and pellets were washed twice in 10 volumes of PBS, each time pelleting at 15,000 x *g* for 1 min and discarding the supernatant. Washed pellets were resuspended in 300 µl sterile distilled water (sdw), 100 µl 20 % Chelex-100 resin suspended in PBS added, then the sample was heated for 10 min to 100°C, and finally spun at 15,000 x *g* for 1 min. The resulting supernatant was transferred to fresh tubes and stored at 4 °C and –20 °C prior to agarose-TBE gel electrophoresis for determination of DNA concentration and use as a template for PCR.

2.2 TRIzol Extraction of Total RNA from *P. falciparum*

Total RNA was extracted from blood stage parasite cultures using TRIzol Reagent, according to the method of Helen Taylor (personal communication). Cells at a parasitaemia of 5-15 % were harvested by centrifugation on a bench top centrifuge at 1,800 x *g*, 4 min, the supernatant removed and the pellet was resuspended by shaking in

10 pellet volumes of TRIzol, pre-warmed to 37 °C. The sample was left at RT for 5 min, after which 2 pellet volumes of chloroform were added, the sample was shaken for 15 sec, and then left at RT for 3 min. Aqueous and non-aqueous layers were separated by centrifugation at 3,000 x *g*, 30 min, at 4 °C, and 0.6 x pellet volume of aqueous phase was transferred to a 1.5 ml microfuge tube containing 0.5 x pellet volume of isopropanol. (i.e. if the original pellet was 1 ml, then one would expect 0.6 ml of aqueous phase per 1 ml of TRIzol added, thus 0.6 ml of aqueous phase was placed with 0.5 ml of isopropanol in a 1.5 ml tube). Samples were either left on ice for 60 min, or stored at 4 °C for several days before continuing the extraction. Samples were centrifuged at 14,000 x *g*, 30 min at 4 °C in a cooled microfuge, the supernatant aspirated, and tubes inverted and air dried for 5 min. The dried RNA was carefully resuspended in 0.1 x pellet volume of formamide, heated at 60 °C for 10 min, cooled briefly on ice, then transferred to a new tube and stored at –20 °C. Prior to storage the absorbance at 260 nm was determined, adding 1 µl of sample to 1 ml of water, with 1 µl of formamide in 1 ml of water as the blank.

2.3 Agarose Gel Electrophoresis

DNA samples were loaded with 6x loading buffer into 0.5 – 2 % agarose, 1 x TBE or TAE gels and separated by electrophoresis at 10 V cm^{-1} (Sambrook *et al.* 1989). DNA size markers were used as recommended by manufacturers (see Appendix), to estimate band sizes.

RNA samples were separated in agarose - guanidine thiocyanate gels (Goda and Minton 1995). The gel apparatus was cleaned by soaking in 1 % SDS for 2 hours, rinsed in distilled water and air-dried. A 1 % agarose, 1 x TBE gel was made using freshly

prepared reagents, melted in a microwave, cooled to 55 °C and 1 M guanidine thiocyanate added to a final concentration of 5 mM; the solution was poured into the gel mould and left to set for 30 min. RNA samples resuspended in formamide were heated at 60 °C for 10 min, placed on ice and loaded into the wells with 6 x loading buffer. RNA was initially run into the gels at 10 V cm^{-1} for 10 - 15 min, then at 7 V cm^{-1} for 3 - 4 hours, until the bromophenol blue dye front had migrated approximately 10 cm along the gel. RNA size markers were used as necessary (see Appendix).

Nucleic acids were visualised either by addition of ethidium bromide to a final concentration of 0.5 μg ml^{-1} to the gel prior to casting, or by incubation of the gel in a solution of 0.5 μg ml^{-1} ethidium bromide, 1 x TAE / TBE for 30 min following electrophoresis. Ethidium bromide incorporated into nucleic acid molecules was visualised with a long-wavelength ultra violet transilluminator and Polaroid photos taken to give a permanent record.

2.4 Cloning of PCR Amplification Products

PCR products were ligated directly into TA vector pCR®2.1 using either the Original TA Cloning® or TOPO® TA Cloning kits and transformed into INVαF' and TOP10F' *E. coli* respectively as described in Invitrogen's guidelines (see Appendix for *E. coli* genotypes). As AmpliTaq and AmpliTaq Gold polymerases add a single deoxyadenosine (A) overhang to the 3' ends of PCR products, TA vectors are supplied linearised with 3' deoxythymidine (T) overhangs, enabling ligation of the PCR product with the plasmid. Insertion of the PCR product into the multiple cloning site (MCS)

disrupts the LacZα gene, preventing β-galactosidase production and hydrolysis of X-gal, enabling the identification of recombinant colonies by blue/white screening.

Ligations using the Original TA kit were in 10 µl volumes, with 50 ng of pCR®2.1, and 1 : 1, 3 : 1 w/w ratios of PCR product to vector. Reactions were incubated at 16 °C overnight, with 4 U T4 DNA Ligase in 1x ligation buffer, and stored at –20 °C until transformation of INVαF' *E. coli.* Ligations with 10 ng of pCR®2.1-TOPO, and a 1 : 1 w/w ratio of insert to vector, were made to 5 µl with sdw, incubated 5 min at RT, and stored at –20 °C until transformation into TOP10F' *E. coli.*

Transformations of *E. coli* were carried out using the following protocol. To 50 µl of competent cells on ice, 2 µl of 0.5 M β-ME and 2 µl of ligation reaction were added. The cells were incubated on ice, 30 min, heat shocked at 42 °C, 30 sec, and transferred to ice for 2 min. Two hundred and fifty microlitres of SOC medium was added to the cells, and cells grown in a horizontal shaking incubator (225 rpm) at 37 °C for 1 hr. Cells were plated onto LB-agar containing 50 µg ml^{-1} ampicillin, 40 µl of 40 mg ml^{-1} X-Gal (INVαF' cells), plus 40 µl of 40 mg ml^{-1} IPTG (TOP10F' cells). Plates were incubated at 37 °C, overnight, followed by selection of single recombinant (white) colonies using sterile toothpicks. Selected colonies were amplified by growth in 3 ml of LB medium, 50 µg ml^{-1} ampicillin, overnight at 37 °C, with horizontal shaking at 225 rpm. Stabilates were made by mixing 0.5 - 1 ml of overnight culture with 0.1 volume of 10 x Hogness Freezing Buffer, leaving 30 - 60 min at RT, and storing at –70 °C.

When confirmation of the presence of an insert in a plasmid was required prior to colony selection and amplification, a recombinant colony was picked with a toothpick and smeared on the inside of a 500 µl PCR tube prior to inoculation into LB medium.

PCRs were then performed using these tubes either with M-13 and M-21 primers, or with the primers originally used to amplify the insert, and the resultant product analysed by agarose gel electrophoresis.

2.5 Plasmid DNA Purification

Plasmid DNA was extracted and purified from 3 ml overnight cultures by SNAP miniprep (Invitrogen) according to the manufacturer's instructions. Cells were pelleted at 14,000 x *g*, 2 min, in a microfuge, resuspended in 150 µl resuspension buffer, lysed in 150 µl lysis buffer, and 150 µl ice cold precipitation salt solution added, followed by centrifugation at 14,000 x *g*, 5 min. To the supernatant, 600 µl binding buffer was added, and plasmid DNA bound to resin in a SNAP minicolumn by centrifugation at 3000 x *g*, 30 sec. Contaminants were removed with 500 µl wash buffer, followed by 900 µl final wash buffer, each time centrifuging as before. The resin was dried by centrifugation at 14,000 x *g* for 1 min, and plasmid DNA eluted by the addition of 60 µl sdw, incubated at RT for 3 min, followed by centrifugation at 14,000 x *g* for 30 sec, and storage at either 4 °C or –20 °C.

2.6 Restriction Digests

To confirm the presence of an insert in purified TA vector, analytical restriction digests were carried out in 20 µl volumes using 5 U *Eco* R1, 0.5 µg plasmid DNA, and 2 µl of the recommended 10 x buffer (NBL / Boehringer Mannheim), incubated at 37 °C, overnight, followed by resolution by agarose-TBE gel electrophoresis.

Preparative plasmid digests were carried out using 5 U of each restriction enzyme per µg of plasmid in 50 µl reaction volumes.

2.7 δ-Rhodamine Dye Terminator Cycle Sequencing

Inserts in SNAP purified plasmids were sequenced using the ABI PRISM™ δRhodamine terminator cycle sequencing ready reaction kit. Reactions were made up on ice in 200 µl thin walled PCR tubes, and consisted of 8 µl terminator ready reaction mix, 200 – 500 ng plasmid DNA, 4 µl of 0.8 ρm μl^{-1} primer, and the volume made up to 20 µl with sdw. Reactions were thermo-cycled on a PTC-100™ Programmable Thermal Controller as follows, 25 cycles of rapid thermal ramp to 96 °C, 96 °C for 45 sec, rapid thermal ramp to 50 °C*; 50 °C for 30 sec, rapid thermal ramp to 60 °C, 60 °C for 4 min; followed by a rapid thermal ramp to 4 °C, for 24 hrs (*temperature dependent on the Tm of sequencing primer).

Excess dye terminators were removed from extension products by ethanol precipitation using either of the following methods. The 20 µl reactions were added to a mixture of 2 µl of 3 M potassium acetate, 50 µl 96 % ethanol, then incubated on ice for 10 min. Extension products were pelleted at 14,000 x *g* 15 min, the supernatant aspirated, the pellet resuspended in 250 µl 70 % ethanol, then spun at 14,000 x *g* for 10 min, and the supernatant aspirated. Ethanol was evaporated from the pellet by incubation at RT for 15 min, and the resulting dried pellets stored at –20 °C until electrophoresis.

Alternatively the 20 µl sequencing reactions were aliquoted into 0.5 ml microfuge tubes, 74 µl of 70 % ethanol, 0.5 mM $MgCl_2$ added and samples vortexed for 10 seconds. Samples were then incubated at RT for 1 - 2 hrs, the washed DNA pelleted

by centrifugation at 13,000 x *g* for 10 min, and the supernatant discarded. Samples were briefly re-centrifuged and any residual supernatant removed. Samples were then heated at 90 °C for 1 min with the tube lids open, followed by storage at –20 °C.

2.8 Automated Sequencing and Sequence Analysis

Sequencing samples prepared in Section 2.7 were resuspended in 2 µl of a loading buffer consisting of a 5 : 1 ratio of deionised formamide, and 25 mM EDTA / 50 mg ml^{-1} Blue dextran. Samples were denatured at 95°C, 5 min, and cooled on ice until loading. 1.5 µl of denatured samples were loaded per well into 36 well 5 % acrylamide gels, and run on an ABI PRISM 377™ Automated Sequencer using the appropriate run module, matrix and dyeset programmes for δrhodamine dye terminator reactions (as specified in manufacturer's guidelines).

Chromatograms were viewed and if necessary data re-extracted using ABI Sequencing Analysis 2.1.1. ABI Factura 1.2 was used to remove ambiguous sequence from the beginning and end of sequence reads. ABI AutoAssembler 3.1 enabled the alignment of overlapping sequences into a contig, manual correction of mis-called bases, removal of vector sequence, and assembly of a consensus DNA sequence. MacVector 6.5 sequence analysis software (Eastman Kodak) was used for further analysis of consensus sequences, in particular restriction enzyme site identification, primer design and sequence alignment.

2.9 SDS PAGE

Protein samples were heated 100 °C, 5 min, in SDS sample cocktail in the presence or absence of 0.1 M DTT, centrifuged 14,000 x *g*, 5 min to remove any insoluble material, and separated by SDS-PAGE on 8 - 15 % mini-gels by the method of Laemmli (Laemmli 1970). Various pre-stained SDS-PAGE standards were used depending on the expected size of protein being analysed (see Appendix). Following electrophoretic separation, proteins were visualised by incubating gels in Coomassie blue stain for 15 min, followed by overnight destaining in a 7 % acetic acid, 20 % methanol solution.

2.10 Western Blot Analysis

Proteins resolved by SDS-PAGE were blotted onto nylon-reinforced nitro-cellulose membrane (Optitran / Protran) in cooled Western Blot Buffer at 50 V, overnight, or 60 V, 5 hrs. Following blotting, non-specific binding was blocked with 5 % BSA in PBS, 1 hr at RT on a horizontal shaker. Blots were incubated with primary antibody diluted between 1/50 and 1/2000 in PBS, 5 % BSA, for 1 - 2 hrs at RT. Primary antibody binding was detected by either Alkaline Phosphatase (AP) or Horse Radish Peroxidase (HRP)-conjugated secondary antibody detection systems.

For AP detection, non-specifically bound primary antibody was removed by 3 x 5 min washes in PBS, 0.5 % Tween 20, 1 x 5 min wash in PBS, followed by incubation with AP-conjugated secondary antibody (see Appendix) at a 1/1000 dilution in PBS for 1 hr. Unbound second antibody was removed by 3 x 5 min PBS, 0.5 % Tween 20 washes, followed by a 5 min wash in 0.5 M Tris-HCl pH 9.6. AP activity was detected by precipitation of an insoluble, blue colour, on addition of Sigma FAST™ BCIP/NBT

buffered substrate (1 tablet dissolved in 10 ml water). Colour formation was stopped after 10 min by washing in sdw.

For HRP detection, blots were washed 3 x 5 min with PBS, 0.5 % Tween 20, incubated 30 min - 1 hr with HRP-conjugated anti-primary antibody (see Appendix) diluted 1/1000 to 1/2000 in PBS, 0.05 % Tween 20. Blots were washed 3 x 5 min in PBS, 0.5 % Tween 20, followed by 2 x 5 min washes in PBS. Supersignal® West Pico Chemiluminescent Substrates (Pierce) were added to the blot for 60 sec, drained off and the blot exposed to Kodak Biomax MR1 film. When required chloronaphthol colour development was performed after HRP detection. Blots were washed 3 x 5 min in PBS, 5 min in 20 mM Tris-HCl pH 7.4, and then placed in 20 ml of 20 mM Tris–HCl pH 7.4 with 12 µl H_2O_2 mixed with 4 ml of 3 mg ml^{-1} chloronaphthol in methanol. On colour development the reaction was stopped by washing with PBS.

2.11 Dialysis, Desalting and Concentration of Fusion Proteins

Dialysis tubing was prepared by boiling for 10 min in 50 mM EDTA pH 8.0, subsequent cooling to RT, washing with distilled water, boiling 5 min in distilled water, followed by cooling and storage at 4 °C. Prior to use, tubing was extensively washed with sdw then PBS. Fusion proteins were dialysed twice into 5 L PBS at 4 °C for 5 hrs through 12 - 14 kDa molecular mass cut-off dialysis tubing (Medicell International).

Fusion proteins were desalted by gel filtration using a Sephadex G-25M PD-10 column (Amersham Pharmacia Biotech). The column was equilibrated with 25 ml of PBS, 2.5 ml of fusion protein sample was added to the column, the run-through discarded, and protein eluted with 3.5 ml of PBS.

Dialysed fusion proteins were concentrated either by ultrafiltration with an Amicon stirred cell unit through a 10 kDa molecular mass cut-off membrane, or by centrifuge concentrators (Amicon / Whatman) with 10 or 30 kDa molecular mass cut-off membranes, according to manufacturers' instructions.

2.12 Determination of Fusion Protein Concentration

The concentration of GST-fusion proteins was determined by micro-BCA assay (Pierce). This assay uses the reduction of Cu^{2+} by proteins in alkaline environments, to chelate 2 molecules of bicinchoninic acid with the tetradentate-Cu^{1+} complex, forming a purple complex that exhibits absorbance between 540 - 590nm. The complex formation depends on the presence of cysteine, tyrosine and tryptophan. This absorbance is linear with increasing protein concentration.

Both the protein to be measured and the BSA standard (2.0 mg ml^{-1}) were serially diluted in PBS, the reaction performed in microtiter plates as per guidelines, and absorbance read at 540 nm.

2.13 Indirect Immunofluorescence Antibody Assay

Cells from asynchronous and synchronous blood stage cultures (FCB-1, T9/96, and 3D7) were harvested by centrifugation, transferred to microfuge tubes and briefly pulsed on a microfuge. Pellets were resuspended in RPMI AlbuMAX, either to a 50 % haematocrit of which 5 µl was used to make thin blood-smears on polylysine coated slides, or to a 5 % haematocrit and 8 µl spotted onto each well of 15 well multitest slides. Slides were dried in a laminar flow hood, and either fixed (as described below) for

immediate use, or wrapped in foil and stored in the presence of self indicating silica gel granules (BDH) at –20 °C. Alternatively thin blood smears of schizonts isolated by Percoll or Plasmagel treatment were prepared (Muni Grainger, personal communication).

Prior to use slides were defrosted for 5 min at 37 °C, wells were marked out on thin blood smears using a permanent marker pen, and parasites fixed at RT in either acetone or a 50 : 50 mix of acetone/methanol for 30 sec – 2 min, and then air dried at RT.

Primary antibodies were diluted between 1/10 and 1/10,000 in PBS, 1 % BSA. On addition of 8 – 20 µl of diluted primary antibody the slides were incubated at 37 °C, 30 min - 1 hr in a humid chamber. Unbound primary antibody was removed by 3 x 5 min washes in an excess of PBS at RT with shaking, excess liquid was aspirated, and the slide briefly dried with a hairdryer and 8 – 20 µl of second antibody added at a 1/50 - 1/2000 dilution in PBS, containing 1 % BSA. Secondary antibodies were specific to the primary antibody and conjugated to either of the following fluorophores: FITC, Oregon Green, TRITC, or Texas Red. Slides were incubated at 37 °C for 30 min - 1 hr, and washed 3 times in PBS as before to remove unbound antibody.

To visualise nuclear material, DAPI staining was performed for 5 seconds after 2 x 5 min PBS washes, and washed again in PBS as before. When using FITC and Oregon Green fluorophores, red blood cells were visualised by staining slides for 5 sec in 0.01 % Evans Blue. The Evans Blue step was missed when using Texas red or TRITC as it causes background fluorescence at the emission wavelength used for these fluorophores. Slides were washed in PBS, excess liquid aspirated, the slide briefly dried with a hairdryer and a drop of Citifluor (a glycerol / PBS mix that minimises background

fluorescence) added per well. A coverslip was laid over the wells and sealed using standard clear nail varnish. Slides were stored wrapped in foil at 4 °C prior to viewing.

Dual labelling with a tertiary antibody specific to another protein of interest was performed after the PBS washes removing unbound second antibody. This was detected using a fourth anti-tertiary antibody, conjugated to an alternative fluorophore to that of the secondary antibody. The tertiary and quaternary antibodies were diluted, incubated and washed in a similar fashion as the primary and secondary antibodies, and DAPI staining performed as before.

Slides were viewed either on a Zeiss Epifluorescent microscope or a Delta Vision Olympus Epifluorescent microscope. Using the Zeiss microscope, slides were viewed with x 60 and x 100 epifluorescent objectives, Evans blue stained red blood cells and schizonts indicated by the presence of haemozoin were visualised by light microscopy, whilst fluorophores were visualised using the appropriate excitation and emission filters. Photographs were taken with a built in camera, using 1600 ASA Kodak slide film, kindly developed by the NIMR Photographics Department. Alternatively slides were viewed with a Delta Vision Olympus Epifluorescent microscope using a x 60 or x 100 objective with the appropriate filter set for each fluorophore. Images were acquired with a digital camera using the Delta Vision programme to determine image settings, and saved onto a Silicon Graphic computer. Acquired images were manipulated using the SoftWorks programme on the Silicon Graphic computer, saved as tiff files, and further manipulated using Adobe Photoshop versions 5.5 and 6.5.

METHOD SECTION TWO : IDENTIFICATION OF THE GENE CODING FOR MEROZOITE SURFACE PROTEIN-7

2.14 Database Searches with the MSP-7_{22} and MSP-7_{19} N-Terminal Sequences

The International Malaria Genome Sequencing Project is currently sequencing the 14 chromosomes of *P. falciparum*, and releasing the obtained nucleotide sequences to the public domain via the World Wide Web (Wirth 1998). The sequencing projects were supported by awards from the National Institute of Allergy and Infectious Diseases, National Institutes of Health, The Wellcome Trust, the Burroughs Wellcome Fund, and the U.S. Department of Defence.

The N-terminal amino acid sequences for T9/96 MSP-7_{22} (SETDTQSKNEQEPST) and MSP-7_{19} (EVQKPAQGGESTFQK) were used to TBlastN search all public *Plasmodium falciparum* sequence databases (Altschul *et al.* 1997) (See Appendix for all web sites searched). The single gel read sequence PNACJ17TF was retrieved from the partially sequenced Chromosome 14 of *P. falciparum* strain 3D7 on the TIGR web site. This coded for the first 13 N-terminal amino acids of MSP-7_{22}. This sequence was in turn used as the query sequence to BlastN search the malaria sequence databases to extend the nucleotide sequence coding for MSP-7_{22}, and any upstream sequences.

2.15 Identification of Downstream *msp-7* Sequence

As database searches identified PNACJ17TF of 1140 nucleotides, the 3' end of which coded for the first 13 N-terminal amino acids of MSP-7_{22} and no further

downstream sequences were retrieved, vectorette PCR was used to obtain DNA sequence downstream of the MSP-7_{22} N-terminus.

2.15.0 First Vectorette PCR Step

Oligonucleotide primer p22F3 complementary to the 5' strand of the retrieved sequence PNACJ17TF, was used to amplify sequence downstream of the MSP-7_{22} N-terminus, by vectorette PCR, a form of one-sided PCR (Hengen 1995). Five libraries consisting of T9/96 genomic DNA digested with either *Alu* I, *Dra* I, *Rsa* I, *Sau* 3AI, or *Xho* II restriction enzymes, and ligated to Vectorette-II 5' and 3' linkers, were used (supplied by R. Gunaratne (Gunaratne *et al.* 2000)).

PCR reactions were performed in 500 µl microfuge tubes using AmpliTaq Gold, which enables hot-start PCR and prevents non-specific priming. The reaction mixture components were made up on ice and consisted of: 1 µl of appropriate Vectorette library, 2.5U AmpliTaq Gold, 25 ρm p22F3, 25 ρm Vectorette II primer, 3 mM $MgCl_2$, 10 µl of 10 x PCR Buffer II, 10 µl of 2.5 mM dNTPs, and made up to 100 µl with sdw. Reactions were overlaid with 30 µl of mineral oil to prevent evaporation of the reagents during thermo-cycling. Two controls were used, a positive control primer NMTvec4 (25 ρM), was used with the *Sau* 3A1 digested library (expected product 500 bp), a negative control of sdw (no template DNA) was used with p22F3. (See Appendix for primer sequences).

Reactions were thermo-cycled on a Programmable Thermal Controller (PTC-100, Genetic Research Instrumentation) as follows: 94 °C for 12 min; 40 cycles of denaturing at 94 °C for 1 min, annealing at 55 °C for 2 min; extension at 72 °C for 3 min; followed by a final extension step of 72 °C for 10 min, and a 4°C step for 24 hrs.

PCR products were resolved by agarose-TBE gel electrophoresis, stained with ethidium bromide (0.5 μg ml^{-1}) in 1 x TBE, and viewed on a long wave ultraviolet transilluminator.

2.15.1 Cloning into TA Vector and Sequencing of Vectorette Products

PCR products from vectorette PCR were ligated with TA vector pCR®2.1, transformed into INVαF' *E. coli,* and recombinant colonies selected by blue / white screening. Plasmid DNA was extracted using SNAP minipreps and the presence of the correct size insert was determined by restriction enzyme digestion with *Eco* R1.

Inserts were δrhodamine dye terminator cycle sequenced, from both 5' and 3' ends, with primers M13revA and M13-21 (Tm 55 °C) that anneal to regions just outside the MCS of pCR2.1 (2.7), and analysed as described in Section 2.8. Sequences from vectorette library products were assembled into contigs forming consensus sequences, to which primers were designed using MacVector 5.0 / 6.5 to obtain further downstream sequences from the next vectorette PCR step.

2.15.2 Further Vectorette PCR Steps

To walk down the *msp-7* gene, two further vectorette PCR reads were required, using oligonucleotides that were based on nucleotide sequence obtained in the previous vectorette PCR. These oligonucleotides were p22F4, and p22F5, and with the exception of an annealing temperature of 60 °C, conditions were as before.

2.16 Identification of the Entire *msp-7* Gene

Sequences from the vectorette PCR steps (Section 2.15), were assembled with the upstream sequence obtained in Section 2.14, into a contig using AutoAssembler, and a

best-fit consensus sequence obtained for *msp-7* from T9/96 and 3D7 strains. This was analysed using MacVector for the presence of restriction sites, open reading frames, introns, exons, amino acid translations, secondary structure and a putative amino acid sequence. The DNA and amino acid sequences were used to search public databases for homologous DNA sequences and proteins.

The putative amino acid sequence was submitted to a variety of primary and secondary protein structure prediction programmes available on the World Wide Web (see Appendix for www sites).

2.17 Mass Spectrometry Analysis of MSP-7_{22} to Confirm the Primary Sequence

The soluble MSP-1 complex was purified by C. Trucco and M. Grainger, from the culture medium of T9/96 parasites by binding to and elution from a X509 monoclonal antibody affinity column (Blackman and Holder 1992; Pachebat *et al.* 2001). The MSP-1 complex was fractionated by SDS-PAGE (Stafford *et al.* 1994), and the 22 kDa and 19 kDa components were digested with trypsin and analysed by peptide mass fingerprinting using a Bruker Reflex-III matrix-assisted laser desorption/ionisation time-of-flight (MALDI-TOF) mass spectrometer (Bruker Daltonics, Bremen, Germany), essentially as described previously (Pachebat *et al.* 2001; Trucco *et al.* 2001).

2.18 RT PCR Confirmation of the *msp-7* Sequence

To confirm the supposition that there were no introns present in the *msp-7* coding region, and that the proposed start and finish sites of the *msp-7* open reading frame were

correct, RT PCR was performed on total RNA extracted from 3D7 parasites using primers that spanned the *msp-7* coding region.

2.18.0 Reverse Transcription PCR to Produce cDNA

Total RNA from an asynchronous culture of 3D7 parasites was subjected to DNase treatment as follows: a mixture of 10 µl of RNA, 1 x PCR Buffer II, 3 mM $MgCl_2$, 4 µl of 10 mM dNTPs, 4 µl of RNasin, 4 µl of DNase was made up to 40 µl with sdw, incubated at 37 °C for 60 min, and the Dnase then inactivated by heating at 75 °C for 5 min. The RNA was stored on ice until the reverse transcription step.

Eight microlitres of Dnase-treated RNA was used as the reverse transcriptase negative control (rt-), to this was added 1 µl of Random primer stock at 750 ng μl^{-1} and 1 µl sdw. To the remaining 32 µl (designated rt+) was added 4 µl of the random primer stock and 4 µl of Superscript II Reverse Transcriptase. Both rt+ and rt- samples were incubated at 25 °C for 10 min, 42 °C for 30 min, 95 °C for 3 min, 4 °C for 3 hrs, and the cDNA stored at –20 °C until use as a template for PCR.

2.18.1 Testing cDNA for Introns in *msp-7* Sequences

The primer pairs pfp22F / p22R2, p22Fexp / p22Rexp, and p22F6 / pfp22R were used to amplify regions of *msp-7* by PCR from the 3D7 cDNA. The rt+ samples were amplified in duplicate, and compared with the results from negative controls of rt- sample and sdw respectively, and a positive control amplified from chelex-purified 3D7 gDNA. Reactions consisted of 5 µl of the appropriate template, 1 x PCR Buffer II, 0.25 mM dNTPs, 3 mM $MgCl_2$, 1 unit of AmpliTaq Gold, with sdw to make the volume up to 100µl, and a mineral oil overlay. Reactions were cycled as previously described (Section 2.15.0) with the exception of an annealing temperature of 58 °C for 40 cycles, and

products were analysed by agarose-TBE electrophoresis. Products were ligated into TOPO-TA vector, transformed into *E. coli*, and selected recombinants sequenced.

2.19 Amplification and Sequencing of *msp-7* from Parasites with Different MSP-1 Allelic Types

Since initial PCR reactions with FCB-1 gDNA indicated that *msp-7* was present in parasites with Wellcome MSP-1 allelic type, and that products were the same size as those amplified from MAD-20 type gDNA (data not shown), it was decided to sequence *msp-7* from genomic FCB-1 gDNA to compare the level of conservation in both Wellcome and MAD-20 like clones.

Msp-7 was amplified by PCR from FCB-1 gDNA (provided by Helen Taylor) using primer pairs pre22Fexp / pre22Rexp, and p22Fexp / p22Rexp. Reaction conditions were as follows:- 100 ng gDNA, 2.5 U AmpliTaq Gold, 1 x PCR Buffer II, 3 mM $MgCl_2$, 50 ρm forward primer, 50 ρm reverse primer, 10 µl, 0.25 mM dNTPs, the volume made up to 100 µl with sdw, and the reaction overlaid with 30 µl of mineral oil. Reactions were thermocycled as previously described (Section 2.15.0) with the exception of an annealing temperature of 48 °C, and 25 cycles instead of 40. To determine the FCB-1 *msp-7* sequence in regions dictated by primer sequence the primer pairs pfp22F / p22R2, and p22F3 / pfp22R were used with identical PCR conditions except for a 55 °C annealing temperature. Products were ligated into TOPO-TA vector, transformed into *E. coli*, and selected recombinants sequenced.

METHOD SECTION THREE : PRODUCTION OF TOOLS TO INVESTIGATE MSP-7 BIOSYNTHESIS

2.20 Production of GST-Fusion Proteins

To study the cleavage and association of the precursor MSP-7 protein with MSP-1, Glutathione-S-Transferase tagged – MSP-7A and MSP-7B fusion proteins were produced with the aim of raising antibodies against N- (MSP-7A) and C-terminal (MSP-7B) regions of MSP-7 (Figure 2.0).

DNA coding for *msp-7a* and *msp-7b* was amplified by PCR from *P. falciparum* gDNA and ligated in frame into pGEX-3X (Pharmacia Biotech) via incorporated *Bam*H1 and *Eco*R1 sites (Figure 2.1 and Appendix for map of pGEX-3X). The optimal conditions for maximal protein expression were determined, and N-terminal tagged GST-MSP-7A and GST-MSP-7B were purified from bacterial lysates using glutathione agarose columns.

2.20.0 PCR Amplification of *msp-7a* and *msp-7b* and Preparation for Cloning

Using primers pre22Fexp, pre22Rexp, p22Fexp, p22Rexp with *Bam*H1 and *Eco*R1 restriction sites incorporated, *msp-7a* and *msp-7b* were amplified by PCR from 3D7 and T9/96 gDNA respectively (Figure 2.1). Reaction conditions and thermo-cycling were as in Section 2.19, with the exception of an annealing temperature of 56 °C and 60 °C for the primer pairs pre22F / Rexp and p22F / Rexp respectively.

The 463 bp *msp-7a* product was cloned in TA vector, and selected recombinants sequenced to confirm there were no errors introduced by the AmpliTaq polymerase.

Msp-7a was excised from TA plasmid with *Bam* H1 / *Eco* R1 restriction endonucleases (5 U μg^{-1} DNA), and purified using Geneclean II (Invitrogen) according to manufacturer's instructions.

The 528 bp *msp-7b* was purified from PCR reactions using QIAquick PCR Purification Spin Columns (Qiagen), followed by removal of primer ends with *Bam* H1 and *Eco* R1 restriction endonucleases (5 U μg^{-1} of DNA), and the digested *msp-7b* fragment purified using Geneclean II.

2.20.1 Cloning into pGEX-3X and Transformation of *E. coli*

Digested *msp-7a* and *msp-7b* were ligated to *Bam*H1 / *Eco*R1 cut pGEX-3X, and used to transform DH5α™ (Life Technologies) and BL21-Gold (Stratagene) competent *E. coli* respectively according to the supplier's instructions. Colonies were analysed for the presence of the inserts as described in Section 2.4. DNA from positive colonies was amplified, purified and sequenced to ensure the inserts were in frame with the pGEX-3X open reading frame.

2.20.2 Small Scale GST Fusion Protein Induction of Expression

Selected pGEX-3X-*msp-7a* and pGEX-3X-*msp-7b* recombinants were grown overnight at 37 °C in 1 ml LB, 50 $\mu g\ ml^{-1}$ ampicillin. Two hundred µl of overnight culture was added to 0.8 ml LB, 50 $\mu g\ ml^{-1}$ ampicillin, grown at 37 °C for 1 hr, then induced with 0.1 mM IPTG, and grown for 5 hr at 37°C. Cells were pelleted at 14,000 x *g*, 2 min, resuspended in 1 x SDS sample cocktail with DTT, and freeze-thawed twice to lyse cells and fragment DNA. Proteins were resolved on 12.5 % SDS-PAGE gels, and fusion protein visualised by coomassie blue staining, and western blot analysis with either mouse anti-GST polyclonal serum (1/100 dilution), goat anti-GST polyclonal

serum (1/1000), or rabbit anti-MSP-7_{22} polyclonal serum (1/300) and the appropriate AP-conjugated secondary antibody.

Optimal expression of GST fusion proteins was determined by a time course as follows: 2 ml of an overnight culture was diluted 1 : 5 with 8 ml of LB, 50 μg ml^{-1} ampicillin, and incubated at 37 °C for 1 hr. After 1 hr, 1 ml of the suspension was pelleted (T = 0), and expression induced in the remaining culture with 0.1 mM IPTG. Samples were taken every hour for 5 hours (T = 1 to 5), and prepared and analysed as before to determine the time of maximal protein expression.

2.20.3 Large Scale Induction and Purification of GST-Fusion Proteins

GST-MSP-7A and GST-MSP-7B fusion proteins were purified from 500 ml cultures. An overnight culture was diluted 1 : 10 into fresh TB broth, 50 μg ml^{-1} ampicillin, grown at 37 °C until OD_{600} = 0.6 (log phase), followed by induction with 0.1 mM IPTG for 3 hr at 37 °C. Bacteria were pelleted at 4000 x *g*, 10 min, 4 °C, and stored at –70 °C until required.

Solublisation was performed on ice to prevent breakdown of fusion proteins by bacterial or external proteases. Pellets were thawed, resuspended in 40 ml of lysis buffer consisting of 50 mM Tris-HCl, 1 mM EDTA, pH 8.0, 0.2 % NP40 (plus a Complete™ protease inhibitor cocktail tablet), lysozyme added to 1 mg ml^{-1}, incubated on ice 1 hr, followed by addition to a final concentration of 1 mM $MgSO_4$, 10 μg ml^{-1} DNase, then incubated on ice for 1 hr. The crude extract was centrifuged at 10, 000 x *g*, 10 min, 4 °C, followed by clarification of the supernatant at 30,000 x *g* for 1.5 hrs. Clarified supernatant was loaded onto a 5 ml column of pre-swollen glutathione agarose (binding capacity 8 mg of protein ml^{-1} of beads) at 10 ml hr^{-1}. Non-specific bacterial proteins were

removed in 10 column volumes of lysis buffer, followed by 10 column volumes of 50 mM Tris-HCl, 1 mM EDTA pH 8.0. GST fusion proteins were eluted with 5 mM reduced glutathione in 50 mM Tris-HCl, 1 mM EDTA pH 8.0, and 2 - 3 ml fractions of collected on a fraction collector. The peak of GST-fusion protein elution was determined at 280 nm using a UV-1 monitor.

Fractions of the eluted GST fusion protein were analysed by SDS-PAGE and western blotted for analysis with anti-GST antibodies (Sections 2.9 – 10). Fractions containing fusion protein were dialysed against PBS to remove reduced glutathione, followed by concentration, and quantification using the micro BCA test (Sections 2.11 - 12). Concentrated proteins were western blotted and analysed with anti-GST antibodies to determine the quantity of fusion protein breakdown products, and with anti-MSP-7_{22} antibodies to determine the reactivity of the fusion proteins to anti-MSP-7_{22} antibodies.

2.21 Production of 6*Histidine – MSP-7B Fusion Protein

To determine the structure of MSP-7_{22}, large amounts of protein are required, for example to carry out NMR or crystallisation studies. Thus the recombinant fusion protein needs to be easily expressed, purified using native conditions, and have an epitope tag that is small enough not to affect the conformation of the protein. Six-histidine epitope tagged recombinant proteins have these benefits and are easily expressed and purified in native conditions. The C-terminal region of MSP-7, MSP-7B was expressed using the pTRC-HisC bacterial expression system as a N-terminal 6*Histidine-tagged fusion protein (6*His-MSP-7B) (Figure 2.2). The 6*His-MSP-7B fusion protein was to be used as a tool to screen for hybridomas expressing anti-MSP-7B monoclonal antibodies.

Msp-7b was digested out of pGEX-3X-*msp-7b* using *Bam* HI and *Eco* RI restriction endonucleases and purified using Geneclean II, before ligation into *Bam* H1 and *Eco* R1 digested pTRC-HisC (Invitrogen), and transformation into BL21G *E. coli* (Figure 2.3). Recombinant colonies were selected for expression of the N-terminal 6*His–MSP-7B as in Section 2.20.2 with the exception of induction of expression at 1 mM IPTG, and western blot analysis with Anti-Xpress mouse monoclonal antibody (Invitrogen) that binds an eight amino acid epitope present in the N-terminal tag.

Maximal expression of 6*His-MSP-7B was determined by time course as in Section 2.20.2, with the exception of induction with 1 mM IPTG, and solubilisation of the fusion protein in 100 µl of 0.2 % NP40 lysis buffer (lysis buffer as in Section 2.20.3) followed by SDS-PAGE and western blot analysis with the anti-Xpress antibody and rabbit anti-MSP-7_{22} serum.

To purify expressed 6*His-MSP-7B from the host bacterial cells, bacteria from a 100 ml culture were lysed, solubilised fusion protein bound onto a 5 ml ProBond™ resin column (Invitrogen), and purified using native conditions using the Xpress System Protein Purification kit (Invitrogen). An overnight culture was diluted 1/10 into 100 ml of TB, 50 µg ml^{-1} ampicillin, grown at 37 °C until OD_{600} = 0.6, and then expression was induced by addition of 1 mM IPTG, for 2 hr at 37°C. Bacteria were pelleted at 4000 x *g*, 10 min, 4 °C, and 6*His-MSP-7B solubilised in native conditions as per Invitrogen's guidelines. Briefly the bacterial pellet was resuspended in 20 ml of 20 mM phosphate, 500 mM NaCl pH 7.8, lysozyme added to 1 mg ml^{-1}, then incubated on ice 15 min, sonicated for 3 x 10 second bursts at medium intensity, followed by 3 cycles of flash freezing in an ethanol-dry ice slurry and thawing at 37 °C. Ten µg ml^{-1} DNase and 1 mM $MgCl_2$ were added to the mixture and incubated 1 hr on ice. Insoluble debris was

removed by centrifugation at 3000 x *g*, 15 min, 4°C, and the lysate cleared by filtering through a 0.45 μm filter. Solubilised protein was batch bound to the ProBond resin, washed, and eluted with increasing concentrations of imidazole as per guidelines with the exception of a final 750 mM imidazole elution step to remove tightly bound fusion protein. Eluted 6*His-MSP-7B was dialysed against PBS to remove imidazole prior to storage at –20 °C, and SDS-PAGE and western blot analysis of purified protein.

2.22 Polyclonal Sera and Monoclonal Antibody Production

To produce polyclonal sera against the N-terminal and C-terminal regions of the MSP-7 precursor, Balb C mice were immunised with GST-MSP-7A and GST-MSP-7B fusion proteins. To isolate a monoclonal antibody specific to MSP-7B, splenocytes from a mouse immunised with GST-MSP-7B, were fused with myeloma cells, and hybridomas cloned by limiting dilution.* Hybridomas were screened for expression of anti-MSP-7A antibody by IFAT and western blot analysis with 6*His-MSP-7B fusion protein. *(With thanks to Terry Scott-Finnigan who kindly performed this procedure).

2.22.0 Production of Anti GST-MSP-7A and GST-MSP-7B Polyclonal Sera

The recombinant GST-fusion proteins GST-MSP-7A and GST-MSP-7B (prepared in Section 2.20.3) were used to raise polyclonal sera in Balb C mice in accordance to Home Office guidelines (Harlow and Lane 1988). (Immunisations kindly performed by Sola Ogun and Terry Scott-Finnigan). Three 8 week-old female Balb C mice designated Group A, 1-3 and Group B, 1-3 were immunised with GST-MSP-7A or GST-MSP-7B fusion protein respectively. Equal amounts of protein were used to immunise both Groups A and B via the intraperitoneal route. Mice were primed with an initial 20 μg of protein homogenised with Complete Freund's Adjuvant, followed by boosts of 50 μg of protein with Incomplete Freund's Adjuvant (see Table 2.0).

Table 2.0 Timetable for Raising of Mouse Anti-MSP-7A and MSP-7B Polyclonal Sera

Day	Technique	Protein / adjuvant
0,	*Prime*	20 μg in 100 μl PBS 100 μl complete Freund's Adjuvant
21,	*First boost*	50 μg in 100 μl PBS 100 μl incomplete Freund's Adjuvant
37,	1st tail bleed, serum for IFAT	
42,	*Second Boost*	50 μg in 100 μl PBS 100 μl incomplete Freund's Adjuvant
56,	2nd tail bleed, serum for IFAT	
83,	*Third Boost*	50 μg in 100 μl PBS 100 μl incomplete Freund's Adjuvant
90,	3rd tail bleed, serum for IFAT	
92,	**Mouse B1 (GST-MSP-7B)** *Fourth Boost*	50 μg in 100 μl PBS 100 μl incomplete Freund's Adjuvant
98,	**Mouse B1** Blood taken for isolation of serum. Spleen removed for hybridoma production.	

Prior to analysis of antibody titre by IFAT, blood from tail bleeds was clotted for 3 hrs at RT, centrifuged at 14,000 x *g* for 10 min, serum transferred to a fresh microfuge tube and stored at –20 °C. Antibody titre was determined by IFAT with acetone fixed FCB-1, T9/96 or 3D7 parasites (Section 2.13), using sera diluted in PBS, 1 % BSA as follows: 1/50, 1/100, 1/500, 1/1000, 1/2000, 1/4000, 1/8000, 1/16000. Positive IFAT control antibodies were either 8A12 (anti-MSP-1 MAD-20), 2F10 (anti-MSP-1 Wellcome), or rabbit anti-MSP-7_{22} (1/300). Normal mouse serum (pre-immune) diluted 1/50 in PBS, 1 % BSA was used as a negative control.

Mouse B1 showed the highest antibody titre by IFAT after the third boost. A fourth boost was performed on Mouse B1, to increase the proportion of anti-MSP-7B specific B cells in the spleen. Six days later mouse B1 was killed using a Schedule One method, blood collected for isolation of serum and the spleen removed for hybridoma production (2.22.1). Mouse B1 serum was analysed by IFAT and diluted 1/500 in PBS, 1 % BSA for western blot analysis of fusion proteins.

A further 5 female Balb C mice were immunised with GST-MSP-7B as previously described, being primed with 20 µg of GST-MSP-7B, followed by 3 boosts of 50 µg of GST-MSP-7B, before being killed and the sera isolated as before.

2.22.1 Monoclonal Anti-MSP-7B Antibody Production

To produce a monoclonal antibody specific to MSP-7B, splenocytes removed from Mouse B1 were fused with SP2/0 - AG14 myeloma cells (Harlow and Lane 1988). Briefly, myeloma cells were fused with splenocytes at a 1 : 1.4 ratio in 50 % PEG, finally resuspending in 100 ml HAT medium prior to plating 100 µl into 10 x 96 well Microtest plates. These were grown at 37 °C in a CO_2 incubator. Fusion of myelomas with splenocytes and growth with aminopterin that inhibits the *de novo* nucleotide

synthesis pathway, results in death of unfused myeloma cells and selection of fusion cells that are salvage pathway positive, of which hypoxanthine and thymidine are precursors.

Plates were examined by microscopy for the presence and growth of hybridoma colonies. Two weeks after fusion, 50 µl of supernatant was removed from each well and tested by ELISA against plates coated with 1 µg ml^{-1} of 6*His-MSP-7B in sodium carbonate buffer pH 9.6, using an anti-Mouse IgG HRP conjugated second antibody, with OPD colour formation. Supernatants from ELISA positive wells were tested by IFAT. Since initial results suggested that the 6*His-MSP-7B contained co-purified *E. coli* proteins, hybridomas were re-screened by IFAT 3 weeks after fusion. To check IFAT positive hybridomas were producing antibodies specific to MSP-7B, supernatant from IFAT positive wells was used to probe 6His*MSP-7B by western blot analysis, using the HRP method (Figure 2.4).

IFAT and western blot positive hybridoma cells were cloned by limiting dilution in HT medium by diluting the selected hybridoma colony to 10^2, 10^1, 10^0 cells ml^{-1} of HT medium, and plating out 96 x 100 µl into microtiter plates for each of the 10^2, and 10^1 cells ml^{-1} dilutions, and 96 x 100 µl into 3 plates for the 10^0 cells ml^{-1} dilution. Hybridomas were grown at 37 °C in a CO_2 incubator and once colonies had developed, supernatants were tested by IFAT and western blot analysis with 6*His-MSP-7B, and positives selected for cloning by limiting dilution as before (Figure 2.4). Testing of supernatants and cloning by limiting dilution was repeated until all hybridoma colonies were positive and hence clonal.

2.22.2 Determination of JP1 Mouse Monoclonal Antibody Isotype

Since the JP1 anti-MSP-7B mouse monoclonal antibody gave weak fluorescence by IFAT using anti-mouse IgG FITC conjugated secondary antibodies and weak signals by chemo-luminescent western blotting with anti-mouse IgG HRP conjugated secondary antibodies, it was decided to determine the antibody isotype of the JP-1 monoclonal using a mouse monoclonal isotype detection kit (Sigma #ISO-1).

The JP-1 culture supernatant and a control mouse monoclonal of IgG2a isotype were tested in screw top assay tubes as follows. One isotyping strip was incubated with 2 ml of each hybridoma supernatant for 30 min on a horizontal shaker, the supernatant was aspirated and the strip washed in 4 ml of PBS, 0.05 % Tween 20, 1 % BSA wash buffer for 5 min with shaking. The wash buffer was discarded and the strip incubated for 30 min with shaking with biotinylated anti-mouse immunoglobulins diluted 1/50 in wash buffer. This was aspirated, the strip washed as before, then incubated for 15 min in 2 ml of ExtraAvidin-Peroxidase diluted 1/50 in wash buffer. The strip was washed in wash buffer as before, followed by a 5 min wash in 4 ml PBS, before the addition of 4 ml of the substrate solution. This was incubated until a clear red insoluble signal was obtained for the isotype signal and positive control, following which the reaction was stopped by immersion in 0.1M NaOH for 2 min. Strips were rinsed in distilled water then air dried prior to storage.

METHOD SECTION FOUR : INVESTIGATING THE BIOSYNTHESIS OF MEROZOITE SURFACE PROTEIN - 7

2.23 Northern Blot Analysis of *msp-7* Transcription

2.23.0 Initial Northern Blot Analysis of *msp-7* Transcription

Total RNA from ring, trophozoite, and schizont stages of a 3D7 parasite blood culture, separated by electrophoresis on an agarose-TBE-guanidine thiocyanate gel, was Northern blotted onto nitrocellulose by Helen Taylor. This was probed with [α-^{32}P] dATP labelled *msp-7b* specific to MSP-7 and analysed by autoradiography.

2.23.1 [α-^{32}P] dATP Labelling of *msp-7b*

The probe *msp-7b* (528 bp) (amplified and purified in Section 2.20.0) was labelled with 30 µCi of [α-^{32}P] dATP using the Prime-It II® Random Primer Labelling Kit following the manufacturers' instructions (Stratgene). Briefly, 25 ng of *msp-7b* was made up to 24 µl with sdw, 10 µl of random oligonucleotides added, a small hole made in the lid and the reaction heated at 100 °C for 5 min, then cooled to RT. To this was added 10 µl of 5 x *dATP primer buffer, 3 µl of [α-^{32}P] dATP at 10 Ci µl^{-1}, the contents mixed with a pipette tip and 1 µl of Exo(-) Klenow enzyme (5 U µl^{-1}) added. This was incubated at 37 °C for 5 min and the reaction stopped with 2 µl of stop mix.

Radiolabelled probe was separated from unincorporated [α-^{32}P] dATP by gel filtration through a NICK Sephadex G-50 column (Pharmacia Biotech), following the manufacturer's instructions. The NICK Column was equilibrated with 3 ml of equilibration buffer (10 mM Tris-HCl, pH 7.5, 1 mM EDTA), and the reaction mix

added to the column with 400 µl of equilibration buffer. The radiolabelled probe was eluted with an additional 400 µl of equilibration buffer, and then denatured at 100 °C for 2 min before hybridisation to the Northern blotted RNA.

2.23.2 Analysis of RNA by Northern Hybridisation

The Northern blot was incubated at 55 °C with prehybridisation solution consisting of 6 x SSC, 5 x Denhardt's reagent, 0.5 % SDS, 100 µg ml^{-1} denatured salmon sperm DNA, 50 % formamide at 55 °C, with gentle rotation in a Hybaid bottle. The denatured probe was added to the prehybridisation solution and hybridised overnight at 55 °C. Unbound probe was removed with a low stringency wash of 2 x SSC, 0.1 % SDS, at RT for 5 min, followed by a second higher stringency wash of 2 x SSC, 0.1 % SDS, at 55 °C for 15 min. The blot was wrapped in Saran wrap to prevent desiccation which would result in irreversible binding of the probe, exposed to Kodak Biomax MR1 film at -70 °C O/N and developed as before.

2.23.3 Analysis of *msp-7* Transcription at Two Hour Time Points Throughout the *P. falciparum* 3D7 Erythrocytic Cycle

2.23.3.0 Total RNA Collected at Two Hour Time Points

Total RNA from synchronised 3D7 parasites was collected at 2 hour intervals throughout a 48 hour period. This work was done in association with Helen Taylor, Malika Kaviratne, Irene Ling and Muni Grainger.

Mature erythrocytic schizonts of *P. falciparum* strain 3D7 enriched by plasmagel and percoll treatment were incubated with fresh erythrocytes for 30 min then sorbitol treated for 30 min to lyse any remaining schizonts, giving highly synchronised rings in a 30 minute window, at a 10 % parasitaemia. The time of addition of red blood cells to the

schizonts was taken as time zero (T = 0). The highly synchronised rings were aliquoted into 24 x 5 ml culture flasks giving a 20 % haematocrit, and cultured at 37 °C. Every 2 hours over a period of 48 hrs, parasites in one flask were resuspended, two thin blood smears made and Giemsa stained, and the parasites pelleted by centrifugation at 300 x *g*, 5 minutes, giving a 0.7 ml pellet of infected red blood cells for each time point. The supernatant was aspirated and the pellet resuspended in 10 pellet volumes of TRIzol pre-warmed to 37 °C, and 1 ml aliquots of the resuspended pellet dispensed into RNase-free 1.5 ml Eppendorf tubes, labelled with the appropriate time point, and stored at –70 °C until processing.

2.23.3.1 Extraction of RNA from Collected Time Points

Total RNA was extracted from the 1 ml volumes of each time point, where each 1 ml volume contained the equivalent of a 100 µl pellet of infected rbc, following the protocol described in Section 2.2. The RNA extracted from each 1 ml sample was resuspended in 20 µl of formamide, the replicate samples were pooled for each time point, prior to electrophoresis and Northern blotting.

2.23.3.2 Northern Blotting of RNA Time Points

The concentration of RNA isolated from each time point was determined, and equal volumes of RNA from each time point run on an agarose-guanidine thiocyanate gel, this was stained with ethidium bromide, photographed and then Northern blotted (Performed by Shahid Khan). The stage of the parasite at each time point was confirmed by light microscopy and photography of the giemsa stained slides.

2.23.3.3 Northern Blot Analysis with *msp-7b* and *stevor*

The Northern blot was hybridised with a number of stage specific probes including *msp-7b* and *stevor* (Cheng *et al.* 1998). Twenty five ng of purified *msp-7b* amplified from 3D7 gDNA, was labelled with 30 μCi of [α-^{32}P] dATP using the Prime It II Random Primer labelling kit, purified by running through a NICK column, and denatured, essentially as described in Section 2.23.1.

The blot was prehybridised in 0.5 M sodium phosphate buffer pH 7.2, 7 % SDS at 55 °C for 2 hours with gentle rotation in a Hybaid bottle, the denatured probe was added to the prehybridisation buffer and hybridised overnight at 55 °C. Unbound probe was removed with a low stringency wash in 2 x SSC, 0.1 % SDS, at RT for 15 min, followed by a second higher stringency wash in 2 x SSC, 0.1 % SDS, at 65 °C for 15 min. The blot was covered in Saran wrap and exposed to Kodak Biomax MR1 film at -70 °C and developed as before.

Hybridised probes were stripped from the blot by heating the blot to 100°C in 0.1 x SSC, 0.5 % SDS, and leaving to cool at RT with gentle shaking. The stripped blot was stored until required in Saran wrap with 2 x SSC at RT to prevent desiccation.

2.24 Western Blot Analysis of MSP-7 in Schizonts, Merozoites and Shed MSP-1 Complex

Samples of enriched schizonts were either lysed directly into SDS-PAGE sample cocktail (SC) with or without DTT, or treated with 1 % saponin in the presence of protease inhibitors to lyse red blood cells, before resuspending the parasites in SDS-PAGE SC. Merozoites samples either supplied washed as in Section 2.0.1 or as pellets from MSP-1 processing assays by Simon Wilkins and Chairat Uthaipibull (Section 2.32)

were resuspended directly into SDS-PAGE sample cocktail (SC). Shed MSP-1 complex, purified by Carlotta Trucco and Muni Grainger as described in Section 2.17, was diluted in PBS and mixed with SDS-PAGE SC. On addition of SDS-PAGE SC the sample was heated at 100 °C for 5 min and if required subjected to 3 freeze-thaw cycles, each time freezing in a methanol-dry ice bath, thawing at 100 °C 5 min, followed by centrifugation on a microfuge at 13,000 x *g* for 10 min to pellet cellular debris.

Protein preparations from schizonts, merozoites and shed MSP-1 complex were separated by SDS-PAGE and western blotted as described in Sections 2.9 - 10. The western blotted proteins were probed with anti-MSP-7 antibodies and binding detected using HRP conjugated secondary antibodies as described in Section 2.10.

2.25 Immunofluorescence with Anti-MSP-1 and MSP-7 Antibodies in Schizonts and Merozoites

Smears of synchronous and asynchronous 3D7, T9/96 and FCB-1 parasites were tested by IFA with a variety of antibodies against MSP-1, MSP-7 and other malarial proteins, as described in Section 2.13. Antibody binding was mainly detected using FITC and Oregon green fluorophore-conjugated secondary antibodies.

2.26 Dual Immunofluorescence to Visualise the Location of MSP-7 in Relation to MSP-1

Mature enriched schizont smears prepared by Muni Grainger were fixed in acetone / methanol and tested by dual IFA as described in section 2.13. Slides were viewed and images captured using the Delta Vision epifluorescent microscope as

previously described. The resulting green and red wavelength images were merged and co-localisation of proteins indicated by a yellow colour.

2.27 Metabolic-Radiolabelling of Schizont Proteins

Enriched *P. falciparum* schizonts were metabolically radiolabelled with L-[^{35}S] methionine and L-[^{35}S] cysteine PRO-MIX^{TM} *in vitro* cell labelling mix (Amersham Pharmacia Biotech #SJQ 0079), which results in the incorporation of radiolabelled methionine and cysteine into proteins translated during the labelling procedure. All radioactive procedures were performed in compliance with the *NIMR Radioactive Usage Guidelines*.

2.27.0 Metabolic L-[^{35}S] Methionine and L-[^{35}S] Cysteine Labelling of Schizonts

Synchronous *P. falciparum* 3D7 or T9/96 schizonts enriched by Percoll and Plasmagel treatment were washed twice by resuspending in 9 volumes of serum free (SF) RPMI and pelleting at 300 x *g* for 5 min. The quality and development of schizonts were checked, by Giemsa staining as previously described (Section 2.0). Two hundred micro-litres of washed schizonts were aliquoted into 15 ml centrifuge tubes and washed twice in 9 ml of SF methionine- and cysteine free RPMI, each time pelleting at 300 x *g* for 5 min. The schizonts were resuspended to a 2 % haematocrit in 10 ml of labelling medium pre-warmed to 37 °C (9 ml SF Methionine/Cysteine free RPMI, 1 ml 0.22 µm filtered human AB+ serum, 1 % glutamine) in a 10 ml tissue culture flask. Schizonts were metabolically labelled by adding PRO-MIX^{TM} to a final concentration of 100 µCi ml^{-1}, the mixture gently agitated, then gassed with CO_2 and incubated at 37 °C for 2 hours.

The radiolabelled parasites were resuspended into a 15 ml centrifuge tube, the schizonts pelleted by centrifugation at 300 x *g* for 5 min, and the supernatant containing unincorporated radiolabel and any radiolabelled proteins released during labelling stored at –80 °C. Unincorporated radiolabel was removed by washing the pellet twice in 14 ml of SF RPMI, each time resuspending the pellet, centrifuging at 300 x *g* for 5 min. The washed radiolabelled schizonts were resuspended in 5 ml of PBS, aliquoted in 1 ml volumes to screw cap microtubes, pelleted on a microcentrifuge at 13,000 x *g*, 5 min, the supernatant discarded, and the 40 µl pellets of [^{35}S] methionine / cysteine labelled schizonts stored at –70 °C prior to solubilisation in the presence of a variety of detergents (Section 2.28).

2.27.1 L-[^{35}S] Methionine and L-[^{35}S] Cysteine Labelling of Shed MSP-1 Complex

A synchronous population of *P. falciparum* 3D7 or T9/96 schizonts was prepared and incubated with PRO-MIX^{TM} radiolabel as before. After incubation the radiolabelled schizonts were pelleted by centrifugation at 300 x *g* for 5 min, and washed twice in 14 ml of RPMI AlbuMAX. The washed cells were resuspended in 10 ml of RPMI AlbuMAX, 1 % glutamine, transferred to a 10 ml tissue culture flask, gassed with CO_2 and incubated at 37 °C overnight to allow merozoite release. The culture was resuspended into a 15 ml centrifuge tube and pelleted at 300 x *g* for 5 min. Supernatant containing radiolabelled shed MSP-1 complex was aliquoted in 1 ml volumes into 1.5 ml screw cap microfuge tubes, pelleted and stored at –70 °C prior to analysis by immunoprecipitation. The pellet containing the remaining schizonts was stored at –70°C.

2.28 Solubilisation of Radiolabelled Schizont Proteins

[^{35}S] Methionine and Cysteine radiolabelled proteins were released by lysis of schizonts and solubilised with a variety of detergents, in the presence of protease inhibitors. The non-ionic detergent Nonidet P40 (NP40) was used to solubilise proteins in their native conformation, and to maintain protein complexes. To break apart protein-protein complexes, proteins were solubilised in the mildly denaturing, ionic detergent sodium deoxycholate (DOC). The harsh detergent sodium dodecyl sulphate (SDS) was used to denature schizont proteins.

2.28.0 Lysis of Schizonts and Solubilisation in NP40 or DOC Solubilisation Buffers

A pellet of radiolabelled schizonts (20 – 40 µl) was thawed directly from -70°C into 20 to 25 x pellet volumes of either ice cold 0.5 % DOC or 1 % NP40 solubilisation buffers. The pellet was resuspended and vortexed, placed on ice for 30 min with occasional vortexing, and transferred to prechilled Beckman centrifuge tubes for clarification by centrifugation on a TL-100 Ultracentrifuge at 55,000 rpm, 45 min, 4 °C. The supernatant was aliquoted in 100-200 µl volumes into prechilled 1.5 ml screw top microfuge tubes, and either used immediately for immunoprecipitations or snap-frozen in a dry ice-ethanol slurry before storage at –70 °C. This contained the equivalent of 4 – 8 µl of schizonts in each aliquot of solubilised protein tested by immunoprecipitation.

2.28.1 Lysis of Schizonts and Solubilisation in SDS Solubilisation Buffer

A pellet of radiolabelled schizonts was thawed into 2.5 x pellet volume of 1 % SDS solubilisation buffer. The pellet was resuspended as above, boiled at 100 °C, 5 min, then cooled on ice. To this was added 9 x volumes of 0.5 % DOC solubilisation buffer, the sample mixed, left on ice for 10 min, before clarification on the TL-100 Ultracentrifuge as in Section 2.28.0. The supernatant was aliquoted in 100 – 200 µl

volumes into prechilled 1.5 ml screw top microfuge tubes, and either used immediately for immunoprecipitations or snap-frozen in a dry ice-ethanol slurry before storage at –70 °C.

2.29 Immunoprecipitation of Soluble Radiolabelled Proteins

[^{35}S]-Methionine and Cysteine Radiolabelled proteins either solubilised in detergent (Section 2.28) or present as a soluble complex in culture supernatant (2.27.1), were immunoprecipitated by the addition of monoclonal or polyclonal antibodies specific to the protein of interest, resulting in the formation of specific antibody-antigen complexes. The antibody-antigen complex was captured via the Fc receptor of the complexed antibodies by Protein G Sepharose (Prot G), washed to remove non-specific contaminants and analysed by SDS-PAGE and autoradiography.

To each 100 - 200µl aliquot of solubilised radiolabelled proteins was added 5 µg of monoclonal antibody, or 2 - 10µl of polyclonal antisera. The sample was kept overnight on ice at 4 °C, and then added to 100 µl of "dry" Protein G Sepharose. Protein G Sepharose was prepared from an ethanol slurry by 3 washes in an excess of PBS, each time pelleting the sepharose by centrifugation at 200 x *g*, finally resuspending the pellet at a 1 : 1 ratio with PBS and storage at 4 °C. "Dry" Protein G Sepharose was prepared by briefly centrifuging an aliquot of 1 : 1 Prot G / PBS mix in microfuge tubes and removal of the PBS. The Ag–Ab-Protein G mix was rotated at 4 °C for 4 hours to bind any Ab-Ag complex to Protein G, followed by centrifugation at 13,000 x *g*, for 1 min at 4 °C. The supernatant was kept at –80 °C for further analysis, whilst the pellet containing the Ag–Ab-Protein G sepharose complex was washed to remove any unbound antibodies or

proteins. NP40 solubilised samples were washed 2 or 3 times in Immunoprecipitation Wash Buffer I (IPWB I), followed by 4 washes in Immunoprecipitation Wash Buffer II (IPWB II), whilst DOC solubilised samples were washed twice in IPWB II to remove any DOC which would otherwise form an emulsion with the NaCl in IPWB I, followed by 2 washes in IPWB I, and an additional 2 washes in IPWB II. Each wash was performed as follows: the pellets were re-suspended in 500 µl of ice-cold wash buffer either by vortexing or pippetting, spun at 13,000 x *g*, 1 min, at 4 °C, and the supernatant removed.

The washed Ag-Ab-Protein G complex was resuspended in 50 µl of 2 x SC + DTT, boiled at 100 °C for 5 min, spun at 13,000 x *g*, 1 min, and aliquots of the S/N loaded onto 8 - 15 % SDS-PAGE minigels. These were run as previously described, then stained with Coomassie blue for 5 min and destained for 30 min, enabling visualisation of the antibody chains. The gel was incubated in Amplify for 30 min, dried at 70 °C, 1 hr, followed by exposure to BioMax film at –70 °C for various time periods depending on the half-life of the radiolabel and volume of sample loaded on the gel.

2.30 Brefeldin A Inhibition of Radiolabelled Schizont Protein Trafficking

The effect of Brefeldin A (BFA) on MSP-7 processing and complex formation was determined by incubation of early and late schizonts with BFA followed by metabolic radiolabelling. Since BFA blocks protein transport between the Endoplasmic reticulum and Golgi-like apparatus, its use allows determination of any pre-Golgi processing events or complex formations.

One hundred micro-litre aliquots of early schizonts were resuspended to a 2 % haematocrit in 5 ml of labelling medium. BFA prepared as a 1 mg ml^{-1} stock solution in methanol was added to a final concentration of 5 μg ml^{-1} to the schizonts, the cultures were gassed and incubated at 37 °C for 30 min. A control was similarly treated with 25 μl of methanol. The BFA pre-treated and control schizonts were metabolically labelled by the addition of PRO-MIX™ to 200 μCi ml^{-1} and cultured at 37 °C for 1 hr. The culture was pelleted at 300 x *g* for 3 min, the supernatant transferred to –80 °C, and the cell pellet washed twice in SF RPMI as before, resuspended in 2.5 ml of PBS, transferred in 1 ml aliquots to screw cap tubes and pelleted by centrifugation at 13,000 x *g* for 5 min, discarding the supernatant. The pellets were either solubilised immediately or stored until required at -70°C.

Two hundred micro-litre aliquots of late schizonts were resuspended at a 4 % haematocrit in 5 ml of labelling medium, and cultured with 10 μg ml^{-1} BFA for 1 hour, before the addition of PRO-MIX to 200 μCi ml^{-1} and incubation at 37°C for 2 hours. The schizonts were then pelleted, washed and stored as before.

2.31 Pulse Chase of Radiolabelled MSP-7 in T9/96 Schizonts

Processing of the MSP-7 precursor and its formation of a complex with MSP-1 was investigated by pre-treating mature schizonts with BFA which blocks protein transport between the Endoplasmic reticulum and Golgi apparatus and any subsequent complex formation and processing events, then pulsing with PRO-MIX in the presence of BFA, resulting in an excess of metabolically labelled MSP-7 precursor, and initiating the chase by reversing the inhibition on removal of BFA and radiolabel. A second pulse-

chase was performed without BFA to determine the timing of any processing events after the Golgi apparatus.

A culture of highly synchronised 41 – 44 hr old schizonts at a 5.6 % parasitaemia was pelleted at 2000 rpm for 10 min on a Beckmann J6B centrifuge, and washed twice in 50 ml of SF Met / Cys free RPMI pre-warmed to 37°C. The washed pellet of 1.5 ml rbc (at 5.6 % parasitaemia = 84 µl of schizonts) was resuspended in 10 ml of pre-warmed labelling medium with 10 µg ml^{-1} of BFA, and cultured in a small tissue culture flask for 30 min at 37°C. The culture was then pulsed by adding PRO-MIX™ to a final concentration of 200 µCi ml^{-1}, and incubated at 37 °C for 30 min.

The chase was initiated by transferring the culture to a 15 ml centrifuge tube, pelleting at 300 x *g* for 5 min, and resuspending the pellet in 15 ml of pre-warmed RPMI AlbuMAX, 1 % glutamine. At this point 2 x 1 ml samples were taken (Zero Hour Time Point) these were immediately processed as described below. The resuspended culture was transferred into a 15 ml tissue culture flask, gassed and cultured at 37°C. Two x 1 ml aliquots were subsequently removed from the flask at 0.5, 1, 2, 3, 5 and 8 hour time points after the zero hour, and processed immediately. The remaining culture was gassed before being returned to the incubator.

At each time point the 2 x 1 ml samples were placed in pre-chilled screw cap microtubes containing 10 µl of 10 % sodium azide, giving a final concentration of 0.1 % sodium azide. These were immediately pulsed on a cooled microfuge, the supernatant transferred to a fresh prechilled tube and snap frozen in a methanol-dry ice bath, whilst the pellet was resuspended in 1 ml of ice cold PBS, 0.1 % sodium azide, pulsed as before, the wash discarded and the pellet snap-frozen and stored at –70 °C.

Each time point consisted of 2 tubes, each containing the pellet from 1 ml of culture contained the equivalent of 100µl of rbc, which with a parasitaemia of 5.6 % gives 5.6 µl of schizonts per tube. As each time point was to be analysed by immunoprecipitation under ionic and non-ionic conditions, for every time point each 100 µl pellet was solubilised in 550 µl of either 1 % NP40 or 0.5 % DOC solubilisation buffers as described previously (Section 2.28), and the solubilised proteins aliquoted in 100 µl volumes into screw cap tubes and stored at –70°C until required. Aliquots of 100 µl of solubilised protein containing the equivalent of 0.86 µl of schizonts were then analysed by immunoprecipitation with a specific antibody or antisera.

An additional pulse chase was performed without BFA, pulsing 200 µl of synchronised mature nucleated schizonts with 300 µCi ml^{-1} of PRO-MIX for 10 min, followed by initiation of the chase by culture in normal medium with samples taken at 0, 5, 10, 20, 30, 60 and 120 minutes after initiation of the chase. Samples from each time point were solubilised and analysed by immunoprecipitation as before, with the exception of having the equivalent of 2.22 µl of schizonts per 100 µl of solubilised protein per immunoprecipitation.

2.32 Two-Dimensional Tryptic Digest Peptide Mapping

Immunoprecipitated [S^{35}] labelled proteins were separated by SDS-PAGE, visualised by autoradiography and the appropriate bands excised from the gel. Proteins in the excised gel slices were subjected to tryptic digestion and the resulting peptide fragments separated in 2-dimensions by electrophoresis followed by chromatography. The resulting 2-D peptide maps were visualised by autoradiography.

Washed Ag-Ab-Protein G complexes were resuspended in an equal volume of 2 x SC with 0.1 M DTT, boiled at 100 °C for 5 min, spun at 13,000 x *g* for 1 min, then cooled to RT. Samples were alkylated by adding 0.2 volumes of freshly made 1 M white iodoacetamide in 0.2 M Tris-HCl pH 8.2, vortexed at RT and then incubated at 37 °C for 30 min.

The reduced and alkylated samples were loaded in 100 µl volumes into a large 10 % SDS-PAGE gel and separated at 35 mA for 3 hours. After electrophoresis the gel was fixed for a total of 30 min in 2 changes of an excess of destain, dried for 2 hours and exposed to autoradiography film for 2 days at –80 °C. Using the developed autoradiograph as a guide, the appropriate protein bands were excised with fresh scalpels and placed in sterile microtubes. The remaining gel was checked by autoradiography to check that the correct bands had been excised.

Excised bands were rehydrated in 1 ml of 0.2 M NH_4HCO_3 for 30 min at RT with shaking. The supernatant was removed and rehydrated gels incubated as before in 1 ml of a 1 : 1 acetonitrile (ACN) : 0.2 M NH_4HCO_3 mix, the S/N removed and this wash repeated. Gels were rinsed briefly in 50 % ACN in sdw, then washed in 500 µl volumes of neat ACN for 15 min at RT until the gel turned white. The gel slice was completely dried using a speed vac prior to tryptic digestion.

Fresh 1 mg ml^{-1} trypsin was prepared in ice-cold sdw, then diluted to 0.1 mg ml^{-1} in 25 mM NH_4HCO_3. Each gel slice was swollen in 100 µl of 0.1 mg ml^{-1} trypsin solution for 15 min on ice, placed at 37 °C for 30 min, then an additional 100 µl of 25 mM NH_4HCO_3 was added and the sample mixed before digestion overnight at 37 °C on a vortex shaker.

Following tryptic digestion the supernatant was transferred to a fresh microfuge tube on ice, and 150 µl of 60 % ACN in DDW added to the gel to extract any remaining peptides, this was vortexed for 1 hour at RT, and the resulting supernatant pooled with the previously extracted supernatant still on ice. The peptide extraction step was repeated twice with 150 µl, then 40 µl of 60 % ACN, and all the supernatants pooled on ice. The pooled supernatant was spun for 2 min at 13,000 x *g* in a microfuge, the clarified supernatant transferred to a fresh tube and any residual proteins re-extracted from the gel pellet by incubation with 10 µl of 60 % ACN for 30 min with vortexing. All the supernatants were then pooled and clarified again by centrifugation and the resulting supernatant containing tryptic peptides dried down in a Speed vac at medium speed until virtually dry. To this was added 50 µl of 20 % pyridine, and the samples vortexed and dried down for a further 2 hrs in the Speed Vac. The dried samples were freeze-dried O/N to remove any residual NH_4HCO_3, then mixed with 10 µl of 20 % aqueous pyridine prior to spotting onto thin layer chromatography (TLC) plates (Merck plastic-backed cellulose, 0.1 mM thickness #5577).

Each sample was loaded onto a separate TLC plate as follows:- 10 µl of sample was loaded in multiple applications of 0.2 µl, each time drying the applied spot with a hairdryer before adding further applications. Once the sample was dried, 5 µl of marker dyes (0.2 mg ml^{-1} xylene cyanol FF, 0.5 mg ml^{-1} DNP lysine) were added to the same position and dried as before. Samples loaded onto TLC plates were subjected to electrophoresis at 250 V for 1.5 hrs, then 300 V for 30 min using cooled first dimension electrophoresis buffer at pH 4.4 (2 % pyridine, 4 % acetic acid, 15 % acetone, 79 % DDW). The plates were air dried for 30 min and then subjected to separation in the second dimension, ascending chromatography using the ascending chromatography

buffer (7.5 % acetic acid, 25 % pyridine, 37.5 % butanol, 30 % DDW) in a saturated chamber for approximately 1 hr until the solvent was close to the top of the plate. Each TLC plate was air dried for 30 min, then sprayed 3 times with ENHANCE spray drying the plates between applications, and then exposed for several days/weeks to autoradiography film at –80 °C.

2.33 Effect of Anti-MSP-7 Antibodies on MSP-1 Secondary Processing and MSP-7 Processing Events

MSP-1 secondary processing assays were performed on merozoite preparations, with the guidance of Chairat Uthaipibull, following his modification of an assay described previously (Blackman *et al.* 1994; Uthaipibull *et al.* 2001).

2.33.0 The MSP-1 Secondary Processing Assay

Assays always included the following controls; a "positive processing" control sample of merozoites resuspended in reaction buffer only; a "negative processing" control sample of merozoites resuspended in reaction buffer with 1 mM PMSF, and a zero hour control as described above. Aliquots of polyclonal mouse sera against GST-MSP-7A and GST-MSP-7B and the JP-1 anti-MSP-7B monoclonal were tested in the assay as follows.

Washed 3D7 merozoites were resuspended in ice-cold 50 mM Tris-HCl pH 7.5, 10 mM $CaCl_2$, 2 mM $MgCl_2$ plus protease inhibitors 10 μg ml^{-1} leupeptin, 10 μg ml^{-1} Aprotinin, 10 μg ml^{-1} Antipain dihydrochloride, and 74 μg ml^{-1} TLCK. Fifteen micro-litre aliquots of about 1 x 10^9 merozoites were dispensed into 1.5 ml centrifuge tubes on ice, containing 5 μl of protease inhibitors or antibodies as appropriate, giving a total

reaction volume of 20 µl. Merozoites were maintained on ice for 30 minutes to allow antibody binding, then pelleted in a microfuge cooled to 4 °C, at 13,000 x *g* for 5 min. Ten micro-litres of the S/N was transferred to another tube on ice containing 10 µl of 2 x SC. Processing of the zero hour (0 hr) control was stopped at this point by the addition of 10 µl of 2 x SC to the pellet, this was then stored on ice until the experiment was completed. The remaining reactions in the reduced volume of 10 µl were transferred to a 37 °C water bath for one hour to allow processing to proceed. The samples were pulsed, placed on ice and the reaction stopped by the addition of 10 µl of 2 x SC, the merozoites resuspended by pippetting, boiled at 100 °C for 5 min, and cell debris pelleted at 13,000 x *g* for 10 min on a microcentrifuge.

2.33.1 Analysis of the MSP-1 Secondary Processing Assay

Samples from the processing assay were loaded in 16µl aliquots into 12.5 % SDS-PAGE gels, separated by electrophoresis and western blotted. The presence of MSP-1_{33} showing that MSP-1_{42} had undergone secondary processing was detected by probing the western blot with biotinylated X509.

The blot was blocked in PBS, 5 % BSA, 0.5 % Tween 20 for 1 hr, washed for 5 min in PBS, 0.5 % Tween, then incubated with biotinylated X509 diluted 1 in 400 in PBS, 0.1 % BSA for 2 hours at RT. Unbound antibody was removed with 2 x 5 min PBS, 0.5 % Tween washes, and the bound biotinylated X509 detected by incubation with streptavidin HRP conjugate diluted 1 in 2000 in PBS, 0.5 % Tween for 1 hour at RT. The blot was washed 3 x 5 min in PBS, 0.5 % Tween to remove any unbound streptavidin, exposed to ECL reagents and chemo-luminescence detected by autoradiography.

2.33.2 Analysis of MSP-7_{22} to MSP-7_{19} Processing

To determine if processing of MSP-7_{22} to MSP-7_{19} was affected by inhibition of MSP-1 secondary processing, or by the presence of anti-MSP-7 antibodies, the blot probed in Section 2.32.1, was washed in sdw and PBS to remove any ECL reagents, and then probed with rabbit anti-MSP-7_{22} polyclonal sera which was detected by AP BCIP / NBT colour formation as briefly described below.

The washed blot was blocked in PBS, 5 % BSA for 1 hour, probed with rabbit anti-MSP-7_{22} polyclonal sera diluted 1 in 200 in PBS, 5 % BSA for 1 hour, washed 3 x 5 min in PBS, 0.5 % Tween 20, then washed for 5 min in PBS, before incubation with secondary AP conjugated goat anti-rabbit IgG, (adsorbed with human serum proteins, Sigma, A-3812) diluted 1/1000 in PBS, for 1 hr. Unbound secondary antibody was removed with 3 x 5 min PBS, 0.5 % Tween washes, followed by a 5 min wash in 0.5 M Tris-HCl pH 9.6, and colour formation on addition of the BCIP / NBT solution.

Figure 2.0 Expression of Regions of MSP-7 as N-Terminal Glutathione–S-Transferase Tagged Fusion Proteins

The MSP-7 precursor of 351 amino acids is predicted to undergo cleavage between amino acid residues 176 - 177, giving rise to the C-terminal product, MSP-7_{22}, that is detected in the primary processed MSP-1 polypeptide complex on the merozoite surface.

In order to characterize this apparent processing reaction, two regions of MSP-7, designated MSP-7A (residues 23 - 176) and MSP-7B (residues 177 - 351), were expressed as N-terminal Glutathione-S-Transferase (GST) tagged - fusion proteins. These GST fusion proteins were to be immunised into mice to raise antisera against the N-terminal and C-terminal regions of MSP-7.

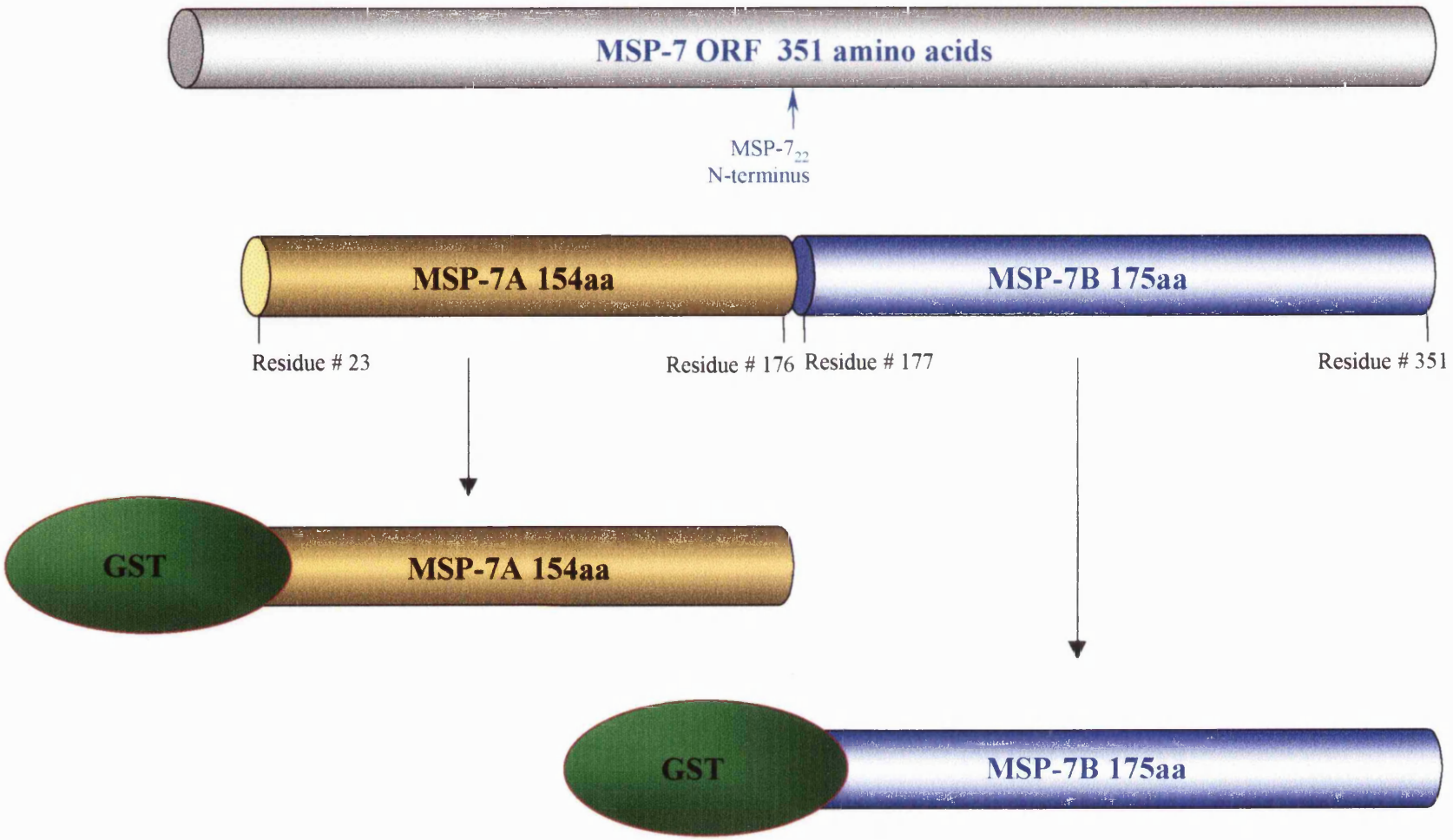
MSP-7 ORF 351 amino acids
MSP-7$_{22}$
N-terminus
MSP-7A 154aa
MSP-7B 175aa
Residue # 23
Residue # 176
Residue # 177
Residue # 351
GST
MSP-7A 154aa
GST
MSP-7B 175aa

Figure 2.1 Amplification of *msp-7a* and *msp-7b* and Insertion into pGEX-3X Bacterial Expression Plasmid

The primers pairs pre22Fexp / pre22Rexp and p22Fexp / p22Rexp were designed to respectively amplify *msp-7a* and *msp-7b* from 3D7 and T9/96 *Pf* gDNA. The forward (Fexp) and reverse (Rexp) primers had *Bam* H1 and *Eco* R1 restriction sites respectively incorporated into them.

The 463 bp *msp-7a* PCR product was ligated into TA plasmid, and recombinant colonies analysed for the presence of *msp-7a* by restriction digestion with *Eco* R1. The *msp-7a* insert in a selected TA clone was sequenced to confirm *msp-7a* had been correctly amplified, and was then *Bam* H1 and *Eco* R1 digested out of the TA multiple cloning site.

The 528 bp *msp-7b* PCR product was purified with a QIAquick PCR purification spin column, and the 5' and 3' primer ends removed from the purified *msp-7b* PCR product by *Bam* H1 and *Eco* R1 digestion.

Both the *Bam* H1 and *Eco* R1 digested *msp-7a* and *msp-7b* fragments were purified using Geneclean II, then ligated to *Bam* H1 and *Eco* R1 digested pGEX-3X plasmid, with the MSP-7A or MSP-7B open reading frames in frame with that of GST.

The pGEX-3X-*msp-7a* and pGEX-3X-*msp-7b* plasmids were transformed into competent DH5α™ and BL-21Gold™ *E. coli* respectively, and recombinant colonies tested by PCR for the presence of the appropriate insert, followed by sequencing with pGEX-3X primers.

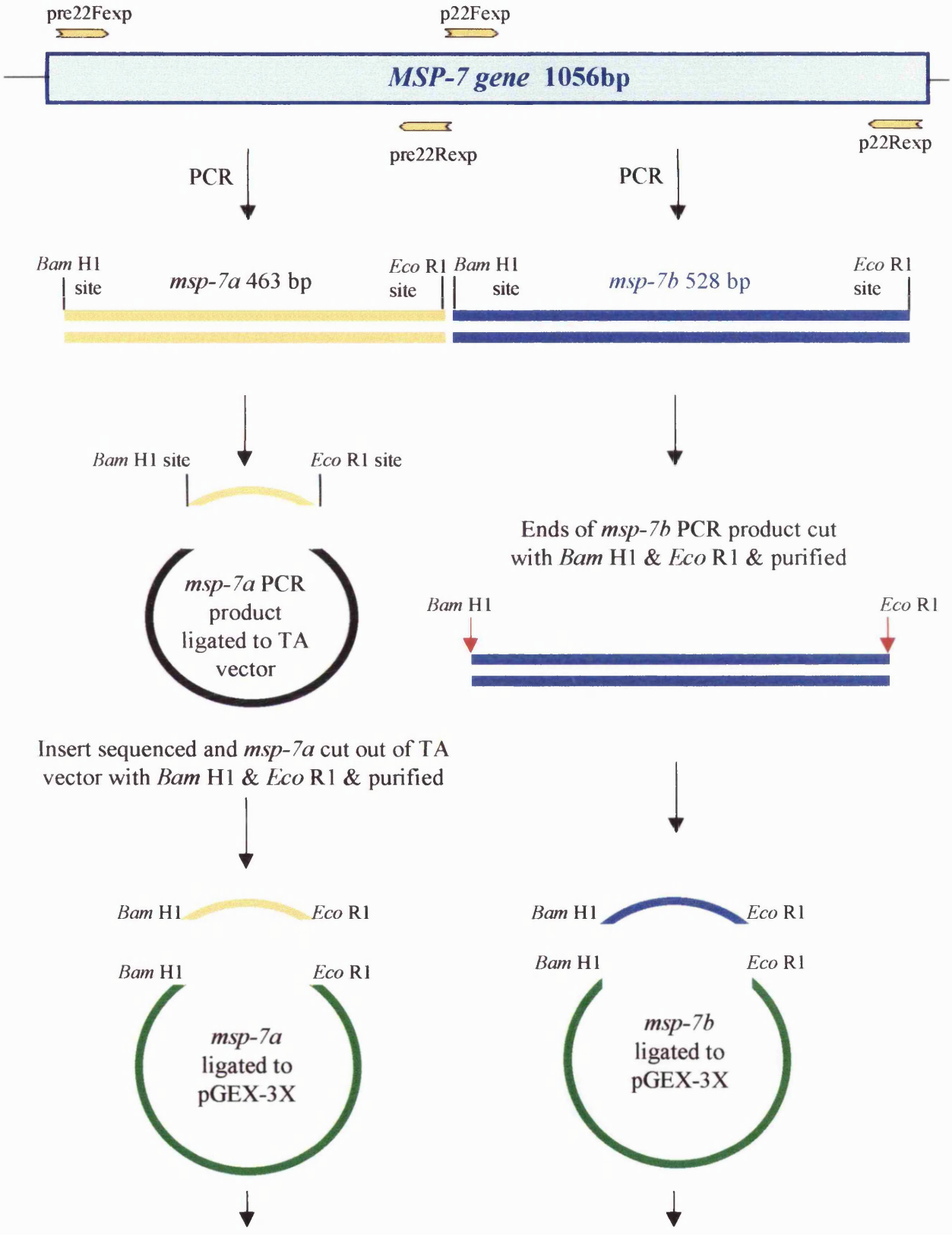
pre22Fexp
p22Fexp
MSP-7 gene 1056bp
pre22Rexp
p22Rexp
PCR
PCR
Bam H1 site
msp-7a 463 bp
Eco R1 site
Bam H1 site
msp-7b 528 bp
Eco R1 site
Bam H1 site
Eco R1 site
msp-7a PCR product ligated to TA vector
Ends of msp-7b PCR product cut with Bam H1 & Eco R1 & purified
Bam H1
Eco R1
Insert sequenced and msp-7a cut out of TA vector with Bam H1 & Eco R1 & purified
Bam H1
Eco R1
Bam H1
Eco R1
msp-7a ligated to pGEX-3X
Bam H1
Eco R1
Bam H1
Eco R1
msp-7b ligated to pGEX-3X
msp-7a-pGEX-3X transformed into DH5α E. coli and insert confirmed by PCR and sequencing
msp-7b-pGEX-3X transformed into BL21-G E. coli and insert confirmed by PCR and sequencing

Figure 2.2 Expression of MSP-7B as an N-terminal 6-Histidine Tagged Fusion Protein

The C-terminal half of MSP-7, designated MSP-7B (residues 177 – 351), was expressed as a 6-Histidine N-terminal tagged fusion protein using the pTRC-HisC bacterial expression system. The 6*His-MSP-7B fusion protein was to be used as a tool to aid in the cloning of an anti-MSP-7B mouse monoclonal antibody and possibly to determine the structure of MSP-7_{22}.

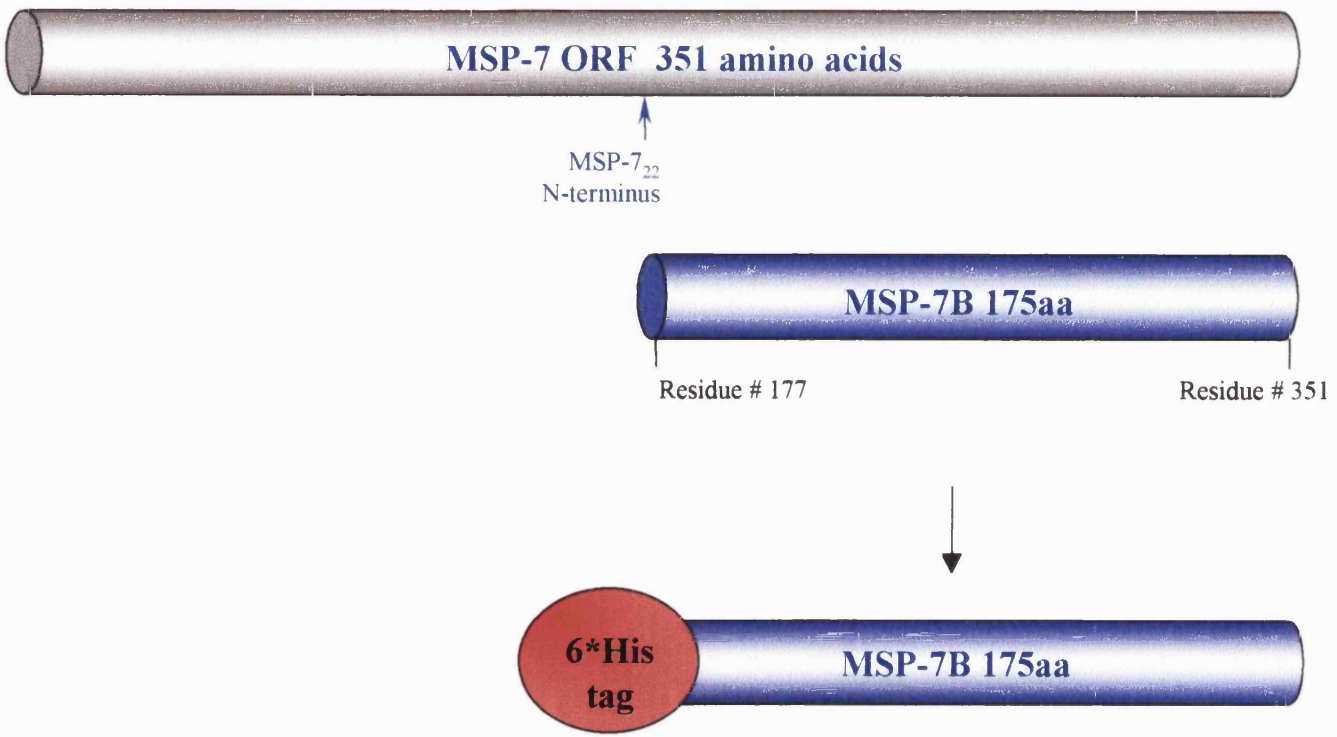
MSP-7 ORF 351 amino acids
MSP-7$_{22}$
N-terminus
MSP-7B 175aa
Residue # 177
Residue # 351
6*His tag
MSP-7B 175aa

Figure 2.3 Insertion of *msp-7b* into the MCS of pTRC-HisC Bacterial Expression Plasmid

The 528 bp *msp-7b* insert was digested out of pGEX-3X-*msp-7b* with *Bam* H1 and *Eco* R1 restriction enzymes and purified using Geneclean II. The digested and purified *msp-7b* fragment was ligated directly with pTRC-HisC that had been similarly digested with *Bam* H1 and *Eco* R1, with the MSP-7B ORF in-frame with that of the N-terminal histidine expression tag.

The resulting pTRC-HisC-*msp-7b* plasmid was transformed into competent BL-21Gold™ *E. coli*, and the presence of the *msp-7b* insert in recombinant colonies confirmed by restriction digestion analysis with *Bam* H1 and *Eco* R1.

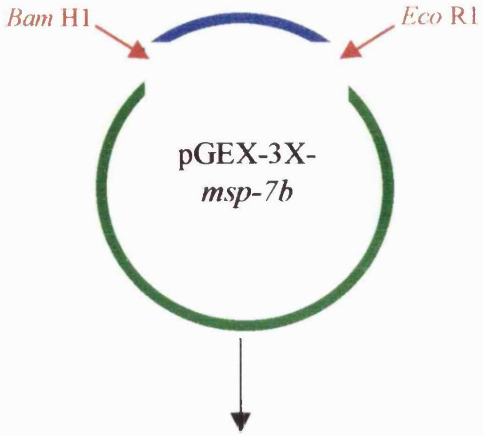

msp-7 cut out of pGEX-3X-*msp-7b* with *Bam* H1 & *Eco* R1

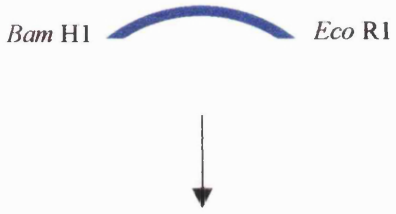

Cut *msp-7b* fragment purified with Geneclean

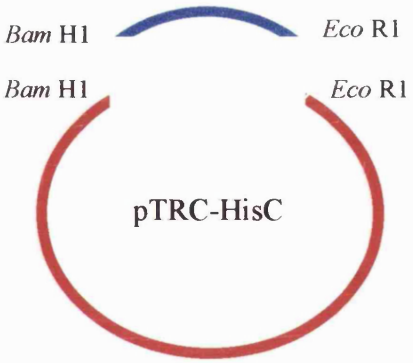

Purified *msp-7b* fragment ligated to *Bam* H1 & *Eco* R1 digested pTRC-HisC

pTRC-HisC-*msp-7b* transformed into competent BL21-Gold *E. coli.*

Presence of *msp-7b* insert in pTRC-HisC-*msp-7b* clones confirmed by restriction digestion with *Bam*H1 & *Eco*R1

Figure 2.4 Production of JP-1 Anti-MSP-7B Monoclonal Antibody

The supernatants from each well of the primary hybridoma culture were tested by IFAT against blood stage parasites using multi-well slides. Antibody binding was detected with a secondary anti-mouse IgG FITC-conjugated antibody. The presence of antibodies to MSP-7B in IFAT positive supernatants was confirmed by probing western blotted 6*His-MSP-7B with the culture supernatant, and antibody binding detected using a secondary anti-mouse IgG peroxidase conjugated antibody and HRP chemo-luminescence.

Colonies from one well that was IFAT and western blot positive, were cloned by limiting dilution, and allowed to undergo growth before testing of supernatants by IFAT as before. Colonies from one well that showed reactivity with parasites by IFAT and with 6*His-MSP-7B, were cloned by limiting dilution as before.

This procedure was repeated until a hybridoma colony had been cloned over three limiting dilution steps, and the resulting hybridoma supernatants 100 % positive by IFAT and western blot analysis of 6*His-MSP-7B.

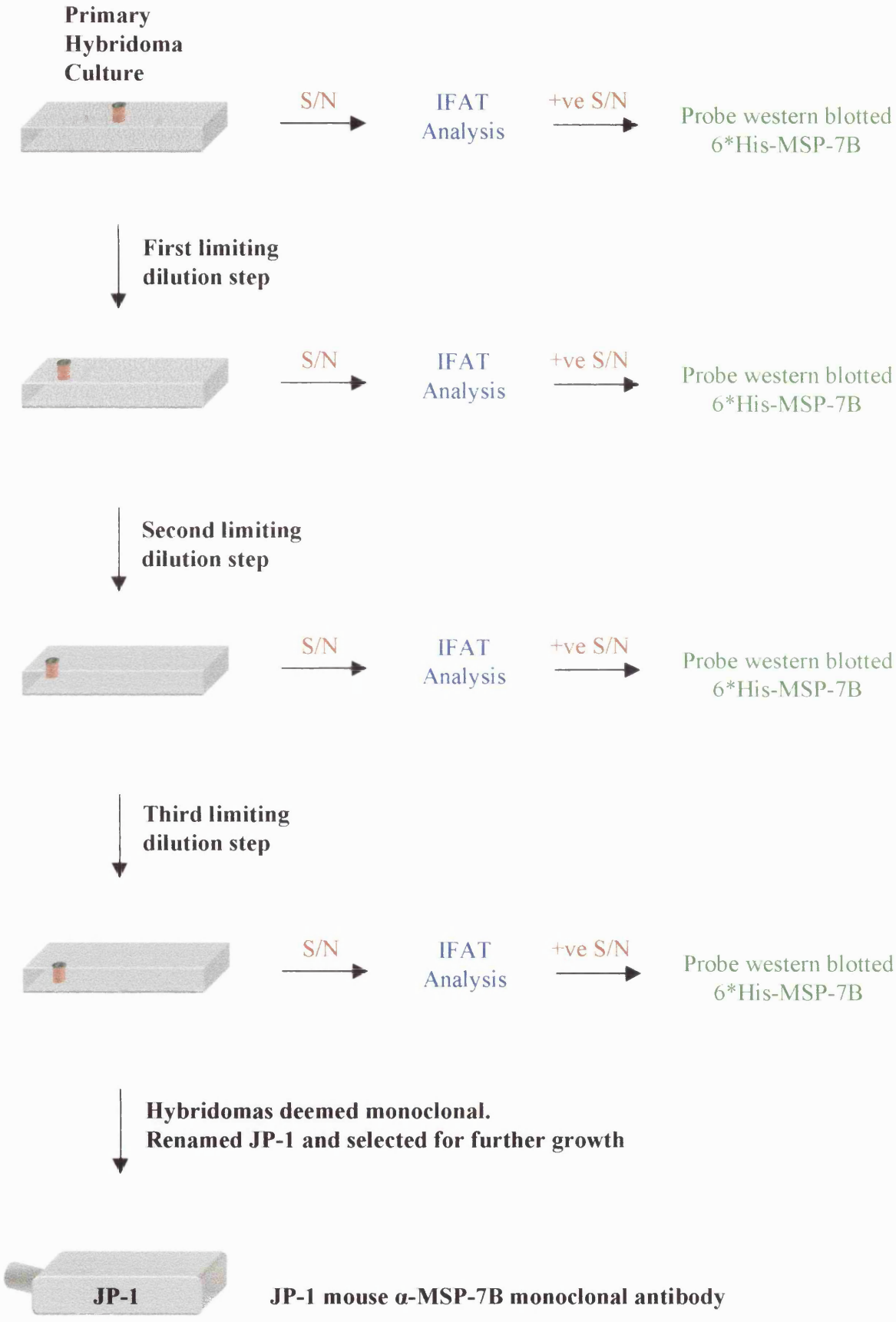
Primary
Hybridoma
Culture
S/N
IFAT
Analysis
+ve S/N
Probe western blotted
6*His-MSP-7B
First limiting
dilution step
S/N
IFAT
Analysis
+ve S/N
Probe western blotted
6*His-MSP-7B
Second limiting
dilution step
S/N
IFAT
Analysis
+ve S/N
Probe western blotted
6*His-MSP-7B
Third limiting
dilution step
S/N
IFAT
Analysis
+ve S/N
Probe western blotted
6*His-MSP-7B
Hybridomas deemed monoclonal.
Renamed JP-1 and selected for further growth
JP-1
JP-1 mouse α-MSP-7B monoclonal antibody

CHAPTHER THREE : THE MEROZOITE SURFACE PROTEIN - 7 GENE AND PROTEIN

SECTION ONE : IDENTIFICATION OF THE MSP-7 GENE

3.0 Database Searches with the MSP-7_{22} and MSP-7_{19} N-Terminal Amino Acid Sequences

The partially sequenced *Plasmodium falciparum* 3D7 genome databases were TBLASTN searched with the MSP-7_{22} and MSP-7_{19} T9/96 N-terminal amino acid sequences (as described in Section 2.14). On searching with the MSP-7_{22} N-terminal sequence, PNACJ17TF, a 627 nucleotide sequence, was retrieved from the unfinished Chromosome 14 TIGR database (Figure 3.0). Nucleotides 42 to 1 of PNACJ17TF, when translated in the –1 frame, coded for 13 out of 14 of the MSP-7_{22} N-terminal amino acids, with 585 nucleotides upstream of the MSP-7_{22} start site. Nucleotides 569 to 1 coded for an open reading frame in the same frame as the MSP-7_{22} N-terminal sequence, suggesting that MSP-7_{22} is part of a larger precursor protein.

PNACJ17TF showed no significant homology with the MSP-6_{36} or MSP-7_{19} N-terminal sequences. No sequences homologous to the MSP-7_{19} N-terminal sequence were recovered from the *P. falciparum* genome databases. The PNACJ17TF nucleotide sequence was used to BLASTN search the *P. falciparum* sequence databases for additional sequences to extend the downstream nucleotide sequence coding for MSP-7_{22}. No sequences downstream of PNACJ17TF were retrieved although two reads were retrieved that coded for additional upstream sequence (see Section 3.2 for details).

3.1 Identification of Downstream *msp-7* Sequence by Vectorette II PCR

In order to obtain the entire nucleotide sequence coding for MSP-7_{22} and MSP-7_{19}, Vectorette II PCR was used to walk down the *msp-7* gene. Vectorette PCR is a one-sided PCR technique in which only one primer specific to the gene of interest is required to amplify an unknown sequence (see Figure 3.1 for a description of Vectorette PCR) (Allen *et al.* 1994).

Two Vectorette PCR amplification steps were required to walk down the *msp-7* gene until reaching a stop codon.

3.1.0 First Vectorette PCR Step

Primer p22F3 was designed to complement sequence ~104 bp upstream of the MSP-7_{22} N-terminus. Vectorette II PCR using p22F3 resulted in amplification products from 3 Vectorette libraries, of 470 bp (*Alu* I), 372 bp (*Dra* I), 195 bp (*Rsa* I) (See Figure 3.2A). The positive PCR control of NMTvec4 with the *Sau* 3A1 library gave the expected 500bp product, whilst the negative PCR control of p22F3 with sdw was negative.

Each of the p22F3 Vectorette products were ligated into TA vector and selected clones sequenced in both 5' and 3' directions using M13revA and M13-21 primers that are complementary to sites in the TA vector MCS. The sequences were edited and assembled into a contig from which a 470 bp consensus sequence was made. The consensus sequence overlapped the PNACJ17TF sequence by 175 bp, giving 295 bp of previously unknown downstream *msp-7* sequence (Figure 3.2B).

Translating the consensus sequence in all 6 frames identified an open reading frame that contained the MSP-7_{22} N-terminal amino acid sequence followed by the MSP-7_{19} N-terminal amino acid sequence, confirming that the DNA amplified coded for the

MSP-7 polypeptides. It also confirmed the hypothesis that MSP-7_{22} and MSP-7_{19} are related and that MSP-7_{19} is the product of N-terminal cleavage of MSP-7_{22}.

3.1.1 Second Vectorette PCR Step

A second Vectorette PCR step was performed to obtain more downstream sequence coding for MSP-7, and to confirm the sequence from the first Vectorette step. Primers p22F4 and p22F5 were designed downstream of the *Rsa* I and *Dra* I restriction sites, respectively, on the first Vectorette consensus sequence.

Amplification products obtained with the p22F4 primer were 263 bp (*Alu* I), 164 bp (*Dra* I) and 481 bp (*Rsa* I); and with the p22F5 primer a 272 bp (*Rsa* I) product was obtained (Figure 3.3A). These were ligated into TA vector and selected clones sequenced. The positive control of p22F3 with the *Dra* I Vectorette library gave the expected 372 bp product, whilst the negative controls of p22F4 and p22F5 with sdw only were consistently negative.

The second Vectorette PCR step sequences were aligned with the first Vectorette PCR step consensus sequence, forming a 688 bp contig, that showed an overlap of 263 bp and extended the known downstream sequence by 218 bp (Figure 3.3B). Translation of the contig identified an open reading frame that ended at a TAA stop codon at nucleotides 661 - 663, suggesting that the C-terminal end of the gene coding for MSP-7 had been identified.

3.2 Identification of the Entire *msp*-7 Gene and Further Database Searches

The 688bp contig made from both Vectorette PCR steps was aligned with the 3D7 PNACJ17TF sequence and formed a contig of 1140 bp. When the contig was translated into all 6 frames, an uninterrupted open reading frame, coding for a putative

351 amino acid protein was identified (Figure 3.4). The MSP-7_{22} and MSP-7_{19} N-termini sequences start at residues 177 and 195 respectively, suggesting that MSP-7_{22} and MSP-7_{19} are part of a larger previously unknown precursor protein called Merozoite Surface Protein 7 (MSP-7). The MSP-7 precursor is coded by a gene of 1056 nucleotides, called *msp-7* (see Section 3.4).

There were no nucleotide differences in the overlap between the T9/96 Vectorette and retrieved 3D7 sequences, suggesting that the *msp-7* sequence is identical in these related lines of the cultured *P. falciparum* parasite.

To extend the known sequence upstream and downstream of the putative *msp-7* start and stop sites, regions of the 1140bp *msp-7* contig were used to BLASTN search the 3D7 *P. falciparum* sequence databases. Two entries PNAAG29TR (701 bp) and PNAJO60TF (358 bp) were retrieved from the Chromosome 14 database, and used to assemble a 1935 bp contig, with 570 nucleotides upstream of the putative *msp-7* start site, and 309 nucleotides downstream of the putative *msp-7* stop site.

No introns were detected in the *msp-7* sequence nor exons in the non-coding regions in the 1935 bp contig, suggesting that *msp-7* has a single exon structure. Northern blotting was used to confirm the expected size of the transcript and RT-PCR used to certify the absence of introns in sequence upstream and downstream of the *msp-7* gene (see Section 3.3).

During the course of this project the *P. falciparum* genome sequencing databases were regularly searched with the *msp-7* consensus and MSP-7 amino acid sequences using BLASTN and TBLASTN. Homologous sequences were obtained from several chromosome specific sequencing projects, these confirmed the T9/96 / 3D7 *msp-7* sequence and extended the known sequence 5' and 3' of *msp-7*. Contamination of chromosome specific libraries with sequences deriving from a number of other

chromosomes is common. This is because chromosome specific libraries are prepared from chromosomes separated by Pulsed Field Gel electrophoresis, and hence often contaminated due to the presence of co-migrating chromosomes. As chromosome specific shotgun sequences have undergone assembly, many reads initially suspected to be from Chromosome 14 have since been assigned to several other chromosomes. The *msp-7* gene is currently placed on contigs assigned to Chromosome 10, although this location may change as the *P. falciparum* genome sequencing project nears completion.

3.3 Confirmation of Single Exon Structure for *msp-7*

Analysis of known DNA sequence upstream and downstream of the *msp-7* gene confirmed the putative start sites or introns. To check the assumption that *msp-7* has a single exon structure, the expected size of the transcript was confirmed by Northern blotting, and the position of the start and the stop sites of translation confirmed by sequencing of RT-PCR products.

3.3.0 Northern Blotting Analysis of Ring, Trophozoite and Schizont Stages

To determine the transcript length of *msp-7*, a Northern blot of 3D7 ring, trophozoite and schizont stage specific total RNA was probed with a [α-^{32}P] dATP labelled 3D7 *msp-7b* probe. If the *msp-7* open reading frame was 1056 bp long then the expected transcript length would be approximately 2000 - 3000 nucleotides, taking into account untranslated regions either side of the coding sequence.

The *msp-7b* probe hybridised to a band of RNA of approximately 2,500 nucleotides, from all 3 stages of the asexual blood cycle, with the highest intensity of binding occurring with the schizont stage RNA (Figure 3.5). This confirms the expected size of the mRNA precursor, suggesting that the 1056 bp sequence codes for the entire

msp-7 gene and is not part of a far larger transcribed gene. The parasites from which the RNA was collected were synchronised, although results using other gene specific probes suggest schizont RNA may be present in all stages (results not shown) explaining why the *msp-7* transcript was also identified in RNA isolated from ring and trophozoite stages.

3.3.1 RT-PCR Results Confirm Start/Stop Sites and No Introns in 3D7 *msp-7*

The primer pairs pfp22F, p22R2 and p22F6, pfp22R were used to amplify regions covering the putative start and stop sites of *msp-7*, from duplicate reverse transcriptase positive (rt+) 3D7 cDNA samples and 3D7 gDNA (positive PCR control).

Amplification products of 686 bp (pfp22F, p22R2) and 230 bp (p22F6, pfp22R) were analysed by agarose gel electrophoresis, giving identically-sized amplification products for both rt+ and gDNA samples, suggesting there were no large introns in the amplified regions (Figure 3.6). Reverse transcriptase negative (rt-) and H_2O only (negative PCR control) samples, with the same primer pairs were consistently negative.

The pfp22F, p22R2 and p22F6, pfp22R amplification products were ligated into TOPO-TA vector, and selected clones sequenced with M13revA and M13-21 primers. The sequences were assembled, edited, and the rt+ and gDNA sequences aligned with each other and the 3D7 / T9/96 *msp-7* sequence. There were no nucleotide differences between regions of *msp-7* amplified from cDNA and gDNA, confirming the putative *msp-7* start and stop sites are correct, and that *msp-7* has a single exon structure.

SECTION TWO : THE MSP-7 GENE AND PROTEIN

3.4 The Full Length *msp-7* Gene and MSP-7 Protein

The full length T9/96 / 3D7 *P. falciparum* gene for merozoite surface protein 7 *(msp-7)* was determined to be 1056 nucleotides long and has a single exon structure (Figure 3.7). The *msp-7* sequence starts at an ATG, has no introns, and is translated into an open reading frame of 351 amino acids that ends in a TAA stop codon (Figure 3.8). The 351 amino acid precursor has been named Merozoite Surface Protein 7 (MSP-7) and has a calculated mass of 41.3 kDa and a pI of 4.74.

MALDI-TOF mass spectrometry of tryptic digested MSP-7_{22} and MSP-7_{19} fragments identified 83% of the expected MSP-7_{22} peptide products and all of the MSP-7_{19} sequence in peptide products (Pachebat *et al.* 2001). This confirmed the *msp-7* sequence was correct and that no post-translational modifications, such as glycosylation of the Asn – Lys - Ser sequence (residues 276 - 278), were present in the MSP-7_{22} polypeptide (Pachebat *et al.* 2001).

The MSP-7_{22} and MSP-7_{19} N-terminal amino acid sequences are located at the C-terminal half of the MSP-7 precursor, suggesting that MSP-7 is cleaved between residues 176 (Gln) and 177 (Ser) into a N-terminal (17.8 kDa) polypeptide and a C-terminal 20.7 kDa (MSP-7_{22}) polypeptide of 175 amino acids (Figure 3.9). The MSP-7_{22} polypeptide is located in the MSP-1 complex on the merozoite surface and undergoes further cleavage of 18 amino acids from the N-terminus between residues 194 (Gln) and 195 (Glu), resulting in a 18.7 kDa (MSP-7_{19}) polypeptide of 157 amino acids, which is detectable in the MSP-1 shed complex (Stafford 1996).

The *msp-7* nucleotide and amino acid sequences were used to search the EMBL, TrEMBL and SWIS-PROT databases using the appropriate BLASTN, BLASTP and TBLASTN search engines, but no significant matches with non-*Plasmodium* proteins were identified.

3.5 *msp-7* Nucleotide Homology Between Different Isolates of *P. falciparum*

MSP-1 is found in two major sequence allelic types in *P. falciparum*: MAD20-type (e.g. 3D7, T9/96 lines) and Wellcome-type (e.g. FCB-1and K1 line) (Tanabe *et al.* 1987). The *msp-6* gene, that codes for the precursor of the MSP-6_{36} polypeptide found in the shed MSP-1 complex, shows no sequence variation in any of these parasite lines, suggesting that MSP-6_{36} is binding to a region of MSP-1 that is conserved in both MSP-1 allelic forms (Trucco *et al.* 2001). There are no nucleotide differences in *msp-7* from the T9/96 and 3D7 lines, suggesting that *msp-7* is highly conserved. Since MSP-7_{22} and MSP-7_{19} are bound to the shed MSP-1 complex of both MSP-1 forms, FCB-1 *msp-7* was amplified and sequenced to determine if MSP-7 was highly conserved or identical in parasites of both MAD20 and Wellcome MSP-1 type lines.

Msp-7 was amplified from FCB-1 gDNA with four primer pairs (Section 2.19) resulting in four overlapping PCR products of: 686 bp (pfp22F, p22R2); 463 bp (pre22Fexp, pre22Rexp); 779 bp (p22F3, pfp22R); and 528 bp (p22Fexp, p22Rexp). These were cloned into TOPO-TA vector, the inserts sequenced, assembled into contigs and compared with the T9/96 / 3D7 *msp-7* sequence (Figure 3.10). There are only 4 nucleotide differences between the T9/96 / 3D7 and the FCB-1 *msp-7* sequences, at positions 580 (C → A); 623 (A → G); 694 (A → G); 722 (G → A). As separate PCR reactions were performed using primers that amplified overlapping regions of this region, the changes in the nucleotide sequence cannot be attributed to errors introduced

by the lack of proof reading ability of the AmpliTaq Gold polymerase. These nucleotide differences code for 4 amino acid changes in the MSP-7_{22} polypeptide at residues: 194 (Glutamine → Lysine), 208 (Glutamine → Arginine), 232 (Lysine → Glutamic acid) and 241 (Glycine → Aspartic acid) (Figure 3.11).

Therefore *Pfmsp-7* is highly conserved. All of the amino acid differences are in the MSP-7_{22} region of the protein. These differences may be involved with the specificity of cleavage during the MSP-7_{22} to MSP-7_{19} processing step, or in changes to the MSP-1 / MSP-7 binding site possibly affected by allelic variation in the MSP-1 amino acid sequence. Further analysis of the *msp-1* and *msp-7* sequences in different *P. falciparum* strains and field isolates is required to investigate this hypothesis.

There is a possibility that *msp-7* is part of a multigene family in *P. falciparum*, since some unique genes have been identified from the malarial databases that share sequence similarity at the protein level with the C-terminal beta sheet of MSP-7 (see Section 3.7) (Pachebat *et al.* 2001).

3.6 Secondary Protein Structure and Pattern Database Predictions of MSP-7

The MSP-7 amino acid sequence was entered into a variety of secondary structure prediction programs and used to search pattern databases to identify conserved motifs present in MSP-7.

3.6.0 Signal and Trans-Membrane Domain Prediction

To determine whether the MSP-7 precursor was targeted to the merozoite surface by a signal sequence and if MSP-7 had any transmembrane domains, the 351 residue sequence was submitted to signal sequence and trans-membrane prediction programs.

Psort II and SignalP, using networks trained on eukaryotic data, gave differing results. Psort II, using a combination of PSG and von Heijne's method, did not predict a N-terminal signal peptide, instead using the *k*-nearest neighbour (*k*-NN) algorithm to predict the following probabilities of location for MSP-7; 34.8 % nuclear, 21.7 % extracellular / cell surface, 17.4 % mitochondrial, 13.0 % cytoplasmic, 8.7 % vacuolar, 4.3 % vesicles of secretory system. However, Signal P predicted a putative signal sequence of 27 amino acids, with the most likely cleavage site between residues 27 (Ser) and 28 (Thr) (Figure 3.8). Until a signal prediction program trained on protozoan or *Plasmodium* signal sequences is available, and since MSP-7_{22} has been located on the merozoite surface suggesting it is targeted to the plasma membrane (McBride and Heidrich 1987; Stafford *et al.* 1996), the Signal P prediction can be assumed to be correct. Similarity of the predicted MSP-7 signal sequence with other malarial surface proteins associated with the MSP-1 complex, such as MSP-6 remains to be elucidated.

TMpred and DAS transmembrane prediction servers denominate a possible transmembrane helix between residues 2 to 21. Assuming MSP-7 has a signal sequence of 27 residues and not a transmembrane domain at the N-terminus, the resulting 324 amino acid protein would have a predicted molecular mass of 38.5 kDa and an estimated pI of 4.52.

3.6.1 Secondary Protein Structure

A combination of the Chou-Fasman and Robson-Garnier secondary structure prediction programs available on MacVector 6.5, and the Profile fed neural network systems from HeiDelberg (PHD) sub programs PHDsec and PHDacc were used to

predict the secondary structure and solvent accessibility for *Pf*MSP-7. As no homologues were identified in SWIS-PROT the expected accuracy of the PHD prediction programs was only between 62 – 66 %. The secondary structure of MSP-7 is predominantly alpha helical with two small regions of beta sheet and several beta turns indicating the protein is highly flexible (See Figure 3.12).

SMART sub-program SEG predicted that residues: 7 - 20, 37 - 52, 62 - 75, 92 - 113, 328 - 339 are of low compositional complexity whilst Prospero predicted the presence of two internal repeats between residues 117 - 252, and 125 - 262.

MSP-7 is mainly hydrophilic, with a negative charge cluster at residues 94 – 148, which may form the core backbone of the structure. Psort II predicted a coiled-coil region from residues 234 (Lys) to 261 (Tyr) with a hydrophobic region in the coil perhaps a putative region for interaction with MSP-1.

3.6.2 Pattern Database Searches

The MSP-7 amino acid sequence was used as the query sequence to search a number of secondary or pattern databases for conserved motifs that could give an indication of function for MSP-7.

PHD and ScanProsite searches of the PROSITE database predicted the presence in MSP-7 of a number of patterns including N-glycosylation, kinase phosphorylation and N-myristoylation sites, although these are probably false positives. Additionally a PrintsScan search of the PRINTS fingerprint database predicted the presence of tropomyosin (residues 66 – 84, 229 – 258, and 332 – 358), and alpha-tubulin (residues 236 – 249, and 299 – 315) motifs in MSP-7.

A PRODOM domain search performed by PHD recovered no significant homologous domains, whilst a Pfam search for Hidden Markov Models and a NCBI-CD profile search were negative. The BLOCKS search engine was used to search the

BLOCKS + and PRINTS 23.0 databases for similarity to highly conserved aligned motifs but no significant matches were obtained.

These results do not predict a known function for MSP-7. This may be because the motifs present in MSP-7 remain to be discovered or that the programs used in the analysis are not sophisticated or comprehensive enough to deal with protozoan motifs.

3.6.3 Sequence Conservation Between *Pf* MSP-7 Processing Sites and Other Merozoite Surface Proteins

The *Pf* MSP-7_{22} cleavage site shows similarity to protease cleavage sites at the start of MSP-1_{30} (MSP-1 primary processing site) and MSP-6_{36} (Figure 3.13A). This suggests that the protease responsible for these cleavages has a similar specificity. Since the cleavages are all predicted to occur at the same stage of merozoite development and the C-terminal products are known to be complexed together in the shed MSP-1 complex, it is possible that the same protease is responsible for these cleavages. Once an inhibitor of the protease SERPH that is predicted to be responsible for primary MSP-1 processing is discovered, this hypothesis can be tested (Blackman 2000).

The *Pf* MSP-$7_{22\text{-}19}$ N-terminal sequences, especially the N-terminal region of MSP-7_{19}, show similarity to a motif in the MSP-2 gene family (Figure 3.13B). This requires further analysis of MSP-2 processing and binding sites before any hypothesis concerning this motif can be made with confidence.

3.7 MSP-7 Homologues

MSP-1 orthologues are ubiquitous in *Plasmodium* species. *Pf* MSP-7 is highly conserved suggesting that the regions of MSP-1 binding to MSP-6 and MSP-7 are also conserved either at the primary or at the secondary structural level. It has also been

suggested that there are proteins similar in size to MSP-7_{22} associated with the shed MSP-1 complex in *P. chabaudi* (Stafford 1996). Preliminary PCR experiments using *Pfmsp-7* primers with the gDNA of several species of *Plasmodia*, resulted in the ampification of bands in *P.yoelii, P.vivax, and P. berghei* samples (data not shown). Hence it is reasonable to hypothesise that orthologues to MSP-7 may be present in other *Plasmodium* species.

TBLASTN database searches with the MSP-7 amino acid sequence identified a homologous sequence in the partial *P. yoelii* 17X database (contig 966, http://www.tigr.org) that at the amino acid level is 23 % identical and 50 % similar to that of *Pf* MSP-7 (Pachebat *et al.* 2001). The *Pf* MSP-7 amino acid sequence was aligned with the putative *Py* MSP-7 and the alignment used to predict the secondary structural characteristics of MSP-7 conserved between the two *Plasmodium* species (Pachebat *et al.* 2001).

The C-terminal beta sheet of *Pf* MSP-7 has a high sequence similarity to *Py* MSP-7 and to several unique proteins found in the partial *P. falciparum, P. berghei* and *P. vivax* genome databases, suggesting *msp-7* may be part of a multigene family present in several *Plasmodium* species. A multiple alignment (Figure 3.14) and pattern of the region covering residues 309 to 326 of *Pf* MSP-7, and residues 352 to 369 of the multiple alignment, (F-[KD]-[NK]-[YFN]-[IMV]-[YH]-G-[VIL]-[YN]-[SG]-[FY]-A-K-[QRK]-[HYN]-[SN]-[HY]-L) was used to for iterative PSI- and PHI-BLAST protein database searches but no additional homologues outside of malaria proteins were found (Pachebat *et al.* 2001).

The MSP-7_{22} and MSP-7_{19} polypeptides are associated with both allelic forms of MSP-1 in *P. falciparum*, and the *Pf msp-7* gene is highly conserved in these 2 allelic forms; *Py* and *Pb* MSP-7 orthologues have been identified and a 22 kDa protein is

associated with the shed MSP-1 complex in *P. chabaudi*; hence it is hypothesised that MSP-7 orthologues are present in all *Plasmodia.* As more *Plasmodium* genomes are sequenced in the comparative sequencing projects, this hypothesis can be verified.

It is also hypothesised that these MSP-7 orthologues are likely to show a high level of conservation of the primary or secondary structure in the region of MSP-7 that interacts with MSP-1, with the corresponding binding site on MSP-1 also expected to be highly conserved in all *Plasmodium* species.

It is unknown if this C-terminal beta sheet that characterises the MSP-7 multigene family is the region coding for the MSP-1 – MSP-7 binding motif, or if this region of homology is part of a motif coding for an unknown and unrelated function common to several *Plasmodium* proteins. As the function of the C-terminal beta sheet is unknown, and no homologues have been discovered outside of *Plasmodium* databases, further work is required to elucidate the function of this MSP-7 multigene family.

3.8 SUMMARY

The nucleotide sequence coding for MSP-7_{22} and MSP-7_{19} has been identified by a variety of sequence database searches and Vectorette PCR reads. The sequence is part of a larger gene that has been named merozoite surface protein 7 (*msp-7*).

The *msp-7* gene is 1056 nucleotides long and codes in one open reading frame for a 351 amino acid precursor that has been named Merozoite Surface Protein 7 (MSP-7). MALDI-TOF mass spectrophotometer analysis of trypsin-digested MSP-7_{22} and MSP-7_{19}, confirms that the correct gene has been identified, and that MSP-7_{22} is not modified by N-glycosylation (Pachebat *et al.* 2001).

The MSP-7_{22} and MSP-7_{19} N-terminal amino acid sequences have been located to the C-terminal half of the MSP-7 precursor, suggesting the precursor undergoes N-terminal cleavage to MSP-7_{22}, before MSP-7_{22} is detected bound to the primary processed MSP-1 polypeptide complex on the merozoite surface. MSP-7_{22} undergoes a further cleavage removing 18 amino acids from the N-terminus, resulting in MSP-7_{19} (18.7 kDa) that is detectable in the shed MSP-1 complex.

The MSP-7_{22} cleavage site shows similarity to the MSP-6 to MSP-6_{36} protease cleavage sites, and to the primary processing site of MSP-1 that gives rise to MSP-1_{30} (Stafford 1996; Pachebat *et al.* 2001; Trucco *et al.* 2001). All three cleavages are predicted to occur around the time of merozoite release, and since the cleavage sites are similar and the products complexed together on the merozoite surface, it is possible that the same protease is responsible for all three processing reactions. Additionally the MSP-7_{19} cleavage site shows similarity with a motif in MSP-2, the relevance of this remains to be elucidated.

In *P. falciparum,* MSP-7 is highly conserved with only 4 amino acid differences in parasite lines that code for the MAD-20 and Wellcome MSP-1 alleles. These amino acid differences are all in the MSP-7_{22} – MSP-7_{19} N-terminal region, suggesting they may be involved either: in specificity of the protease involved in cleavage of MSP-7_{22} to MSP-7_{19}, or in changes to the MSP-1 binding site. As *Pf* MSP-7 is highly conserved and undergoes little variation, this suggests that the MSP-1 – MSP-7 binding site is also highly conserved, with the MSP-7 binding site on MSP-1 either coded for by a conserved region of the MSP-1 amino acid sequence or part of a highly conserved secondary / tertiary structure of MSP-1. If the assignment of *msp-7* to chromosome 10 is correct, then it is possible that *msp-1* and *msp-7* are closely linked, and perhaps subjected to similar transcriptional regulation. It would also suggest that the allelic differences shown

by MSP-7 are related to differences between the 2 allelic types of MSP-1. This will become clearer once the *P. falciparum* genome has been assembled.

The degree of *Pf msp-7* conservation also suggests that MSP-7 is either not subjected to selective immune pressure, although antibodies to MSP-7_{22} are present in humans exposed to malaria (Stafford 1996), or that MSP-7 is highly conserved because it has an essential function bound to MSP-1 during the development of the merozoite and erythrocyte invasion.

Sequences showing similarity with the C-terminus of MSP-7 have been retrieved from the *P. falciparum* databases, suggesting that MSP-7 may be part of a multigene family. Additionally orthologues to MSP-7 have been detected in *P. yoelii*, *P. berghei*, and *P. vivax* and it is hypothesised that MSP-7 orthologues play an important if currently unknown role complexed to MSP-1 on the surface of merozoites in all *Plasmodia*.

Figure 3.0 TBLASTN 1.4.6 Results of MSP-7_{22} N-terminus vs. Chromosome 14 Individual Sequence Reads

The MSP-7_{22} N-terminal sequence of 25 amino acids from (Stafford *et al.* 1994) was used to TBLASTN (Version 1.4.6.) search the *Plasmodium falciparum* 3D7 genome databases.

A 627 nucleotide sequence (PNACJ17TF), was identified in the unfinished Chromosome 14 TIGR database, which on the date of searching consisted of 10,526 sequences and 5,512,334 total nucleotides.

Nucleotides 42 to 1 of PNACJ17TF when translated in the –1 frame, coded for 13 out of 14 MSP-7_{22} N-terminal amino acids (13/14 Identities, 13/14 positives). The non-identical amino acids are shown in red.

TBLASTN 1.4.6

Query = MSP-7_{22} N-terminus (25 letters)

10,526 sequences; 5,512,334 total letters.

Sequences producing High-scoring Segment Pairs:	Reading Frame	High Score	Smallest Sum Probability P (N)	N
>PNACJ17TF	**-1**	**61**	**0.029**	**1**

>PNACJ17TF

Length = 627

Minus Strand HSPs:

Score = 61 (25.9 bits), Expect = 0.030, P = 0.029
Identities 13/14 (92%), Positives 13/14 (92%), Frame –1,

MSP-7_{22} N-terminus	1	**SETDTQSKNEQEPS**	14
		SETDTQSKNEQE S	
PNACJ17TF	42	**SETDTQSKNEQEIS**	1

Release date: unknown
Posted date: 4:57 PM EDT Apr 17, 1998
# of letters in database: 5,512,334
# of sequences in database: 10,526
# of database sequences satisfying E: 1
No. of states in DFA: 102 (10 KB)
Total size of DFA: 12 KB (64 KB)

Figure 3.1 Description of Vectorette PCR

The Vectorette libraries used in this experiment consisted of T9/96 *P. falciparum* gDNA digested with either *Alu* I, *Dra* I, *Rsa* I, *Sau* 3AI or *Xho* II restriction endonucleases, and ligated to double stranded Vectorette II units (shown in red) at the 5' and 3' ends of the digested DNA (Gunaratne *et al.* 2000). The 5' strand of each Vectorette II unit is mismatched (mismatched top strand), this determines the specificity of the PCR reaction, as the Vectorette primer (VP) is homologous to the 3' strand of the unit.

On the first round of PCR the Vectorette primer is unable to hybridise to the mismatched strand, and so unable to extend the 5' strand. Only the primer specific to the known sequence (initiating primer, IP) is able to hybridise on the first PCR cycle, producing a product complementary to the bottom strand of the Vectorette unit.

In the second PCR cycle the Vectorette II primer anneals to the product made in the first round, and makes a complementary copy. After this second cycle, PCR occurs as normal with both primers binding to and amplifying the amplification products from the first two rounds.

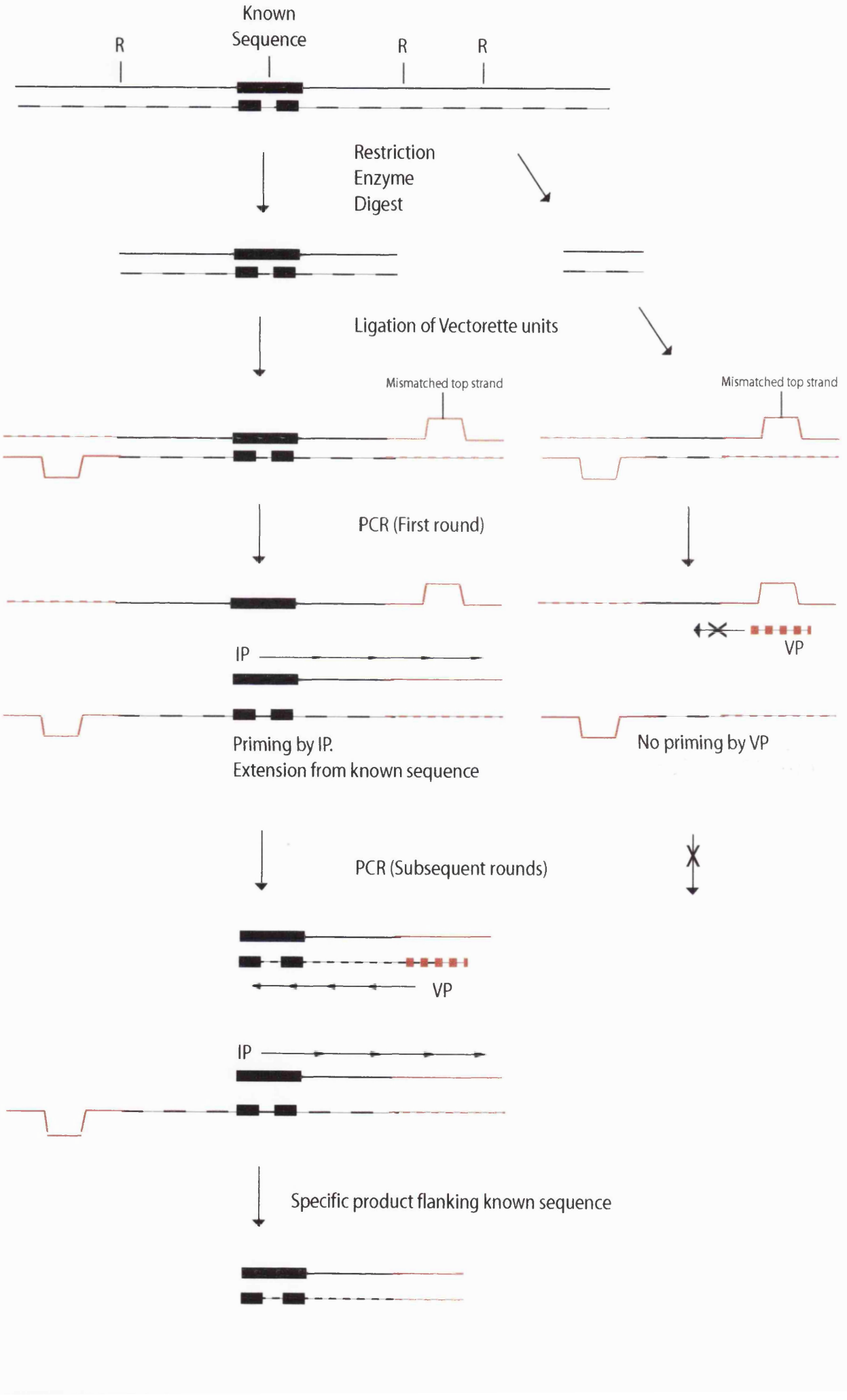
Known
Sequence
R
R
R
Restriction
Enzyme
Digest
Ligation of Vectorette units
Mismatched top strand
Mismatched top strand
PCR (First round)
IP
VP
Priming by IP.
Extension from known sequence
No priming by VP
PCR (Subsequent rounds)
VP
IP
Specific product flanking known sequence

Figure 3.2 First Vectorette Library PCR Step

A Analysis of First Vectorette Library PCR Products

Products from the Vectorette PCR reaction with p22F3 were separated by 1 % agarose-TBE gel electrophoresis, the gel incubated in a solution of 10 μg ml^{-1} ethidium bromide, 1 x TBE and the DNA visualised by ultraviolet illumination.

Loading Order on gel (from left to right): 200 bp marker; p22F3 vs. Vectorette *Alu* I, *Dra* I, *Rsa* I, *Sau* 3AI or *Xho* II libraries; negative control p22F3 (no template / H_2O); positive control (NMTvec4 vs. *Sau* 3A1).

Amplification products of 470bp (*Alu* I), 372bp (*Dra* I), 195bp (*Rsa* I) were visualised on the gel. The positive control of NMTvec4 vs. (*Sau* 3A1) gave the expected 500 bp product. No amplification products were seen in the negative control of p22F3 with no template.

B Schematic of the Aligned First Vectorette PCR Sequences with the Retrieved Chromosome 14 Sequence Read PNACJ17TF.

The PNACJ17TF sequence (truncated, red) is shown with the position of the primer p22F3 (▬) and the start of the sequence coding for the MSP-7_{22} N-terminus indicated.

The sequences (hatched blue) of the Vectorette *Alu* I, *Dra* I, *Rsa* I library PCR products obtained using the p22F3 primer were aligned with each other into a contig forming a 470 bp consensus sequence (solid blue).

A comparison of the 470 bp first Vectorette PCR consensus sequence with the PNACJ17TF sequence (red) showed an overlap of 175 nucleotides and extended the known downstream *msp-7* sequence by 295 bp.

Alu I, *Dra* I and *Rsa* I restriction enzyme sites are indicated. The p22F3 primer is shown as a yellow arrow. Sequence coding for the start of the MSP-7_{22} and MSP-7_{19} N-termini is indicated.

A

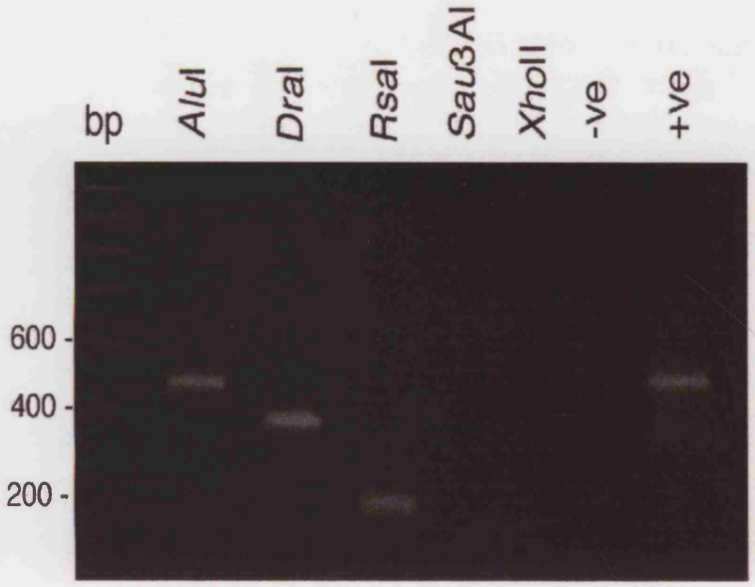
bp
AluI
DraI
RsaI
Sau3AI
XhoII
-ve
+ve
600 -
400 -
200 -

B

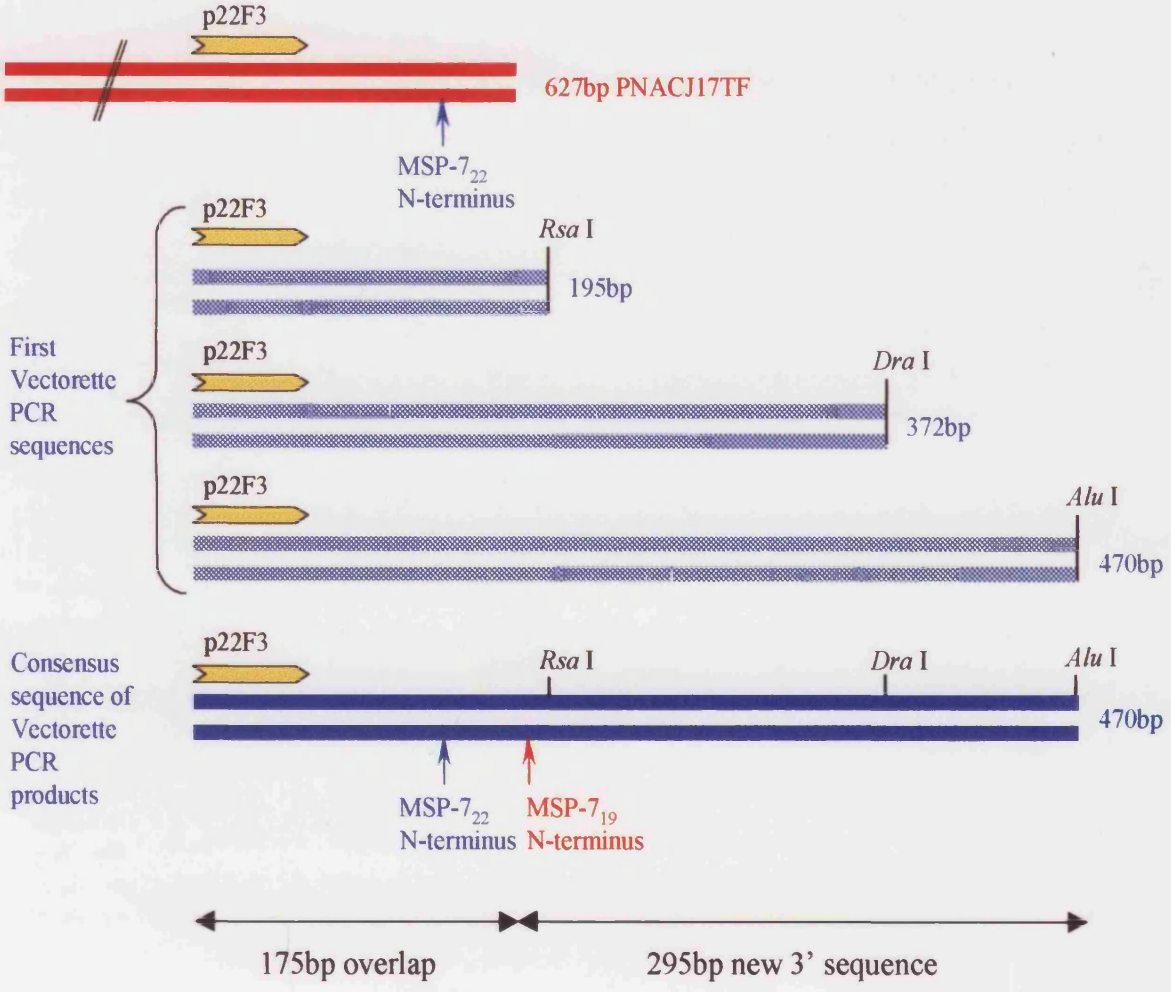
p22F3
627bp PNACJ17TF
MSP-7 22 N-terminus
First Vectorette PCR sequences
p22F3
Rsa I
195bp
p22F3
Dra I
372bp
p22F3
Alu I
470bp
Consensus sequence of Vectorette PCR products
p22F3
Rsa I
Dra I
Alu I
470bp
MSP-7 22 N-terminus
MSP-7 19 N-terminus
175bp overlap
295bp new 3' sequence

A

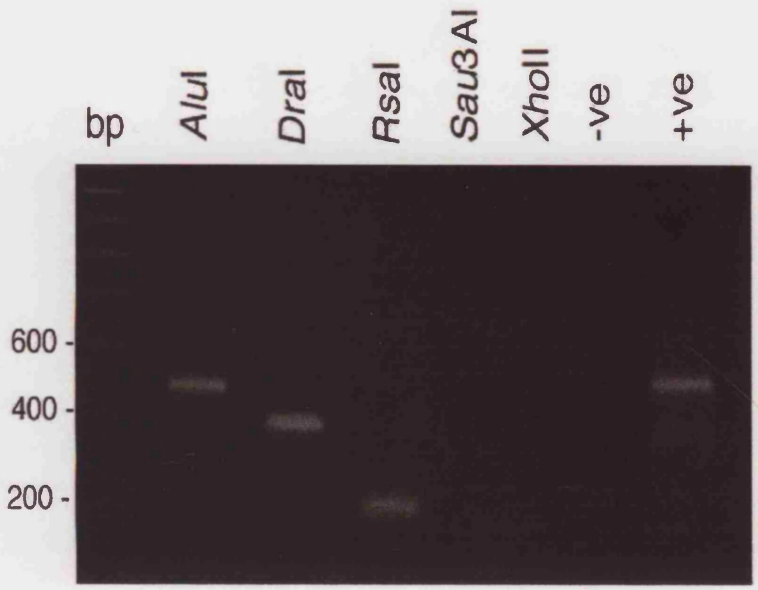
bp
AluI
DraI
RsaI
Sau3AI
XhoII
-ve
+ve
600 -
400 -
200 -

B

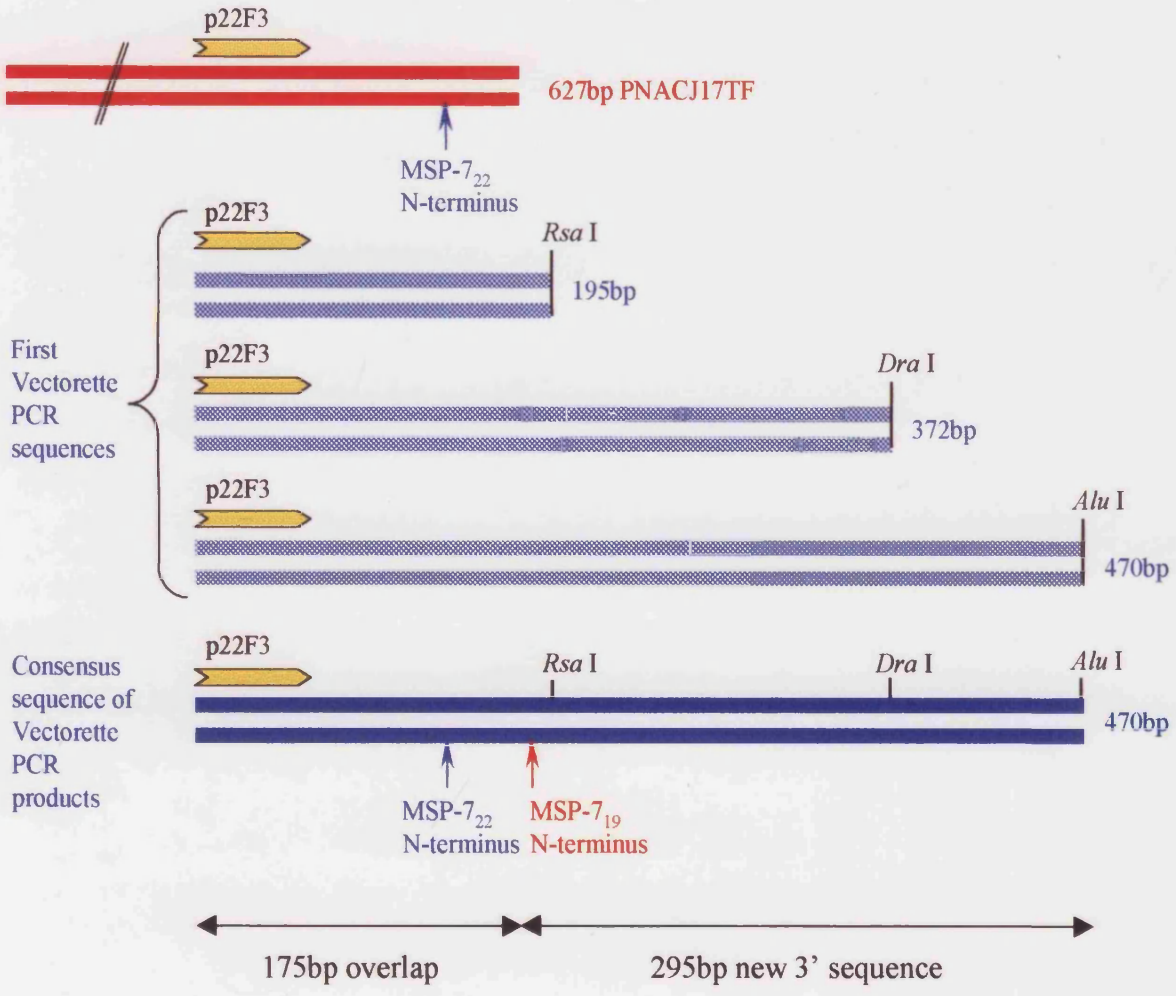
p22F3
627bp PNACJ17TF
MSP-7 22 N-terminus
p22F3
Rsa I
195bp
First Vectorette PCR sequences
p22F3
Dra I
372bp
p22F3
Alu I
470bp
Consensus sequence of Vectorette PCR products
p22F3
Rsa I
Dra I
Alu I
470bp
MSP-7 22 N-terminus
MSP-7 19 N-terminus
175bp overlap
295bp new 3' sequence

Figure 3.3 Second Vectorette Library PCR Step

A Analysis of Second Vectorette Library PCR Products

Products from the Vectorette PCR reaction with primers p22F4 and p22F5 were analysed by 1 % agarose-TBE gel electrophoresis, the gel incubated in a solution of 10 $\mu g\ ml^{-1}$ ethidium bromide, 1xTBE and the DNA visualised by ultraviolet illumination.

Loading Order on gel (from left to right): 200 bp marker; p22F4 vs. Vectorette *Alu* I, *Dra* I, *Rsa* I, *Sau* 3AI or *Xho* II libraries, negative control p22F4 (no template / sdw), positive control (p22F3 vs. *Dra* I), p22F5 vs. Vectorette *Rsa* I library.

Amplification products of 263 bp (*Alu* I), 164 bp (*Dra* I) and 481 bp (*Rsa* I) were obtained with p22F4. Only one product was obtained using p22F5, giving a 271 bp product with the *Rsa* I library. The positive control of p22F3 gave the expected 372 bp (*Dra* I) product, whilst negative controls of p22F4 and p22F5 (not shown) with no template (sdw) gave no products.

B Schematic of the Aligned Second Vectorette PCR Sequences with the First Vectorette Consensus Sequence

Primers p22F4 and p22F5 were designed against the first Vectorette PCR consensus sequence, for use in a second Vectorette PCR step, to extend the known downstream sequence of *msp-7*.

The Vectorette *Alu* I, *Dra* I and *Rsa* I library PCR products obtained with p22F4 and p22F5 were sequenced and the sequences (hatched blue) aligned with the first Vectorette consensus sequence showing an overlap of 263 bp and extending the known downstream sequence by 218 nucleotides. A 688 bp consensus sequence (blue) was made from the alignment, the translation of which identified an open reading frame coding for both the MSP-7_{22} and MSP-7_{19} N-terminal amino acid sequences and a TAA stop codon.

Alu I, *Dra* I and *Rsa* I restriction enzyme sites are indicated. Primers are shown as yellow arrows (▬). The size of each of the Vectorette products is shown in bp. Sequence coding for the start of the MSP-7_{22} and MSP-7_{19} N-termini is indicated. The TAA stop codon is shown in red.

A

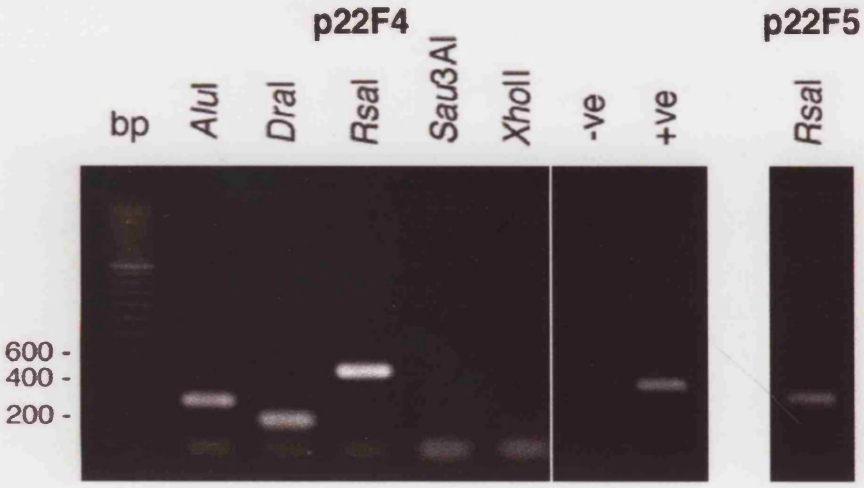
p22F4
p22F5
bp
AluI
DraI
RsaI
Sau3AI
XhoII
-ve
+ve
RsaI
600 -
400 -
200 -

B

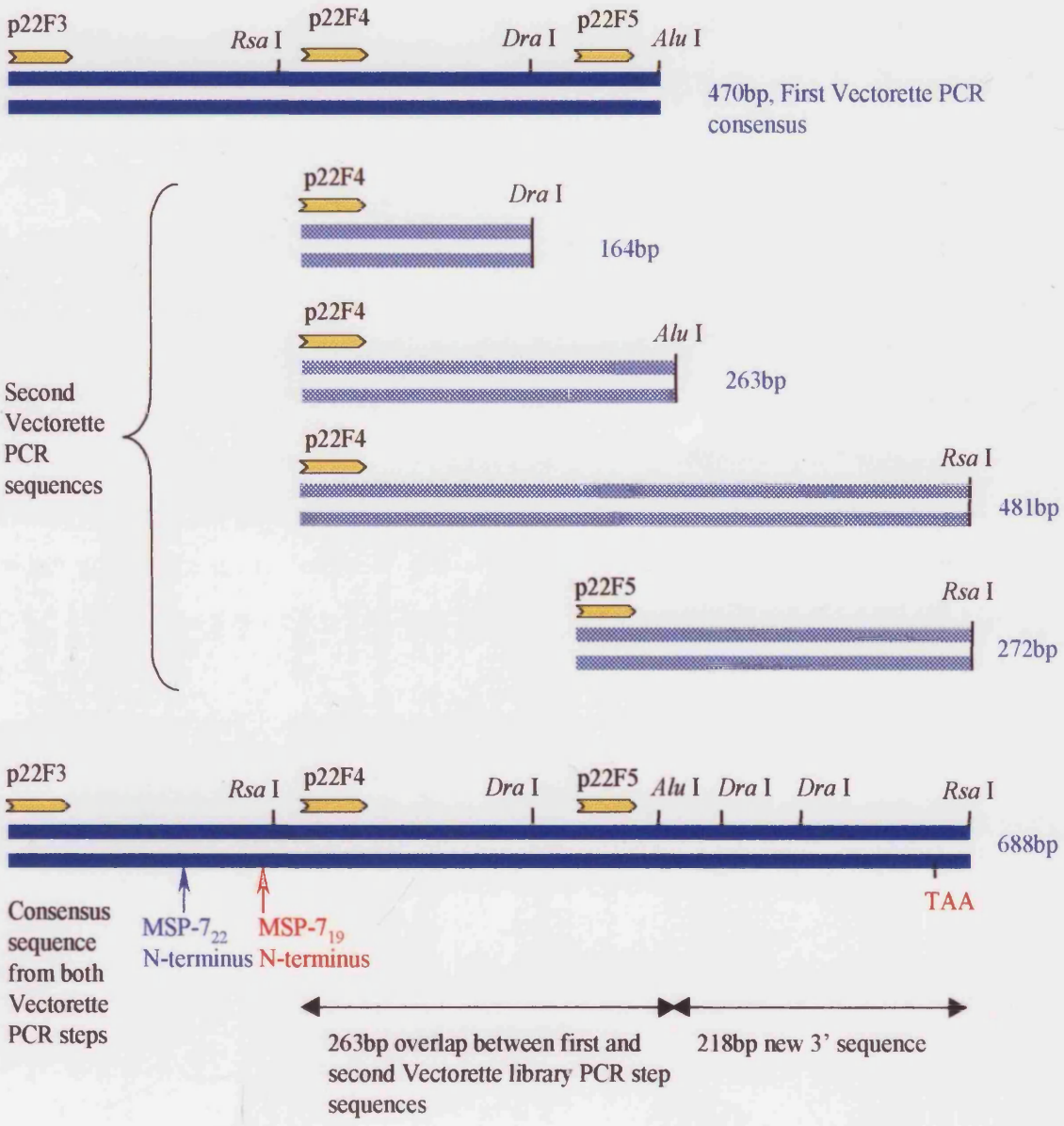
p22F3
Rsa I
p22F4
Dra I
p22F5
Alu I
470bp, First Vectorette PCR consensus
Second Vectorette PCR sequences
164bp
263bp
481bp
272bp
688bp
TAA
Consensus sequence from both Vectorette PCR steps
MSP-7 22 N-terminus
MSP-7 19 N-terminus
263bp overlap between first and second Vectorette library PCR step sequences
218bp new 3' sequence

Figure 3.4 Schematic of the Identification of the Putative *msp-7* Gene

The 688 bp consensus sequence of the Vectorette PCR steps (blue), was aligned with the PNACJ17TF sequence (red), forming a 1140 bp contig (green). On translation into all 6 frames, an uninterrupted open reading frame of 351 amino acids, starting at an ATG start codon at 58 bp and ending in a TAA stop codon at 1113 bp, was identified.

The MSP-7_{22} and MSP-7_{19} N-termini sequences start respectively at residues 177 and 195 of MSP-7, suggesting that the MSP-7_{22} and MSP-7_{19} polypeptides are N-terminal cleavage products of the larger precursor.

This previously unknown protein has been named Merozoite Surface Protein 7 (MSP-7), and is coded for by the *msp-7* gene of 1056 nucleotides.

Alu I, *Dra* I, *Rsa* I and *Sau* 3AI restriction enzyme sites are indicated. Primers are shown as yellow arrows (). Sequence coding for the start of the MSP-7_{22} and MSP-7_{19} N-termini is indicated. The ATG start and TAA stop codons are shown in red.

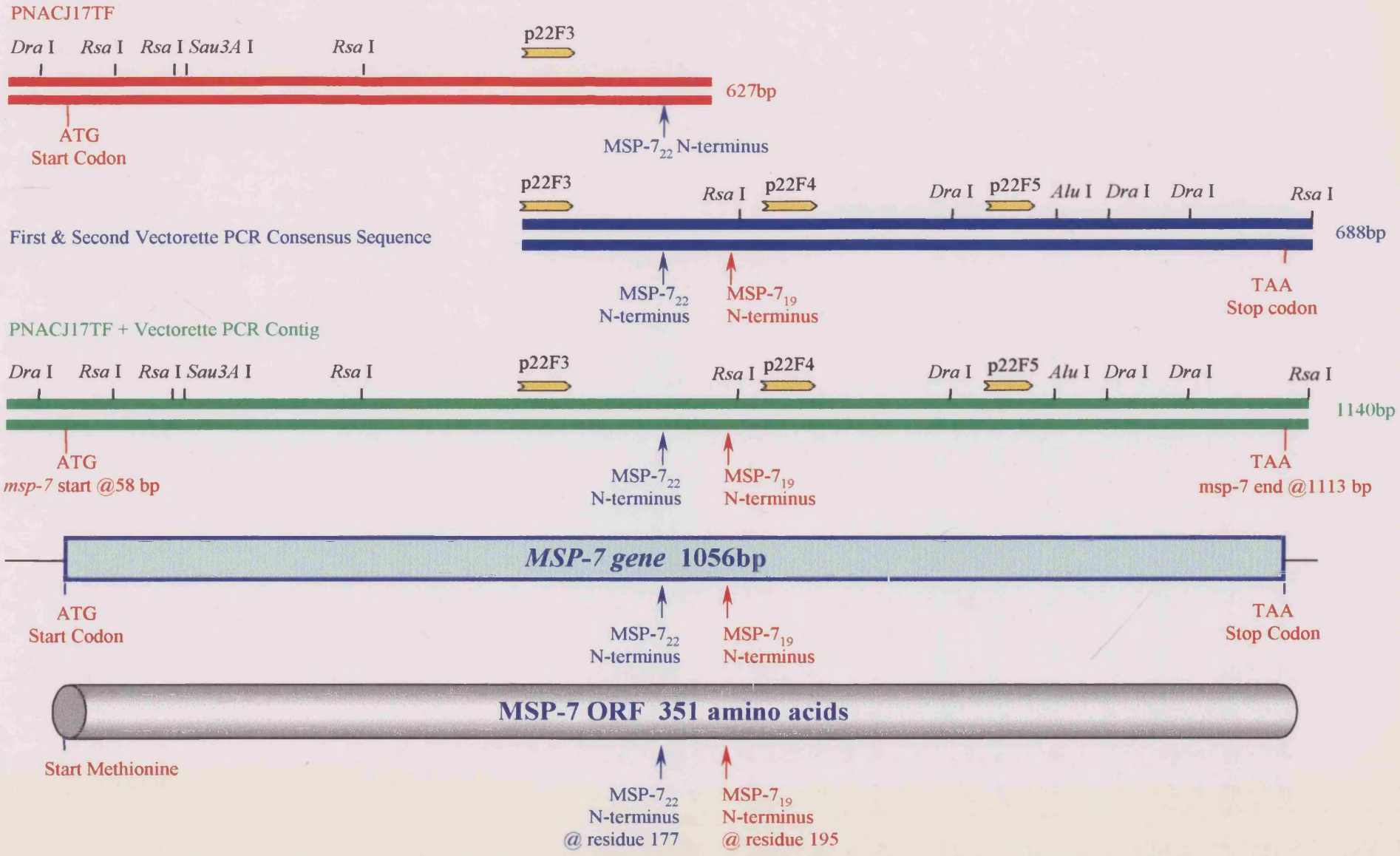
PNACJ17TF
Dra I
Rsa I
Rsa I Sau3A I
Rsa I
p22F3
627bp
ATG
Start Codon
MSP-7 22 N-terminus
First & Second Vectorette PCR Consensus Sequence
p22F3
Rsa I
p22F4
Dra I
p22F5
Alu I
Dra I
Dra I
Rsa I
688bp
MSP-7 22
N-terminus
MSP-7 19
N-terminus
TAA
Stop codon
PNACJ17TF + Vectorette PCR Contig
Dra I
Rsa I
Rsa I Sau3A I
Rsa I
p22F3
Rsa I
p22F4
Dra I
p22F5
Alu I
Dra I
Dra I
Rsa I
1140bp
ATG
msp-7 start @58 bp
MSP-7 22
N-terminus
MSP-7 19
N-terminus
TAA
msp-7 end @1113 bp
MSP-7 gene 1056bp
ATG
Start Codon
MSP-7 22
N-terminus
MSP-7 19
N-terminus
TAA
Stop Codon
MSP-7 ORF 351 amino acids
Start Methionine
MSP-7 22
N-terminus
@ residue 177
MSP-7 19
N-terminus
@ residue 195

Figure 3.5 Identification of the *msp-7* Transcript by Probing A Northern Blot

To determine the size of the *msp*-7 transcript, a Northern blot of total RNA from ring, trophozoite and schizont stages of 3D7 parasites was probed with [α-^{32}P] dATP labeled *msp-7b* as described in Method Sections 2.23.

The probe hybridised to a transcript of approximately 2.5 kb in size, in all stages of the asexual blood cycle, with the highest intensity occurring in schizont stage RNA. This suggested that the *msp-7* transcript had been identified and that the 1056 bp *msp-7* gene has a single exon structure, and that *msp-7* is transcribed mainly in schizonts.

(With thanks to Helen Taylor for supplying the Northern Blot).

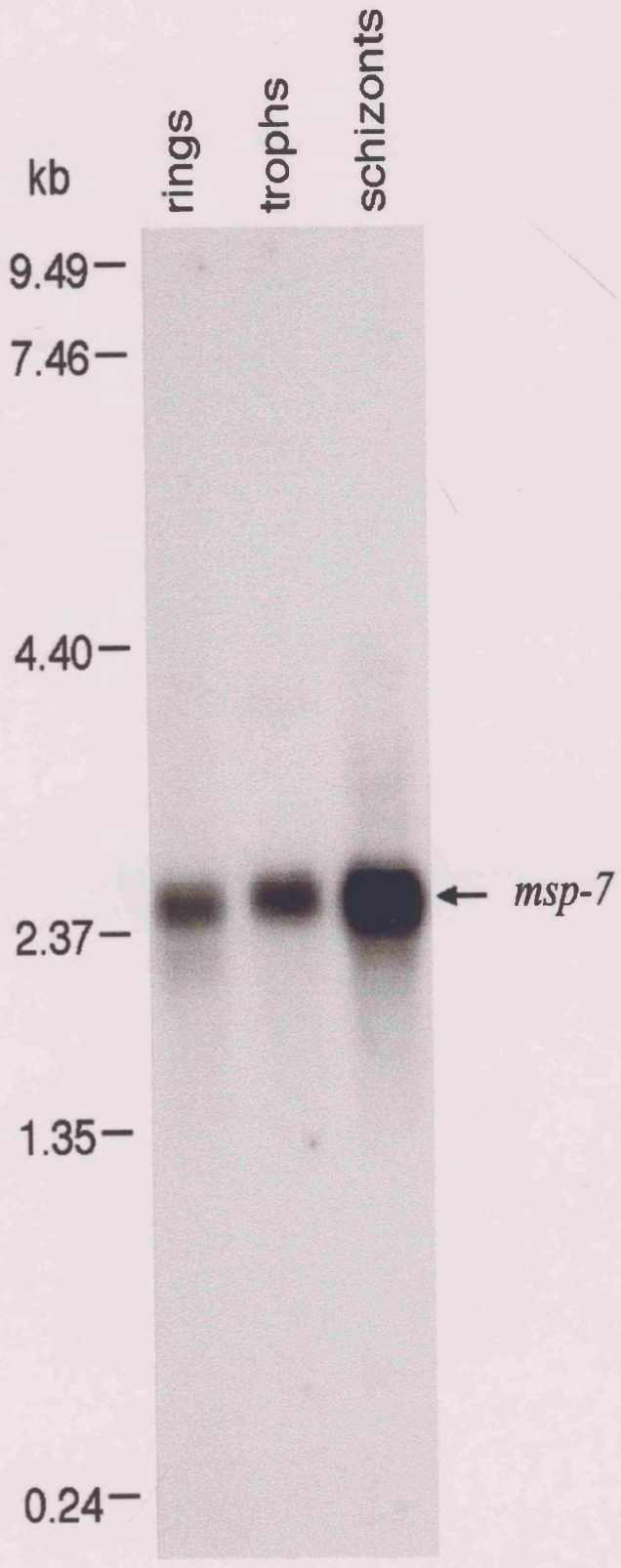
kb
rings
trophs
schizonts
9.49
7.46
4.40
2.37
1.35
0.24
msp-7

Figure 3.6 RT-PCR of 3D7 *msp-7* to Confirm Start and Stop Sites

The primer pairs pfp22F, p22R2 (**A**) and p22F6, pfp22R (**B**) were used to amplify the putative start and stop sites of *msp-7*. Reactions were performed on: duplicate reverse transcriptase positive 3D7 cDNA samples (rt+(1) and rt+(2)); reverse transcriptase negative 3D7 mRNA samples (rt-); a PCR negative control of sdw only (sdw); and a PCR positive control of 3D7 gDNA (gDNA).

Amplification products were analysed by 1 % agarose-TBE gel electrophoresis. Nucleic acids were visualised by incubating the gel in 10 μg ml^{-1} ethidium bromide, 1 x TBE, followed by ultraviolet illumination. Loading order on gel (from left to right):

A (pfp22F, p22R2): 100 bp marker, rt+(1), rt+(2), rt-, gDNA, sdw.

B (p22F6, pfp22R): 100 bp marker, rt+(1), rt+(2), rt-, gDNA, sdw.

Amplification products of 686 bp (pfp22F, p22R2) and 230 bp (p22F6, pfp22R) were obtained for both rt+ and gDNA samples, whilst the reverse transcriptase negative, and the control of sdw only were consistently negative, giving no PCR products.

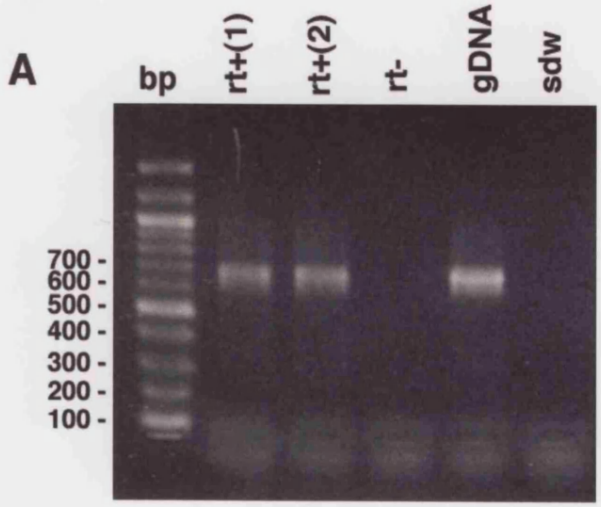
A
bp
rt+(1)
rt+(2)
rt-
gDNA
sdw
700 -
600 -
500 -
400 -
300 -
200 -
100 -

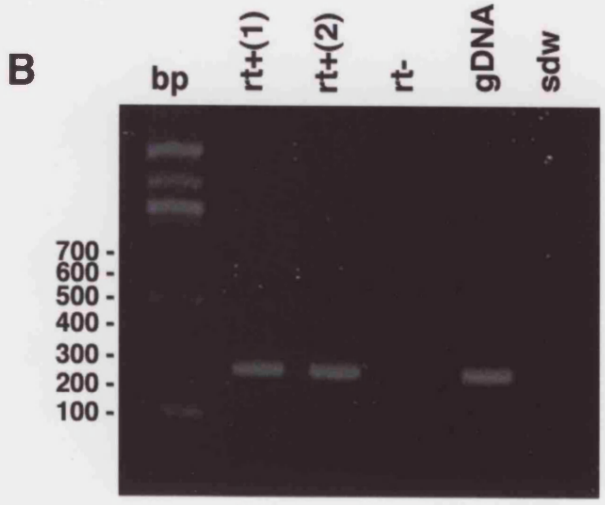
B
bp
rt+(1)
rt+(2)
rt-
gDNA
sdw
700 -
600 -
500 -
400 -
300 -
200 -
100 -

Figure 3.7 The *P. falciparum* 3D7 and T9/96 *msp-7* Gene

The nucleotide sequence for the 1056 bp gene for *msp-7* is identical for 3D7 and T9/96 lines of *P. falciparum*. The gene consists of 1056 nucleotides and has no introns. Start (ATG) and stop (TAA) codons are underlined.

A = Adenine; T = Thymine; C = Cytosine; G = Guanine


ATGAAGAGTA ATATCATATT TTATTTTTCT TTTTTTTGTG TGTACTTATA 50
CTATGTTTCG TGTAATCAAT CAACTCATAG TACACCAGTA AATAATGAAG 100
AAGATCAAGA AGAATTATAT ATTAAAAATA AAAAATTGGA AAAACTAAAA 150
AATATAGTAT CAGGAGATTT TGTTGGAAAT TATAAAAATA ATGAAGAATT 200
ATTAAACAAA AAAATTGAAG AATTACAAAA CAGTAAAGAA AAAAATGTAC 250
ATGTATTAAT TAATGGAAAT TCAATTATTG ATGAAATAGA AAAAAATGAA 300
GAAAATGATG ATAACGAAGA AAATAATGAT GATGACAATA CATATGAATT 350
AGATATGAAT GATGACACAT TCTTAGGACA AAATAACGAT TCACATTTTG 400
AAAATGTTGA TGATGACGCA GTAGAAAATG AACAAGAAGA TGAAAACAAG 450
GAAAAATCAG AATCATTTCC ATTATTCCAA AATTTAGGAT TATTCGGTAA 500
AAACGTATTA TCAAAGGTAA AGGCACAAAG TGAAACAGAT ACTCAATCTA 550
AAAATGAACA AGAGATATCA ACACAAGGAC AAGAAGTACA AAAACCAGCA 600
CAAGGAGGAG AATCGACATT TCAAAAAGAC CTAGATAAGA AATTATATAA 650
TTTAGGAGAT GTTTTTAATC ATGTAGTTGA TATTTCAAAC AAAAAGAACA 700
AAATAAATCT CGATGAATAT GGTAAAAAAT ATACAGATTT CAAAAAAGAA 750
TATGAAGACT TCGTTTTAAA TTCTAAAGAA TATGATATAA TCAAAAATCT 800
AATAATTATG TTTGGTCAAG AAGATAATAA GAGTAAAAAT GGCAAAACGG 850
ATATTGTAAG TGAAGCTAAA CATATGACTG AAATTTTCAT AAAACTATTT 900
AAAGATAAGG AATACCATGA ACAATTTAAA AATTATATTT ATGGTGTTTA 950
TAGTTATGCA AAACAAAATA GTCACTTAAG TGAGAAAAAA ATAAAACCAG 1000
AAGAGGAATA TAAAAAATTC TTAGAATATT CATTTAATTT ACTAAACACA 1050
ATGTAA 1056

Figure 3.8 The *P. falciparum* MSP-7 Amino Acid Sequence

The *msp-7* gene from 3D7 / T9/96 lines of *P. falciparum* was translated giving an open reading frame of 351 amino acids. The 351 amino acid sequence has been named Merozoite Surface Protein 7 and has a calculated mass of 41.3 kDa.

MSP-7 has a 27 amino acid signal peptide with the predicted site of cleavage (indicated by ↓) between residues 27 and 28, the resulting 324 amino acid protein has a calculated mass of 38.5 kDa.

The MSP-7_{22} and MSP-7_{19} N-termini start at residues 177 and 195, where ↓ indicates the N-terminal cleavage sites. This suggests that MSP-7 is cleaved between residues 176 and 177 into an N-terminal polypeptide product of 149 amino acids and C-terminal MSP-7_{22} 175 amino acid polypeptide product. The MSP-7_{22} polypeptide undergoes further cleavage at residues 194 and 195 of MSP-7, removing 18 amino acids from the N-terminus to give the 157 amino acid polypeptide (MSP-7_{19}).

A = Alanine; C = Cysteine; D = Aspartic acid; E = Glutamic acid; F = Phenylalanine; G = Glycine; H = Histidine; I = Isoleucine; K = Lysine; L = Leucine; M = Methionine; N = Asparagine; P = Proline; Q = Glutamine; S = Serine; T = Threonine; V = Valine; Y = Tyrosine. * indicates a stop codon.

= hydrophobic, non-polar residues; = hydrophilic residues; = hydrophobic, acidic residues.

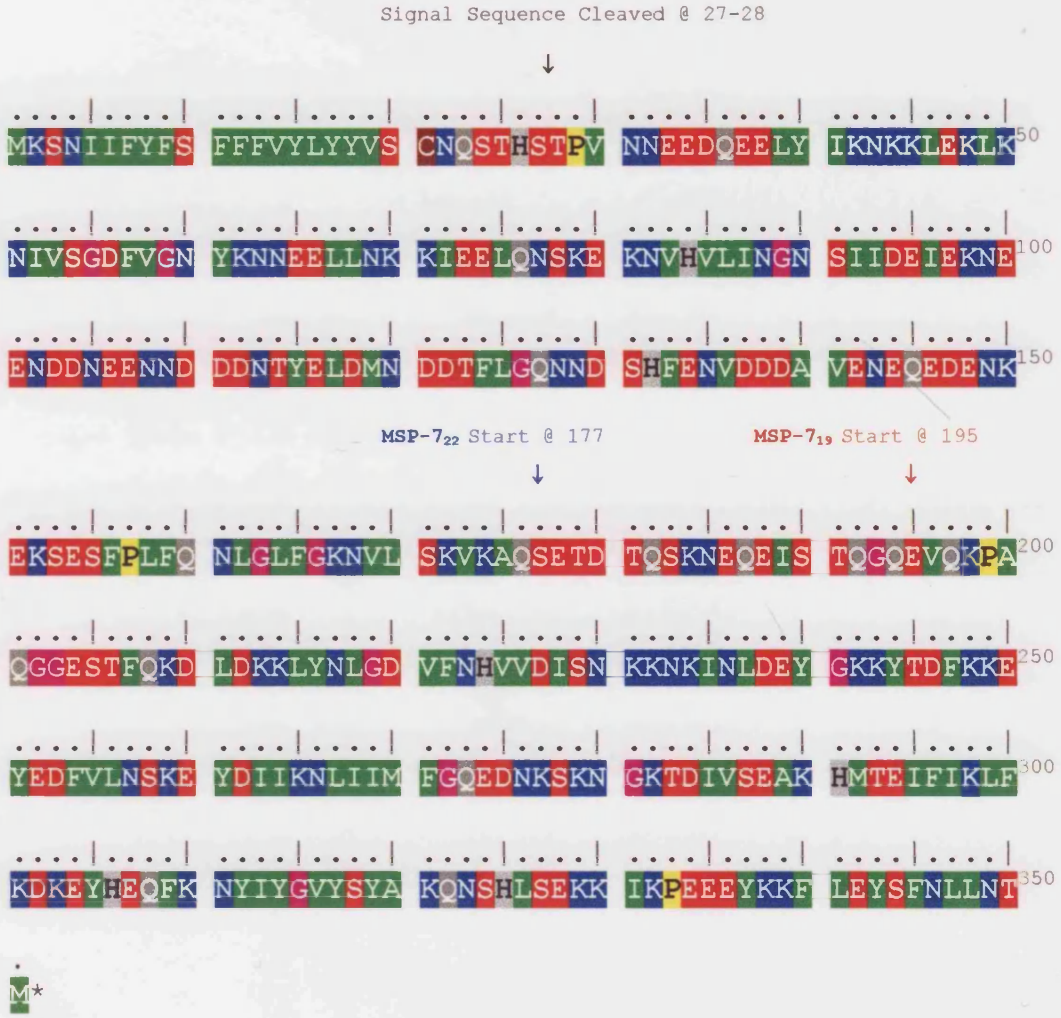
Signal Sequence Cleaved @ 27-28
MKSNIIFYFS FFFVYLYYVS CNQSTHSTPV NNEEDQEELY IKNKKLEKLK 50
NIVSGDFVGN YKNNEELLNK KIEELQNSKE KNVHVLINGN SIIDEIEKNE 100
ENDDNEENND DDNTYELDMN DDTFLGQNND SHFENVDDDA VENEQEDENK 150
MSP-7$_{22}$ Start @ 177
MSP-7$_{19}$ Start @ 195
EKSESFPLFQ NLGLFGKNVL SKVKAQSETD TQSKNEQEIS TQGQEVQKPA 200
QGGESTFQKD LDKKLYNLGD VFNHVVDISN KKNKINLDEY GKKYTDFKKE 250
YEDFVLNSKE YDIIKNLIIM FGQEDNKSKN GKTDIVSEAK HMTEIFIKLF 300
KDKEYHEQFK NYIYGVYSYA KQNSHLSEKK IKPEEEYKKF LEYSFNLLNT 350
M*

Figure 3.9 The Basic Structure and Processing Sites of MSP-7

Schematic of the 351 amino acid MSP-7 protein (grey), with the predicted cleavage sites and resulting polypeptide products indicated.

The signal sequence of 27 amino acids (pink) is cleaved from the N-terminus of MSP-7, leaving a 324 amino acid protein. Cleavage at residues 176 - 177 gives rise to a predicted 149 amino acid N-terminal polypeptide (grey), and a 175 amino acid C-terminal product MSP-7_{22} (blue). Cleavage of 18 amino acids (blue) from the N-terminus of MSP-7_{22} gives a 157 amino acid polypeptide (red), MSP-7_{19}.

The N-terminal amino acid sequences at the MSP-7_{22} and MSP-7_{19} cleavage sites are shown.

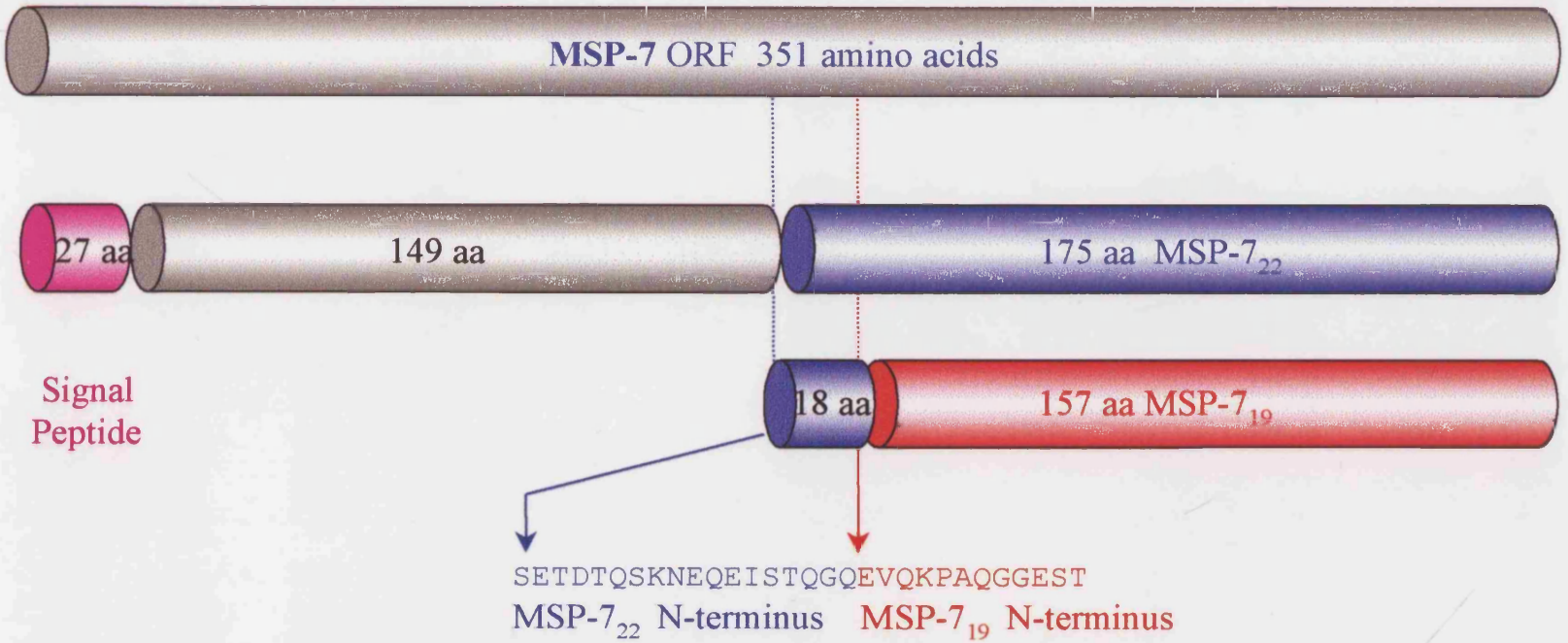
MSP-7 ORF 351 amino acids
27 aa
149 aa
175 aa MSP-7$_{22}$
Signal Peptide
18 aa
157 aa MSP-7$_{19}$
SETDTQSKNEQEISTQGQEVQKPAQGGEST
MSP-7$_{22}$ N-terminus
MSP-7$_{19}$ N-terminus

Figure 3.10 Alignment of FCB-1 and 3D7 *P. falciparum msp-7*

The amplified FCB-1 *msp-7* sequence was aligned with that of 3D7 *msp-7*. Only four nucleotide differences (indicated by ▼) were detected between the 3D7 and FCB-1 sequences at positions: 580 (C → A), 623 (A → G), 694 (A → G), and 722 (G → A).

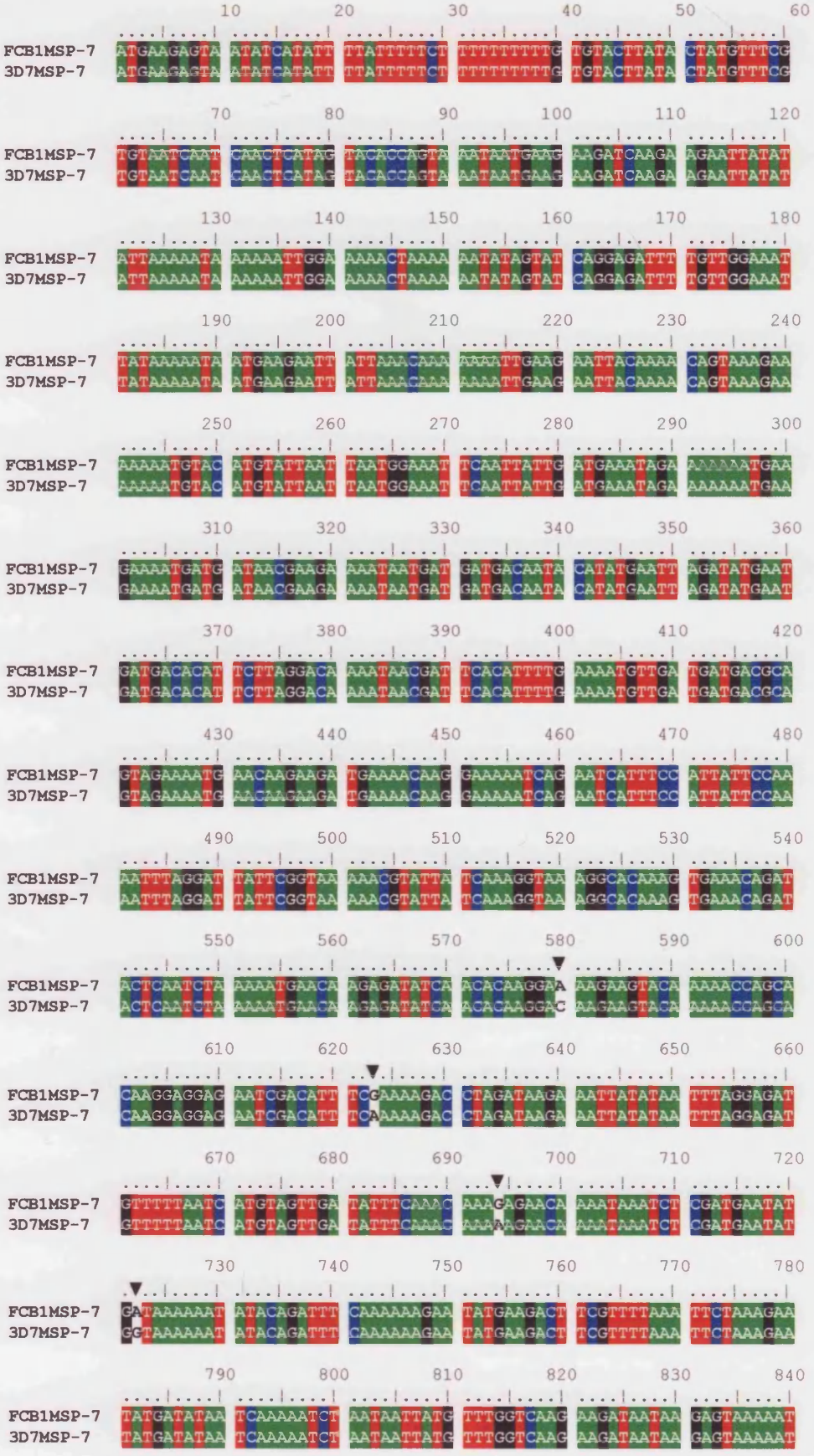

continued overpage

Figure 3.10 continued

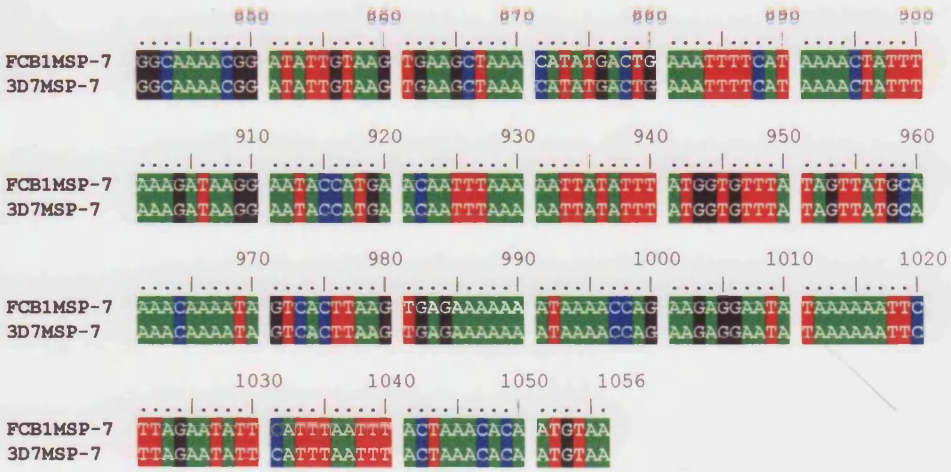
850 860 870 880 890 900
FCB1MSP-7 GGCAAAACGG ATATTGTAAG TGAAGCTAAA CATATGACTG AAATTTTCAT AAAACTATTT
3D7MSP-7 GGCAAAACGG ATATTGTAAG TGAAGCTAAA CATATGACTG AAATTTTCAT AAAACTATTT
910 920 930 940 950 960
FCB1MSP-7 AAAGATAAGG AATACCATGA ACAATTTAAA AATTATATTT ATGGTGTTTA TAGTTATGCA
3D7MSP-7 AAAGATAAGG AATACCATGA ACAATTTAAA AATTATATTT ATGGTGTTTA TAGTTATGCA
970 980 990 1000 1010 1020
FCB1MSP-7 AAACAAAATA GTCACTTAAG TGAGAAAAAA ATAAAACCAG AAGAGGAATA TAAAAAATTC
3D7MSP-7 AAACAAAATA GTCACTTAAG TGAGAAAAAA ATAAAACCAG AAGAGGAATA TAAAAAATTC
1030 1040 1050 1056
FCB1MSP-7 TTAGAATATT CATTTAATTT ACTAAACACA ATGTAA
3D7MSP-7 TTAGAATATT CATTTAATTT ACTAAACACA ATGTAA

Figure 3.11 Sequence Conservation of the *Pf* MSP-7 Protein in FCB-1 and 3D7 Lines.

The *Pf* FCB-1 and 3D7 MSP-7 amino acid sequences were aligned using Clustal W. Amino acid differences are indicated by ▼. * indicates a stop codon.

There are only 4 amino acid differences between *Pf* MSP-7 in these 2 lines, all of which are in the MSP-7_{22} region of the polypeptide. These are at residues: 194 (Glutamine → Lysine), 208 (Glutamine → Arginine), 232 (Lysine → Glutamic acid) and 241 (Glycine → Aspartic acid).

As the MSP-7_{22} polypeptide is found bound to the MSP-1 complex on the merozoite surface, and undergoes N-terminal cleavage to MSP-7_{19} which is found bound to the MSP-1 complex shed on merozoite invasion, the high degree of sequence conservation suggests that MSP-7_{22} binds to a conserved region of MSP-1.

A = Alanine; C = Cysteine; D = Aspartic acid; E = Glutamic acid; F = Phenylalanine; G = Glycine; H = Histidine; I = Isoleucine; K = Lysine; L = Leucine; M = Methionine; N = Asparagine; P = Proline; Q = Glutamine; R = Arginine S = Serine; T = Threonine; V = Valine; Y = Tyrosine.

= hydrophobic, non-polar residues; = hydrophilic residues; = hydrophobic, acidic residues.

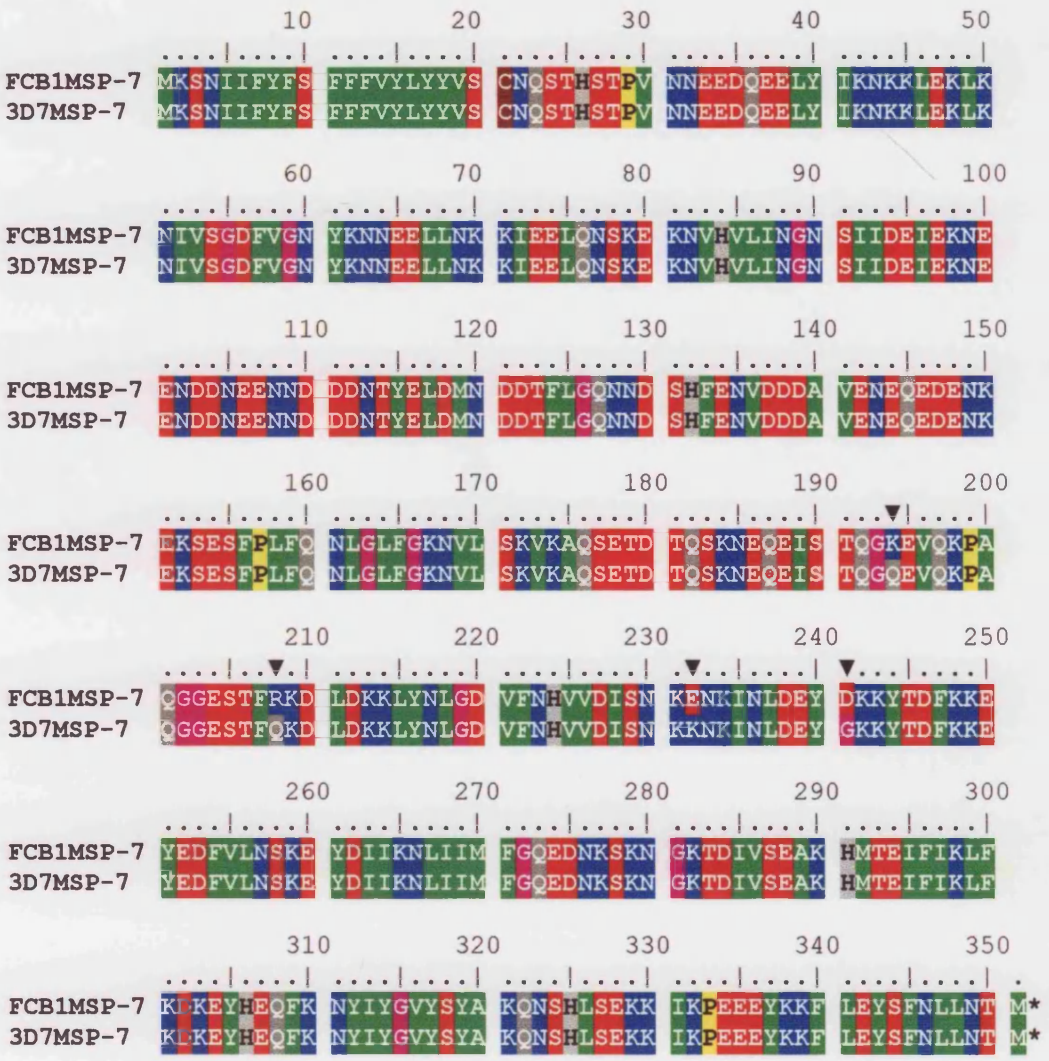
10 20 30 40 50
FCB1MSP-7 MKSNIIFYFS FFFVYLYYVS CNQSTHSTPV NNEEDQEELY IKNKKLEKLK
3D7MSP-7 MKSNIIFYFS FFFVYLYYVS CNQSTHSTPV NNEEDQEELY IKNKKLEKLK
60 70 80 90 100
FCB1MSP-7 NIVSGDFVGN YKNNEELLNK KIEELQNSKE KNVHVLINGN SIIDEIEKNE
3D7MSP-7 NIVSGDFVGN YKNNEELLNK KIEELQNSKE KNVHVLINGN SIIDEIEKNE
110 120 130 140 150
FCB1MSP-7 ENDDNEENND DDNTYELDMN DDTFLGQNND SHQFENVDDDA VENEQEDENK
3D7MSP-7 ENDDNEENND DDNTYELDMN DDTFLGQNND SHQFENVDDDA VENEQEDENK
160 170 180 190 200
FCB1MSP-7 EKSESFPLFQ NLGLFGKNVL SKVKAQSETD TQSKNEQEIS TQGKEVQKPA
3D7MSP-7 EKSESFPLFQ NLGLFGKNVL SKVKAQSETD TQSKNEQEIS TQGQEVQKPA
210 220 230 240 250
FCB1MSP-7 QGGESTFRKD LDKKLYNLGD VFNHVVDISN KENKINLDEY DKKYTDFKKE
3D7MSP-7 QGGESTFQKD LDKKLYNLGD VFNHVVDISN KKNKINLDEY GKKYTDFKKE
260 270 280 290 300
FCB1MSP-7 YEDFVLNSKE YDIIKNLIIM FGQEDNKSKN GKTDIVSEAK HMTEIFIKLF
3D7MSP-7 YEDFVLNSKE YDIIKNLIIM FGQEDNKSKN GKTDIVSEAK HMTEIFIKLF
310 320 330 340 350
FCB1MSP-7 KDKEYHEQFK NYIYGVYSYA KQNSHLSEKK IKPEEEYKKF LEYSFNLLNT M*
3D7MSP-7 KLKEYHEQFK NYIYGVYSYA KQNSHLSEKK IKPEEEYKKF LEYSFNLLNT M*

Figure 3.12 Secondary Structure and Solvent Accessibility of *Pf* MSP-7

Secondary structure of *Pf*MSP-7 was predicted by a combination of the Chou-Fasman and Robson-Garnier methods and confirmed with the PHDsec predictions. The secondary structure of MSP-7 is predominantly alpha helical with two small regions of beta sheet and several beta turns indicating the protein is highly flexible. Solvent accessibility was determined by PHDacc. SMART predicted that residues: 7 - 20, 37 - 52, 62 - 75, 92 - 113, 328 - 339 are of low compositional complexity, and Prospero predicted the presence of two internal repeats between residues 117 - 252, and 125 - 262.

The 351 amino acid sequence for 3D7 and T9/96 *P. falciparum* MSP-7 is shown in full, with amino acid differences in the FCB-1 line indicated on the lines below. The putative signal peptide is shown in red, and the cleavage sites producing MSP-7_{22} and MSP-7_{19} are shown(↓). Predicted alpha helices ( ) and beta sheets ( ) are indicated below the sequence with an indication of the predicted surface accessibility of the residues within these structures (b, buried; e, exposed).

See Appendix for web site addresses at which these bioinformatics programmes are available.

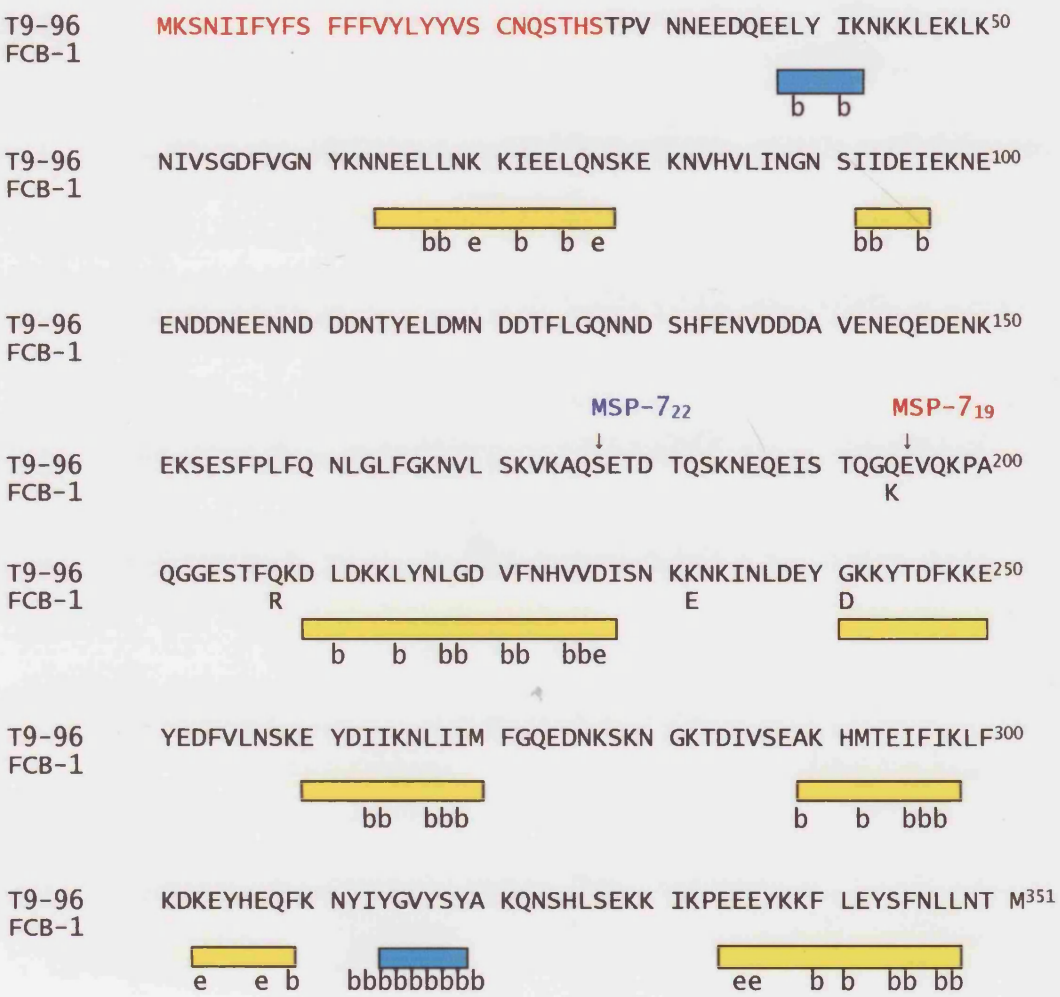
T9-96 MKSNIIFYFS FFFVYLYYVS CNQSTHSTPV NNEEDQEELY IKNKKLEKLK50
FCB-1
b b
T9-96 NIVSGDFVGN YKNNEELLNK KIEELQNSKE KNVHVLINGN SIIDEIEKNE100
FCB-1
bb e b b e
bb b
T9-96 ENDDNEENND DDNTYELDMN DDTFLGQNND SHFENVDDDA VENEQEDENK150
FCB-1
MSP-722
MSP-719
T9-96 EKSESFPLFQ NLGLFGKNVL SKVKAQSETD TQSKNEQEIS TQGQEVQKPA200
FCB-1
K
T9-96 QGGESTFQKD LDKKLYNLGD VFNHVVDISN KKNKINLDEY GKKYTDFKKE250
FCB-1
R
E
D
b b bb bb bbe
T9-96 YEDFVLNSKE YDIIKNLIIM FGQEDNKSKN GKTDIVSEAK HMTEIFIKLF300
FCB-1
bb bbb
b b bbb
T9-96 KDKEYHEQFK NYIYGVYSYA KQNSHLSEKK IKPEEEYKKF LEYSFNLLNT M351
FCB-1
e e b
bbbbbbbbb
ee b b bb bb

Figure 3.13 Conservation of Processing Sites Throughout Merozoite Surface Proteins

A Alignment of the MSP-1_{30}, MSP-6 and MSP-7_{22} Cleavage Sites.

The MSP-7_{22} cleavage site shows similarity to protease cleavage sites that give rise to MSP-1_{30} and MSP-6_{36}.

The amino acid sequences were aligned to compare the protease cleavage sites at the start of MSP-7_{22}, MSP-6_{36} and MSP-1_{30}. The cleavage site is shown (↓), together with the amino acid residues that are identical (▮) or similar (▮) in the three peptide sequences.

B Alignment of *Pf* MSP-$7_{22\text{-}19}$ with a Motif Present in the MSP-2 Protein Family.

The *Pf* MSP-$7_{22\text{-}19}$ N-terminal amino acid sequence, in particular the cleavage site that gives rise to MSP-7_{19} shows similarity to a motif in the MSP-2 gene family. An alignment of the *Pf* MSP-$7_{22\text{-}19}$ N-terminal amino acid sequence with an alignment of amino acid residues 201 to 250 of the MSP-2 protein family, gives a consensus sequence of **G.EVQKP.Q..ES T.** The MSP-7_{19} cleavage site is shown (↓).

A = Alanine; C = Cysteine; D = Aspartic acid; E = Glutamic acid; F = Phenylalanine; G = Glycine; H = Histidine; I = Isoleucine; K = Lysine; L = Leucine; M = Methionine; N = Asparagine; P = Proline; Q = Glutamine; R = Arginine S = Serine; T = Threonine; V = Valine; Y = Tyrosine. * indicates a stop codon.

▮ = hydrophobic, non-polar residues; ▮ = hydrophilic residues; ▮ = hydrophobic, acidic residues.

A


MSP-7
MSP-6
MSP-1
NVLSKVKAQ SETDTQS
NITQVVQAN SETNKNP
SITQPLVAA SETTEDG

B

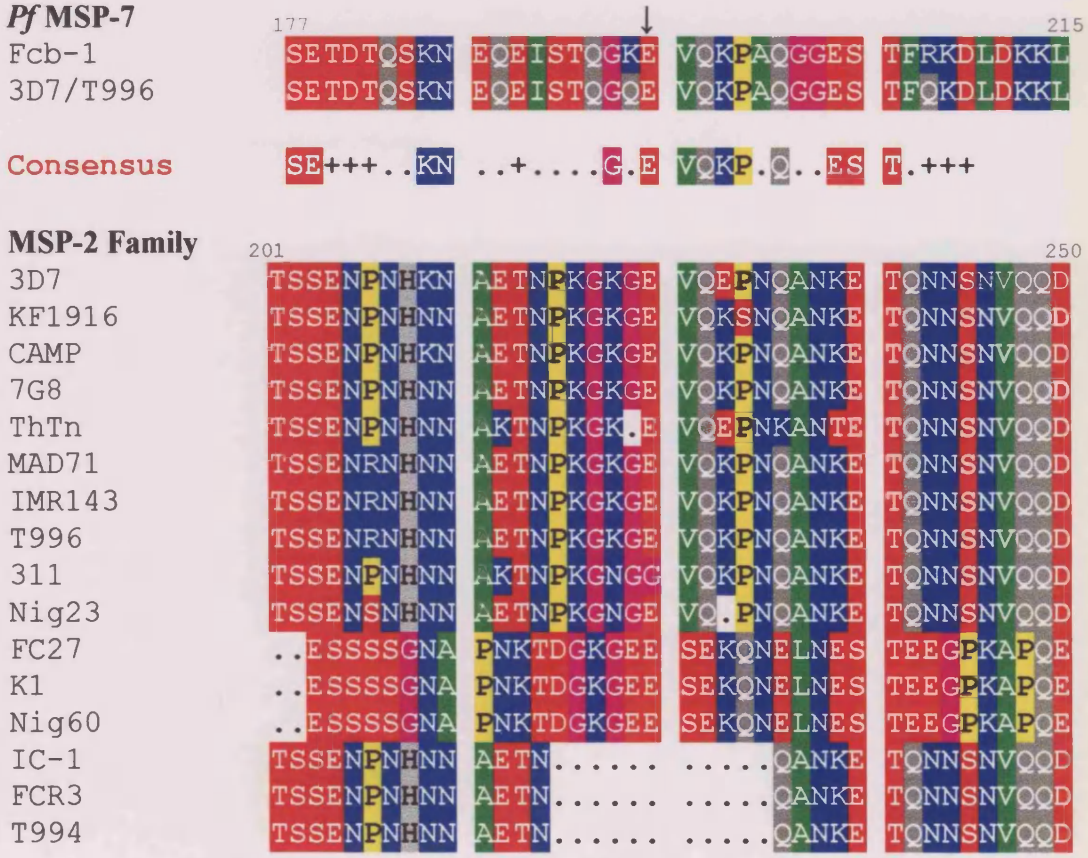
Pf MSP-7
177
215
Fcb-1
3D7/T996
SETDTQSKN EQEISTQGKE VQKPAQGGES TFRKDLDKKL
SETDTQSKN EQEISTQGQE VQKPAQGGES TFQKDLDKKL
Consensus
SE+++..KN ..+....G.E VQKP.Q..ES T.+++
MSP-2 Family
201
250
3D7
KF1916
CAMP
7G8
ThTn
MAD71
IMR143
T996
311
Nig23
FC27
K1
Nig60
IC-1
FCR3
T994
TSSENPNHKN AETNPKGKGE VQEPNQANKE TQNNSNVQQD
TSSENPNHNN AETNPKGKGE VQKSNQANKE TQNNSNVQQD
TSSENPNHKN AETNPKGKGE VQKPNQANKE TQNNSNVQQD
TSSENPNHNN AETNPKGKGE VQKPNQANKE TQNNSNVQQD
TSSENPNHNN AKTNPKGK.E VQEPNKANTE TQNNSNVQQD
TSSENRNHNN AETNPKGKGE VQKPNQANKE TQNNSNVQQD
TSSENRNHNN AETNPKGKGE VQKPNQANKE TQNNSNVQQD
TSSENRNHNN AETNPKGKGE VQKPNQANKE TQNNSNVQQD
TSSENPNHNN AKTNPKGNGG VQKPNQANKE TQNNSNVQQD
TSSENSNHNN AETNPKGNGE VQ.PNQANKE TQNNSNVQQD
..ESSSSGNA PNKTDGKGEE SEKQNELNES TEEGPKAPQE
..ESSSSGNA PNKTDGKGEE SEKQNELNES TEEGPKAPQE
..ESSSSGNA PNKTDGKGEE SEKQNELNES TEEGPKAPQE
TSSENPNHNN AETN..... .....QANKE TQNNSNVQQD
TSSENPNHNN AETN..... .....QANKE TQNNSNVQQD
TSSENPNHNN AETN..... .....QANKE TQNNSNVQQD

Figure 3.14 Homologues of MSP-7 in *Plasmodia*

A multiple alignment of the *Pf* MSP-7 amino acid sequence, with the amino acid sequences of *Py* MSP-7 (966rc1) and putative MSP-7 homologues retrieved from the *P. falciparum* (prefix MAL), *P. berghei* (Pb) and *P. vivax* (Pv) genome databases.

The C-terminal beta sheet of *Pf* MSP-7 has a high sequence similarity to the *Py* MSP-7 orthologue, and other unique proteins found in the partial *P. falciparum*, *P. berghei* and *P. vivax* Genome databases, suggesting that they may form part of a multigene family.

A pattern of the region covering residues 352 to 369 of the alignment, (F-[KD]-[NK]-[YFN]-[IMV]-[YH]-G-[VIL]-[YN]-[SG]-[FY]-A-K-[QRK]-[HYN]-[SN]-[HY]-L) was used to refine the iterative PSI- and PHI-BLAST protein database searches, but no sequences outside of the Plasmodia databases were recovered.

A = Alanine; C = Cysteine; D = Aspartic acid; E = Glutamic acid; F = Phenylalanine; G = Glycine; H = Histidine; I = Isoleucine; K = Lysine; L = Leucine; M = Methionine; N = Asparagine; P = Proline; Q = Glutamine; R = Arginine S = Serine; T = Threonine; V = Valine; W = Tryptophan; Y = Tyrosine. * indicates a stop codon.

= hydrophobic, non-polar residues; = hydrophilic residues; = hydrophobic, acidic residues.

(With thanks to Tony Holder, Irene Ling, Delmiro Fernandez-Reyes and Ruwani Gunaratne).

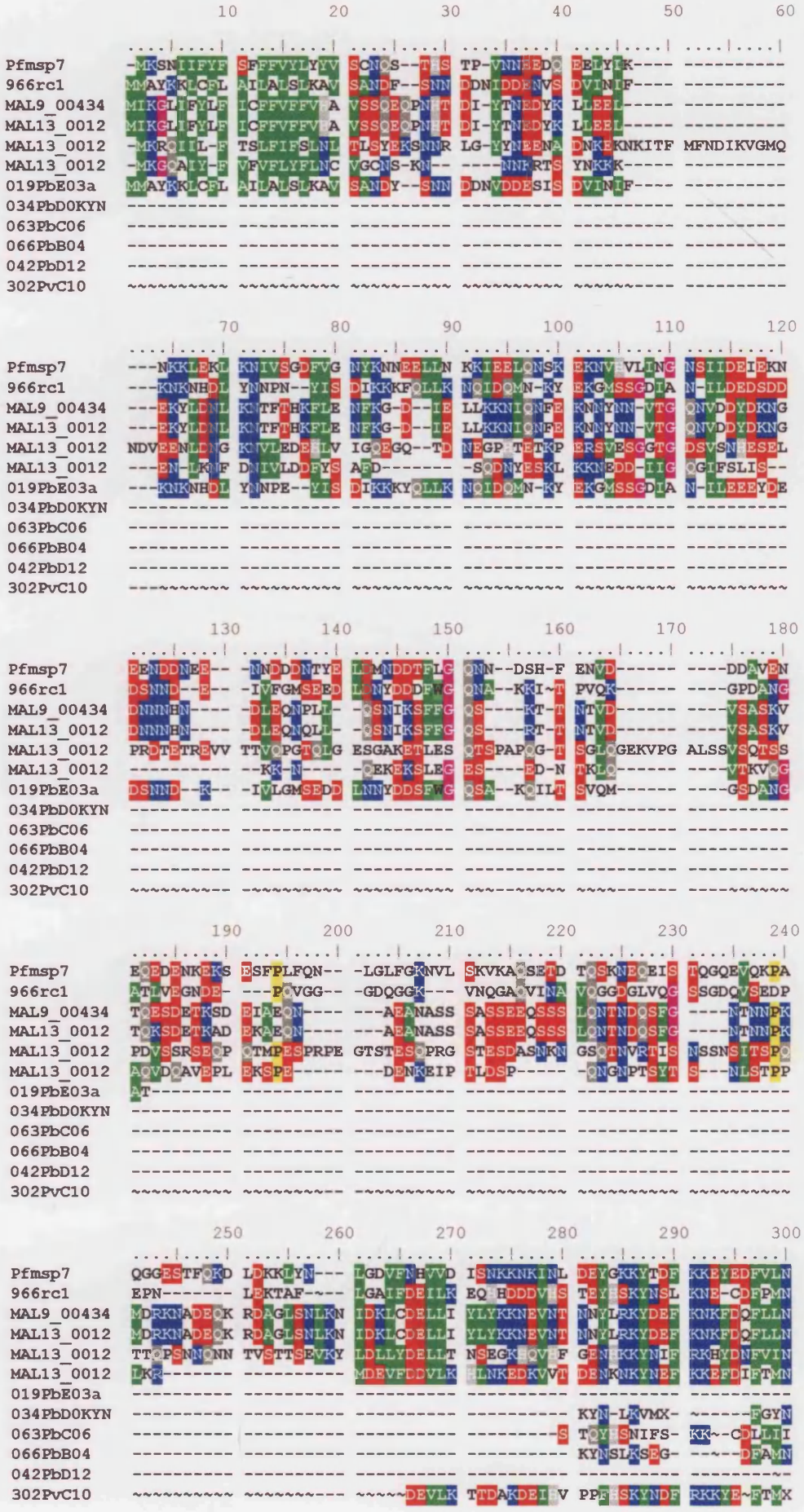
10 20 30 40 50 60
Pfmsp7
966rc1
MAL9_00434
MAL13_0012
MAL13_0012
MAL13_0012
019PbE03a
034PbD0KYN
063PbC06
066PbB04
042PbD12
302PvC10
70 80 90 100 110 120
130 140 150 160 170 180
190 200 210 220 230 240
250 260 270 280 290 300

continued

Figure 3.14 continued

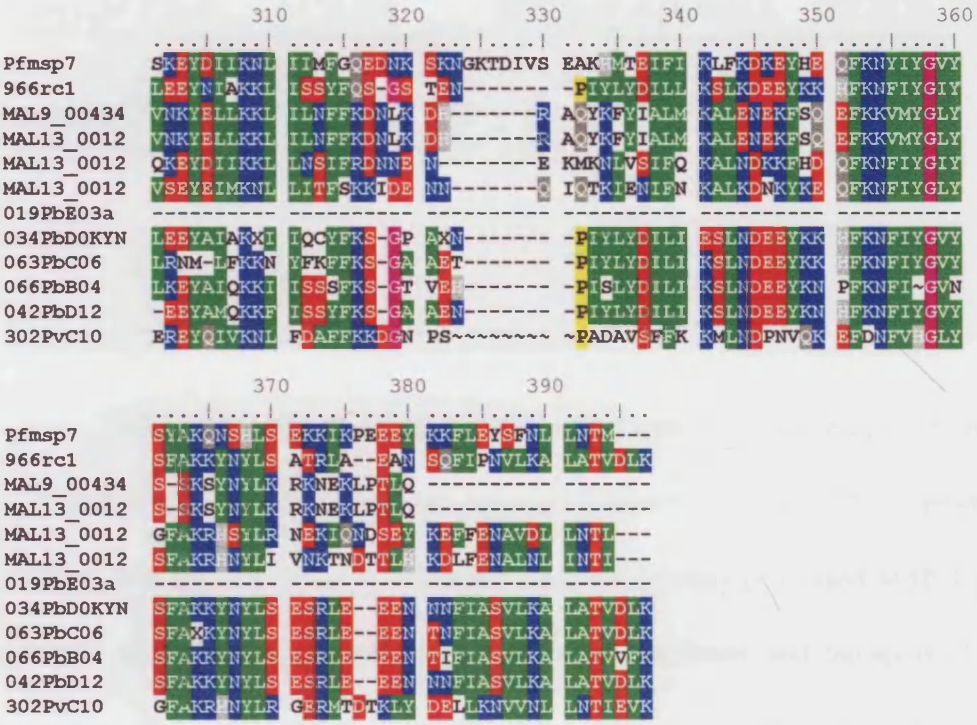
310
320
330
340
350
360
Pfmsp7
966rc1
MAL9_00434
MAL13_0012
MAL13_0012
MAL13_0012
019PbE03a
034PbD0KYN
063PbC06
066PbB04
042PbD12
302PvC10
370
380
390
Pfmsp7
966rc1
MAL9_00434
MAL13_0012
MAL13_0012
MAL13_0012
019PbE03a
034PbD0KYN
063PbC06
066PbB04
042PbD12
302PvC10

CHAPTER FOUR : PREPARING TOOLS FOR INVESTIGATING MSP - 7

4.0 Production of Glutathione-S-Transferase Tagged MSP-7 Proteins

Preliminary analysis of the MSP-7 amino acid sequence suggested that the 41.3 kDa precursor undergoes cleavage between residues 176 and 177, to produce the C-terminal product, MSP-7_{22}, that is detected in the primary processed MSP-1 polypeptide complex on the merozoite surface. To study the translation and transport of the MSP-7 precursor in the developing merozoite, in particular its cleavage events and time of association with MSP-1, antibodies specific to MSP-7 were required. Two regions of MSP-7, designated MSP-7A (residues 23 - 176) and MSP-7B (residues 177 - 351), were expressed as N-terminal GST-fusion proteins with the aim of immunising mice to raise antisera against these regions of MSP-7, for use as tools to investigate MSP-7 biosynthesis and processing.

4.0.0 Amplification of *msp-7a* and Insertion into pGEX-3X

The primers pre22Fexp and pre22Rexp were used to amplify *msp-7a* from 3D7 *Pf* gDNA (See Figure 4.0). The 463 bp *msp-7a* PCR product was ligated into TA plasmid, and 10 recombinant (white) colonies selected for further growth and plasmid purification. Sequencing of the *msp-7a* insert in the MCS with M13-21 and M13revA primers confirmed that *msp-7a* sequence had been correctly amplified. As the pre22Fexp and pre22Rexp primers had *Bam* H1 and *Eco* R1 restriction enzyme sites incorporated into them, *msp-7a* was digested out of a selected recombinant clone with the appropriate enzymes, purified using the Geneclean II kit and ligated into *Bam* H1 and *Eco* R1 digested pGEX-3X plasmid so that the MSP-7A ORF was in-frame with the GST ORF.

The resulting pGEX-3X-*msp-7a* plasmid was transformed into competent DH5α™ *E. coli* and 10 colonies subsequently selected for further growth, and the presence of the *msp-7a* insert confirmed by PCR and sequencing.

4.0.1 Amplification of *msp-7b* and Insertion into pGEX-3X

msp-7b was amplified from T9/96 *Pf* gDNA using the primers p22Fexp and p22Rexp (See Figure 4.1). The 528 bp *msp-7b* PCR product was purified using a QIAquick PCR purification spin column, the primer ends removed by *Bam* H1 and *Eco* R1 restriction enzyme digestion, followed by another spin column purification step, and ligation to *Bam* H1 and *Eco* R1 digested pGEX-3X plasmid so that the MSP-7B and the GST open reading frames were in frame. The resulting pGEX-3X-*msp-7b* plasmid was transformed into competent BL21-Gold™ *E. coli.* Recombinant colonies that were PCR positive for *msp-7b* were selected for further growth and sequenced, confirming that the inserted *msp-7b* sequence was correct and the MSP-7B ORF in frame with that of GST.

4.0.2 Time Course to Determine Optimal Expression of GST-MSP-7A

To balance the optimal expression of the GST-MSP-7A fusion protein with the least amount of fusion protein degradation, a time course was performed in which a selected DH5α pGEX-3X-*msp-7a* colony was cultured at 37°C to log phase growth, and expression of the GST-MSP-7A fusion protein induced with 0.1 mM IPTG whilst culturing at 37°C. Samples of the induced bacteria were taken at 1 hour intervals from induction for 5 hours, and pelleted by centrifugation. The bacterial pellets were lysed directly into SDS-sample buffer, reduced with DTT to break any disulphide bonds between cysteine residues, and the proteins separated on 12.5 % SDS-PAGE gels, prior to detection by Coomassie Blue staining and western blot analysis with mouse anti-GST serum (Figure 4.2A).

The GST-MSP-7A fusion protein was expressed in DH5α cells with an apparent mass of 46 kDa (predicted mass 44.5 kDa), in sufficient quantities to be detected by Coomassie Blue staining. Analysis of the western blotted time course samples with mouse anti-GST antibodies confirmed that the expressed 46 kDa protein visible on the Coomassie stained gel was the full length GST-fusion protein. It also suggested that GST-MSP-7A was degrading in the bacteria during induction, with numerous bands below 46 kDa recognized by anti-GST antibodies. The pattern of degradation stayed constant throughout the experiment, but the quantity of breakdown products increased with each hour following induction. It is likely that the MSP-7A component of the fusion protein was breaking down probably from the C-terminus of the construct, as the anti-GST antibody epitope remained present in all of the breakdown products, the majority of which were larger than GST alone.

Balancing the expression of full size GST-MSP-7A with the quantity of breakdown products at each hour post induction, suggested that the optimal period of GST-MSP-7A induction with 0.1 mM IPTG at 37°C, was 3 hours. The 4 and 5 hour samples showed little difference with that of 3 hours in terms of the quantity of full size GST-MSP-7A, whilst showing an increase in the proportion of breakdown products.

4.0.3 Small Scale Expression of GST-MSP-7B Fusion Protein

As GST-MSP-7A showed optimal expression at 37°C by 3 hours post induction, a selected pGEX-3X-*msp-7b* clone was similarly induced with 0.1 mM IPTG for 3 hours at 37°C. Post induction the bacteria were pelleted and the bacterial pellet lysed directly into SDS-sample buffer with DTT. Proteins were separated on a 12.5 % SDS-PAGE gel and detected by Coomassie Blue staining and western blot analysis with mouse anti-GST serum (Figure 4.2B).

The GST-MSP-7B fusion protein was expressed in BL21-Gold cells with an apparent mass of 44 kDa (predicted 47 kDa) in sufficient quantities to be detected by Coomassie Blue staining. Again there was a significant degree of degradation of the fusion protein with numerous bands below 44 kDa recognised by anti-GST antibodies. This was probably due to the action of bacterial proteases during the expression period, despite the BL21-Gold *E. coli* being defective in OmpT and Lon protease production.

Hence both GST-MSP-7A and GST-MSP-7B fusion proteins are expressed in significant quantities by 3 hours at 37°C following induction of expression with 0.1 mM IPTG. However the fusion proteins were being degraded during expression, probably from the C-terminus by bacterial proteases during the 3 hour period of induction, and perhaps as a consequence of their over-expression in the bacterial host cells.

Both fusion proteins were found to be partially soluble in a solution containing 0.2 % NP40, a non-ionic detergent, with the majority of proteins present in the soluble fraction, but a significant proportion was present in the insoluble fractions (data not shown). This partial solubility may be due to over-expression of the fusion proteins in the bacteria, resulting in the formation of inclusion bodies containing a significant proportion of the expressed protein aggregated to RNA, which would be insoluble under non-denaturing conditions.

4.0.4 Large Scale Purification of GST-MSP-7A and GST-MSP-7B

DH5α pGex-3X-*msp-7a* and BL21-Gold pGEX-3X-*msp-7b* colonies, selected for optimal GST-MSP-7A, and GST-MSP-7B protein expression, were cultured in a 600 ml volume of either LB or TB medium, at 37°C to log phase growth, and expression of the fusion constructs induced for 3 hours with 0.1 mM IPTG, before lysis of the bacterial pellet and solubilisation of proteins in their native state in ice-cold lysis buffer containing a non-ionic detergent (0.2 % NP40) and protease inhibitors. The solubilised protein

fraction was clarified by ultra-centrifugation, the clarified fraction passed down a glutathione agarose bead column, binding the GST component of the fusion proteins to the glutathione agarose beads. Bacterial proteins that did not exhibit specific binding to glutathione were removed during the column washing steps, and the GST-fusion proteins eluted by competition of the glutathione binding site with 5 mM reduced glutathione. Eluted GST-fusion proteins were dialysed into PBS-A and concentrated either by ultra-filtration or with centrifuge concentrators, before quantification by BCA analysis.

Yields of 3 mg of protein per litre of culture for GST-MSP-7A and 1.2 mg of protein per litre of culture for GST-MSP-7B were determined by BCA analysis. The concentrated, purified fusion proteins were analysed on 12.5 % SDS-PAGE gels and either Coomassie Blue stained or western blotted and probed with goat anti-GST antibodies or rabbit anti-MSP-7_{22} serum (Figure 4.3).

Western blot analysis with anti-GST serum confirmed the mass of the purified GST fusion proteins as 46 kDa for GST-MSP-7A and 44 kDa for GST-MSP-7B (Figure 4.3B). The purified fusion proteins still contained numerous breakdown products of the original GST-fusion proteins, despite the inclusion of protease inhibitors and handling of all samples either on ice or at 4°C. Analysis of western blotted GST-MSP-7A, GST-MSP-7B and GST, with rabbit anti-MSP-7_{22} serum and sheep anti-rabbit IgG alkaline phosphatase conjugated antibodies, recognised the GST-MSP-7B fusion protein, but not GST-MSP-7A or GST alone (Figure 4.3C). This suggested that MSP-7_{22} epitopes were present in the MSP-7B fusion protein but not MSP-7A, confirming that the C-terminal half of MSP-7 is actually MSP-7_{22}.

Comparing the pattern of breakdown in the purified proteins to that in bacterial samples lysed directly into SDS-sample cocktail (Figure 4.2A & B), confirmed that the degradation was occurring in the bacteria during expression of the proteins and was not

due to the action of external proteases during cell lysis, solubilisation and purification steps. Induction at 27°C to reduce the action of bacterial proteases during induction was attempted, although no significant decrease in the quantity of breakdown products was seen, and no attempts were made to transform the plasmids into alternative protease deficient strains of *E. coli,* as the quality of the purified proteins was deemed sufficient to raise antisera by immunisation of mice.

4.1 Production of 6-Histidine Tagged MSP-7B Protein

MSP-7B was expressed as a 6-Histidine N-terminal tagged protein using the pTRC-HisC bacterial expression system (Figure 4.4A). The 6*His-MSP-7B fusion protein was to be used as a tool to screen for monoclonal anti-MSP-7B antibodies and for future studies of the structure of MSP-7B by NMR.

4.1.0 Insertion of *msp-7b* into the pTRC-HisC plasmid

The 528 bp *msp-7B* insert was digested out of pGEX-3X-*msp-7b* with *Bam* H1 and *Eco* R1 enzymes, and following purification ligated directly into pTRC-HisC that had been similarly digested with *Bam* H1 and *Eco* R1 (Figure 4.4B). The circularized pTRC-HisC-*msp-7b* was successfully transformed into BL21-Gold *E. coli*, and the presence of the *msp-7b* insert in recombinant colonies confirmed by PCR and restriction digestion.

4.1.1 Small Scale Expression of 6*Histidine tagged-MSP-7B

Selected BL21-Gold pTRC-HisC-*msp-7b* clones were cultured to log phase growth at 37°C, then expression of the 6*His-MSP-7B protein induced with 1 mM IPTG for 5 hours. Bacterial pellets were lysed in SDS-sample cocktail with DTT, proteins separated on 12.5% SDS-PAGE gels and detected with Coomassie Blue stain (data not

shown). Comparing induced to non-induced samples, showed that the 6*His-MSP-7B fusion protein ran with an apparent size of 30 kDa (expected size 21 kDa) and was expressed in sufficient quantity to be visible on a Coomassie Blue stained gel. The discrepancy between the predicted and actual size of the fusion protein was unusual and suggested to be due to the nature of the amino acids in the fusion protein.

The BL21-Gold-6*His-*msp-7b* clone that showed the highest level of 6*His-MSP-7B expression was chosen for optimization of fusion protein expression.

4.1.2 Solubility and Time Course of 6*His-MSP-7B

A time course to determine the time of maximum 6*His-MSP-7B expression was performed at 37°C. Following induction with 1 mM IPTG, bacterial samples were removed and pelleted at hourly intervals over 5 hours. The bacterial cells were lysed in the presence of lysozyme, followed by DNase treatment and solubilisation of proteins in 0.2 % NP40 lysis buffer. NP40 soluble and insoluble fractions from each time point were separated on 12.5 % SDS-PAGE gels and either stained with Coomassie Blue or subjected to western blot analysis with mouse anti-Xpress (Figure 4.5) and rabbit anti-MSP-7_{22} antibodies (data not shown). The expressed 6*His-MSP-7B protein was determined to be partially soluble in the non-ionic detergent NP40 (0.2 %), with approximately one third of the expressed 6*His-MSP-7B fusion protein being solubilised. The anti-Xpress-tag and anti-MSP-7_{22} antibodies both recognized a band at 30 kDa confirming it was 6*His-MSP-7B. The quantity of expressed 6*His-MSP-7B increased with each hour, with a corresponding increase in the proportion of insoluble to soluble 6*His-MSP-7B with time, with approximately 75 % of expressed protein being insoluble in 0.2 % NP40 by 5 hours post induction. The time of maximum level of expression of soluble 6*His-MSP-7B fusion protein was between 2 - 3 hours post induction.

Solubilising 6*His-MSP-7B under native conditions of 20 mM phosphate, 500 mM NaCl (as recommended by Invitrogen) resulted in a similar pattern of solubility, suggesting that, as with the pGEX-3X-*msp-7b* construct, induction of 6*His-MSP-7B expression at 37°C in BL21-Gold *E. coli* resulted in the over-expression of fusion protein and the formation of fusion protein – RNA aggregates or inclusion bodies, that prevented solubilisation of a significant quantity of the expressed fusion protein under non-denaturing conditions.

4.1.3 Large Scale Purification of 6*His-MSP-7B

To obtain 6*His-MSP-7B for analysis of the antibody response of the GST-MSP-7B immunised mice, and to screen hybridoma colonies by ELISA, large scale expression of 6*His-MSP-7B was performed. The resulting 6*His-MSP-7B fusion protein was partially solubilised under native conditions and run down an IMAC Probond resin column, binding the 6*His tag to the Nickel matrix. Non-specifically bound proteins were removed by high stringency washes, and the 6*His-MSP-7B eluted by competition with increasing concentrations of imidazole to a final concentration of 750 mM. Analysis of the eluted fractions by SDS-PAGE (data not shown) suggested bacterial proteins of approximately 70 kDa were co-eluted with the 30 kDa fusion protein, most probably due to the washes prior to elution being of insufficient stringency, or because bacterial proteins bound to the Nickel resin with high specificity. The final 750 mM imidazole elution contained the least quantity of contaminating proteins and was used for ELISA and western blot analysis after dialysis into PBS and concentration.

Western blot analysis of purified 6*His-MSP-7B with rabbit anti-MSP-7_{22} polyclonal serum (absorbed with *E. coli* proteins) recognised only a band at 30 kDa, the 6*His-MSP-7B protein, whilst mouse anti-MSP-7B polyclonal serum (raised against the GST-MSP-7B fusion protein) bound to an additional band of approximately 70 kDa,

suggesting that bacterial proteins were still present in the purified samples (Figure 4.6). The 70 kDa protein is likely to be heat shock protein, a common contaminant in bacterial fusion protein expression systems. The presence of this protein in the purified sample may explain the large number of false positive results obtained when using purified 6*His-MSP-7B as the antigen in an antibody capture ELISA for isolation of an anti-MSP-7B monoclonal antibody (Section 4.2.1). However western blotted purified 6*His-MSP-7B was suitable for screening hybridoma supernatants as the presence of anti-MSP-7B antibodies would be identified by binding to the 30 kDa 6*His-MSP-7B on the western blot.

4.2 Anti-MSP-7 Antibody Production

The GST-MSP-7A and GST-MSP-7B fusion proteins were used to immunise female Balb C mice to induce a specific IgG antibody response against the MSP-7 components of the fusion protein constructs. Three mice were immunized with GST-MSP-7A, and 8 mice immunized with GST-MSP-7B as described in section 2.7. Serum was tested by IFAT on fixed *P. falciparum* parasites, and collected for further analysis by western blot and immunoprecipitation experiments. A monoclonal antibody to MSP-7B was raised, and following problems with characterization using standard anti-mouse IgG antibodies, the monoclonal antibody isotype was determined to be of the IgA isotype.

4.2.0 Raising Polyclonal Mouse Anti-MSP-7A and MSP-7B Sera

Immunisation of female Balb C mice with the GST-MSP-7A and GST-MSP-7B fusion proteins induced a specific IgG antibody response against *P. falciparum* parasites as determined by IFAT with mixed stage asexual parasites, using sera from tail bleeds taken 1 week after the third fusion protein boost. Two of 3 mice immunised with GST-

MSP-7A had detectable antibody titres by IFAT of 1/4000 to 1/8000; whilst 6 of 8 mice immunised with GST-MSP-7B showed antibody titres of 1/4000 to 1/8000 against blood stage *P. falciparum* parasites.

Both the anti-GST-MSP-7A and anti-GST-MSP-7B sera were positive by IFAT against FCB-1 (Wellcome MSP-1 type), 3D7 and T9/96 (MAD-20 MSP-1 type) acetone or acetone/methanol fixed schizonts, presenting a bunch of grapes-like binding pattern similar to that obtained with α-MSP-1 antibodies and with rabbit α-MSP-7_{22} sera (Stafford *et al.* 1996), but not ring or trophozoite stages (Figure 4.7). This suggests that regions of both MSP-7A and MSP-7B proteins are present on or close to the schizont and developing merozoite surface, but are not carried into an invaded red blood cell on merozoite entry. This ties in with the preliminary Northern blot analysis (Section 3.2.1) that showed a high level of MSP-7 transcription in schizonts, suggesting that the MSP-7 protein is only translated as the merozoites start to develop in schizonts. The antisera showed cross-reactivity with both FCB-1 and T9-96 parasites, confirming that the FCB-1, T9-96 and 3D7 strains of *P. falciparum* share MSP-7 antibody binding epitopes, as predicted from the high degree of MSP-7 amino acid conservation (See section 3.3.1).

Serum isolated from mouse B1 (anti-GST-MSP-7B) gave an antibody titre of 1/8000 by IFAT. Western blot analysis of 6*His-MSP-7B with the mouse B1 serum diluted to 1/500 in PBS, 1 % BSA, showed that it contained antibodies specific to both the recombinant MSP-7B component of the fusion protein, confirming the IFAT results that the antibodies were specific to MSP-7, and to higher molecular mass proteins presumed to be the *E. coli* HSP-70 co-purified with the fusion protein (Figure 4.6).

The anti-GST-MSP-7A and anti-GST-MSP-7B polyclonal sera were used to characterize the biosynthesis and function of MSP-7 in developing schizonts, the results of which are presented in Chapter 5.

4.2.1 JP-1 Mouse Anti-MSP-7B Monoclonal Antibody Production

In order to produce a monoclonal antibody specific to MSP-7B, one IFAT positive mouse (B1) immunized with GST-MSP-7B was boosted for a fourth time and the spleen removed 6 days later for extraction of splenocytes. Serum isolated from the mouse at the time of death gave an antibody titre of 1/8000 by IFAT and bound to western blotted MSP-7B fusion proteins (Section 4.2.0).

SP2-10-AG14 myeloma cells were grown in the presence of the purine analog 8-azaguanine that selects for myeloma cells deficient in the nucleotide salvage pathway. Splenocytes removed from mouse B1 were fused with the nucleotide salvage pathway deficient myeloma cells and the resulting hybridoma fusion cells positively selected by growth in hypoxanthine, aminopterin and thymidine (HAT) medium. Aminopterin inhibits the de novo purine and pyrimidine synthesis pathway, resulting in the death of all unfused myeloma cells that revert to the defunct nucleotide salvage pathway. Hypoxanthine and thymidine select for fusion cells that are salvage pathway positive.

Supernatant from hybridoma cultures were initially tested by ELISA using 1μg ml^{-1} 6*His-MSP-7B recombinant protein as the antigen and positives determined as having a cut off value of $A_{492nm} = 0.5$. Supernatants from ELISA positive colonies were tested by IFAT as before, to ensure the expressed antibodies exhibited the correct 'bunch of grapes-like' pattern of fluorescence as seen in section 4.2.0. No fluorescence and hence antibody binding to blood stage parasites was detected by IFAT. Since the purified 6*His-MSP-7B protein was later found to contain *E. coli* HSP-70 proteins that had co-eluted with the fusion protein, it was predicted that the ELISA positive supernatants were probably false negatives, and it was decided to instigate an alternative method of screening hybridoma supernatants using parasites fixed on multi-well IFAT slides and confirmation of IFAT positive supernatants by western blot analysis of 6*His-MSP-7B.

After an additional 2 weeks growth to increase the antibody titre in the culture supernatant, the primary hybridoma colony supernatants were re-screened by IFAT (Figure 4.8). Supernatant from five wells of the primary hybridoma cell line was identified as being IFAT positive. Of these, cells from one well (Plate 8, well A5) that showed the best fluorescence pattern and bound to western blotted 6*His-MSP-7B and had been positive by ELISA, were selected for cloning by limiting dilution in Hypoxanthine and Thymidine (HT) medium. Supernatants from wells with colonies from the first limiting dilution step were screened by IFAT and western blot analysis. Colonies from one positive well (Plate 1, well B2) were selected and cloned in a second limiting dilution step. Supernatants from colonies from the second cloning step were tested by IFAT and western blot analysis, and one positive well selected (Plate 1, well F3) for a third cloning by limiting dilution step. By the third cloning step all the resulting hybridoma colonies were producing antibody in the culture supernatant that gave an identical fluorescence pattern on schizonts to that of the mouse B1 anti-GST-MSP-7B serum, and bound strongly to western blotted 6*His-MSP-7B. A hybridoma in one well (Plate 2, well G10) from the third cloning step, was deemed monoclonal, named JP-1, and selected for further growth. The JP-1 tissue culture supernatant was harvested and used to analyse the specificity and sensitivity of the JP-1 monoclonal antibody in IFAT and western blot analyses.

4.2.2 Analysis of the JP-1 Anti-MSP-7B Mouse Monoclonal Antibody Isotype

The monoclonal JP-1 antibody was detected binding to 6*His-MSP-7B and GST-MSP-7B fusion proteins, but not to GST only, when tested by western blot analysis with a secondary anti-mouse polyvalent antibody. However when a secondary anti-mouse IgG-specific antibody was used for either western blot analysis or IFAT, the sensitivity of the assays decreased, suggesting that the JP-1 isotype was not IgG.

To determine the isotype of the mouse JP-1 monoclonal antibody, the JP-1 hybridoma supernatant was tested with the Sigma ImmunoType Mouse Monoclonal Antibody Isotyping Kit. JP-1 was determined to be a mouse monoclonal IgA antibody (See Figure 4.9A). A mouse monoclonal antibody of IgG2a isotype was used as a positive control, confirming that the isotyping test worked.

The development of an anti-MSP-7B IgA antibody is somewhat unusual as mouse monoclonal antibodies are predominantly IgG1 isotypes, and IgA is usually associated with mucosal immunity, not with protection against blood borne diseases. The presence of an IgA B cell may be a result of the intra-peritoneal immunisation of the mice, although the majority of anti-MSP-7 antibodies in the serum were predominantly IgG isotypes, since they were bound strongly by secondary α-mouse IgG specific antibodies during IFAT and western blot analyses (data not shown).

Following determination of the IgA isotype for JP-1, IFAT analysis of acetone – methanol fixed 3D7 *P. falciparum* parasites, using the JP-1 culture supernatant at a 1/10 dilution and a secondary anti-mouse IgA specific antibody, showed increased sensitivity, when compared to a FITC-conjugated anti-mouse IgG secondary antibody (Figure 4.9B-D). This confirmed the isotyping result that JP-1 is a mouse IgA monoclonal antibody. The low intensity of fluorescence with the anti-mouse IgG antibodies may be due to cross reactivity between the κ and λ light chains of IgA and IgG molecules. The JP-1 anti-MSP-7B monoclonal was detected binding at the edges of developing merozoites in schizonts, and on the surface of released merozoites prior to invasion of red blood cells. This confirmed that the JP-1 monoclonal binds to the MSP-7_{22} component of MSP-7 during merozoite development, and to MSP-7_{22} in released merozoites whilst in the MSP-1 complex prior to secondary MSP-1 processing.

4.3 SUMMARY

Analysis of the MSP-7 amino acid sequence suggests that the MSP-7_{22} polypeptide in the shed MSP-1 complex is derived from cleavage of MSP-7 between residues 176 and 177. The N-terminal region of MSP-7 (MSP-7A) and the MSP-7_{22} C-terminal region (MSP-7B) were expressed in the pGEX-3X bacterial expression system as recombinant N-terminal tagged Glutathione-S-Transferase fusion proteins. Both GST-MSP-7A (46 kDa) and GST-MSP-7B (44 kDa) were purified as soluble proteins in non-denaturing conditions, yielding 3 mg of protein per litre of culture of GST-MSP-7A, and 1.2 mg of protein per litre of culture of GST-MSP-7B. The purified samples contained both full-length GST fusion proteins, and fragments of the expressed proteins that had undergone C-terminal degradation by host bacterial proteases during the expression period. GST-MSP-7B was recognized by the rabbit anti-MSP-7_{22} serum, confirming that MSP-7_{22} is part of MSP-7.

MSP-7B was also expressed in the pTRC-HisC bacterial expression system as a 6*Histidine tagged N-terminal tagged protein. The 30 kDa 6*His-MSP-7B was purified by IMAC as a soluble protein under native conditions, and purified 6*His-MSP-7B used as a tool to screen for an anti-MSP-7B mouse monoclonal antibody.

Immunisation of Balb C mice with the GST-MSP-7A and GST-MSP-7B fusion proteins induced specific anti-GST-MSP-7A and anti-GST-MSP-7B antibody titres of between 1/4000 to 1/8000, as determined by IFAT of *P. falciparum* blood stage parasites. The mouse sera bound to what is presumed to be MSP-7, on the surface of developing merozoites in schizonts, with a similar fluorescence pattern to each other and to anti-MSP-1 antibodies. Additionally the anti-MSP-7 antibodies recognized parasites by IFAT from both FCB-1 (Welcome MSP-1 type) and 3D7 / T9-96 (MAD-20 MSP-1 type) strains of *P. falciparum*, suggesting that the antibodies show cross-reactivity

between strains of *P. falciparum* as predicted from the highly conserved MSP-7 amino acid sequence.

A hybridoma expressing monoclonal anti-MSP-7B antibody (JP-1) was produced and isolated by a combination of IFAT and western blot screening, and the JP-1 monoclonal antibody isotype was determined to be IgA. When tested by IFAT the JP-1 anti-MSP-7B monoclonal binds specifically to the surface of developing merozoites in mature schizonts and to released merozoites.

It is hypothesised from these preliminary IFAT results, that the 41.3 kDa MSP-7 precursor is translated during merozoite development, and that it is located, close to MSP-1, on or around the surface of the developing merozoite. As the anti-MSP-7A and anti-MSP-7B IFAT patterns were very similar, it was unclear whether the full length MSP-7 precursor was present on the surface of the developing merozoites, or if MSP-7 had already undergone cleavage at residues 176 - 177 and both the predicted N- and C-terminal cleavage products were transported to the surface of developing merozoites. Further analyses using the anti-MSP-7 antibodies to characterise the biosynthesis and processing events of MSP-7 are described in the next chapter.

Figure 4.0 Amplification of *msp-7a* and Insertion into the pGEX-3X Bacterial Expression Plasmid

A) The primers pre22Fexp and pre22Rexp were used to PCR amplify the 463 bp *msp-7a* from 3D7 *Pf* gDNA.

The 463 bp *msp-7a* PCR product was ligated into TA plasmid, and recombinant colonies analysed by *Eco* R1 restriction digestion for the presence of the *msp-7a* insert. The insert in selected clones was sequenced with M23-21 and M13-revA primers, confirming that the *msp-7a* sequence had been correctly amplified.

B) As the primers pre22Fexp and pre22Rexp had *Bam* H1 and *Eco* R1 restriction enzyme sites respectively incorporated into them, *msp-7a* was digested out of a selected TA plasmid clone with *Bam* H1 and *Eco* R1.

The *Eco* R1 / *Bam* H1 digested *msp-7a* fragment was purified using Geneclean II, and then ligated into *Bam* H1 and *Eco* R1 digested pGEX-3X plasmid, so that the MSP-7A ORF was in frame with the GST ORF. The resulting pGEX-3X-*msp-7a* plasmid was transformed into competent DH5α™ *E. coli.*

C) The presence of the *msp-7a* insert in recombinant colonies was confirmed by PCR using the pre22Fexp and pre22Rexp primers, using gDNA as a positive PCR control (+ve), and sdw as a negative PCR control (-ve), and the insert sequenced with pGEX-3X primers.

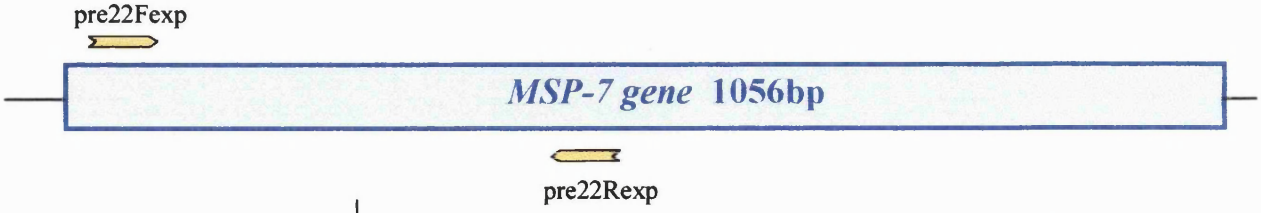

PCR

msp-7a 463 bp PCR Product

Bam H1 site

Eco R1 site

Bam H1 site

Eco R1 site

msp-7a PCR product ligated to TA vector

Insert sequenced and *msp-7a* cut out of TA vector with *Bam* H1 & *Eco* R1, & purified

Bam H1

Eco R1

Bam H1

Eco R1

msp-7a ligated to pGEX-3X

pGEX-3X-*msp-7a* transformed into competent DH5α *E. coli.* Insert confirmed by PCR and sequencing

A

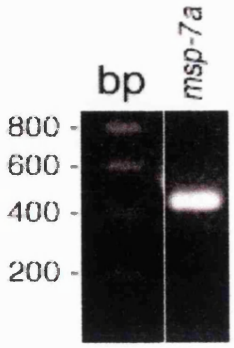

B

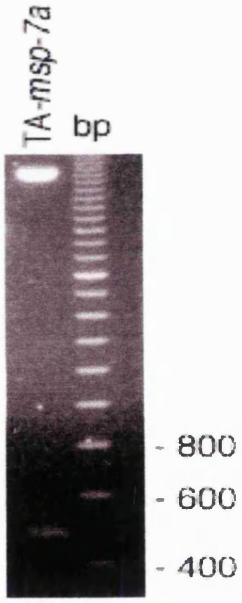

C

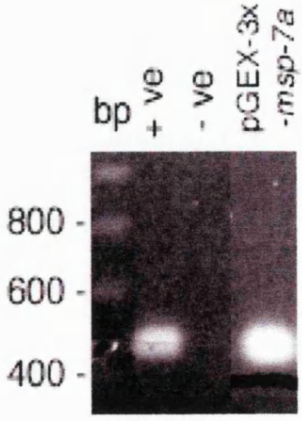

Figure 4.1 Preparation of *msp-7b* for GST-Fusion Protein Production

A) The 528 bp *msp-7b* was PCR amplified from T9/96 *Pf* gDNA using the primers p22Fexp and p22Rexp that have *Bam* H1 and *Eco* R1 restriction sites respectively incorporated into them.

B) The *msp-7b* PCR product was purified with a QIAquick PCR purification spin column (*msp-7b*), the 5' and 3' primer ends removed from the purified *msp-7b* PCR product by *Bam* H1 and *Eco* R1 endonuclease restriction enzyme digestion (*msp-7b* cut), and the digested *msp-7b* fragment purified with a Geneclean II purification step (*msp-7b* cut & purified).

The *Bam* H1 / *Eco* R1 digested *msp-7b* was ligated into *Bam* H1 and *Eco* R1 digested pGEX-3X plasmid ensuring the MSP-7B and GST ORFs were in frame.

C) The pGEX-3X-*msp-7b* plasmid was transformed into competent BL21-Gold™ *E. coli*. The presence of *msp-7b* in recombinant colonies (pGEX-3X-*msp-7b*) was confirmed by PCR with p22Fexp and p22Rexp primers, using gDNA as a positive PCR control (+ve), and sdw as a negative PCR control (-ve). The insert was then sequenced with pGEX-3X primers.

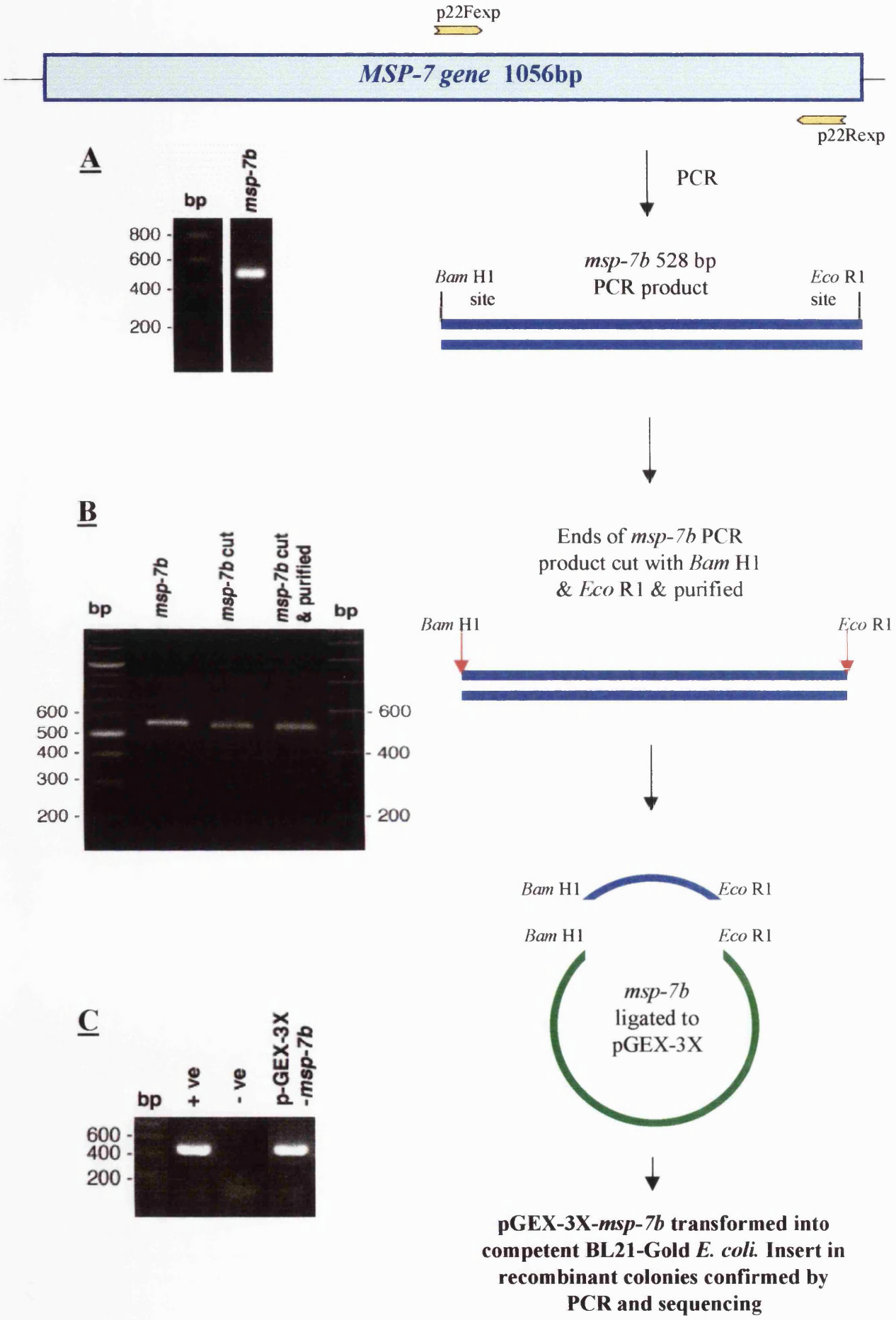
p22Fexp
MSP-7 gene 1056bp
p22Rexp
A
bp
msp-7b
800
600
400
200
PCR
msp-7b 528 bp
PCR product
Bam H1
site
Eco R1
site
B
bp
msp-7b
msp-7b cut
msp-7b cut
& purified
bp
600
500
400
300
200
600
400
200
Ends of msp-7b PCR
product cut with Bam H1
& Eco R1 & purified
Bam H1
Eco R1
Bam H1
Eco R1
Bam H1
Eco R1
msp-7b
ligated to
pGEX-3X
C
bp
+ ve
- ve
p-GEX-3X
-msp-7b
600
400
200
pGEX-3X-msp-7b transformed into
competent BL21-Gold E. coli. Insert in
recombinant colonies confirmed by
PCR and sequencing

Figure 4.2 Expression Analysis of GST-MSP-7A and GST-MSP-7B

A) Time Course Analysis of GST-MSP-7A Expression

A selected DH5α-pGEX-3X-*msp-7a* colony was cultured at 37°C to log phase growth then induced with 0.1 mM IPTG to express GST-MSP-7A. Samples of the induced bacteria were taken at 1 hour intervals from the point of induction for 5 hours (T = 0 to T = 5), pelleted and cells lysed into SDS-sample cocktail with DTT. Proteins from each time point (T=0 to T=5) were separated on 12.5 % SDS-PAGE gels alongside a non-induced control sample (-ve), and purified GST protein (GST). The SDS-PAGE gel was Western blotted and probed with mouse anti-GST serum, and binding detected with sheep anti-mouse IgG AP conjugated antibodies and NBT / BCIP colour development.

GST-MSP-7A ran with an apparent mass of 46 kDa that was recognized by anti-GST antibodies, confirming it was the full length GST-MSP-7A fusion protein. GST-MSP-7A was expressed in significant quantities within 1 hour of induction (T = 1) when compared to the T = 0 control. The quantity of expressed GST-MSP-7A increased with each hour post induction, as did the intensity of bands below 46 kDa recognized by anti-GST antibodies, suggesting that GST-MSP-7A was being degraded by bacterial proteases during expression. Balancing the optimal expression of full size GST-MSP-7A with the least quantity of breakdown products, suggests that the optimal time of expression appeared to be 3 hours post induction (T = 3).

B) Western Blot Analysis of Small Scale GST-MSP-7B Expression

Recombinant pGEX-3X-*msp-7b* and pGEX-3X BL21-Gold colonies were induced with 0.1 mM IPTG for 3 hours at 37°C. Induced (+) and non-induced (-) bacterial pellets were lysed directly into SDS-sample buffer with DTT, and protein samples separated on a 12.5 % SDS-PAGE gel, western blotted and probed with mouse anti-GST serum, followed by sheep anti-mouse IgG AP-conjugated antibodies and NBT/BCIP colour development.

Comparing non-induced and induced samples identified a 44 kDa protein (GST-MSP-7B) present only in the pGEX-3X-*msp-7b* induced sample, which was recognized by anti-GST antibodies. Hence GST-MSP-7B is expressed in large quantities by 3 hours of induction with IPTG. The anti-GST antibodies also bound to a number of bands below 44 kDa suggesting that as with GST-MSP-7A, the fusion protein was being degraded by bacterial proteases during the 3 hour expression period.

A

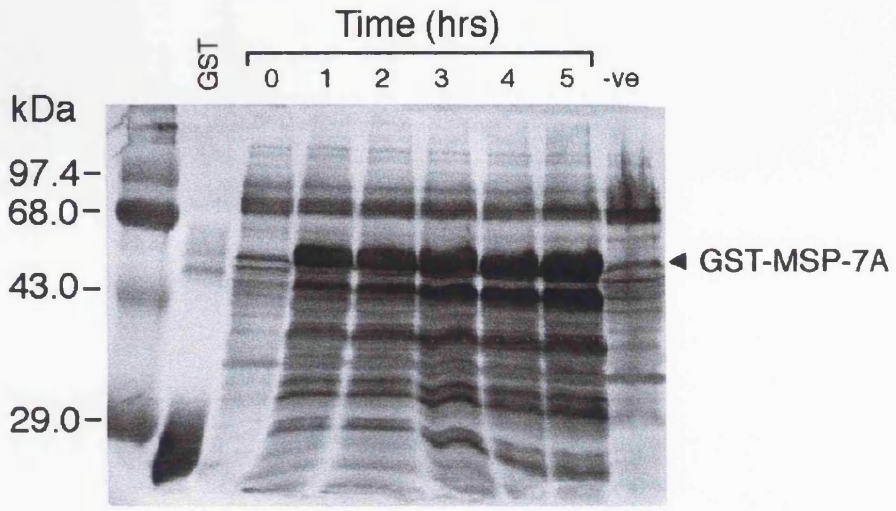
Time (hrs)
GST
0
1
2
3
4
5
-ve
kDa
97.4
68.0
43.0
29.0
GST-MSP-7A

B

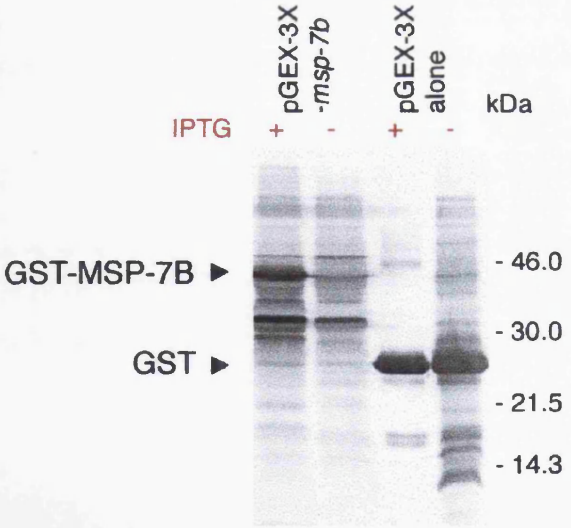
pGEX-3X -msp-7b
pGEX-3X alone
kDa
IPTG
+
-
+
-
GST-MSP-7B
GST
46.0
30.0
21.5
14.3

Figure 4.3 Analysis of GST-MSP-7A and GST-MSP-7B Purified Proteins

A) Coomassie Blue stained 12.5 % SDS-PAGE gel of the purified and concentrated GST-MSP-7A (apparent mass 46 kDa) and GST-MSP-7B (apparent mass 44 kDa) fusion proteins. Both proteins have a number of smaller fragments that have co-purified with the full size fusion protein and match the pattern of breakdown seen in the induced bacterial samples (Figure 4.2 A and B).

B) Western blot analysis of purified GST-MSP-7A, GST-MSP-7B and GST, probed with goat anti-GST antibodies and secondary AP-conjugated anti-goat IgG antibodies, and detected with NBT / BCIP colour development. The anti-GST antibodies bound all three full length proteins at 46 kDa (GST-MSP-7A), 44 kDa (GST-MSP-7B) and 26 kDa (GST). The purified GST-MSP-A and GST-MSP-7B fusion protein breakdown products were recognized by the anti-GST antibodies with the same pattern as seen in the Coomassie Blue stained gel (Section A), and in the induced bacteria (Figure 4.2 A and B). The breakdown products have obviously retained both the glutathione binding site and the anti-GST antibody epitopes, suggesting that the fusion proteins are being degraded mostly from the C-terminus of the fusion construct.

C) Western blot analysis of purified GST-MSP-7A, GST-MSP-7B and GST, probed with rabbit anti-MSP-7_{22} serum and secondary AP-conjugated anti-rabbit IgG antibodies and detected with NBT/BCIP colour development. The rabbit α-MSP-7_{22} sera only bound to the 44 kDa GST-MSP-7B and its breakdown products, and not to GST or GST-MSP-7A, confirming that MSP-7B contains the same epitopes as MSP-7_{22} purified from the shed MSP-1 complex.

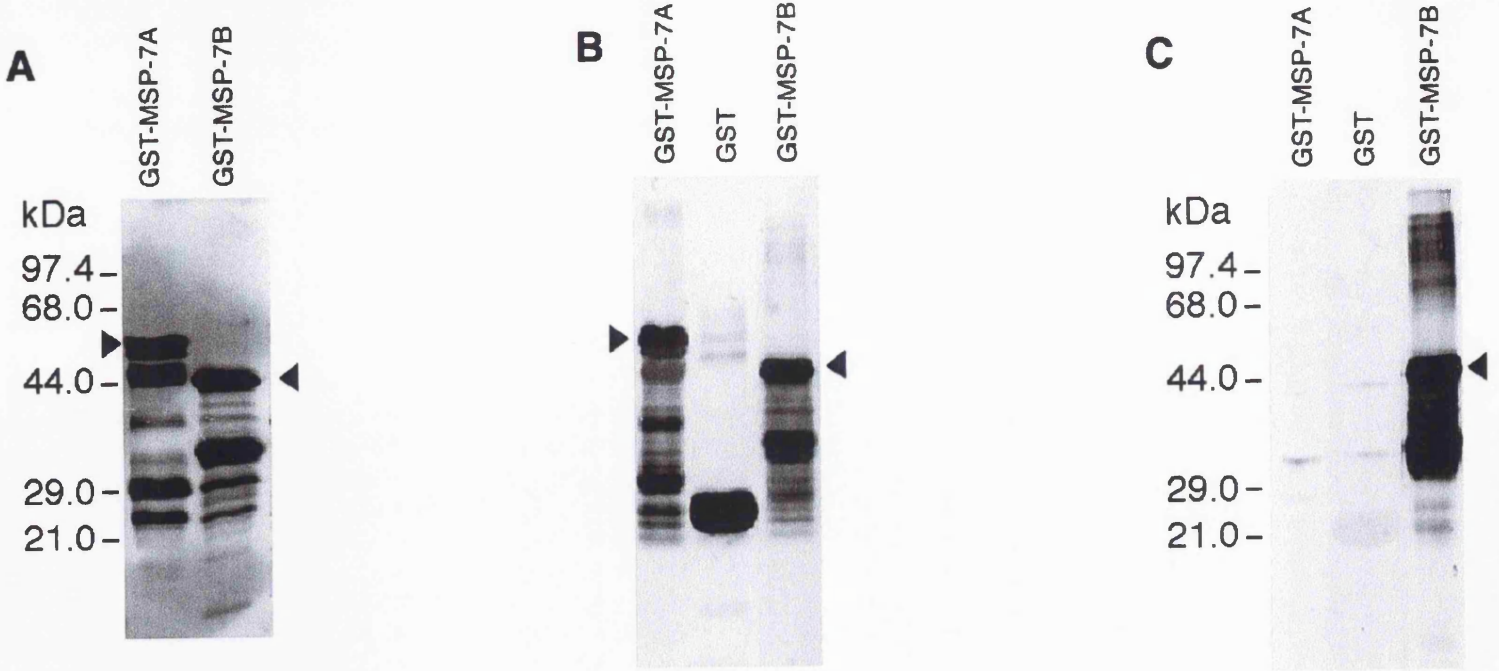
A
GST-MSP-7A
GST-MSP-7B
kDa
97.4
68.0
44.0
29.0
21.0
B
GST-MSP-7A
GST
GST-MSP-7B
C
GST-MSP-7A
GST
GST-MSP-7B
kDa
97.4
68.0
44.0
29.0
21.0

Figure 4.4 Insertion of *msp-7b* into the MCS of pTRC-HisC

A pGEX-3X-*msp-7b* was digested with *Bam* H1 and *Eco* R1 enzymes, and the *msp-7b* insert purified using a Geneclean II kit (*msp-7b* purified).

The digested and purified *msp-7b* was ligated into pTRC-HisC that had been similarly digested with *Bam* H1 and *Eco* R1. The resulting pTRC-HisC-*msp-7b* plasmid was successfully transformed into BL-21G *E. coli.*

B The presence of the *msp-7b* insert in recombinant colonies was confirmed by restriction digestion analysis with *Bam* H1 and *Eco* R1.

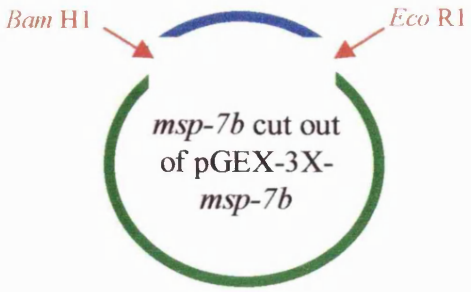

msp-7b fragment Geneclean II purified

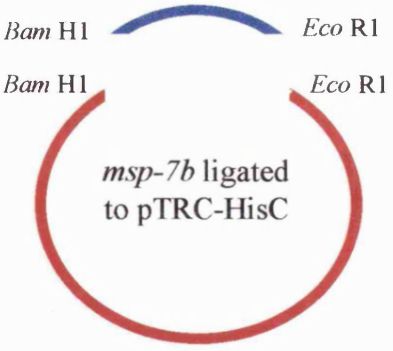

pTRC-HisC-*msp-7b* transformed into competent BL21-Gold *E. coli.*

A

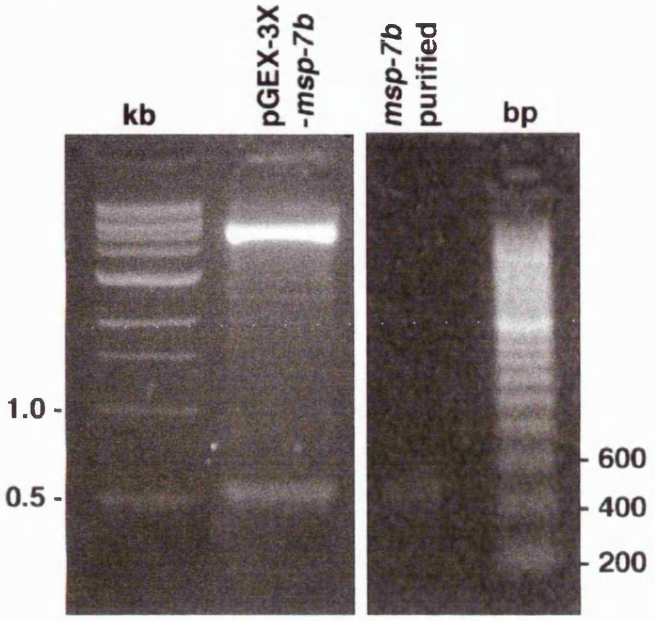

B

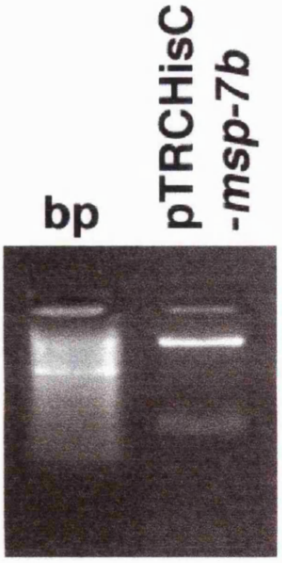

Figure 4.5 Time Course and Solubility Analysis of 6*His-MSP-7B

A selected BL-21-Gold-pTRC-HisC-*msp-7b* clone was grown at 37°C to log phase growth, and expression of 6*His-MSP-7B induced by the addition of 1 mM IPTG. Samples of the induced bacteria were taken at hourly intervals from the point of induction for 5 hours (T = 0 to T = 5). Samples from each time point were pelleted, cells lysed in lysozyme and DNase, and proteins solubilised in 0.2 % of non-ionic detergent NP40.

NP40 soluble (s) and insoluble (p) fractions from each time point were separated on 12.5 % SDS-PAGE gels and Western blotted for analysis with mouse anti-Xpress, followed by secondary sheep anti-mouse IgG AP-conjugated antibodies, and NBT/BCIP colour development.

The anti-Xpress tag antibodies recognized 6*His-MSP-7B with an apparent mass of 30 kDa. Within 1 hour of induction (T = 0) the 6*His-MSP-7B fusion protein was being expressed, giving equal quantities of NP-40 soluble and insoluble proteins. The quantity of expressed 6*His-MSP-7B increased with each hour, with a corresponding increase in the proportion of insoluble to soluble 6*His-MSP-7B with time, with approximately 75 % of expressed protein being insoluble in 0.2 % NP40 by 5 hours post induction (T = 5). The increase in insoluble protein is probably due to over-expression of the fusion protein and formation of inclusion bodies. The maximum level of expression of soluble 6*His-MSP-7B fusion protein was determined to be between 2 - 3 hours post induction (T = 3). Reactivity of antibodies to lysozyme (21 kDa) was noted.


Time of Induction (hrs)
0
1
2
3
4
5
p
s
kDa
46 –
30 –
21 –
6*His-MSP-7B

Figure 4.6 Western Blot Analysis of Purified 6*His-MSP-7B

Purified 6*His-MSP-7B was run on a 12.5 % SDS-PAGE gel, western blotted and probed with a variety of primary antibodies (1-4). Binding of primary antibodies was detected using species appropriate HRP-conjugated secondary antibodies, and visualized by ECL.

1) Rabbit anti-MSP-7_{22} polyclonal serum (pre-absorbed with *E. coli* proteins) recognized only the 30 kDa 6*His-MSP-7B fusion protein.

2) Mouse anti-GST-MSP-7B polyclonal serum bound to both 6*His-MSP-7B and an additional band of approximately 70 kDa. The binding of mouse anti-GST-MSP-7B antibodies to 6*His-MSP-7B, confirms that the GST-MSP-7B immunization procedure raised antibodies specific to MSP-7B, and these recognise denatured MSP-7B epitopes in the 6*His-MSP-7B.

3) Normal (pre-immune) mouse serum (NMS) did not react with any proteins.

4) The anti-MSP-7B JP-1 mouse monoclonal antibody only binds to the 30 kDa 6*His-MSP-7B fusion protein.

Hence the 70 kDa protein was recognized only by mouse anti-GST-MSP-7B sera (2). This suggests that the 70 kDa protein is not a dimer of 6*His-MSP-7B, and is the same bacterial protein that co-eluted with 6*His-MSP-7B during elution from the IMAC at low concentrations of imidazole. This protein may be HSP-70, a common contaminant of bacterial expression systems. The presence of antibodies to HSP-70 in the mouse serum, whilst NMS does not contain any, suggests that either the immunogen inoculated into the immunized mice contained epitopes cross-reactive with HSP-70 or actually contained HSP-70 that had co-purified with the GST-fusion protein, or that the immunisation procedure stimulated anti-HSP antibodies.

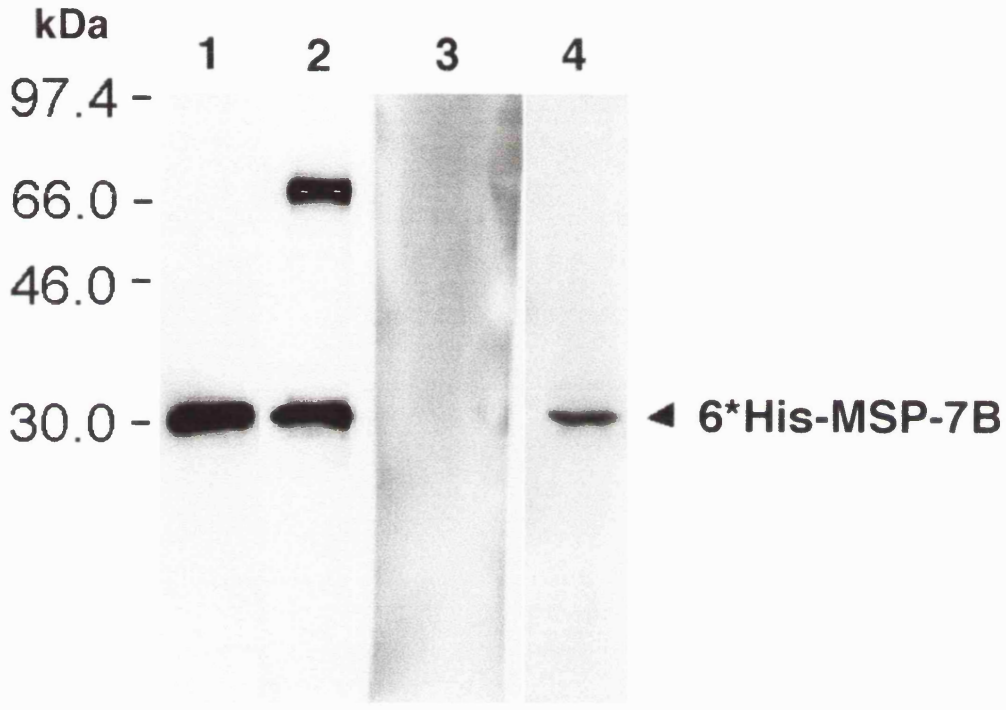
kDa
1
2
3
4
97.4
66.0
46.0
30.0
6*His-MSP-7B

Figure 4.7 IFAT Analysis of Mouse Anti-GST-MSP-7A and Anti-GST-MSP-7B Sera

Sera from mice immunized with either GST-MSP-7A **(A)** or GST-MSP-7B **(B)** fusion proteins were tested by IFAT on acetone-fixed *P. falciparum* non-synchronous blood stage parasites to determine the anti-MSP-7 antibody titres. Monoclonal mouse anti-MSP-1 antibodies **(C)** were used as positive controls, whilst normal mouse serum (NMS) **(D)** was used as the negative control.

Binding of murine antibodies was detected with FITC-conjugated anti-mouse IgG antibodies. Slides were viewed with an Olympus Fluorescent microscope using the appropriate wavelength filters, to visualize Evans Blue stained erythrocytes, and FITC-conjugated antibodies. Light microscopy was used in conjunction with the FITC filters to visualize haemozoin crystals that are indicative of late stage schizonts. Images were captured using a built-in camera and ASA 1600 colour slide film.

Two of 3 mice immunised with GST-MSP-7A gave detectable antibody titres of 1/4000 to 1/8000 by IFAT **(A)**. Six of 8 mice immunised with GST-MSP-7B showed antibody titres of 1/4000 to 1/8000 **(B)**. At these antibody titres both the anti-GST-MSP-7A **(A)** and anti-GST-MSP-7B **(B)** sera bound to late stage schizonts (as determined by presence of haemozoin crystals). Both the anti-MSP-7A and MSP-7B mouse sera bound to schizonts with a bunch of grapes-like pattern, similar to that obtained in schizonts with anti-MSP-1 antibodies **(C)**. Neither the anti-MSP-7A, or MSP-7B antibodies were detected binding to ring or trophozoite stages. This suggests that regions of both MSP-7A and MSP-7B proteins are present on or close to the schizont and developing merozoite surface, and are not carried into an invaded red blood cell on merozoite entry. The NMS **(D)** did not show any reactivity with parasites or red blood cells.

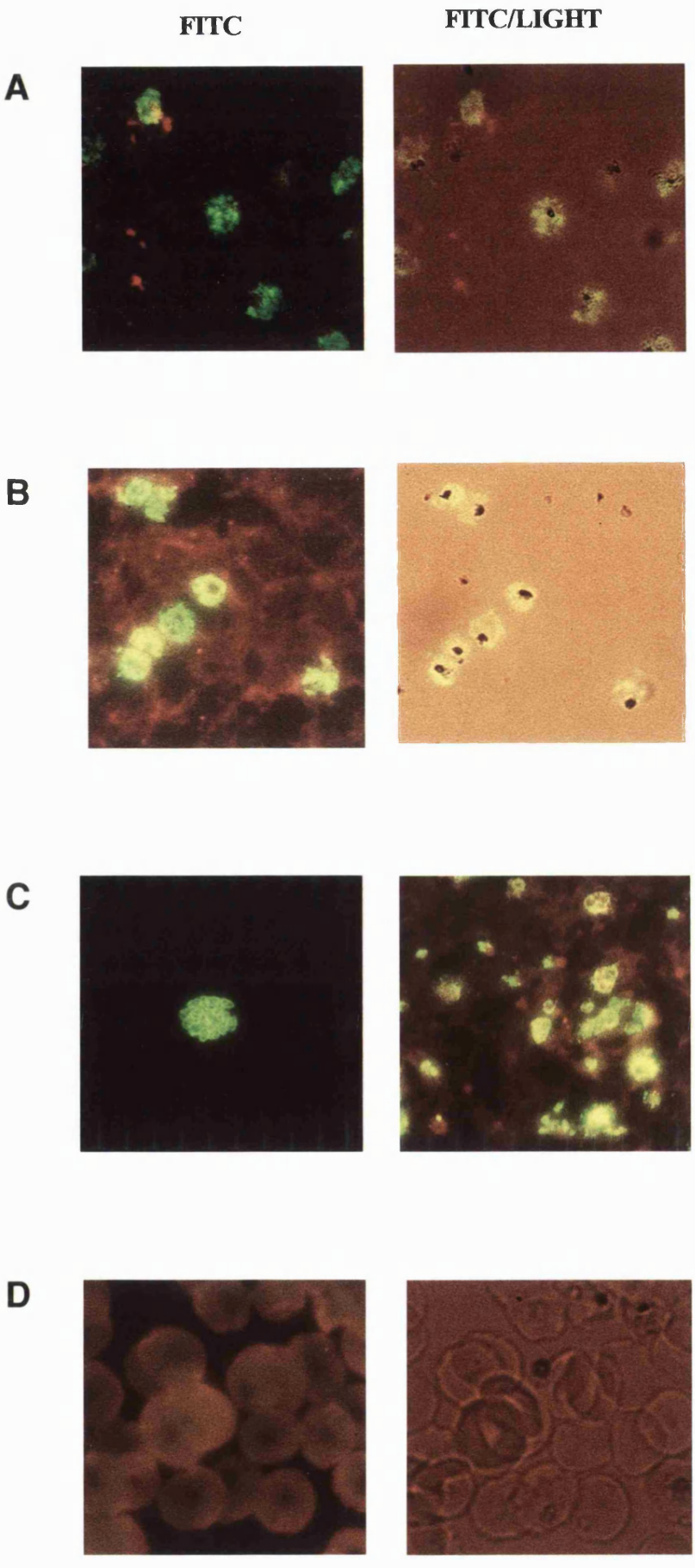
FITC
FITC/LIGHT
A
B
C
D
5μm

Figure 4.8 Production of JP-1 Anti-MSP-7B Monoclonal Antibody

Hybridoma cell culture supernatants were tested by IFAT, using either T9/96 or 3D7 *P. falciparum* mixed blood stage parasites prepared on multi-well IFAT slides. Red blood cells were stained with Evans blue, and light microscopy used to visualize red blood cells and the presence of haemozoin that is indicative of late stage schizonts. Parasite nuclear material was stained with DAPI. Binding of mouse antibodies to parasites was detected by incubation with anti-mouse polyvalent IgG FITC-conjugated antibodies. Slides were viewed on an Olympus Fluorescent microscope, and images were captured using a built-in Olympus camera and ASA 1600 colour slide film.

IFAT positive supernatants were tested for reactivity to western blotted 6*His-MSP-7B fusion protein. Hybridoma supernatants were diluted 1/10 in PBS, 1 % BSA and used to probe western blotted 6*His-MSP-7B. Bound antibodies were detected with a secondary anti-mouse IgG HRP-conjugated antibody and visualised by ECL.

Supernantant from one well (Plate 8, Well A5), of the primary hybridoma culture, showed the best fluorescence pattern with schizonts and bound to the 6*His-MSP-7B fusion protein. Hybridoma cells in this well were then cloned in a limiting dilution step.

Supernatant from Plate 1, Well B2 of the first limiting dilution step, was positive by IFAT and reacted with 6*His-MSP-7B. Cells from this well were cloned in a second limiting dilution step.

The supernatant from colonies in this second cloning step was tested as before, and one IFAT positive well (Plate 1, Well F3) that also bound 6*His-MSP-7B, was selected for a third cloning by limiting dilution step.

By the third cloning step all the resulting hybridoma colonies were producing antibody that gave an identical fluorescence pattern on schizonts to that of the Mouse B1 α-GST-MSP-7B sera, and that bound to the 6*His-MSP-7B fusion protein.

The hybridoma cells in one well (Plate 2 Well G10) from the third cloning step, were deemed monoclonal, named JP-1, and selected for further growth.

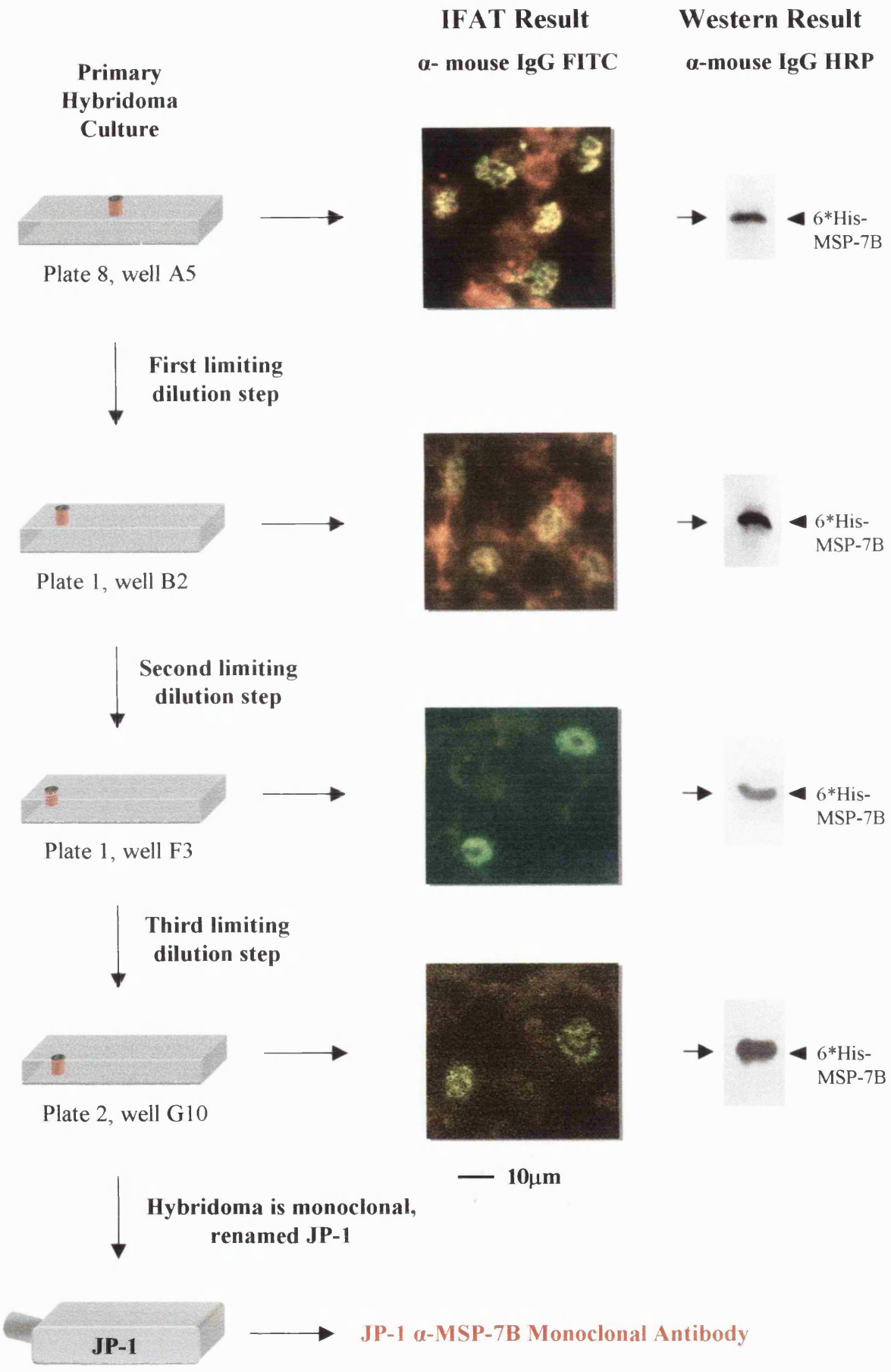
IFAT Result
α- mouse IgG FITC
Western Result
α-mouse IgG HRP
Primary Hybridoma Culture
Plate 8, well A5
6*His-MSP-7B
First limiting dilution step
Plate 1, well B2
6*His-MSP-7B
Second limiting dilution step
Plate 1, well F3
6*His-MSP-7B
Third limiting dilution step
Plate 2, well G10
6*His-MSP-7B
10μm
Hybridoma is monoclonal, renamed JP-1
JP-1
JP-1 α-MSP-7B Monoclonal Antibody

Figure 4.9 Analysis of the JP-1 Anti-MSP-7B Mouse Monoclonal Antibody

A Determination of JP-1 Isotype

The mouse monoclonal JP-1, and a positive control monoclonal antibody of IgG2a isotype were tested using the Sigma ImmunoType Mouse Monoclonal Antibody Isotyping Kit. The positive control gave the correct IgG2a result, whilst JP-1 was determined to be an IgA mouse monoclonal antibody.

B - D IFAT Comparison of JP-1 Detected with Anti-Mouse IgG and Anti-Mouse IgA FITC-conjugated Antibodies

Acetone-methanol fixed *P. falciparum* blood stage parasites were tested by IFAT with either: **(B)** an anti-MSP-1 8A12 mouse monoclonal antibody, **(C - D)** JP-1 culture supernatant at a 1/10 dilution. Slides were also stained with DAPI to stain the nuclear material.

Secondary anti-mouse IgG FITC-conjugated antibodies were used to detect the presence of IgG antibodies bound to schizonts in **(B)** and **(C)**; whilst an anti-mouse IgA specific FITC-conjugated antibody was used to detect the presence of IgA antibodies bound to schizonts in **(D)**. Slides were viewed with the appropriate wavelength filters on Olympus (B – C) and Deltavision (D) epifluorescent microscopes.

Using a secondary anti-mouse IgG FITC-conjugated antibody to detect JP-1 antibody bound to schizonts, the JP-1 monoclonal antibody **(C)** appeared to bind to schizonts with a bunch of grapes pattern similar to that seen with the anti-MSP-1 monoclonal antibody **(B)**, but with a far lower intensity of fluorescence. DAPI images are not shown.

Substituting a secondary anti-mouse IgA specific FITC-conjugated antibody for the anti-IgG antibody resulted in a far greater intensity of fluorescence that enabled better characterization of JP-1 binding to MSP-7B in the developing merozoite **(D)**. DAPI, FITC and merged fluorescent images are shown. This increase in fluorescent intensity confirms the isotyping kit result that the JP-1 mouse monoclonal antibody is of an IgA isotype.

A

B

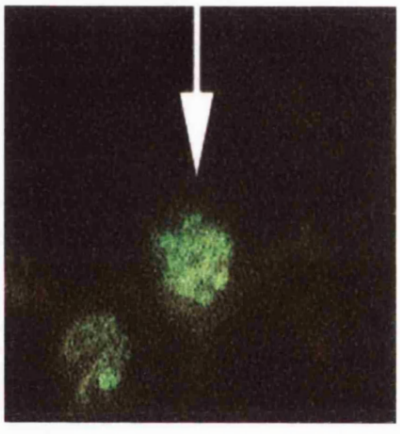

10μm

C

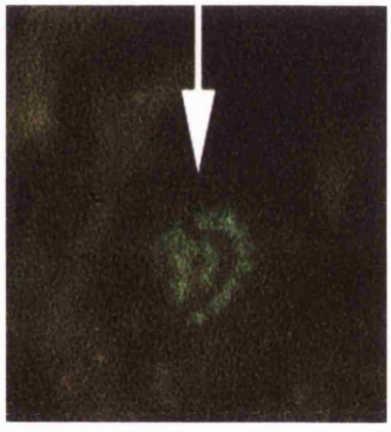

D

DAPI FITC MERGE

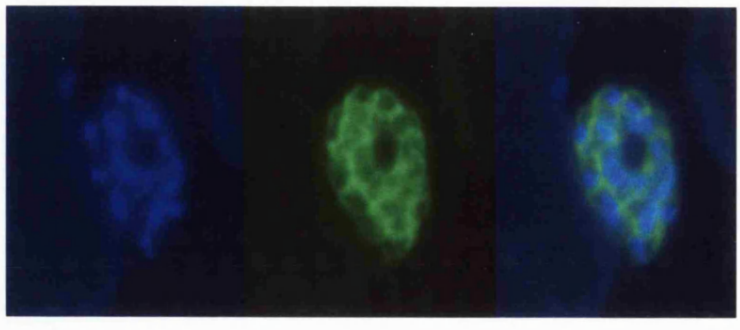

1μm

CHAPTER FIVE : MSP-7 BIOSYNTHESIS

5.0 *msp-7* Transcription Analysis

The preliminary Northern blot analysis of ring, trophozoite and schizont stages (Section 3.3.0) suggested that *msp-7* is transcribed as an mRNA-transcript of approximately 2,500 nucleotides, at a high level in schizonts. To determine the exact time of *msp-7* transcription during the erythrocytic life cycle, and how it is related to *msp-1* transcription, total RNA was collected from highly synchronized 3D7 *P. falciparum* parasites at 2 - hour intervals throughout the 48-hour cycle, and Northern blotted. The Northern blotted RNA was probed with [α-^{32}P] dATP labelled probes *msp-7b*, and *stevor* (a differentially expressed gene) (Cheng *et al.* 1998).

The *msp-7b* probe bound to a band of approx 2,500 nucleotides, present in the 34 - 48 hour samples (Figure 5.0). The intensity of binding to the transcript was low at 34 hours, increased rapidly to a maximum at 36 - 42 hours, and then gradually decreased in the 44 - 48 hour time points. The Giemsa stained parasite images captured for the 34 to 48 hour time points (data not shown), suggest that *msp-7* is transcribed in early to late schizonts. The decrease in the intensity of signal at 44 – 48 hours suggests that *msp-7* transcription decreases as merozoites reach maturity in the schizonts. No binding of *msp-7b* to ring or trophozoite RNA samples (Time points 0 – 32 hours) was seen. The *stevor* probe bound to a transcript of approximately 2400 nucleotides in the 22 – 32 hour time points, as expected.

Hence *msp-7* transcription is stage specific, suggesting that the translated MSP-7 protein has a specific function either in the schizont during merogony, or in the released merozoite.

Comparing the *msp-7* transcription pattern to that previously observed with *msp-1* (Myler 1990; Stafford *et al.* 1996b), suggests that both *msp-1* and *msp-7* are transcribed in schizonts with a very similar pattern. The *msp-1* transcript has been shown by Northern Slot Blot analysis to be present in RNA from 36 to 48 hour erythrocyte stage parasites, with a transcriptional peak at 45 hours (Stafford *et al.* 1996b). This suggests that both *msp-1* and *msp-7* are transcribed and most likely translated at a similar time in the schizont stage.

5.1 Western Blot Analysis of MSP-7 in Schizonts and Merozoites

As *msp-7* is transcribed in *Pf* schizonts 34 – 48 hours post-invasion, it was presumed that the full length MSP-7 protein would be translated in schizonts during this period. To confirm this, western blot analysis of: mature T9-96 schizont proteins (44 – 48 hours development), released T9-96 merozoites, and T9-96 shed MSP-1 complex, was performed with anti-GST-MSP-7A and GST-MSP-7B mouse sera, the anti-MSP-7B JP-1 monoclonal antibody, and pre-immune NMS (Figure 5.1).

Both anti-MSP-7 sera recognised a 48 kDa band in the schizont protein extract, presumed to be the full length MSP-7 precursor (predicted molecular mass of 41.3 kDa). The anti-MSP-7A serum bound weakly to an additional band at approximately 20 kDa, whilst the anti-MSP-7B serum bound strongly to a band at 33 kDa and a doublet at 22 kDa. An additional band at approximately 44 kDa was weakly recognised by the anti-MSP-7B serum. It is unknown whether this polypeptide is related to MSP-7. The anti-GST-MSP-7A antibodies did not bind to the either of the 33 or 44 kDa proteins that were recognised by the anti-GST-MSP-7B serum.

The 22 kDa doublet recognised in schizont proteins by the anti-MSP-7B antibodies, corresponds to the 22 kDa MSP-7_{22} doublet previously seen in merozoites

(Stafford *et al.* 1996a). The presence of the MSP-7_{22} doublet in schizont samples should be treated with caution, as prior to protein extraction, light microscopy of Giemsa-stained samples of the mature schizonts showed the presence of free merozoites. Hence the 22 kDa doublet present in the schizont proteins could originate from released merozoites.

Analysis of the western blotted merozoite proteins, showed that the anti-GST-MSP-7A serum did not react strongly with any merozoite proteins. The anti-MSP-7B antibodies only reacted with 22 kDa and 19 kDa proteins, these were presumed to be MSP-7_{22} and MSP-7_{19} (Stafford *et al.* 1996a). Neither the 48 kDa MSP-7 precursor, nor the 20 and 33 kDa proteins seen in schizonts were present in significant quantities in the merozoite samples.

The anti-GST-MSP-7A antibodies did not react with any proteins in the shed MSP-1 complex. The anti-MSP-7B sera and the JP-1 monoclonal reacted with 22 kDa and 19 kDa polypeptides, these were predicted to be MSP-7_{22} and MSP-7_{19}. Neither the 48 kDa precursor, nor the 20 and 33 kDa proteins seen in schizonts, were detected in the shed MSP-1 complex.

The difference between the predicted mass (41.3 kDa) of the MSP-7 precursor, and its apparent mass by SDS-PAGE (48 kDa) was not unexpected. Several other parasite proteins including MSP-6 have been shown to exhibit this difference between predicted and apparent mass by SDS-PAGE (Trucco *et al.* 2001).

From these western blot results it was predicted that MSP-7 is translated in schizonts as a 48 kDa precursor. In the schizont, the 48 kDa MSP-7 precursor appears to be cleaved into an N-terminal 20 kDa fragment (MSP-7_{20}) recognised by anti-MSP-7A antibodies, and a C-terminal 33 kDa fragment (MSP-7_{33}) recognised by anti-MSP-7B antibodies. Before or during the process of schizont rupture and merozoite release, the

MSP-7_{33} fragment appears to undergo a further N-terminal cleavage, resulting in the 22 kDa (MSP-7_{22}). In both released merozoites, and in the shed MSP-1 complex, the MSP-7_{22} polypeptide appears to have undergone a further partial cleavage at the N-terminus to a 19 kDa (MSP-7_{19}) polypeptide. The presence of MSP-7_{19} in merozoites was surprising, as cell surface radio-iodination studies have previously shown MSP-7_{22} to be predominant on the merozoite surface, with MSP-7_{19} only present in large quantities in the shed MSP-1 complex (McBride and Heidrich 1987; Stafford *et al.* 1994; Stafford *et al.* 1996a). However the 19 kDa band was seen consistently in western blotted merozoite proteins samples, and in MSP-1_{42} processing assay samples in which secondary processing of MSP-1 had not occurred (Section 5.9), suggesting that the presence of MSP-7_{19} in merozoite samples, was probably not an artefact of merozoites that had already undergone further MSP-1 and MSP-7 processing during handling of the samples. The reactivity of the JP-1 monoclonal with both MSP-7_{19} and MSP-7_{22} suggests that its binding epitope is C-terminal to the MSP-7_{22} – MSP-7_{19} cleavage site.

5.2 IFAT Analysis of Schizonts and Merozoites with Anti-MSP-7 Antibodies

The location of MSP-7 proteins in schizonts and released merozoites was determined by immuno-fluorescence. Immature and mature *P. falciparum* schizonts were acetone and methanol fixed, and then tested by IFAT with antibodies to: MSP-1, MSP-7, EBA-175 (microneme specific location) and BiP (ER specific location) (Noe *et al.* 2000) (Figures 5.2 and 5.3).

All the anti-MSP-7 antibodies bound to early- and mid-stage schizonts with a similar pattern. This pattern consists of some fluorescence visible in the cytosol, but the majority outlining the edges of developing merozoites.

Very late-stage schizonts and merozoites released from ruptured schizonts, were not recognized by antibodies to MSP-7A, but were by antibodies to MSP-7B. Antibodies to MSP-7B outlined the edges of merozoites, with hardly any fluorescence in the cytosol. This suggests that by the time a merozoite is fully developed, MSP-7 translation and transport from the ER had ceased. This is consistent with the decrease in the level of the *msp-7* transcript in the final 44 to 48 hours of the life cycle (Section 5.0).

The lack of reactivity shown by anti-MSP-7A sera to very late-stage schizonts, suggests that by the end of merogony, the MSP-7 precursor may have undergone N-terminal cleavage to MSP-7_{33}, with the 20 kDa (MSP-7_{20}) N-terminal cleavage product presumably either degraded or exocytosed from the schizont.

The anti-MSP-7A sera did not bind to released merozoites, this was consistent with the lack of reactivity by IFAT to late stage schizonts, and by western blotting to merozoite proteins (section 5.1). Antibodies to MSP-7B bound to the surface of released merozoites, including merozoites that appeared to be attached to red blood cells. One merozoite appeared to have just shed its coat of surface proteins in the process of invading an erythrocyte, presumably the JP-1 anti-MSP-7B monoclonal antibody recognised the MSP-7_{22} and MSP-7_{19} components of the shed MSP-1 complex.

The fluorescence pattern obtained with the MSP-7A and MSP-7B antibodies in early to mid stage schizonts, and with anti-MSP-7B antibodies in late stage schizonts and released merozoites, was similar to that seen with anti-MSP-1 antibodies. This suggests that the MSP-1 precursor and MSP-7 or its predicted cleavage products MSP-7_{20} and MSP-7_{33} are located in the same regions of early to mid-stage schizonts. It also suggests that MSP-7_{33} or MSP-7_{22} are located with the MSP-1 precursor or its primary processed derivatives on the merozoite surface in late stage schizonts and released merozoites.

The fluorescence pattern of the anti-MSP-1 and anti-MSP-7 antibodies in early *P. falciparum* schizonts, is similar to that previously described for MSP-1 and MAEBL in *Plasmodium yoelii* schizonts at the onset of merogony (Noe *et al.* 2000). In early *P. yoelii* schizonts, MSP-1 and MAEBL have been shown to associate with a tubular reticular network of the ER (TuRNER), prior to being targeted via the Golgi to the parasite plasma membrane and rhoptries respectively (Noe *et al.* 2000).

The fluorescence patterns of antibodies to BiP (ER) and EBA-175 (micronemes) in schizonts and merozoites, were compared to those obtained with antibodies to MSP-1 and MSP-7. Antibodies to BiP highlighted the ER in developing and mature merozoites, whilst antibodies to EBA-175 bound to the apical region of mature merozoites. The BiP fluorescence pattern in early schizonts shows similarities to that seen with MSP-1 and MSP-7. This suggests that at the onset of merogony, MSP-1 and MSP-7 are associated with the ER, in an organelle similar to the TuRNER of *P. yoelii* schizonts (Noe *et al.* 2000). As merogony continues, the MSP-1 and MSP-7 fluorescence pattern changes to one outlining the edges of the mature merozoites, that is distinct from that of BiP and EBA-175 which is highlighting the ER and micronemes. By analogy to *Py*MSP-1, this suggests that by mid- to late-stage merogony, both MSP-1 and MSP-7 have been transported from the TuRNER via the Golgi to the merozoite plasma membrane (Noe *et al.* 2000).

5.3 Dual Immuno-fluorescence with MSP-7 and MSP-1 Antibodies.

To determine if the MSP-7 precursor or the MSP-7_{20} and MSP-7_{33} polypeptides were closely associated with MSP-1 in schizonts, dual immuno-fluorescence was performed. Acetone-methanol fixed schizonts were probed with mouse anti-MSP-7 and rabbit anti-MSP-1 antibodies, followed by the appropriate secondary antibodies

conjugated to either FITC or TRITC fluorophores. Merging the 528 nm (Green) and 617 nm (Red) wavelength images obtained with the anti-MSP-7 and MSP-1 antibodies respectively, showed a significant overlap in the fluorescent images (indicated by yellow) (Figure 5.4).

Antibodies to MSP-1 and MSP-7 co-localised in the cytosol and on the surface of developing merozoites in early- to mid-stage schizonts. Antibodies to both MSP-1 and MSP-7B co-localised on the surface of merozoites in mature schizonts, and on a released merozoite, whilst binding of anti-MSP-7A antibodies was not detected in very late-stage schizonts or on released merozoites (as for section 5.2).

The co-localisation of MSP-1 and MSP-7 in the schizont, indicates that both proteins are closely linked during transport to, and on the surface of the developing merozoite. Hence MSP-1 and MSP-7 appear to share a related transport pathway from the ER or TuRNER via the Golgi to the developing merozoite surface.

The predicted processing of MSP-7 into the 20 and 33 kDa fragments may occur either during transport from the ER to the merozoite plasma membrane, or once MSP-7 is at the merozoite membrane. The co-localisation of antibodies to MSP-7A and MSP-1 on the surface of immature merozoites, suggests that the N-terminal region of MSP-7 (either as the MSP-7 precursor or as the N-terminal cleavage product MSP-7_{20}) remains associated with MSP-1 during translocation to and once at the merozoite surface. Antibodies to MSP-7A do not bind to very mature schizonts, suggesting that by the end of schizogony, the MSP-7 precursor has definitely undergone N-terminal cleavage, leaving just MSP-7_{33} associated with MSP-1 on the merozoite surface. The resulting MSP-7_{20} fragment may be either degraded by proteases in the parasitophorous vacuole, or exocytosed. As MSP-7_{33} is not detected in western blotted merozoites, it is predicted that on or around the time of schizont rupture MSP-7_{33} is degraded to MSP-7_{22}. MSP-7_{22}

or its cleavage product MSP-7_{19} co-localise with MSP-1 on the merozoite surface, until erythrocyte invasion, when secondary processing of MSP-1 results in release of the shed MSP-1 complex containing both MSP-7_{22} and MSP-7_{19}.

5.4 Investigation of MSP-7 Translation and Processing by Immunoprecipitation

The western blot and immuno-fluorescence results suggested that MSP-7 is made in early schizonts as a 48 kDa precursor, which appears to undergo cleavage into 20 kDa (MSP-7_{20}) and 33 kDa (MSP-7_{33}) fragments. The time and location of this cleavage in schizonts is unknown, as antibodies to both regions of MSP-7 bind to the surface of developing merozoites. However as merozoites reach maturity the anti-MSP-7A binding site appears to be lost from the merozoite surface, suggesting that MSP-7_{20} has been either degraded in the parasitophorous vacuole or exocytosed. Around the time of merozoite release, the C-terminal MSP-7_{33} is predicted to undergo cleavage into MSP-7_{22}, which has been identified bound to the primary processed MSP-1 complex on the surface of released merozoites.

To confirm the MSP-7 processing events in schizonts and to determine if the resulting MSP-7 fragments remained in complex after cleavage, schizont stage parasite proteins were metabolically ^{35}S-radiolabelled, and proteins solubilised in either non-ionic (NP-40) or ionic (DOC and SDS (SDS data not shown)) detergents that respectively maintain, or disrupt any potential protein complexes. Proteins were immunoprecipitated using antibodies to MSP-1 and MSP-7, and separated on low percentage SDS-PAGE gels (Figure 5.5A).

Both the mouse anti-GST-MSP-7A and MSP-7B sera bound to MSP-7 epitopes in both native and denatured configurations. The JP-1 anti-MSP-7B monoclonal antibody did not immunoprecipitate any radiolabelled proteins in either native or denatured

configurations and as a result was not used for immunoprecipitation analysis (data not shown). Both of the anti-MSP-7A and MSP-7B mouse sera immunoprecipitated a 48 kDa protein from ionic and non-ionic solubilised samples. The anti-MSP-7A serum also pulled down a 20 kDa protein ($MSP\text{-}7_{20}$), whilst the anti-MSP-7B serum immunoprecipitated a 33 kDa ($MSP\text{-}7_{33}$) protein and a doublet at 22 kDa ($MSP\text{-}7_{22}$), from both NP-40 and DOC solubilised samples. These immunoprecipitated proteins corresponded to the 48 kDa, 33 kDa, 22 kDa and 20 kDa bands detected by the anti-MSP-7 sera in western blotted schizont proteins (section 5.1). The 20 and 33 kDa bands did not co-immunoprecipitate in non-ionic conditions, suggesting that once cleaved the $MSP\text{-}7_{20}$ and $MSP\text{-}7_{33}$ fragments are not in a complex with each other. NMS only immunoprecipitated a band at 70 kDa that was immunoprecipitated by all antisera, this was predicted to be HSP-70 (Section 4.2.0). Interestingly the anti-MSP-1 antibody X509, that binds to block 16 of MSP-1, also appeared to immunoprecipitate bands of 48, 33 and 22 kDa from NP-40 but not DOC solubilsed lysates. (This was further investigated in Section 5.6).

In initial radiolabelling experiments some mature schizonts (44 - 48 hours development) had ruptured during the period of radiolabelling, releasing merozoites, as determined by viewing Giemsa stained slides of labelled parasites. This explains the presence of the 22 kDa ($MSP\text{-}7_{22}$) polypeptide that was immunoprecipitated by the anti-MSP-7B serum. Later experiments (Section 5.6) used earlier stage schizonts that were mostly intact post-labelling and the resulting immunoprecipitations did not pull down the $MSP\text{-}7_{22}$ in significant quantities. This suggests that the predicted processing of $MSP\text{-}7_{33}$ to $MSP\text{-}7_{22}$ may not occur until the time of merozoite release from the schizont.

To determine if MSP-7, $MSP\text{-}7_{33}$ or $MSP\text{-}7_{20}$ were released as soluble proteins on schizont rupture, mature schizonts were radiolabelled, allowed to undergo merozoite

release and reinvasion and soluble released proteins immunoprecipitated from the culture supernatant with anti-MSP-1 and MSP-7 antibodies (Figure 5.6A). Both the anti-MSP-1 and MSP-7B antibodies immunoprecipitated a protein complex identical to that previously described for the shed MSP-1 complex (Stafford *et al.* 1994; Stafford *et al.* 1996a; Trucco *et al.* 2001). The anti-MSP-7A serum did not immunoprecipitate MSP-7_{20} or the MSP-1 shed complex, but did appear to pull down a number of bands that were also immunoprecipitated by the anti-MSP-7B serum, mainly bands at 36 kDa and approximately 48 kDa. The 36 kDa band may be MSP-6_{36}, whilst the 48 kDa band may be the MSP-7 precursor. The significance of this remains to be further investigated.

The anti-MSP-7A serum did not react with purified western blotted shed MSP-1 complex, whilst the anti-MSP-7B serum recognised the MSP-7_{22} and MSP-7_{19} components in the shed complex (Figure 5.6B and C), confirming the western blot results of Section 5.1. This suggests that MSP-7_{20} is probably degraded by proteases in the parasitophorous vacuole before schizont rupture, confirming the IFAT results in which antibodies to MSP-7A did not appear to react with mature schizonts or free merozoites (Section 5.2 - 3).

Hence radio-immuno-precipitations of schizont proteins confirm that MSP-7 is made as a 48 kDa precursor. During schizogony the 48 kDa precursor appears to undergo cleavage into two fragments of 20 kDa (MSP-7_{20}) and 33 kDa (MSP-7_{33}). The cleaved MSP-7_{20} does not remain in complex with MSP-7_{33}, and is probably degraded before the schizont ruptures. MSP-7_{33} is predicted to undergo N-terminal cleavage to MSP-7_{22}, an event that may be related to primary processing of MSP-1 and MSP-6 (Section 3.6.3). On the surface of the released merozoite MSP-7_{22} has been partially cleaved into MSP-7_{19}, and on erythrocyte invasion both MSP-7_{19} and MSP-7_{22} are part

of the shed MSP-1 complex released from the merozoite membrane by secondary processing of MSP-1.

5.5 2D Peptide Mapping of MSP-7 and MSP-7_{33}

To confirm that MSP-7_{33} was the cleavage product of the 48 kDa MSP-7 precursor, radiolabelled schizont proteins were immunoprecipitated with mouse anti-MSP-7B serum, separated on a large 10% SDS-PAGE gel and analysed by autoradiography. The 33 kDa and 48 kDa bands corresponding to MSP-7_{33} and MSP-7 were cut out of the SDS-PAGE gel, digested with trypsin and the tryptic peptides subjected to 2D peptide mapping (See Figure 5.7).

The resulting 2D maps for both MSP-7 and MSP-7_{33} were very similar confirming that the 2 proteins are related, although the result is a little disturbed by the presence of an unfortunate water mark on the MSP-7_{33} 2D peptide map. This confirms the hypothesis that the 48 kDa MSP-7 precursor is cleaved at the N-terminus to a 20 kDa (MSP-7_{20}) fragment that is only recognized by anti-MSP-7A serum, and a 33 kDa fragment (MSP-7_{33}) that is recognized by anti-MSP-7B serum, and has been shown by 2D peptide mapping to be related to the MSP-7 precursor.

Comparing the 2D peptide maps for MSP-7 and MSP-7_{33} to those obtained for MSP-7_{22} and MSP-7_{19} purified from the shed MSP-1 complex (Stafford *et al.* 1996a), shows that the peptide maps have similar patterns, confirming that MSP-7 and MSP-7_{33} are related to MSP-7_{22} and MSP-7_{19}.

Based on these 2D peptide mapping observations and the immunoprecipitation and western blot results, it appears that MSP-7 is translated in schizonts as a 48 kDa protein which then undergoes 3 N-terminal cleavage events. The first MSP-7 cleavage event occurs in schizonts before merozoites reach maturity, cleaving the 48 kDa MSP-7

precursor into MSP-7_{20} (N-terminal 20 kDa fragment) and MSP-7_{33} (C-terminal 33 kDa fragment). MSP-7_{20} is degraded in the schizont. The second event is the cleavage of MSP-7_{33} to MSP-7_{22}, which occurs either in mature schizonts or on merozoite release. It is unknown what happens to the cleaved N-terminal fragment from this event. This cleavage may be mediated by the same protease responsible for primary processing of MSP-1 (See section 3.6.3). The third MSP-7 cleavage, which occurs on the surface of the released merozoite, is the incomplete processing of MSP-7_{22} to MSP-7_{19}, with both polypeptides released from the merozoite surface as part of the shed secondary processed MSP-1 complex.

5.6 MSP-7 and MSP-1 Precursors Form a Complex in Schizonts Before Primary Processing of MSP-1 and MSP-7

The primary processed MSP-1 polypeptides and MSP-7_{22} are in a complex on the surface of free merozoites (Stafford *et al.* 1996a), and dual IFAT results suggest that MSP-1 and MSP-7 are closely associated in the nascent merozoite (Section 5.3). In addition antibodies to MSP-1 and MSP-7B give similar immunoprecipitation patterns of schizont proteins lysed in NP-40 (Section 5.4). Hence it is possible that the MSP-1 and MSP-7 precursors form a complex either at the ER or during transport to the merozoite surface. To determine whether MSP-7 or its cleavage products MSP-7_{20} or MSP-7_{33}, associated with the 195 kDa MSP-1 precursor in schizonts, radiolabelled schizont proteins were solubilised in the presence of either non-ionic (NP-40) or ionic (DOC) detergents, and immunoprecipitated with anti-MSP-1 and anti-MSP-7 antibodies (Figures 5.5B and 5.8).

In non-ionic (NP-40) detergent conditions both the anti-MSP-7A and MSP-7B antibodies immunoprecipitated the 48 kDa MSP-7 precursor, and either MSP-7_{20} or

MSP-7_{33} respectively. Both anti-MSP-7 antibodies also immunoprecipitated a protein of approximately 195 kDa, presumed to be the MSP-1 precursor. The anti-MSP-1_{33} antibody X509, immunoprecipitated the 195 kDa MSP-1 precursor, and proteins of 48 and 33 kDa, that were predicted to be MSP-7 and MSP-7_{33}. X509 did not immunoprecipitate a band at 20 kDa that would correspond with MSP-7_{20}.

Hence, in schizonts the MSP-1 and MSP-7 precursors form a complex in schizonts that is maintained in the presence of non-ionic detergents. On primary processing of MSP-7 in the schizont, MSP-7_{33} remains bound to the MSP-1 precursor, whilst MSP-7_{20} is lost from the complex and degraded.

In DOC solubilised samples, antibodies to MSP-1 immunoprecipitated only the 195 kDa MSP-1 precursor, whilst the anti-MSP-7A and MSP-7B antibodies immunoprecipitated the MSP-7 precursor, and MSP-7_{20} or MSP-7_{33} respectively, but not the MSP-1 precursor. Hence in the presence of DOC any potential MSP-1 – MSP-7 interactions were disrupted, suggesting that MSP-7 is non-covalently bound to MSP-1.

The anti-MSP-1_{83} monoclonal antibody 89.1, immunoprecipitated only the MSP-1 precursor irrespective of the detergent used. This suggests that the 89.1 binding site which has been localised to block 3 of MSP-1, is being blocked upon the interaction between MSP-7 and MSP-1 (Holder 1988) (See section 5.8 for further details). The fact that free MSP-1 precursor is present, (as evidenced by 89.1 binding to MSP-1) suggests that the association of the MSP-1 and MSP-7 precursors may not occur immediately post translation, or that some of the MSP-1 precursor never complexes with MSP-7.

Therefore the 195 kDa MSP-1 precursor forms a complex with the 48 kDa MSP-7 precursor in schizonts. The MSP-1 – MSP-7 precursor complex is maintained in non-ionic, but not ionic detergent conditions. It is likely that the MSP-1 and MSP-7 precursors form a complex soon after translation, or during transport to the merozoite

surface. The presence of free MSP-1 precursor immunoprecipitated by 89.1 suggests that there is a reservoir of unbound MSP-1 precursor, perhaps involved in binding to newly translated MSP-7. The MSP-1 - MSP-7 precursor association occurs before either protein undergoes processing. Following formation of the MSP-1 - MSP-7 precursor complex, MSP-7 undergoes cleavage leaving MSP-7_{33} bound to the MSP-1 precursor whilst, the N-terminal fragment (MSP-7_{20}) is no longer bound to either MSP-1 nor MSP-7_{33}.

As antibodies to MSP-7A have been shown to co-localise with anti-MSP-1 antibodies on the surface of schizonts, but not in very mature schizonts or released merozoites, the primary processing of MSP-7 is predicted to occur after the formation of the MSP-1 – MSP-7 precursor complex, but before merozoite release, either as the complex is transported to the merozoite surface or once it has reached the merozoite membrane. The MSP-7_{20} fragment can be immunoprecipitated from schizonts in large quantities, suggesting that it is not degraded immediately upon its cleavage from MSP-7 and release from the MSP-1 – MSP-7 complex.

As MSP-7_{22} can be immunoprecipitated with both anti-MSP-1 and MSP-7B antibodies from mature schizont samples that have undergone merozoite release, and as MSP-7_{33} is not present in western blotted merozoites, it is predicted that the MSP-1 precursor is in complex with MSP-7_{33} in the developing merozoite, and the cleavage of MSP-7_{33} to MSP-7_{22}, which remains bound to MSP-1, occurs on schizont rupture. The MSP-7_{33} – MSP-7_{22} cleavage site has some similarity with primary processing sites of MSP-1, and with the MSP-6_{36} processing site (Section 3.4.3) (Holder *et al.* 1985; McBride and Heidrich 1987; Trucco *et al.* 2001). As primary processing of MSP-1 is predicted to occur on merozoite release, and as MSP-6_{36} is only detected bound to the primary processed MSP-1 complex, it is possible that the same protease is responsible

for primary processing of MSP-1, cleavage of the MSP-6 to MSP-6_{36} (perhaps catalysing its attachment to the MSP-1 complex), and the MSP-7_{33} to MSP-7_{22} processing event.

5.7 Brefeldin A Inhibits MSP-7 Processing But Not MSP-1 - MSP-7 Precursor Complex Formation

The fungal metabolite Brefeldin A inhibits the classical and alternative secretory pathways in *Plasmodium* species, by inhibiting the transport of proteins between the ER and the *trans*-Golgi of parasites (Das *et al.* 1994; Ogun and Holder 1994; Wiser *et al.* 1997; Blackman *et al.* 1998; Blanco *et al.* 1999; Noe *et al.* 2000; Hayashi *et al.* 2001). BFA is known to inhibit the post-translation processing and transport of MSP-1 in *P. yoelii* (Noe *et al.* 2000) and in *P. berghei* (Wiser *et al.* 1997), causing the MSP-1 precursor to accumulate with the endoplasmic reticulum in a distinct compartment in the parasite. Therefore BFA can be used as a tool to determine the location in the developing merozoite of the formation of the MSP-1 - MSP-7 precursor complex, and the primary processing of MSP-7.

Schizonts were metabolically radiolabelled in the presence or absence (methanol only) of BFA. Radiolabelled schizont proteins were solubilised in the non-ionic detergent NP40 (to maintain any potential protein complexes) and immunoprecipitated with anti-MSP-1, MSP-7A, MSP-7B and NMS antibodies (Figure 5.9).

In the presence of BFA, antibodies to MSP-1, MSP-7A and MSP-7B immunoprecipitated both the 195 kDa MSP-1 precursor and the 48 kDa MSP-7 precursor. Hence Brefeldin A does not block the formation of the MSP-1 and MSP-7 precursor complex, suggesting the MSP-1 and MSP-7 precursors form a non-covalently bound complex prior to the *trans*-Golgi.

Comparison of the proteins immunoprecipitated from BFA and methanol-only treated schizonts, showed less of the 48 kDa (MSP-7) precursor and more of the 20 kDa ($MSP\text{-}7_{20}$) and 33 kDa ($MSP\text{-}7_{33}$) polypeptides in the methanol treated samples than in the BFA treated samples. Therefore the primary processing of the 48 kDa MSP-7 is inhibited by BFA.

In the developing merozoite the MSP-1 precursor forms a complex with the MSP-7 precursor prior to the trans-Golgi. The primary processing of MSP-7 into $MSP\text{-}7_{20}$ and $MSP\text{-}7_{33}$ occurs after the MSP-1 – MSP-7 precursor complex has formed, and is blocked by Brefeldin A, indicating that the cleavage occurs post-Golgi, perhaps during transport to the surface or on the merozoite membrane.

As BFA causes a build up of the MSP-1 - MSP-7 precursor complex, it can be assumed that the precursor complex is transported via the traditional intracellular protein transport pathway, as previously predicted for MSP-1 (Wiser *et al.* 1997).

5.8 Kinetics of MSP-7 translation

Two pulse chase experiments were performed to investigate the kinetics of MSP-1 and MSP-7 complex formation and the primary processing of MSP-7. In the first pulse-chase, schizonts were incubated for 30 minutes with Brefeldin A in conjunction with a pulse of radiolabel, resulting in a build up of labelled precursor complex. The chase was initiated by the removal of the BFA and the radiolabel. Samples from each time point (0 – 5 hours) were solubilised in NP-40 and DOC, and immunoprecipitated with anti-GST-MSP-7A, anti-GST-MSP-7B sera, anti-MSP-1 (89.1) monoclonal antibody and NMS (-ve control) (Figure 5.10). The results showed that the 48 kDa MSP-7 precursor was being cleaved to $MSP\text{-}7_{33}$ and $MSP\text{-}7_{20}$ with a gradual increase in the cleavage products to a maximum by 2 hours (time point 3). There was a corresponding decrease in the

amount of MSP-1 immunoprecipitated by the anti-MSP-7A antibodies, consistent with a decrease in the MSP-7 precursor and the loss of the MSP-7A antibody binding sites from the MSP-1 - MSP-7 complex as the MSP-7_{20} is released. The quantity of MSP-1 immunoprecipitated by the anti-MSP-7B serum remained constant, suggesting that the MSP-1 precursor remains bound to the MSP-7_{33} cleavage product. The amount of free MSP-1 immunoprecipitated by 89.1 decreased with time, which is consistent with a decrease in free MSP-1 precursor as it is bound to the MSP-7 precursor and hence loses its 89.1 binding site. The use of BFA with the pulse may have slowed down protein transport and targeting, and hence delayed any processing events that occur post ER ie MSP-7 processing.

The second pulse chase of synchronised schizonts was initiated with a brief pulse of radiolabel without BFA for 10 minutes, with a chase over 120 minutes. Samples from each time point (0 - 120 mins) were solubilised in NP-40 and immunoprecipitated as before (Figure 5.11). The results suggest that by the end of 10 minutes of labelling (T=0), the MSP-1 and MSP-7 precursors were complexed together, and primary processing of MSP-7 was already occurring. The amount of MSP-1 immunoprecipitated by the anti MSP-7A serum decreased with time, and in proportion to the decrease in full length MSP-7 and corresponding increase in the processed MSP-7_{20} polypeptide. This decrease in MSP-1 is consistent with the predicted loss of the anti-MSP-7A binding site from the precursor complex as the MSP-7 precursor is cleaved, releasing MSP-7_{20} from the MSP-1 – MSP-7 complex. Since the MSP-7_{20} polypeptide increased in quantity with time, MSP-7_{20} is clearly not degraded by proteases immediately after cleavage.

The anti-MSP-7B immunoprecipitation showed a decrease in the full length MSP-7 precursor corresponding to that seen with the anti-MSP-7A serum. The MSP-7B serum also showed an increase in MSP-7_{33} to a maximum by 20 to 30 minutes post

labelling, which correlated to the decrease in MSP-7 and the increase in the MSP-7_{20} cleavage product pulled down with anti-MSP-7A serum. The quantity of MSP-1 precursor immunoprecipitated with the anti-MSP-7B serum remained constant, confirming that the MSP-1 precursor remains bound to the C-terminus of MSP-7 during cleavage of MSP-7 into MSP-7_{33}.

The anti-MSP-1 89.1 antibody immunoprecipitation showed a decrease of free unbound MSP-1 with time. This is consistent with the binding of the MSP-7 precursor to the MSP-1 precursor forming the MSP-1 – MSP-7 precursor complex, resulting in a decrease in unbound MSP-1 precursor with time.

5.9 MSP-1_{42} and MSP-7_{22} Processing Assay

The MSP-7_{33} to MSP-7_{22} processing site shows similarity to that of a MSP-1 primary processing site and MSP-6_{36} cleavage site, and it is likely that these cleavage events occur simultaneously. MSP-7_{22} to MSP-7_{19} processing appears to occur at a similar time in merozoites as MSP-1_{42} secondary processing, suggesting that these processing events were also related (Stafford *et al.* 1996a). Therefore MSP-1 secondary processing assays were performed to determine if anti-MSP-7 antibodies inhibit processing of either MSP-1_{42} or MSP-7_{22}, and to determine if inhibition of MSP-1 secondary processing has an effect on processing of MSP-7_{22}. Processing of MSP-1_{42} was detected by the formation of MSP-1_{33}, whilst processing of MSP-7_{22} was determined to have occurred if MSP-7_{19} was detected in the assay (Figure 5.12).

At the concentrations tested in the assay, neither the mouse anti-GST-MSP-7A, anti-GST-MSP-7B and anti-MSP-$7_{22.1}$ polyclonal sera, nor the JP-1 anti-MSP-7B monoclonal antibody, inhibited secondary processing of MSP-1_{42}, as seen by the formation of the cleavage product MSP-1_{33} in these samples.

The results from the 'Processing Negative' controls of 0 hr (time zero, no MSP-1_{42} processing) and PMSF (inhibits the serine protease responsible for MSP-1_{42} processing) suggested that whilst there was no detectable processing of MSP-1_{42} to MSP-1_{33}, the MSP-7_{22} to MSP-7_{19} processing event had already occurred, with both MSP-7_{22} and MSP-7_{19} detected in the control samples. Hence it is unknown whether the anti-MSP-7 antibodies inhibit processing of MSP-7_{22} in merozoites. The presence of MSP-7_{19} in the zero-hour control suggests that MSP-7_{22} has already undergone processing in merozoites, despite preparation of the merozoites in the presence of calcium chelators. This suggests that the calcium dependent serine protease responsible for the processing of MSP-1_{42} is not the protease responsible for cleavage of MSP-7_{22} to MSP-7_{19} (Blackman and Holder 1992; Blackman *et al.* 1993). Therefore the partial processing of MSP-7_{22} to MSP-7_{19} occurs prior to and appears to be independent of, the secondary processing of MSP-1_{42} to MSP-1_{33} and MSP-1_{19}.

The function of the MSP-7_{22} to MSP-7_{19} processing event is unknown. It does not appear to be an essential prerequisite for MSP-1_{42} processing, as both MSP-7_{22} and MSP-7_{19} are released with the shed MSP-1 complex. This raises the question of when and where does processing of MSP-7_{22} occur in the merozoite, and what class of protease is responsible? Also, if this processing event could be inhibited, what effect, if any, would there be on the secondary processing of MSP-1? The cleavage of MSP-1_{42} appears to occur irrespective of the processing of MSP-7_{22}, with both MSP-7_{22} and MSP-7_{19} identified in the released shed MSP-1 complex. As the MSP-7_{22} to MSP-7_{19} cleavage site has some similarities with MSP-2 could the processing of MSP-7_{22} be an arbitrary event of no biological significance, due to non-specific cleavage by a protease released during erythrocyte invasion?

Further studies will need to be carried out to, determine whether the MSP-7_{22} to MSP-7_{19} processing event has any biological significance, identify the protease responsible and the time and location of cleavage, and how or if the processing event has any effect on MSP-1_{42} processing. Knowing the structure of the MSP-1 –MSP-7 complex on the merozoite surface may help in determining why MSP-7_{22} is processed and what effect this has, if any, on processing of MSP-1_{42}.

5.10 Summary

Msp-7 is transcribed between 34 – 48 hours post invasion of the erythrocytic life cycle, with a peak in transcription between 36 – 44 hours, which coincides with the onset of schizogony and resulting merozoite development in the schizont. The *msp-7* transcription pattern is similar to that previously described for *msp-1* (Stafford *et al.* 1996b), suggesting that *msp-1* and *msp-7* are both transcribed at a similar time during schizogony.

It is suggested that during the schizont stage *msp-1* and *msp-7* are co-transcribed and subsequent translation of the MSP-1 and MSP-7 proteins occurs concurrently. When the merozoites reach maturity in the schizont (46 – 48 hours), there is a decrease in *msp-1* and *msp-7* transcription. Following merozoite release and erythrocyte invasion neither *msp-1* nor *msp-7* are transcribed in ring or trophozoite stages.

The *msp-7* transcript is translated in schizonts as a 48 kDa MSP-7 precursor protein. In the schizont the 48 kDa MSP-7 undergoes two cleavage events (Figure 5.13). The first is the cleavage from the N-terminus of MSP-7, of a 20 kDa polypeptide (MSP-7_{20}). Anti-MSP-7A antibodies bind strongly to the MSP-7 and MSP-7_{20} proteins, whilst anti-MSP-7B antibodies bind MSP-7 and a 33 kDa polypeptide (MSP-7_{33}) presumed to be the C-terminal product of the cleavage. Assuming that the 20 kDa fragment is derived

from N-terminal processing of the 48 kDa MSP-7 precursor, the 33 kDa fragment recognized by the anti-MSP-7B serum in western blots and immunoprecipitations is of the expected size for the C-terminal product of this first cleavage event. It was however surprising that the anti-MSP-7A polyclonal serum did not recognize the N-terminal part of the 33 kDa MSP-7_{33}, as the serum was raised against the full length region of MSP-7, N-terminal to the MSP-7_{22} cleavage site.

To confirm that MSP-7 and MSP-7_{33} were related, 2D-peptide mapping was performed. The 2D peptide maps confirm that MSP-7_{33} and MSP-7 are related to each other, and that MSP-7_{33} is the cleavage product of MSP-7. The MSP-7 and MSP-7_{33} 2D peptide maps show similarities with those previously performed on MSP-7_{22} and MSP-7_{19} purified from the shed MSP-1 complex (Stafford *et al.* 1996a). Hence the MSP-7, MSP-7_{33}, MSP-7_{22}, and MSP-7_{19} polypeptides are related to each other, and predicted to be the C-terminal products of sequential N-terminal cleavage of MSP-7, then MSP-7_{33}, and then MSP-7_{22}.

The MSP-7_{33} undergoes N-terminal cleavage, removing approximately 8 kDa to give MSP-7_{22}. Depending on the maturity of schizonts used, MSP-7_{22} was detected by immunoprecipitation and western blotting in schizont samples, suggesting that some schizonts analysed had burst to release merozoites. MSP-7_{33} is not detectable in merozoites by western blotting, nor is it in the shed MSP-1 complex, suggesting that the cleavage of MSP-7_{33} into MSP-7_{22} occurs just before or as merozoites are released by schizont rupture. The C-terminal region of MSP-7, MSP-7_{22}, is later distinguishable complexed to the primary processed MSP-1 fragments on the surface of mature released merozoites (Stafford *et al.* 1994), and then after merozoite invasion in the shed MSP-1 complex as MSP-7_{22} and its partially processed product MSP-7_{19} (Stafford *et al.* 1996a).

Antibodies raised against the N-terminal (MSP-7A) and C-terminal (MSP-7B) regions of MSP-7 bind to schizonts with a fluorescence pattern similar to that of MSP-1. In early schizonts MSP-7 shares a similar fluorescent pattern to that of BiP, an ER marker, and it is suggested that at the onset of schizogony the newly translated MSP-7 and MSP-1 are initially associated with a transient tubular reticular network of the ER (TuRNER) that forms around the dividing nuclei, as has been described with MSP-1 in *Plasmodium yoelii* (Noe *et al.* 2000).

Dual immuno-fluorescence suggested that MSP-7 and MSP-1 proteins also co-localise on the surface of the developing merozoite in schizonts, and may be co-transported from the ER following translation. This suggested that the MSP-1 and MSP-7 proteins co-localised in the TuRNER, and during transport from the ER to the developing merozoite surface.

Immunoprecipitation of schizont proteins with antibodies against MSP-1 and MSP-7 showed that the 195 kDa (MSP-1) and 48 kDa (MSP-7) precursors form a complex in schizonts before either MSP-1 or MSP-7 underwent primary processing. This complex is non-covalently bound as it is only maintained in non-ionic detergent (NP-40) conditions, whilst the ionic detergent DOC breaks apart the MSP-1 - MSP-7 precursor complex. Hence the MSP-1 - MSP-7 precursor complex forms before processing of either the MSP-1 or the MSP-7 precursors.

The anti-MSP-1_{83} antibody 89.1 does not pull down the MSP-7 precursor in either NP-40 or DOC. This suggests that when the MSP-1 - MSP-7 precursor complex is maintained, the 89.1 binding site on the MSP-1 precursor is disrupted or blocked due to the presence of MSP-7. The binding site of 89.1 has been localised to a region between residues 217 - 466 on Block 3 of MSP-1 (Holder 1988). Therefore the site of interaction between MSP-1 and MSP-7 is probably at the N-terminus region of MSP-1.

This raises the questions how does the binding of MSP-7 affect the structure of the MSP-1 precursor, and the structure of the subsequent primary and secondary processed MSP-1 complex? Is binding of the MSP-7 precursor an essential step in the transport of the MSP-1 precursor to the plasma membrane, or is formation of the MSP-1-MSP-7 complex an essential prerequisite for conformational changes that either present cleavage sites to the proteases responsible for the MSP-1 and MSP-7 processing events, or allow binding of MSP-6_{36} after primary processing of MSP-1?

Additionally as the MSP-7_{33} - MSP-7_{22} cleavage site has similarities to the primary processing sites of MSP-1 and to the site of cleavage of MSP-6 to MSP-6_{36}, is the same protease responsible for all cleavage of all three proteins, and could it be a putative drug target?

Inhibiting the transport of proteins to the developing merozoite surface in schizonts with the classical secretory pathway inhibitor, Brefeldin A (BFA), suggests that the MSP-1 and MSP-7 precursors form a complex on translation or in the ER. As BFA treatment causes a build up of both the MSP-1 and MSP-7 precursors that are complexed together, it can also be concluded that the MSP-1 - MSP-7 complex is transported to the developing merozoite membrane via the classical secretory pathway.

The cleavage of the MSP-7 precursor to MSP-7_{33} is inhibited by BFA, suggesting that the first MSP-7 cleavage event occurs post – Golgi, either during transport of the MSP-1 – MSP-7 precursor complex to the developing merozoite membrane, or once it has reached the merozoite surface. It also suggests that cleavage of the MSP-7 precursor to MSP-7_{33} occurs before primary processing of MSP-1.

Pulse chase analysis of the MSP-1 - MSP-7 precursor complex formation in non-ionic conditions shows a rapid decrease of the MSP-7 precursor with a corresponding increase in the quantity of MSP-7_{33} that remains complexed to the MSP-1 precursor, and

an increase in free MSP-7_{20} that is no longer associated with the MSP-1 complex. This process takes 20 - 30 minutes, which is consistent with the anti-MSP-7A and anti-MSP-7B IFAT results showing a similar pattern of fluorescence on the surface of developing merozoites in schizonts, as the complex would have been transported to the surface in that time, and hence the IFAT results are recognising either the full length MSP-7 precursor or the cleaved MSP-7_{20} and MSP-7_{33} cleaved products on the merozoite surface.

The pulse chase results also suggest that in schizonts the MSP-7_{33} protein is not immediately cleaved into MSP-7_{22}, suggesting that this step occurs later, on or during release of merozoites. The MSP-7_{22} cleavage site shows a significant similarity to a MSP-1 primary processing site, and the MSP-6_{36} cleavage site suggesting that perhaps the protease(s) responsible for primary processing of MSP-1 is also responsible for secondary processing of MSP-7, and cleavage of the MSP-6 precursor to MSP-6_{36}. The timing of the cleavage events would be around the time of merozoite release, which is when MSP-6_{36} is first identified bound to the primary processed MSP-1 complex. One possible candidate for the protease responsible for these processing reactions is the parasitophorous vacuole protease SERPH (Blackman 2000).

Processing of MSP-7_{22} to MSP-7_{19} occurs on the merozoite surface before MSP-1 undergoes secondary processing, and is not inhibited by calcium chelators or serine protease inhibitors. Hence the calcium dependent serine protease responsible for secondary processing of MSP-1_{42} is not responsible for processing of MSP-7_{22} to MSP-7_{19} (Blackman and Holder 1992; Blackman *et al.* 1993). Antibodies to either MSP-7A or MSP-7B do not inhibit the processing of MSP-1_{42}. It is unknown what effect antibodies to either MSP-1 or MSP-7 would have on the processing of MSP-7_{22} to MSP-7_{19}. Ideally

the antibodies to MSP-7 should be tested in an erythrocyte invasion assay to determine if they can inhibit red blood cell invasion.

As both MSP-7_{22} and MSP-7_{19} are present in the shed MSP-1 complex, and MSP-1 and MSP-7 are complexed together in roughly equal stoichiometric amounts, does the presence of MSP-7_{19} have any relevance to the processing of MSP-1_{42} and subsequent release of the shed MSP-1 complex, or is the processing to MSP-7_{19} just an artifact due to an unrelated protease released during merozoite release or erythrocyte invasion?

MSP-7 probably has a specific function either in the developing or released merozoite, most probably in its interaction with MSP-1. It's close association with MSP-1 during translocation to the merozoite surface, high level of conservation and similarity in processing events, suggests that MSP-7 has an essential role in the merozoite. Hence MSP-7 warrants further study to define its importance as part of the structure of the MSP-1 complex, and the function of the three proteolytic cleavages it undergoes whilst complexed to MSP-1.

Figure 5.0 Northern Blot Analysis of the *P. falciparum* Erythrocytic Cycle

Highly synchronized (30 minute time window) 3D7 parasites were collected at 2-hour intervals throughout the 48-hour cycle, and total RNA extracted using the TRIzol method. The total RNA from each time point (0 – 48 hours) was separated by agarose-guanidine thiocyanate electrophoresis. (With thanks to M. Grainger, M. Kavaratne, S. Khan, I. Ling and H. Taylor).

The resulting gel was stained with ethidium bromide, and an ultraviolet illuminated image taken **(A)**, before the RNA was Northern blotted. Giemsa stained slides of parasites from each time point were viewed by light microscopy to confirm the synchronicity of culture (data not shown). The Northern blotted total RNA was probed consecutively with two [α-^{32}P] dATP labelled probes, *stevor* a differentially expressed control **(B)** and *msp-7b* **(C)**.

A) The ethidium bromide stained gel of the total RNA samples showed a gradual increase in the quantity of RNA concurrent with the expected increase in message as the parasite develops from the ring stage to the multinucleated schizont in the infected red blood cell. The lane with RNA markers is indicated by M. Analysis of the Giemsa stained images taken from the 30 – 48 hour time points showed late trophozoites / early schizonts undergoing maturation, with schizont rupture and merozoite release being detected by 48 hours.

B) The control probe *Stevor* bound to the 22 – 32 hour total RNA samples as predicted (Image shown with kind thanks to M. Kaviratne). The positions of RNA size markers are indicated in kb.

C) The *msp-7b* probe recognized a band of approx 2,500 nucleotides in the total RNA samples taken at 34 - 48 hours. The intensity of binding to the transcript was low at 34 hours, increased rapidly to a maximum at 36 - 42 hours, and then gradually decreased in the 44 - 48 hour time points. Hence *msp-7* is transcribed in early to late schizonts, as merozoites are undergoing development. No binding of *msp-7b* to ring or trophozoite RNA samples (Time points 0 – 32 hours) was seen. Hence *msp-7* is transcribed in a stage specific manner during the erythrocytic stage 34 – 48 hours during schizogony.

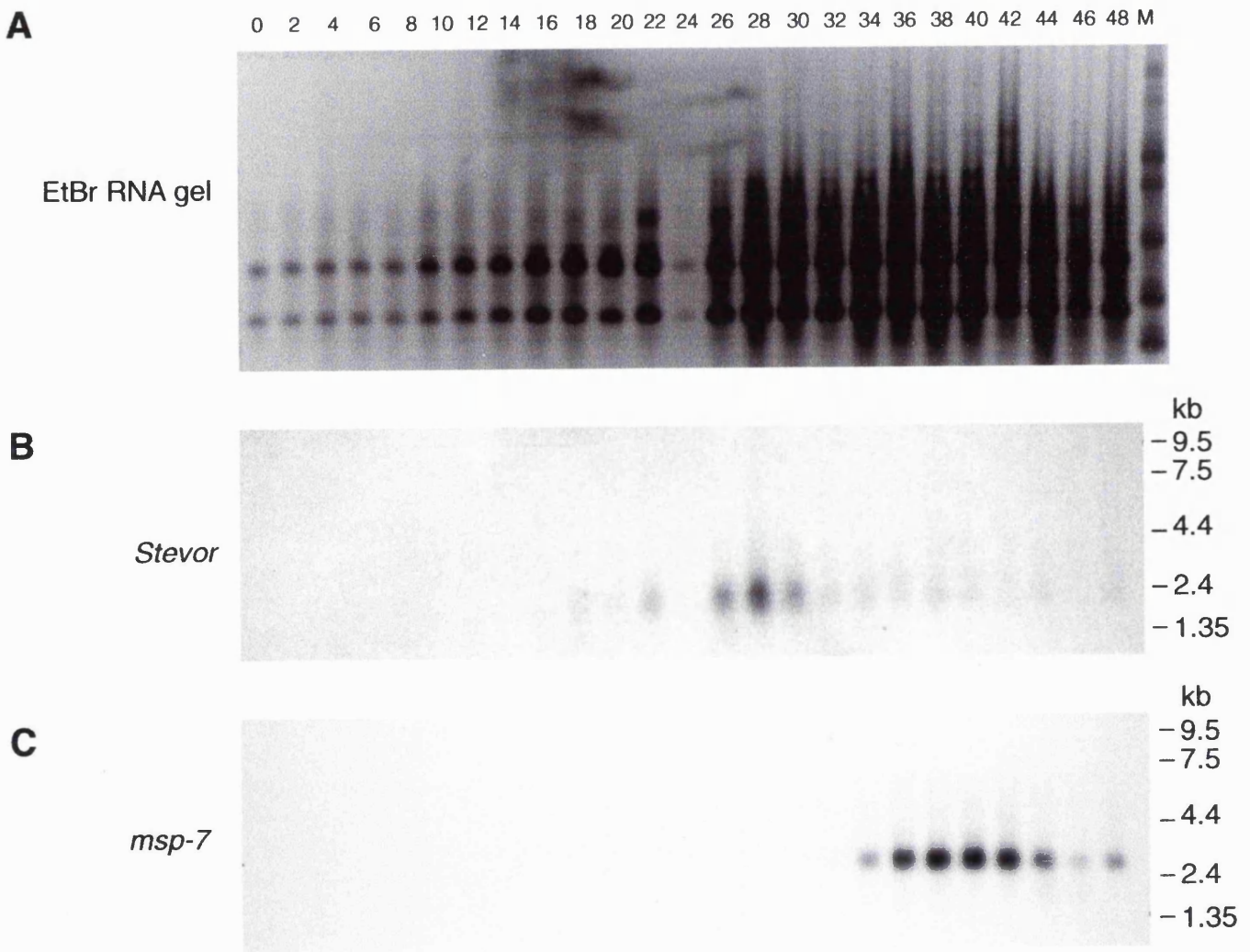
A
0 2 4 6 8 10 12 14 16 18 20 22 24 26 28 30 32 34 36 38 40 42 44 46 48 M
EtBr RNA gel
B
kb
9.5
7.5
4.4
2.4
1.35
Stevor
C
kb
9.5
7.5
4.4
2.4
1.35
msp-7

Figure 5.1 Western Blot Analysis of Schizonts, Merozoites & Shed MSP-1 Complex

A) Mature T9-96 *Pf* schizonts (44 – 48 hours development) were saponin lysed and solubilised into SDS sample cocktail with DTT, separated by SDS-PAGE and Western blotted. The blots were then probed with mouse anti-GST-MSP-7A (αMSP-7A), mouse anti-GSTMSP-7B (αMSP-7B) and NMS. Antibody binding was detected with secondary HRP conjugated anti-mouse IgG antibodies and ECL. Molecular mass markers are indicated in kDa.

Both anti-MSP-7 sera recognise a band at 48 kDa predicted to be the MSP-7 precursor. Anti-GST-MSP-7A also binds weakly to a band at 20 kDa ($MSP\text{-}7_{20}$), whilst anti-GST-MSP-7B binds strongly to a 33 kDa band ($MSP\text{-}7_{33}$) and a doublet at 22 kDa ($MSP\text{-}7_{22}$), and weakly to a band of ~45 kDa. NMS did not react with any specific schizont proteins.

B) Merozoites, collected in presence of calcium chelators and serine protease inhibitors, were lysed directly into SDS sample cocktail, reduced with DTT, separated by SDS-PAGE and western blotted. The blots were then probed with mouse anti-GST-MSP-7A, mouse anti-GST-MSP-7B and NMS. Antibody binding was detected with secondary HRP conjugated anti-mouse IgG antibodies and ECL. Molecular mass markers are indicated in kDa.

NMS and anti-MSP-7A sera do not react with merozoite proteins under reduced conditions. The anti-MSP-7B mouse serum reacts with a band at 22 kDa and another at 19 kDa. These are predicted to be $MSP\text{-}7_{22}$ and $MSP\text{-}7_{19}$.

C) Shed MSP-1 complex recovered from culture supernatant by X509-immunoaffinity purification was reduced with DTT, separated by SDS-PAGE and Western blotted. The blots were probed with mouse anti-GST-MSP-7A, mouse anti-GST-MSP-7B, JP-1 anti-MSP-7B monoclonal antibody and NMS. Primary antibody binding was detected using the appropriate anti-mouse IgA or IgG HRP-conjugated secondary antibodies and ECL. Molecular mass markers are indicated in kDa.

Neither NMS nor anti-MSP-7A serum bind to proteins in the shed MSP-1 complex. Both the anti-MSP-7B serum and the JP-1 monoclonal antibody bound to bands at 22 kDa and 19 kDa. These are predicted to be $MSP\text{-}7_{22}$ and $MSP\text{-}7_{19}$.

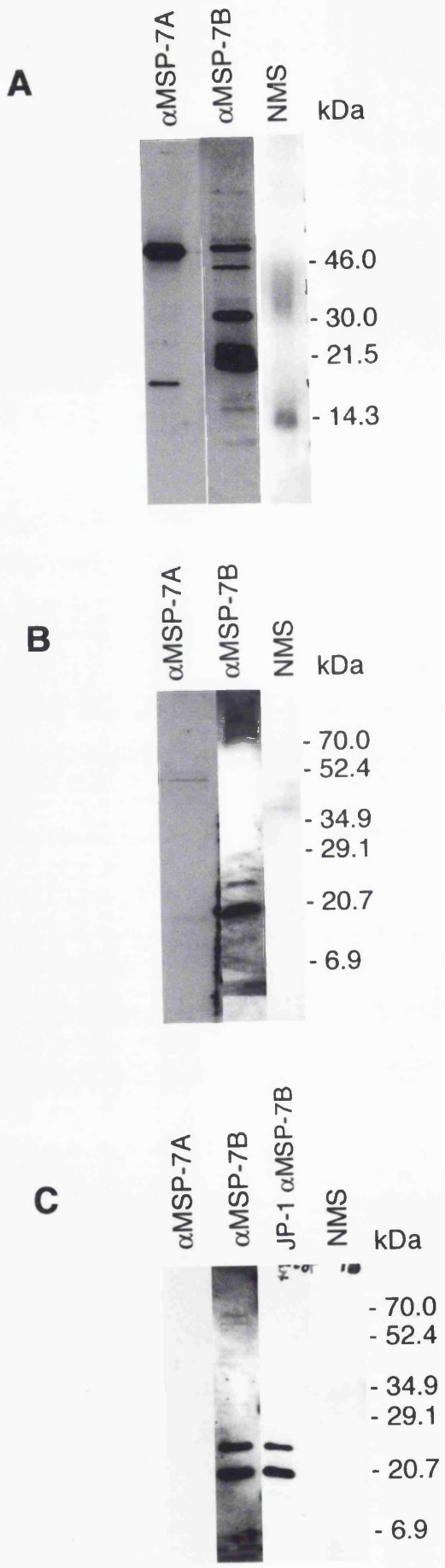
A
αMSP-7A
αMSP-7B
NMS
kDa
- 46.0
- 30.0
- 21.5
- 14.3
B
αMSP-7A
αMSP-7B
NMS
kDa
- 70.0
- 52.4
- 34.9
- 29.1
- 20.7
- 6.9
C
αMSP-7A
αMSP-7B
JP-1 αMSP-7B
NMS
kDa
- 70.0
- 52.4
- 34.9
- 29.1
- 20.7
- 6.9

Figure 5.2 IFAT Analysis of MSP-7 in Schizonts

Acetone/methanol fixed mature *P. falciparum* schizonts were tested by IFAT with the following combinations of primary and secondary antibodies:

- Mouse anti-GST-MSP-7A (**αMSP-7A**) serum, with anti-mouse IgG (γ-chain specific) FITC-conjugated goat antibodies.
- Mouse anti-GST-MSP-7B (**αMSP-7B**) serum, with anti-mouse IgG (γ-chain specific) FITC-conjugated goat antibodies.
- JP-1 anti-MSP-7B (**JP-1 αMSP-7B**) mouse IgA monoclonal antibody with anti-mouse IgA (α-chain specific) FITC-conjugated goat antibodies.
- Rabbit anti-MSP-1 (**Rb αMSP-1**) serum, with anti-rabbit IgG (whole molecule) TRITC-conjugated goat antibodies.
- G13 anti-MSP-1 (**G13 αMSP-1**) mouse IgG monoclonal antibody with anti-mouse IgG (H+L chain) Oregon Green-conjugated goat antibodies.
- Rat anti-BiP (**αBiP**) serum, with anti-rat IgG (H+L chain) Oregon Green-conjugated goat antibodies.
- Rat anti-EBA-175 (**αEBA**) serum, with anti-rat IgG (H+L chain) Oregon Green-conjugated goat antibodies.

Red blood cells were staining with Evans Blue (except with the TRITC fluorophore), and nuclear material stained with DAPI. Slides were viewed with the Deltavision microscope using the appropriate excitation and emission filters for the fluorophores, and images captured using the SoftWorks programme.

The anti-MSP-7 antibodies outline the edges and regions of the cytosol of nascent merozoites during merogony, with a similar pattern to that obtained with anti-MSP-1 antibodies. As merozoites mature the anti- MSP-1 and MSP-7B antibodies are located more distinctly to the merozoite surface, giving a bunch of grapes-like pattern.

The anti-BiP and EBA-175 antibodies highlight distinct regions of developing merozoites. The anti-BiP antibodies highlighted the ER, with a pattern in early- to mid-stage schizonts, which had some similarity to that seen with MSP-1 and MSP-7 antibodies. The anti-EBA-175 antibodies highlighted the micronemes developing in the apical region of the merozoites.

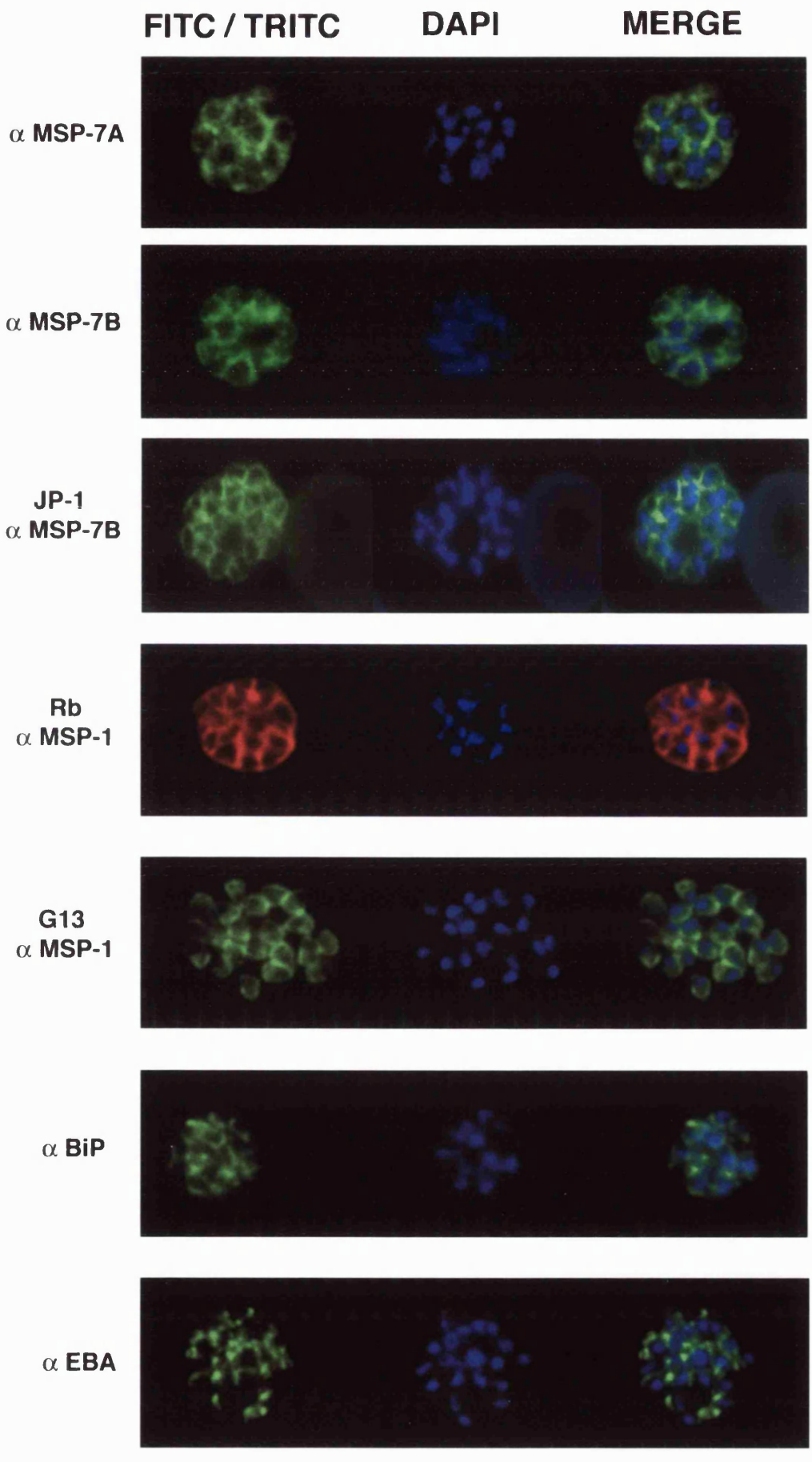
FITC / TRITC
DAPI
MERGE
α MSP-7A
α MSP-7B
JP-1
α MSP-7B
Rb
α MSP-1
G13
α MSP-1
α BiP
α EBA
5μm

Figure 5.3 IFAT Analysis of MSP-7 in Merozoites

Acetone/methanol fixed mature *P. falciparum* schizonts, a proportion of which had ruptured, were tested by IFAT with the following combinations of primary and secondary antibodies:

- JP-1 anti-MSP-7B (**JP-1 αMSP-7B**) mouse IgA monoclonal antibody with anti-mouse IgA (α-chain specific) FITC-conjugated goat antibodies.
- G13 anti-MSP-1 (**G13 αMSP-1**) mouse IgG monoclonal antibody with anti-mouse IgG (H+L chain) Oregon Green-conjugated goat antibodies.
- Rat anti-BiP (**αBiP**) serum, with anti-rat IgG (H+L chain) Oregon Green-conjugated goat antibodies.
- Rat anti-EBA-175 (**αEBA**) serum, with anti-rat IgG (H+L chain) Oregon Green-conjugated goat antibodies.

Red blood cells were staining with Evans Blue, and nuclear material stained with DAPI. Slides were viewed with the Deltavision microscope using the appropriate excitation and emission filters for the fluorophores, and images captured using the SoftWorks programme.

The JP-1 anti-MSP-7B monoclonal antibody bound to the surface of released merozoites with a very similar pattern to that seen with the G13 anti-MSP-1_{33} antibody.

A number released merozoites bound by the JP-1 monoclonal appear to be in the process of attaching to and invading red blood cells. In the fourth set of JP-1 images the merozoite appears to have invaded a red blood cell and shed its coat of surface proteins of which the shed MSP-1 complex, including the MSP-7_{22} and MSP-7_{19} polypeptides recognised by the JP-1 antibody, is likely to be a major component.

The anti-BiP and EBA-175 antibodies bind to locales in merozoites, that are distinct from the surface immuno-fluorescence seen with the anti-MSP-1 or MSP-7 antibodies.

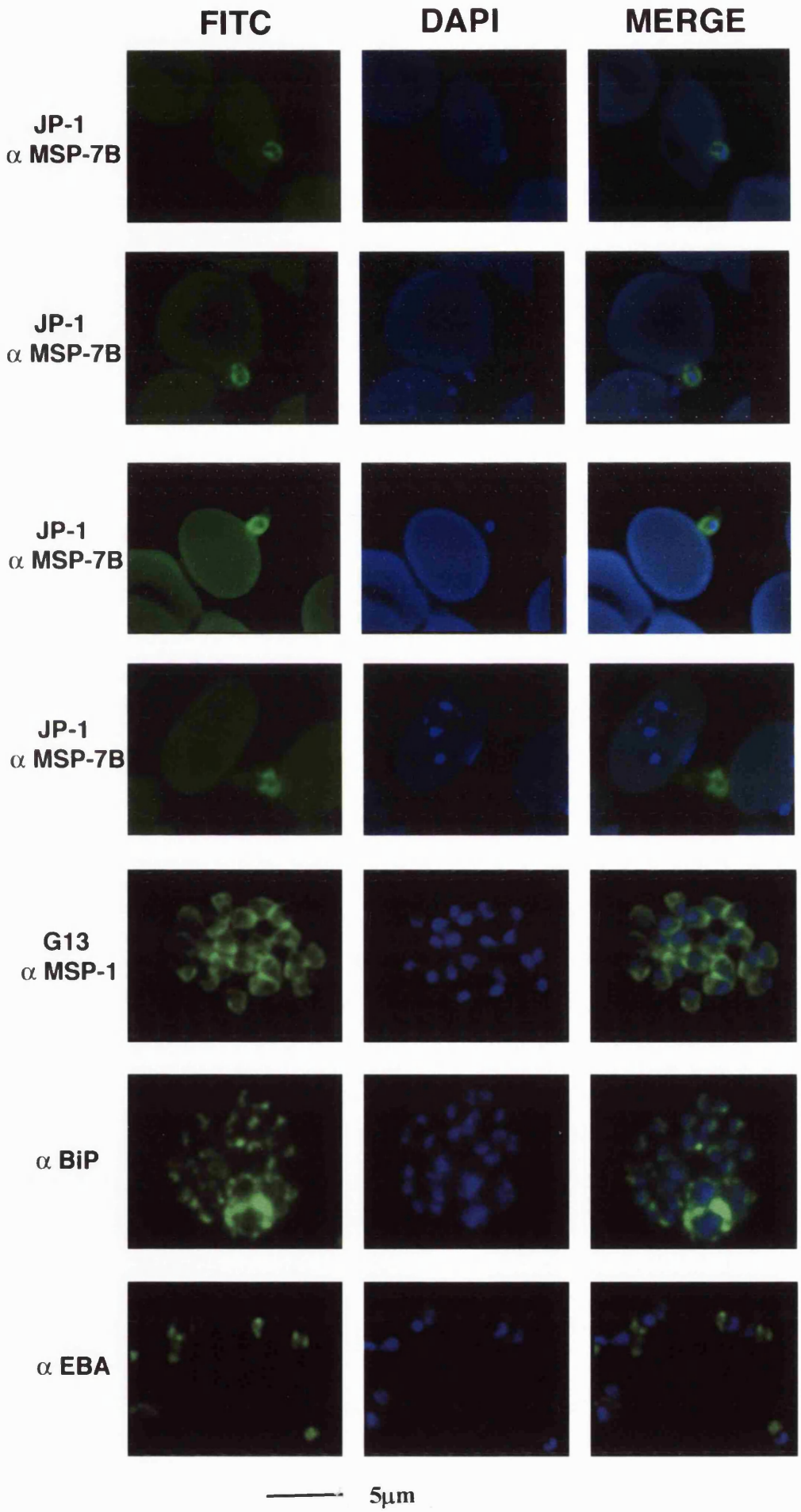
FITC
DAPI
MERGE
JP-1
α MSP-7B
JP-1
α MSP-7B
JP-1
α MSP-7B
JP-1
α MSP-7B
G13
α MSP-1
α BiP
α EBA
5μm

Figure 5.4 Dual Immuno-fluorescence of MSP-7 and MSP-1 antibodies

Dual IFAT was performed on acetone/methanol fixed mature *P. falciparum* schizonts. Parasites were incubated with the first stage antibody combinations A – D as follows:

A) Mouse anti-GST-MSP-7A (**αMSP-7A**) serum, with anti-mouse IgG (γ-chain specific) FITC-conjugated goat antibodies.

B) Mouse anti-GST-MSP-7B (**αMSP-7B**) serum, with anti-mouse IgG (γ-chain specific) FITC-conjugated goat antibodies.

C and D) JP-1 anti-MSP-7B (**JP-1 αMSP-7B**) mouse IgA monoclonal antibody with anti-mouse IgA (α-chain specific) FITC-conjugated goat antibodies.

Parasites were then incubated with the second stage antibody combination of rabbit anti-MSP-1 (**Rb αMSP-1**) serum, with anti rabbit IgG (whole molecule) TRITC-conjugated goat antibodies. Nuclear material was stained with DAPI. Slides were viewed with the Deltavision microscope using combinations of excitation and emission filters appropriate for the fluorophores, and images captured using the SoftWorks programme.

The fluorophores shown are as follows: FITC only; TRITC only; FITC and TRITC merged; DAPI only; FITC, TRITC and DAPI merged (MERGE). Regions of co-localisation between MSP-1 and MSP-7 antibodies are shown as yellow.

Images **A – C** are of schizonts. Image **D** is of a free merozoite, with the insert in the top right corner, showing its actual size in relation to the schizonts shown in A – C.

The results are discussed in the text.

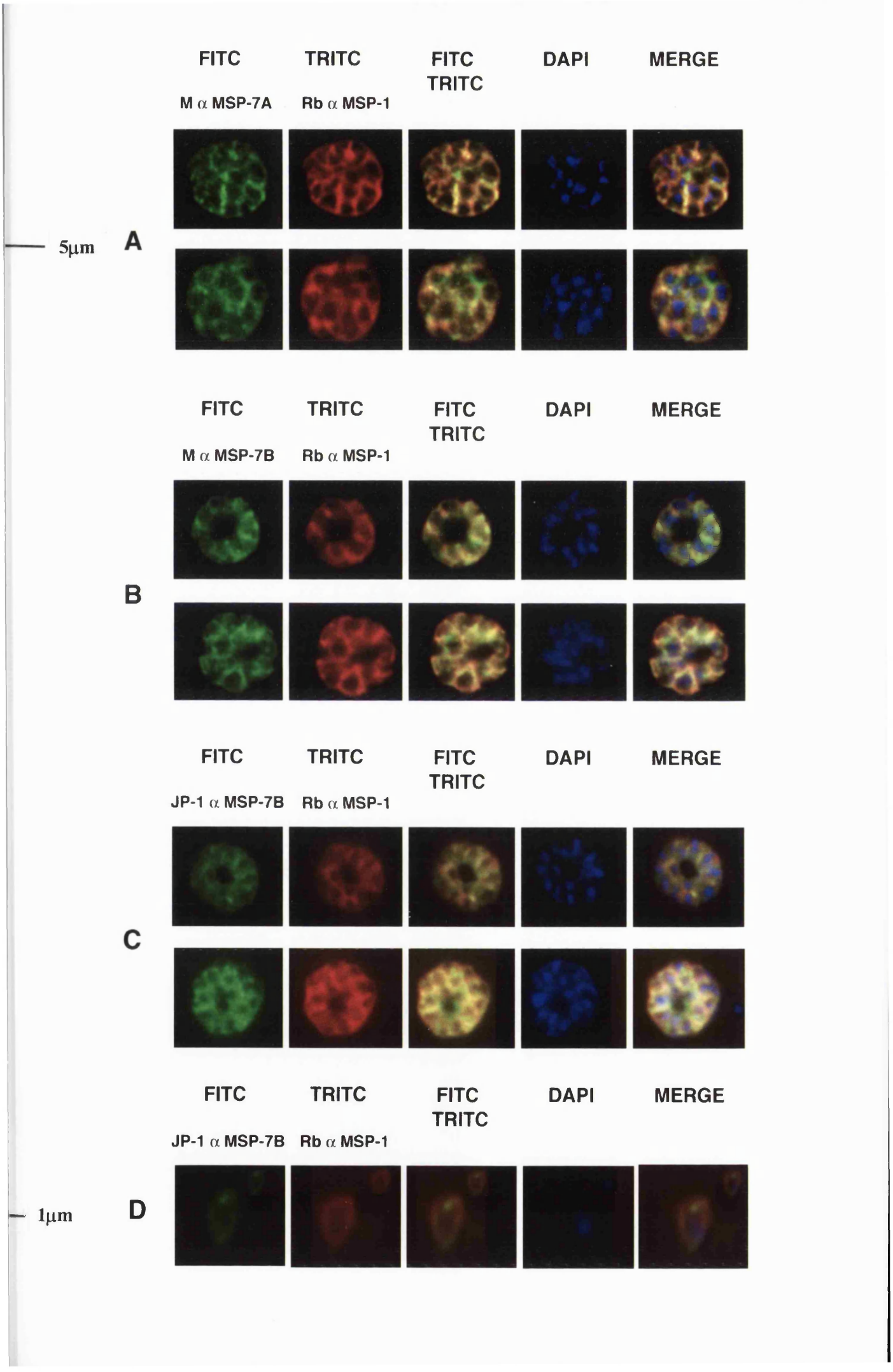
FITC
TRITC
FITC TRITC
DAPI
MERGE
M α MSP-7A
Rb α MSP-1
5μm
A
FITC
TRITC
FITC TRITC
DAPI
MERGE
M α MSP-7B
Rb α MSP-1
B
FITC
TRITC
FITC TRITC
DAPI
MERGE
JP-1 α MSP-7B
Rb α MSP-1
C
FITC
TRITC
FITC TRITC
DAPI
MERGE
JP-1 α MSP-7B
Rb α MSP-1
1μm
D

Figure 5.5 Investigation of MSP-7 Translation and Processing Events by Immunoprecipitation

Mature *P. falciparum* schizonts were metabolically radiolabelled with L-[^{35}S] methionine and L-[^{35}S] cysteine PRO-MIX *in vitro* labelling mix for 2 hours. Following radiolabelling, schizonts were lysed and proteins solubilised in the presence of detergents that either maintain protein complexes (NonidetP40 (**NP40**)), or disrupt them (sodium deoxycholate (**DOC**)). Solubilised proteins were immunoprecipitated with the following antibodies:

- Mouse anti-GST-MSP-7A serum (**MαMSP-7A**)
- Mouse anti-GST-MSP-7B serum (**MαMSP-7B**)
- Anti-MSP-$1_{42/33}$ monoclonal antibody (**X509**)
- Normal mouse serum as a negative control (**NMS**)

Antibody-antigen complexes were precipitated with Protein G Sepharose, washed, reduced with DTT and analysed on **(A)** 12.5% and **(B)** 8% SDS-PAGE minigels. After electrophoresis, antibody chains were visualised by staining with Coomassie blue (data not shown), and immunoprecipitated radiolabelled proteins visualised by incubation with Amplify, followed by exposure to autoradiography film at –70 °C.

The sizes of molecular mass markers are indicted in kDa. Proteins of 195 kDa (MSP-1 precursor), 48 kDa (MSP-7 precursor), 33 kDa (MSP-7_{33}), 22 kDa (MSP-7_{22}), and 20 kDa (MSP-7_{20}) are indicated on the images. Note: solubilisation of the MSP-1 precursor in DOC results in C-terminal cleavage of the MSP-1 precursor, giving a C-terminal protein of approximately 44 – 50 kDa that runs at the same size as the MSP-7 precursor and is recognised by X509.

In the presence of NP40, antibodies to MSP-1 and MSP-7 immunoprecipitate proteins of 48 and 195 kDa. These are predicted to be the MSP-7 and MSP-1 precursors. In the presence of both DOC and NP40, the anti-MSP-7A serum pulls down proteins of 20 and 48 kDa, whilst the anti-MSP-7B serum pulls down proteins of 22, 33 and 48 kDa. X509 also immunoprecipitates proteins of 22 and 33 kDa, but only in the presence of NP40, not DOC. A band of ~70 kDa is present in all NP-40 solubilised samples, this is probably HSP-70 as it is also immunoprecipitated by NMS. Results are discussed further in the text.

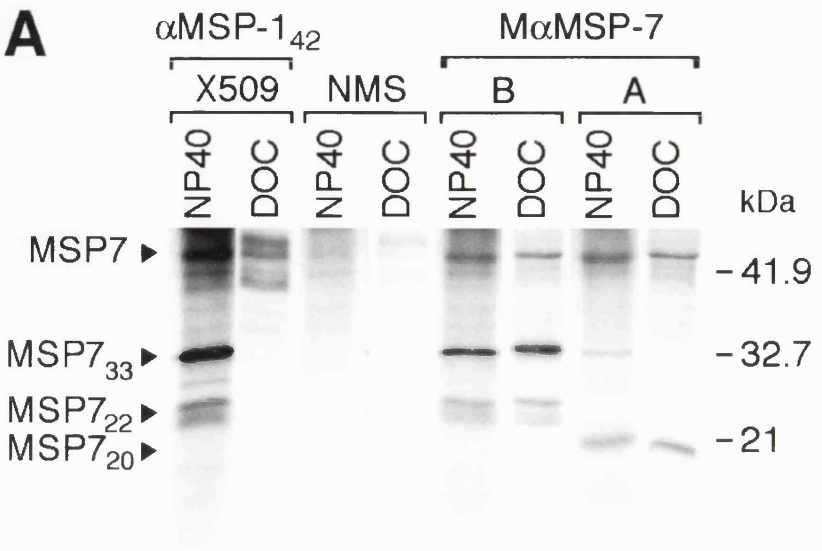
A
αMSP-1$_{42}$
MαMSP-7
X509
NMS
B
A
NP40
DOC
NP40
DOC
NP40
DOC
NP40
DOC
kDa
MSP7
MSP7$_{33}$
MSP7$_{22}$
MSP7$_{20}$
41.9
32.7
21

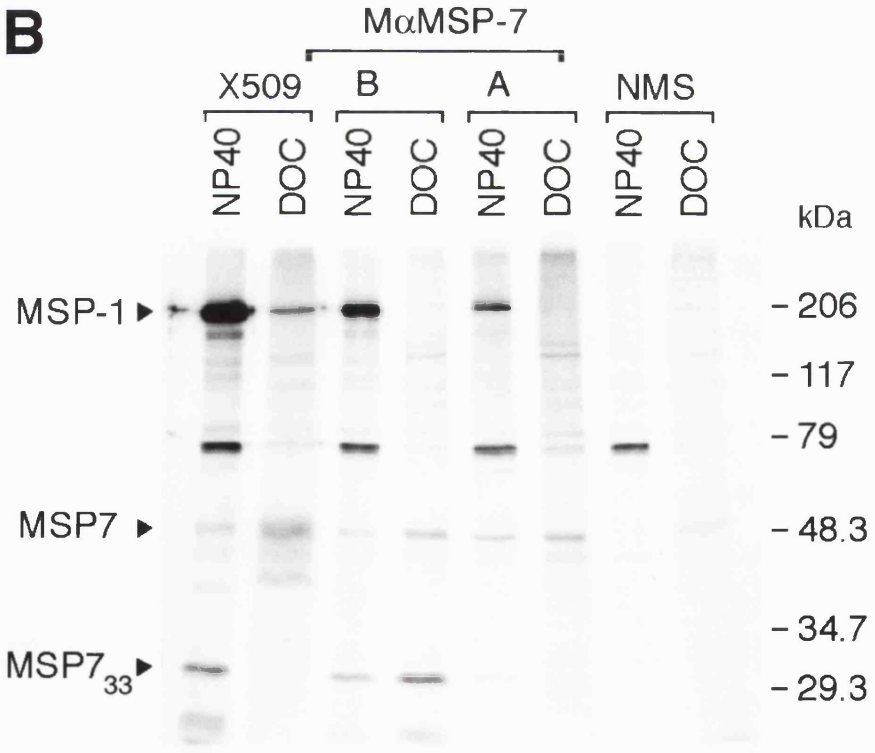
B
MαMSP-7
X509
B
A
NMS
NP40
DOC
NP40
DOC
NP40
DOC
NP40
DOC
kDa
MSP-1
MSP7
MSP7$_{33}$
206
117
79
48.3
34.7
29.3

Figure 5.6 Analysis of MSP-7 Polypeptides Released into the Culture Supernatant

A Mature *P. falciparum* schizonts were metabolically radiolabelled with L-[^{35}S] methionine and L-[^{35}S] cysteine PRO-MIX *in vitro* labelling mix for 2 hours. Following radiolabelling, schizonts were incubated overnight at 37 °C to allow merozoite release. Aliquots of the culture supernatant containing soluble radiolabelled proteins were analysed by immunoprecipitation with the following antibodies:

- Mouse anti-GST-MSP-7A serum (**αMSP-7A**)
- Mouse anti-GST-MSP-7B serum (**αMSP-7B**)
- Anti-MSP-1$_{42/33}$ monoclonal antibody (**X509**)
- Normal mouse serum as a negative control (**NMS**)

Antibody-antigen complexes were precipitated with Protein G Sepharose, and analysed on 12.5% SDS-PAGE mini-gels as described previously.

The polypeptide components of the shed MSP-1 complex are indicated. The anti-MSP-7A antibodies did not immunoprecipitate the 20 kDa (MSP-7$_{20}$) polypeptide, but did pull down several other larger bands. The shed MSP-1 complex is immunoprecipitated by both X509 and the anti-MSP-7B serum. Results are discussed further in the text.

B and C

Soluble shed MSP-1 complex was purified by X509-immunoaffinity purification from the culture supernatant of T9/96 parasites (Performed by C. Trucco and M. Grainger). The shed MSP-1 complex was separated on 12.5% SDS-PAGE minigels, and either Coomassie blue stained **(B)**, or western blotted **(C)**. The polypeptide components of the shed MSP-1 complex are indicated on **(B)**.

The western blotted shed MSP-1 complex was probed with mouse anti-GST-MSP-7A (**αMSP-7A**) and mouse anti-GST-MSP-7B (**αMSP-7B**) sera, and primary antibody binding detected using anti-mouse IgG HRP-conjugated secondary antibodies and ECL.

The anti-MSP-7A serum does not bind to any polypeptides in the shed MSP-1 complex. The anti-MSP-7B recognises two polypeptides of 19 and 22 kDa, which correspond in size to the MSP-7$_{22}$ and MSP-7$_{19}$ components of the shed MSP-1 complex.

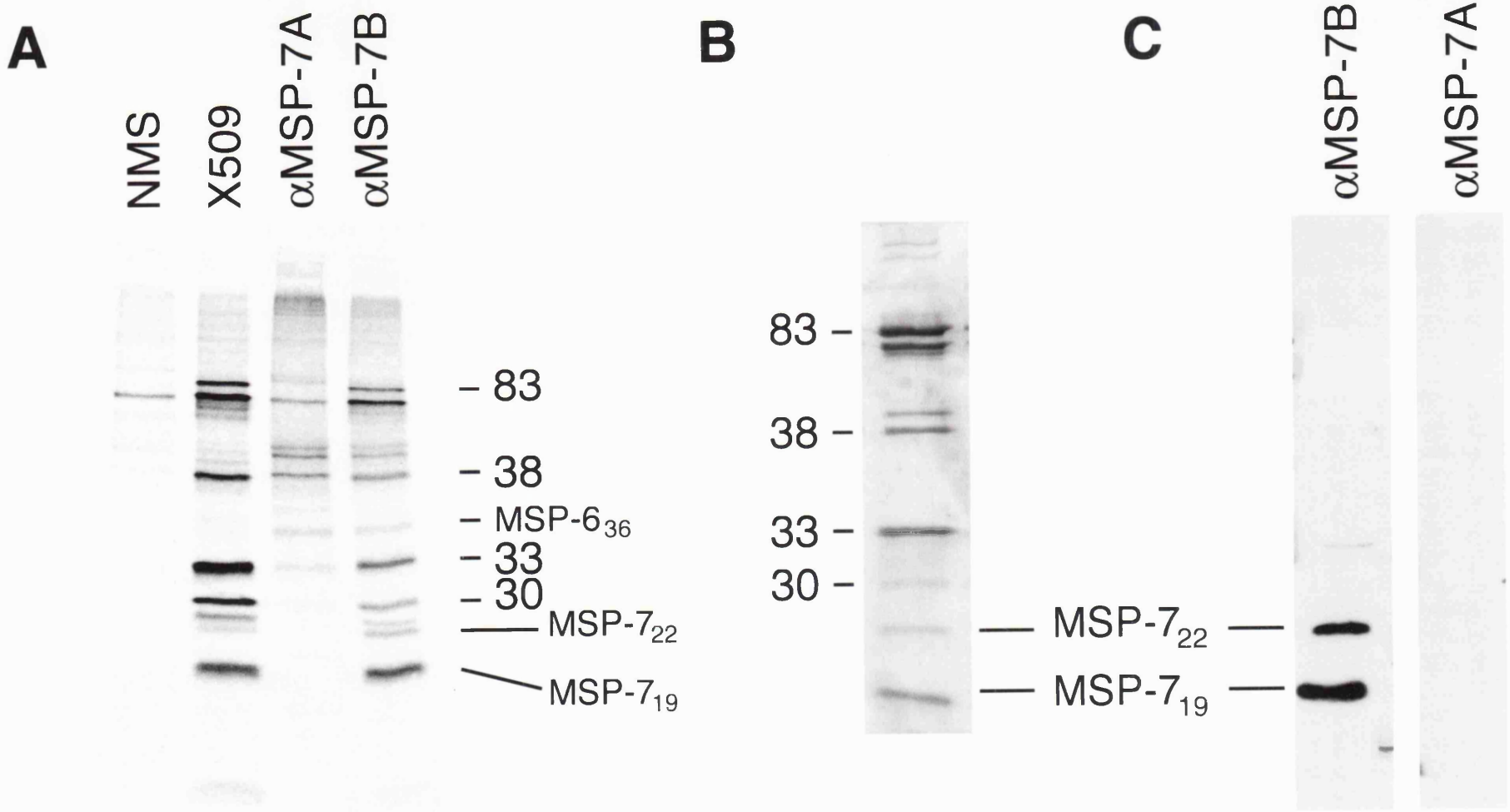
A
NMS
X509
αMSP-7A
αMSP-7B
83
38
MSP-6$_{36}$
33
30
MSP-7$_{22}$
MSP-7$_{19}$
B
83
38
33
30
MSP-7$_{22}$
MSP-7$_{19}$
C
αMSP-7B
αMSP-7A

Figure 5.7 2D Peptide Mapping of MSP-7 Fragments

A) Methionine and Cysteine [^{35}S]-radiolabelled schizont proteins were solubilised in NP-40 and immunoprecipitated with mouse anti-GST-MSP-7B sera followed by precipitation of the antibody-antigen complex with protein G sepharose. The immunoprecipitated proteins were reduced and alkylated prior to separation on a 10 % SDS-PAGE gel. The resulting gel was fixed in destain and exposed to autoradiography film for 2 days at -80 °C. The developed film was used as a guide for excision out of the gel of the 48 kDa band (MSP-7 precursor), and the 33 kDa (MSP-7_{33}) band predicted to be the product of N-terminal cleavage of the MSP-7 precursor.

B) Excised gel slices were rehydrated, washed in ACN and the proteins digested by overnight incubation at 37 °C with tryspin. Digested peptides were extracted from the gel with 60 % ACN washes, dried down in a Speedvac, resuspended in 20 % aqueous pyridine and spotted onto TLC plates, along with xylene cyanol[1] and DNP lysine[2] marker dyes. The peptides were separated in the first dimension by electrophoresis at pH 4.4, and in the second dimension by ascending chromatography. The TLC plates were air dried, sprayed with ENHANCE and exposed to autoradiography film for 2 weeks at -80 °C.

The anti-GST-MSP-7B antibodies immunoprecipitated the 195 kDa MSP-1 precursor, the 48 kDa MSP-7 precursor and the 33 kDa band (MSP-7_{33}), from NP40 solubilised [^{35}S]-labelled schizonts. There was approximately 3 times as much of the 33 kDa band (MSP-7_{33}) than the 48 kDa (MSP-7 precursor), explaining why the resulting signal from the MSP-7 2D peptide map is significantly weaker than that of MSP-7_{33}. Despite the presence of an unfortunate water mark on the MSP-7_{33} 2D map, the trypsin digested fragments from both these bands separated in two dimensions with a very similar pattern. This suggests that the MSP-7 and MSP-7_{33} bands are related, confirming the hypothesis that the 48 kDa MSP-7 precursor undergoes N-terminal cleavage into MSP-7_{20} and MSP-7_{33}.

Comparing the 2D peptide maps for MSP-7 and MSP-7_{33} to those obtained for MSP-7_{22} and MSP-7_{19} purified from the shed MSP-1 Complex [Stafford, 1996 #29], shows that the 2D peptide maps had similar patterns, confirming that MSP-7 and MSP-7_{33} are related to MSP-7_{22} and MSP-7_{19}.

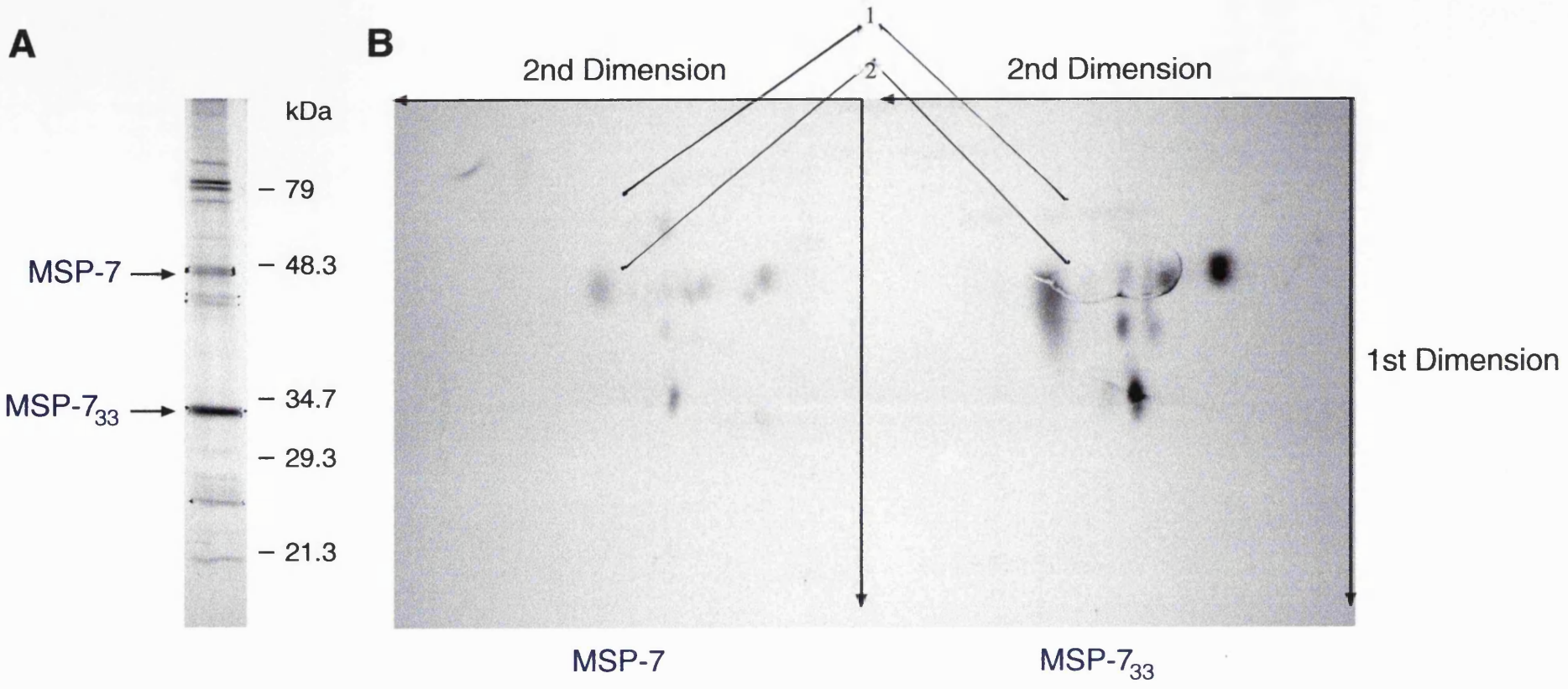
A
kDa
79
48.3
34.7
29.3
21.3
MSP-7
MSP-7$_{33}$
B
1
2
2nd Dimension
2nd Dimension
1st Dimension
MSP-7
MSP-7$_{33}$

Figure 5.8 MSP-7 and MSP-1 Precursors Form Complex Before MSP-1 Primary Processing

Early to mid-stage *P. falciparum* schizonts were metabolically radiolabelled for 2 hours with L-[^{35}S] methionine and L-[^{35}S] cysteine PRO-MIX *in vitro* labelling mix. Schizonts were then lysed and proteins solubilised in a non-ionic detergent that maintains protein complexes (NonidetP40 (**NP40**)), or an ionic detergent that disrupts them (sodium deoxycholate (**DOC**)). Solubilised proteins were immunoprecipitated with the following antibodies:

- Anti-MSP-1_{83} monoclonal mouse antibody (**89.1**)
- Normal mouse serum as a negative control (**NMS**)
- Mouse anti-GST-MSP-7A serum (**MαMSP7A**)
- Mouse anti-GST-MSP-7B serum (**MαMSP7B**)

Antibody-antigen complexes were precipitated with Protein G Sepharose, and analysed on 12.5% SDS-PAGE mini-gels as previously described.

In non-ionic conditions, the anti-MSP-1_{83} antibody, 89.1, immunoprecipitates only the 195 kDa MSP-1 precursor. In the presence of DOC ~40 kDa is cleaved from the C-terminus of the MSP-1 precursor, hence a smaller form of MSP-1 (~160 kDa) is immunoprecipitated by 89.1 from the DOC solubilised proteins. Unlike the anti-MSP-1 antibody, X509, which immunoprecipitates both the 48 kDa MSP-7 and 195 kDa MSP-1 precursors in non-ionic detergent conditions (Figure 5.5A and B), 89.1 does not appear to immunoprecipitate MSP-7.

In non-ionic conditions, both the anti-MSP-7A and MSP-7B sera immunoprecipitate proteins of 48 kDa (MSP-7), and 195 kDa (MSP-1). In the presence of DOC, both of the anti-MSP-7 antibodies immunoprecipitate the 48 kDa MSP-7 precursor, but not the MSP-1 precursor. The anti-MSP-7A serum pulls down a 20 kDa (MSP-7_{20}) protein in both ionic and non-ionic conditions, whilst the anti-MSP-7B serum pulls down a 33 kDa protein (MSP-7_{33}). The high molecular weight bands seen with anti-MSP-7A in the DOC sample are surprising, however these bands are also seen in the NMS lane and may be due cross reacting antibodies in the mouse sera. Results are discussed further in the text.

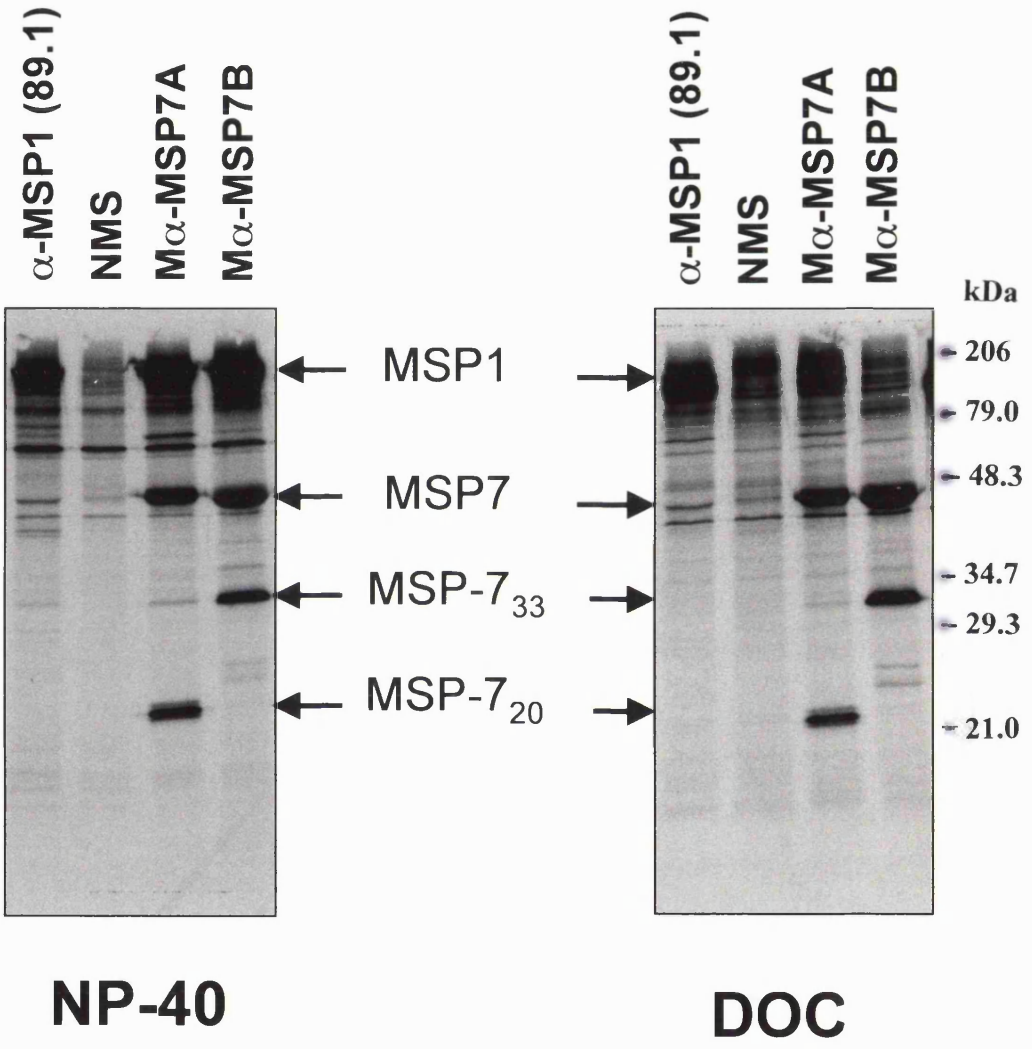
α-MSP1 (89.1)
NMS
Mα-MSP7A
Mα-MSP7B
MSP1
MSP7
MSP-7 33
MSP-7 20
α-MSP1 (89.1)
NMS
Mα-MSP7A
Mα-MSP7B
kDa
206
79.0
48.3
34.7
29.3
21.0
NP-40
DOC

Figure 5.9 Brefeldin A Inhibits MSP-7 Processing But Not MSP-1-MSP-7 Precursor Formation

Schizonts (36 - 40 hours post-invasion) were pre-treated for 30 minutes with Brefeldin A (BFA +) or a methanol control (BFA -), then radiolabelled, whilst in the presence or absence of BFA, for 1 hour with L-[^{35}S] methionine and L-[^{35}S] cysteine PRO-MIX *in vitro* labelling mix. Schizonts were then lysed and proteins solubilised in NonidetP40 (**NP40**), or sodium deoxycholate (**DOC**) (data not shown). NonidetP40 solubilised BFA + / BFA - proteins were immunoprecipitated with the following antibodies:

- Anti-MSP-$1_{42/33}$ X509 monoclonal antibody (**αMSP-1**)
- Mouse anti-GST-MSP-7B serum (**αMSP-7B**)
- Mouse anti-GST-MSP-7A serum (**αMSP-7A**)
- Normal mouse serum as a negative control (**NMS**)

Antibody-antigen complexes were precipitated with Protein G Sepharose, and analysed on 12.5 % SDS-PAGE mini-gels as described previously. The sizes of molecular mass markers are indicated in kDa.

The anti-MSP-1 antibody X509, and both the anti-MSP-7A and B sera, immunoprecipitated the 48 kDa MSP-7 and the 195 kDa MSP-1 precursors from BFA treated schizonts. Comparing immunoprecipitations of proteins from BFA treated parasites with those from methanol treated parasites, shows that the methanol treated (BFA -) parasites have significantly less MSP-7 precursor and significantly more of the 33 kDa (MSP-7_{33}), 22 kDa (MSP-7_{22}), and 20 kDa (MSP-7_{20}) cleavage products.

Hence the formation of the MSP-1 – MSP-7 precursor formation is not inhibited by Brefeldin A, whereas processing of the MSP-7 precursor is inhibited by BFA. Hence the first processing event of MSP-7 occurs post *trans*-Golgi. In addition, the MSP-1 precursor did not appear to have undergone primary processing in the methanol treated parasites, suggesting that MSP-7 is cleaved to MSP-7_{33} before MSP-1 undergoes primary processing.

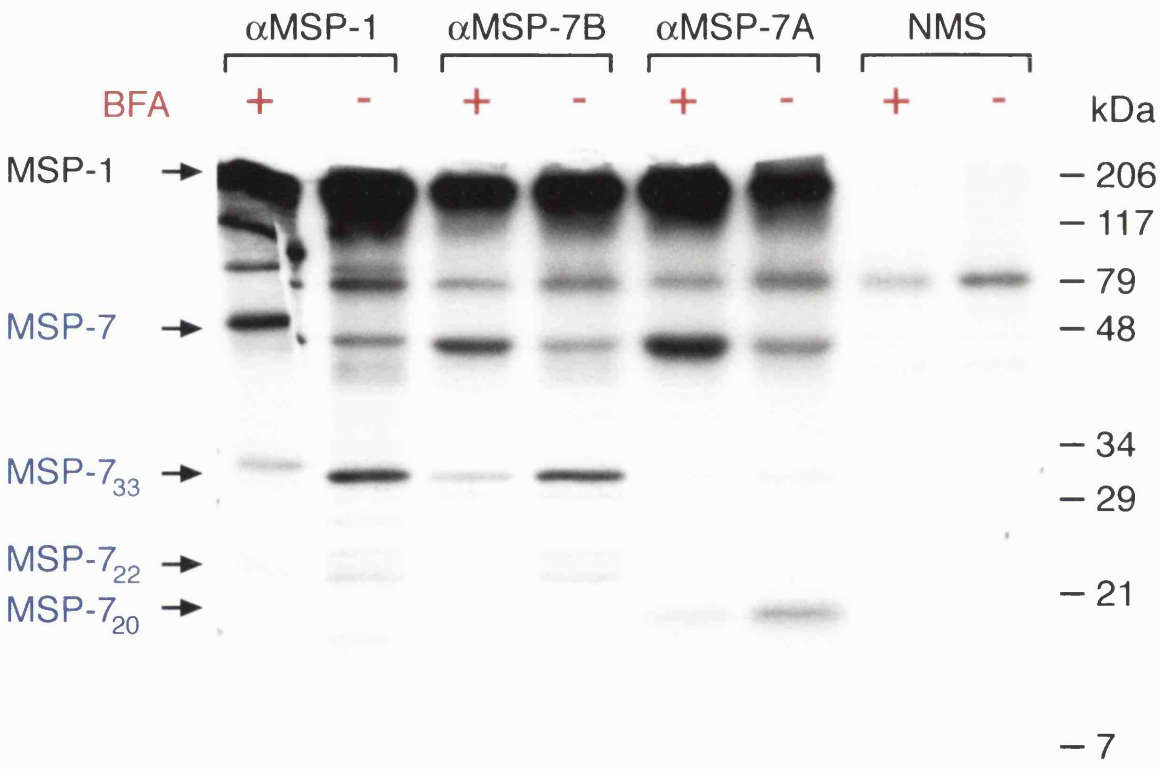
αMSP-1
αMSP-7B
αMSP-7A
NMS
BFA
+
-
+
-
+
-
+
-
kDa
MSP-1
MSP-7
MSP-7$_{33}$
MSP-7$_{22}$
MSP-7$_{20}$
206
117
79
48
34
29
21
7

Figure 5.10 First Pulse Chase Analysis of MSP-7 Translation

Synchronised *P. falciparum* schizonts (41 – 44 hours post-invasion) were pre-treated with Brefeldin A for 30 minutes, followed by a pulse for 30 minutes with L-[^{35}S] methionine and L-[^{35}S] cysteine PRO-MIX *in vitro* labelling mix whilst still in the presence of BFA. This was to give a build up of the MSP-1 and MSP-7 precursors, so that subsequent processing reactions could be followed with ease on initiation of the chase by removal of Brefeldin A and the pulse, since the effect of Brefeldin A on protein transport is reversible. The chase was initiated and samples of the parasites taken at 0, 0.5, 1.0, 2.0, 3.0, 4.0 and 5.0 hours after initiation of the chase. Samples from each time point were divided into two, the parasites lysed and proteins solubilised in the presence of NP40 and DOC. Immunoprecipitations were performed as previously described, on NP40 and DOC solubilised parasites from each time point, using the following antibodies:

(A) Mouse anti-GST-MSP-7A serum

(B) Mouse anti-GST-MSP-7B serum

(C) Anti-MSP-1_{83} 89.1 monoclonal antibody

(D) Normal mouse serum as a negative control

Analysis of the resulting gels, suggest that the MSP-7 precursor binds to the MSP-1 precursor, before the MSP-7 precursor is cleaved to MSP-7_{20} and MSP-7_{33}. The use of Brefeldin A in the Pulse, appears to have slowed down the transport of the MSP-1 – MSP-7 precursor complex through the Golgi, and hence delayed any processing events that occur post-Golgi. Hence processing of the MSP-7 precursor into MSP-7_{20} and MSP-7_{33} was slow, with a gradual increase in the cleavage products to a maximum by 2 hours post-chase. The gradual increase in the quantity of MSP-7_{20} and MSP-7_{33} cleavage products, corresponded with a slight decrease in the quantity of MSP-7 precursor. Additionally the quantity of MSP-1 bound by 89.1 decreased with time. Results are discussed further in the text.

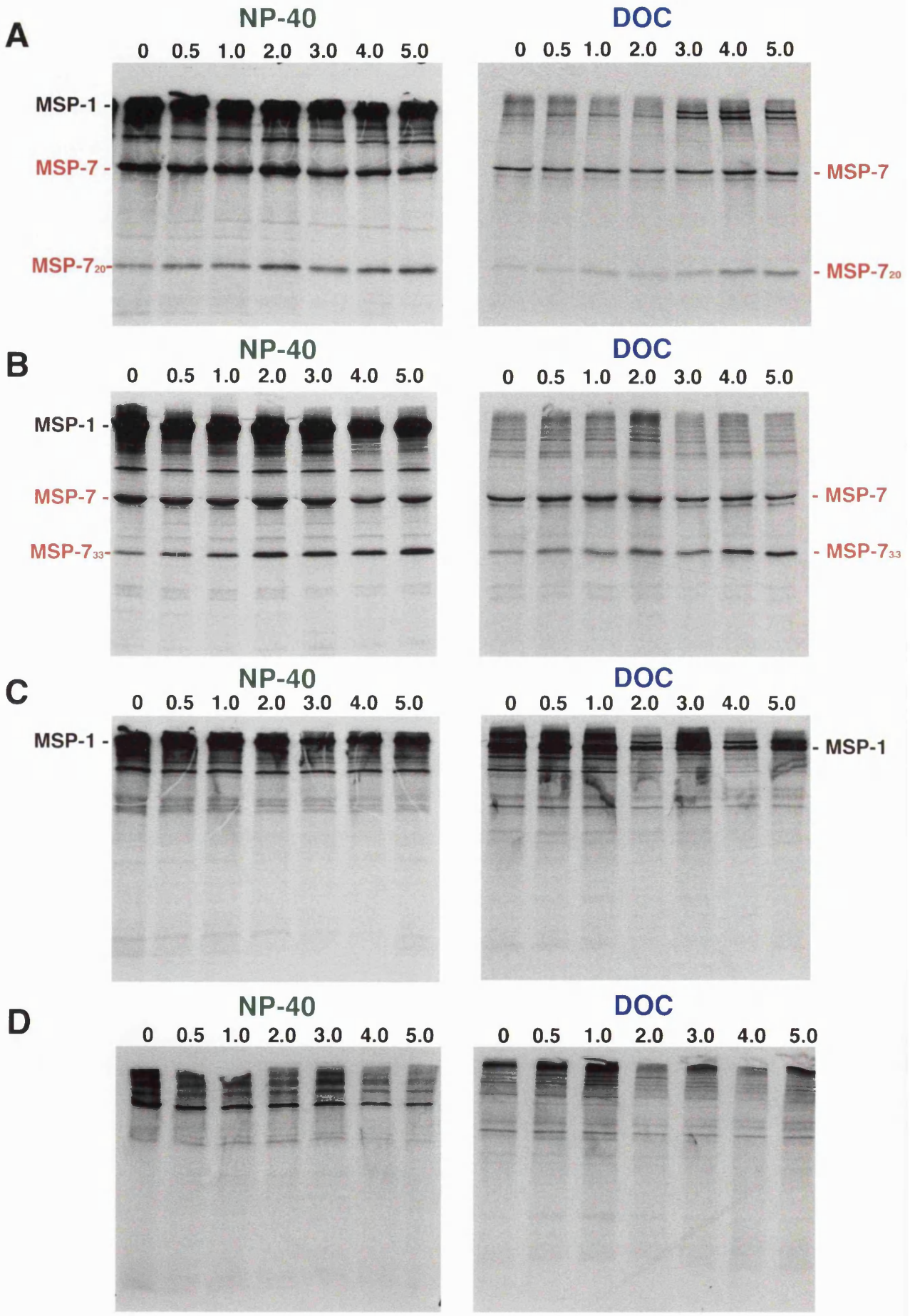
A
NP-40
DOC
0 0.5 1.0 2.0 3.0 4.0 5.0
MSP-1 -
MSP-7 -
MSP-7$_{20}$ -
- MSP-7
- MSP-7$_{20}$
B
NP-40
DOC
0 0.5 1.0 2.0 3.0 4.0 5.0
MSP-1 -
MSP-7 -
MSP-7$_{33}$ -
- MSP-7
- MSP-7$_{33}$
C
NP-40
DOC
0 0.5 1.0 2.0 3.0 4.0 5.0
MSP-1 -
- MSP-1
D
NP-40
DOC
0 0.5 1.0 2.0 3.0 4.0 5.0

Figure 5.11 Second Pulse Chase Analysis of MSP-7 Translation

Synchronised *P. falciparum* mature nucleated schizonts were pulsed with 300 $\mu Ci\ ml^{-1}$ of L-[^{35}S] methionine and L-[^{35}S] cysteine PRO-MIX *in vitro* labelling mix, for 10 minutes. The chase was initiated by culture in normal medium and samples taken at 0, 10, 20, 30, 60 and 120 minutes after initiation of the chase. Samples from each time point were solubilised in NP40 and DOC (data not shown) and analysed by immunoprecipitation as before using the following antibodies:

- Mouse anti-GST-MSP-7B serum (**αMSP7B**)
- Mouse anti-GST-MSP-7A serum (**αMSP7A**)
- Anti-MSP-1_{83} monoclonal mouse antibody (**αMSP1 / 89.1**)

Immunoprecipitations of NP40 solubilised proteins from the first four time points (0 – 30 minutes post-chase) are shown.

Within 10 minutes of adding radiolabel (0 minutes post-chase), the MSP-1 and MSP-7 precursors have already formed a complex, and the MSP-7 precursor is already being processed into MSP-7_{20} and MSP-7_{33}. As the MSP-7 precursor is processed, there is an increase in MSP-7_{20}, and a decrease in MSP-1 precursor immunoprecipitated by the anti-MSP-7A serum. This decrease in MSP-1 is consistent with the predicted loss of the anti-MSP-7A binding site from the precursor complex as MSP-7_{20} is cleaved from the MSP-1 – MSP-7 precursor complex.

The quantity of MSP-1 immunoprecipitated by 89.1 also decreases, this is consistent with the loss of the 89.1 binding site on block 3 of MSP-1, as the MSP-1 – MSP-7 precursor forms. The quantity of MSP-1 precursor bound by the anti-MSP-7B serum remained constant with time, suggesting that the C-terminus of MSP-7_{33} remains bound to the MSP-1 precursor.

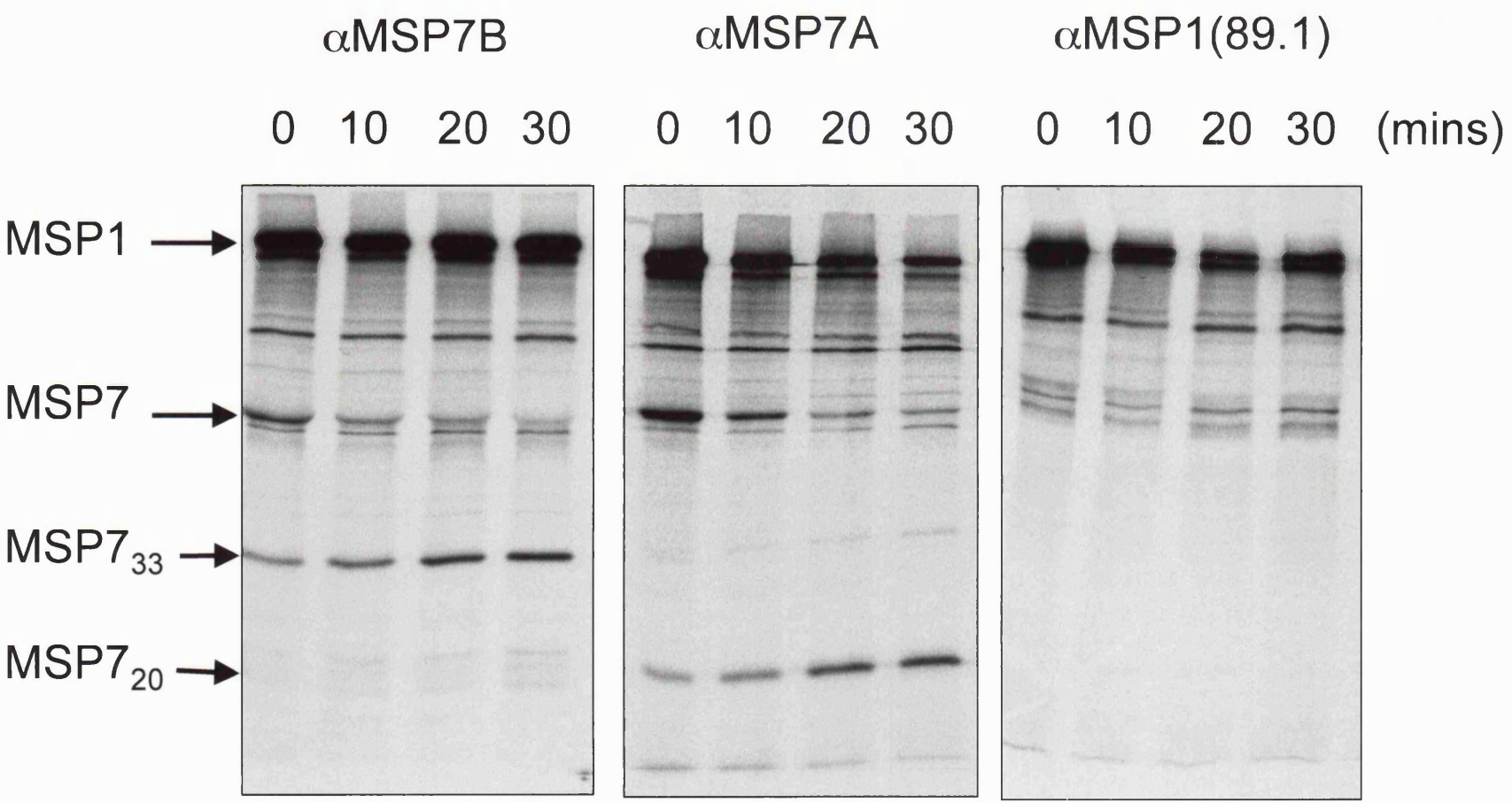
αMSP7B
αMSP7A
αMSP1(89.1)
0 10 20 30
0 10 20 30
0 10 20 30 (mins)
MSP1
MSP7
MSP7 33
MSP7 20

Figure 5.12 Secondary MSP-1_{42} Processing Assay

MSP-1 secondary processing assays were performed on merozoite preparations as described in section 2.18.0, with the guidance of C. Uthaipibull, following his modification of an assay described previously [Blackman, 1994 #4]. Assay samples were analysed and loaded onto a 12.5 % SDS-PAGE gel and Western blotted.

The Western blotted samples were probed as follows:-

A) The presence of MSP-1_{33} indicative of secondary processing of MSP-1_{42} was detected by probing with X509-Biotinylated (anti-MSP-1_{33}) antibody and ECL.

B) The presence of MSP-7_{22} and MSP-7_{19}, was determined by probing with Rabbit anti-MSP-7_{22} serum and binding detected with AP-conjugated secondary anti-rabbit IgG antibodies and NBT / BCIP colour development.

The order of samples on the gel is as follows:-

1) Molecular mass markers, **2**) Shed MSP-1 complex, **3**) Positive Processing control, **4**) Negative processing control (PMSF), **5**) Zero Hour control to check status of MSP-1_{42} in merozoites used in the assay, **6**) mouse anti-GST-MSP-7B serum, **7**) mouse α-MSP-$7_{22.1}$ serum, **8**) JP-1 α-MSP-7B monoclonal culture S/N, **9**) mouse anti-GST-MSP-7A serum (M α-MSP-7A).

A) MSP-1_{33} was present in the positive processing control, but not in the negative (PMSF) or zero hour controls suggesting that the processing assay worked. MSP-7_{33} was detected in all the α-MSP-7 antibodies assay samples, suggesting that when used at 5µl in a total reaction volume of 20µl, there is no inhibition of MSP-1_{42} processing.

B) MSP-7_{22} and MSP-7_{19} were detected in all samples, suggesting that processing of MSP-7_{22} was not inhibited by anti-MSP-7 antibodies. The presence of MSP-7_{22} and MSP-7_{19} in the zero Hour and PMSF processing controls suggests that the processing event is either not inhibited by serine protease inhibitors or occurred prior to merozoite collection and hence secondary processing of MSP-1.

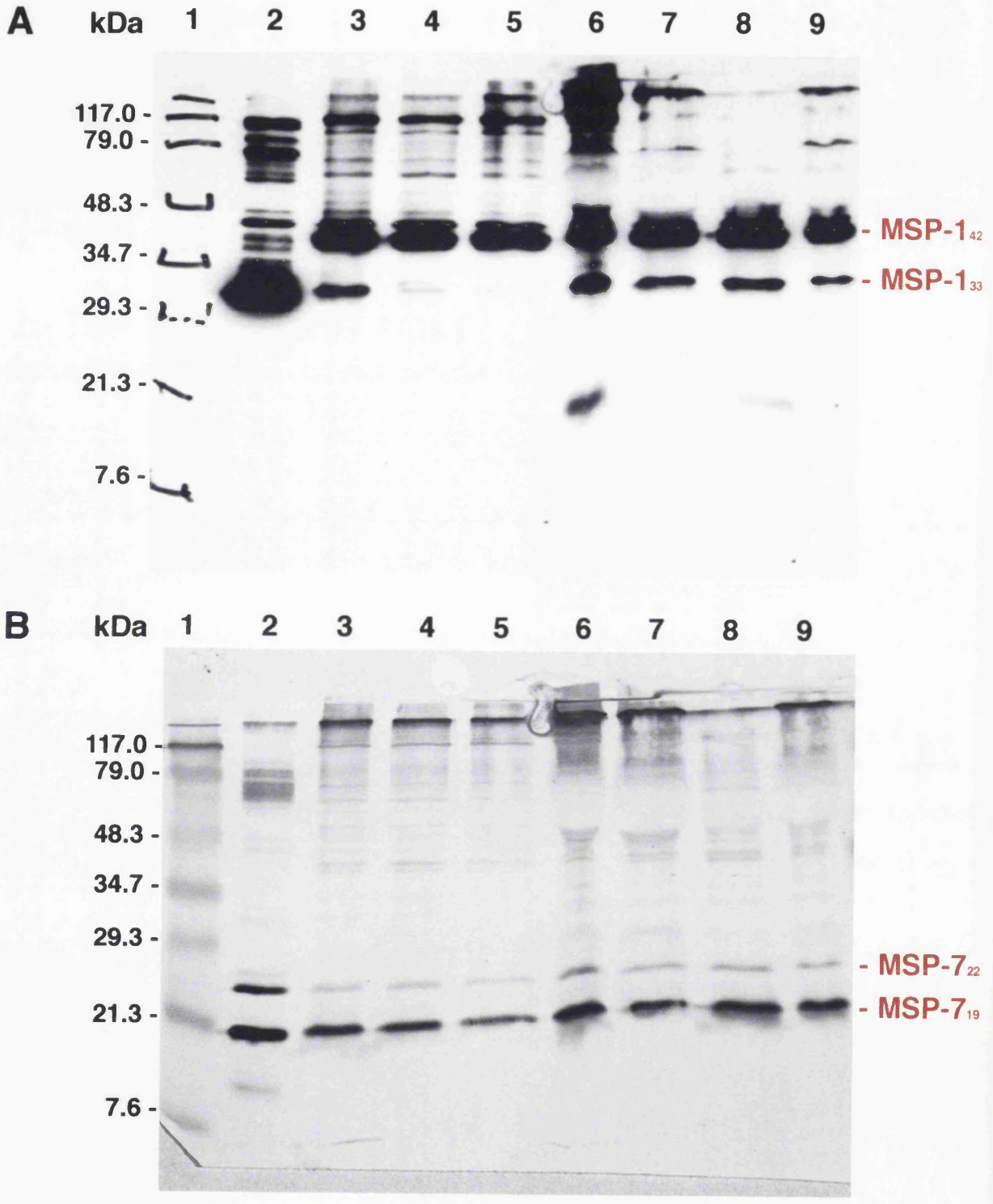
A
kDa
1
2
3
4
5
6
7
8
9
117.0
79.0
48.3
34.7
29.3
21.3
7.6
- MSP-1 42
- MSP-1 33
B
kDa
1
2
3
4
5
6
7
8
9
117.0
79.0
48.3
34.7
29.3
21.3
7.6
- MSP-7 22
- MSP-7 19

Figure 5.13 Schematic of the Predicted MSP-7 Processing Events

The MSP-7 precursor is translated in the schizont as a 48 kDa polypeptide. MSP-7 is predicted to undergo three N-terminal proteolytic cleavages during the processes of merogony, merozoite release and erythrocyte invasion. (This schematic is only taking into account MSP-7 processing events, for a schematic incorporating MSP-7 complex formation with MSP-1 and MSP-6, see Figure 6.0).

The first MSP-7 processing event occurs in the schizont, and involves cleavage of the MSP-7 precursor into an N-terminal 20 kDa polypeptide (MSP-7_{20}) and a C-terminal 33 kDa polypeptide (MSP-7_{33}). Brefeldin A inhibits this processing reaction, hence it occurs post-Golgi, during translocation to, or once at the nascent merozoite surface. IFAT results suggest that both MSP-7_{20} and MSP-7_{33} are on the surface of developing merozoites, but as merozoites reach maturity MSP-7_{20} is lost from the surface, presumably degraded.

The second MSP-7 processing event is predicted to occur around the time of merozoite release, and involves the cleavage of an ~11 kDa fragment from the N-terminus of MSP-7_{33} to give the C-terminal MSP-7_{22}. MSP-7_{22} is part of the primary processed MSP-1 complex on the surface of mature merozoites. This MSP-7 processing event may be mediated by the protease involved in of cleavage of the MSP-1 and MSP-6 precursors (See Figure 6.0).

The third MSP-7 processing reaction appears to have occurred on released merozoites before they undergo erythrocyte invasion, and before secondary processing of MSP-1 (See Figure 6.0). It involves the cleavage of 18 amino acids from the N-terminus of MSP-7_{22}. However this is only a partial cleavage, as both MSP-7_{22} and MSP-7_{19} are present in the shed MSP-1 complex. The presence of calcium chelators and PMSF during merozoite collection do not appear to affect the third processing event, which had been thought to occur concurrently with secondary processing of MSP-1.

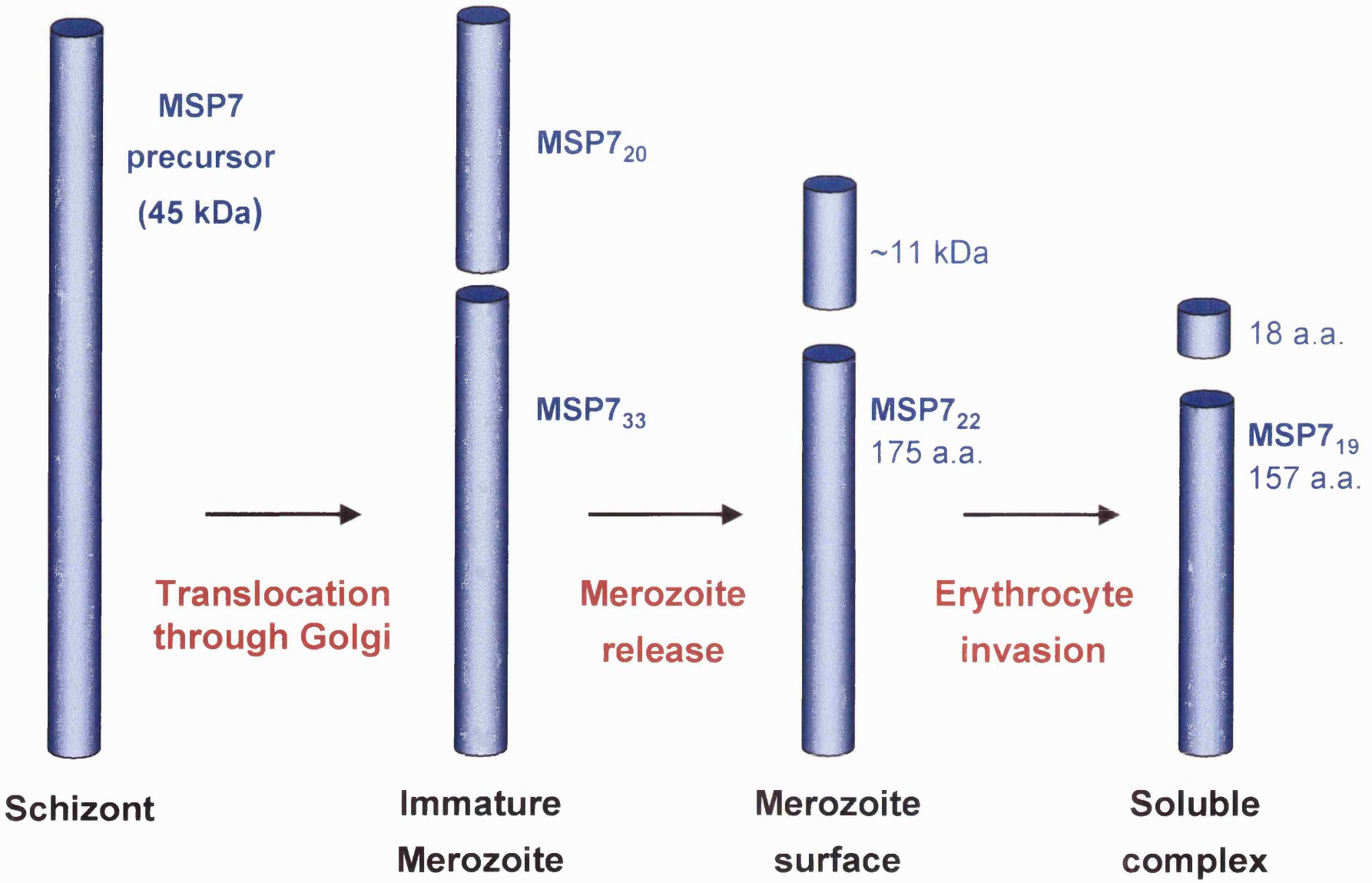
MSP7
precursor
(45 kDa)
MSP7$_{20}$
MSP7$_{33}$
~11 kDa
18 a.a.
MSP7$_{22}$
175 a.a.
MSP7$_{19}$
157 a.a.
Translocation
through Golgi
Merozoite
release
Erythrocyte
invasion
Schizont
Immature
Merozoite
Merozoite
surface
Soluble
complex

CHAPTER SIX : DISCUSSION

Malaria threatens over half of the world's population, and is currently undergoing a global resurgence, predominantly because of the spread of anti-malarial drug resistance and the breakdown of vector control measures. It is essential that new classes of anti-malarial drugs, and targets for an effective vaccine, are identified and utilised to combat this dreadful disease.

The erythrocytic life cycle of the parasite is very important, as the parasite undergoes massive cyclical amplification, exhibits immune evasion and causes all of the pathogenic effects seen in malaria. Blood schizonticides rapidly reduce parasitaemia and morbidity in clinical malaria; whilst in naturally acquired immunity, antibodies to blood stage antigens protect against disease and prevent red blood cell invasion. However drug resistance in malaria, as with other microbes, is reducing the number of drugs available to treat clinical disease, and there is no vaccine that can mimic naturally acquired immunity. Hence the mechanisms by which merozoites develop in the schizont, are subsequently released and invade erythrocytes need to be thoroughly understood to help identify novel drug and vaccine targets.

Whilst antibodies against schizont surface proteins such as EMP prevent cytoadherence, sequestration, and hence by association severe disease, they do not prevent the release of merozoites, which continue the destructive cycle of invasion and amplification in the blood stream. Merozoites are exposed to antibodies for a brief period between release from the schizont and entry into the newly invaded red blood cell. Yet, in naturally acquired immunity, antibodies to merozoite antigens can prevent erythrocyte invasion, suggesting these antigens are potential vaccine candidates. Characterising the

biosynthesis of these merozoite proteins and their role in the invasion process will help to identify novel targets for both vaccine and drug design.

Merozoite surface protein–1 (MSP-1) is a ubiquitous component of the merozoite surface in all *Plasmodium* species. In *P. falciparum msp-1* is an essential gene, which is transcribed and translated during schizogony into a 195 kDa MSP-1 precursor. The MSP-1 amino acid sequence consists of 17 blocks, these are either, highly conserved, moderately conserved or highly diverse (Tanabe *et al.* 1987). This large degree of sequence variation in the highly diverse blocks of MSP-1 is probably a result of immune selection pressure. Yet despite these regions of variation, MSP-1 appears to be functionally conserved throughout the *Plasmodium* genus, suggesting that the conserved and variable blocks of MSP-1 code for essential and non-essential functions respectively (Cowman 2000; O'Donnell *et al.* 2000).

The MSP-1 precursor undergoes two proteolytic processing steps, to expose a 19 kDa polypeptide (MSP-1_{19}) that remains on the merozoite membrane during entry into the invaded erythrocyte (Blackman *et al.* 1990; Blackman *et al.* 1994). MSP-1_{19} is highly conserved, and consists of two EGF-like domains predicted to be involved in binding to sialic acid receptors on the erythrocyte surface, during the invasion process (Blackman *et al.* 1991; Morgan *et al.* 1999). The protease responsible for the first MSP-1 processing events has not been identified, however one potential candidate is the papain-like cysteine protease SERPH (Blackman 2000). The second of the MSP-1 processing events is mediated by a calcium-dependent serine protease, and can be inhibited by serine-protease inhibitors, and by antibodies to MSP-1_{19} that presumably prevent the protease from reaching its substrate (Blackman and Holder 1992; Blackman *et al.* 1993; Chappel and Holder 1993; Uthaipibull *et al.* 2001). Antibodies to MSP-1 are present in the serum of immune individuals, inhibit erythrocyte invasion, and in animal malaria models protect

against parasite challenge (Blackman *et al.* 1990; Shai *et al.* 1995; Lyon *et al.* 1997). Hence MSP-1 plays an essential role in erythrocyte invasion, and is a major chemotherapy and vaccine candidate.

On the surface of the *Plasmodium falciparum* merozoite, the primary processed MSP-1 fragments are in a complex with two additional polypeptides of 22 kDa ($MSP\text{-}7_{22}$) and 36 kDa ($MSP\text{-}6_{36}$) (McBride and Heidrich 1987). On secondary processing of MSP-1, the majority of the MSP-1 complex is shed from the merozoite surface leaving just $MSP\text{-}1_{19}$ bound to the merozoite. The shed MSP-1 complex consists of four MSP-1 derived polypeptides, as well as $MSP\text{-}6_{36}$, $MSP\text{-}7_{22}$ and a 19 kDa ($MSP\text{-}7_{19}$) polypeptide (Stafford *et al.* 1994; Stafford 1996; Stafford *et al.* 1996a; Trucco *et al.* 2001). It was predicted that in the shed complex $MSP\text{-}7_{22}$ is partially cleaved at the N-terminus to give $MSP\text{-}7_{19}$ (Stafford *et al.* 1996a). The gene for MSP-6 has been identified and codes for a 371 amino acid precursor that is cleaved at the N-terminus to give the $MSP\text{-}6_{36}$ polypeptide (Trucco *et al.* 2001).

As $MSP\text{-}7_{22}$ is bound to the primary processed MSP-1, and cleaved to $MSP\text{-}7_{19}$ at a similar time as the second MSP-1 processing step, it was hypothesised that the same protease is responsible. It was also suggested that MSP-7 plays an important role bound to MSP-1 whilst on the merozoite surface.

The aim of my project was to identify the gene coding for MSP-7 in *P. falciparum*, and to characterise the biosynthesis of MSP-7 and its association with MSP-1, with the long-term aim of identifying putative drug or vaccine targets.

I have identified the full-length *P. falciparum msp-7* gene, using a combination of sequence database searches and vectorette PCR steps (Pachebat *et al.* 2001). The *Pfmsp-7* gene consists of 1056 nucleotides, and codes for a precursor of 351 amino acids. MSP-7 is a hydrophilic protein, and has a mainly alpha-helical secondary structure interspersed

with short regions of highly flexible beta sheet turns. The MSP-7_{22} and MSP-7_{19} N-terminal amino acid sequences are located in the C-terminal half of the MSP-7 precursor. This suggested that the MSP-7 precursor underwent at least two N-terminal proteolytic cleavages, the first to MSP-7_{22}, and the second to MSP-7_{19}.

To investigate the biosynthesis of MSP-7, and its predicted processing reactions, the N-terminal region of MSP-7 (MSP-7A) and the C-terminal MSP-7_{22} region (MSP-7B) were expressed as GST-tagged fusion proteins, whilst MSP-7B was also expressed as a His-tagged fusion protein. The GST-MSP-7A and GST-MSP-7B fusion proteins were used to immunise mice to raise antisera, and a monoclonal antibody against MSP-7B was isolated. These reagents were used as tools with which to study the biosynthesis of MSP-7.

The MSP-7 sequence is highly conserved with only four amino acid differences between the 3D7 / T9/96 and FCB-1 lines of *P. falciparum* (Pachebat *et al.* 2001). These four amino acid differences are all in the MSP-7_{22} – MSP-7_{19} N-terminal region, suggesting they may be involved either in specificity of the protease involved in the cleavage of MSP-7_{22} to MSP-7_{19}, or in minor changes to the MSP-1 – MSP-7 binding site that are dictated by MSP-1 allelic variation. MSP-6 also shows little variation between laboratory lines (Trucco *et al.* 2001). The high level of sequence conservation exhibited by both MSP-6 and MSP-7, is in contrast to the dimorphic allelic variation exhibited by MSP-1, suggesting that either, they are not subjected to the same selective immune pressure as MSP-1, or that they play essential roles in the MSP-1 complex. It also suggests that both MSP-6 and MSP-7 bind to highly conserved regions of MSP-1, of which there are five blocks (1, 3, 5, 12 and 17) (Tanabe *et al.* 1987). Of these, block 17 codes for MSP-1_{19} and hence is unlikely to bind either MSP-6 or MSP-7 (Tanabe *et al.* 1987).

A homologue to MSP-7 has been identified in the rodent malaria *P. yoelii* 17X, and it is predicted that MSP-7 homologues are present in several other *Plasmodium* species. Hence MSP-7 probably has an essential function whilst bound to MSP-1 in all *Plasmodia*. The *Pf* and *Py* MSP-7 sequences show a high level of conservation in the region of the C-terminal beta sheet. An alignment of this region shows similarity with several unique proteins in the *Plasmodium* databases, suggesting that they are part of an MSP-7 multi-gene family that is characterised by this C-terminal alignment (Pachebat *et al.* 2001). The function of this conserved C-terminal beta sheet is unknown, although it may be involved in binding to MSP-1. Hence, it is hypothesised that MSP-7 orthologues play an important if currently unknown role complexed to MSP-1 on the surface of merozoites in all *Plasmodium* species.

The *msp-7* gene is transcribed in *P. falciparum* schizonts between 34 – 48 hours post invasion, with a peak in transcription between 36 – 44 hours. This coincides with the onset of schizogony and resulting merozoite development in the schizont. The *msp-7* transcription pattern is similar to that previously described for *msp-1*, suggesting that *msp-1* and *msp-7* are transcribed simultaneously during schizogony (Myler 1990; Stafford *et al.* 1996b).

MSP-7 is translated in schizonts as a 48 kDa MSP-7 precursor protein. Immunofluorescence showed that at the onset of schizogony both MSP-1 and MSP-7 appear to initially associate with a transient tubular reticular network of the ER (TuRNER) that forms around the dividing merozoite nuclei, as has been described with MSP-1 in *Plasmodium yoelii* (Noe *et al.* 2000). MSP-1 and MSP-7 also co-localised on the surface of developing merozoites.

As *msp-1* and *msp-7* appeared to be transcribed simultaneously, with both translated proteins located in the TuRNER and on the developing merozoite surface, it

was predicted that the MSP-1 and MSP-7 precursors were co-transported to the developing merozoite surface. To test this theory, immunoprecipitations of radiolabelled schizont proteins were performed in the presence of ionic or non-ionic detergents.

In this project I have shown that the 48 kDa MSP-7 precursor forms a complex with the 195 kDa MSP-1 precursor in schizonts. This complex is maintained in non-ionic detergent (NP-40) conditions, but disrupted in the presence of the ionic detergent (DOC). Hence the MSP-1 and MSP-7 precursors form a non-covalently bound complex. The MSP-1 - MSP-7 precursor complex forms before either the MSP-1 or the MSP-7 precursors undergo proteolytic processing.

Brefeldin A reversibly inhibits the transport of vesicles from the ER to the *trans*-Golgi (Crary and Haldar 1992; Ogun and Holder 1994; Wiser *et al.* 1997). Treatment of schizonts with Brefeldin A results in an accumulation of the MSP-1 - MSP-7 precursor complex. Therefore the MSP-1 - MSP-7 precursor complex forms before the *trans*-golgi, and is transported to the developing merozoite membrane via the classical secretory pathway (Haldar and Holder 1993). Brefeldin A treatment also significantly inhibits any proteolytic processing of the MSP-1 or MSP-7 precursors. Hence both the MSP-1 and MSP-7 processing events occur post-Golgi, either during translocation to the nascent merozoite surface or once on the surface.

Pulse-chase experiments with antibodies to MSP-1 and MSP-7 show that the MSP-1 – MSP-7 precursor complex forms rapidly post-translation. However in the presence of the non-ionic detergent NP-40, the anti-MSP-1_{83} antibody 89.1 only immunoprecipitates free MSP-1 precursor and not the MSP-7 precursor, with the quantity of immunoprecipitated free MSP-1 decreasing with time. This suggests that either there is a pool of free MSP-1 precursor that is gradually complexed to MSP-7 as it is translated and becomes available, or that the association between MSP-1 and MSP-7 does not occur

immediately post-translation, occurring perhaps instead during vesicular transport from the ER to the Golgi, or during sorting in the Golgi apparatus.

The binding site of 89.1 has been localised to the highly conserved block 3 of MSP-1 (Holder 1988). The decrease with time of free MSP-1 precursor immunoprecipitated by 89.1 (anti-MSP-1_{83}), suggests that on formation of the MSP-1 - MSP-7 precursor complex, the 89.1 binding epitope on the MSP-1 precursor is disrupted or blocked by the presence of MSP-7. Therefore MSP-7 is predicted to bind to block 3 at the N-terminus of MSP-1. This predicted MSP-1 – MSP-7 binding site is in a region of high sequence conservation on MSP-1, suggesting that the highly conserved MSP-7 has an essential function bound to MSP-1 (Tanabe *et al.* 1987).

Two regions of MSP-7 that are C-terminal to the MSP-7_{19} cleavage site are putative sites of interaction with block 3 of MSP-1. The first at residues 234 – 261 is a predicted coiled-coil structure with hydrophobic regions in the coil; whilst the second at residues 309 – 326 is the C-terminal beta sheet that characterises the MSP-7 multi-gene family (Pachebat *et al.* 2001).

Once bound to the MSP-1 precursor, the MSP-7 precursor undergoes 3 proteolytic processing steps (see Figure 6.0).

- The first is the cleavage of the MSP-7 precursor at an unknown site, into a N-terminal 20 kDa polypeptide (MSP-7_{20}) that is lost from the complex, and a C-terminal 33 kDa polypeptide (MSP-7_{33}) that remains bound to the MSP-1 precursor.
- The second is the cleavage of approximately 11 kDa from the N-terminus of MSP-7_{33}, leaving the C-terminal MSP-7_{22} bound to MSP-1. This is predicted to occur simultaneously with MSP-1 primary processing, and processing of MSP-6 to MSP-6_{36}.

- The third is the cleavage of 18 amino acids from the N-terminus of MSP-7_{22} to give MSP-7_{19}. Both MSP-7_{22} and MSP-7_{19} are present in the shed MSP-1 complex, which suggests that MSP-7_{22} is only partially cleaved into MSP-7_{19}.

The first MSP-7 processing step occurs before primary processing of MSP-1, and is inhibited by BFA, suggesting it occurs post–Golgi. Pulse chase analysis of the MSP-1 - MSP-7 precursor complex formation in non-ionic conditions, shows a rapid decrease in the quantity of MSP-7 precursor, with a corresponding increase in the MSP-7_{20} and MSP-7_{33} cleavage products. This process takes 10 - 20 minutes post-translation, which suggests that MSP-7 is cleaved either during transport of the precursor complex to, or once at the developing merozoite surface. If the MSP-1 - MSP-7 precursor complex is transported to the nascent merozoite surface before the MSP-7 precursor is cleaved, it is possible that proteases in the parasitophorous vacuole mediate this primary processing of MSP-7.

MSP-7_{33} remains complexed to the MSP-1 precursor, whilst MSP-7_{20} is lost from the MSP-1 – MSP-7 complex, but MSP-7_{20} does not appear to be immediately degraded. Dual - IFAT results suggest that MSP-7_{20} is closely associated with MSP-1 on the surface of the developing merozoite, but not in mature merozoites. Does MSP-7_{20} remain on the merozoite surface, but distinct from the MSP-1 - MSP-7_{33} complex, perhaps bound to another protein before it is degraded, or is MSP-7_{20} simply released into the parasitophorous vacuole, and subsequently degraded by proteases in the parasitophorous vacuole?

In the second MSP-7 processing event, MSP-7_{33} undergoes N-terminal cleavage of approximately 11 kDa to give MSP-7_{22}, which is predicted to remain bound to block 3 of MSP-1. MSP-7_{33} is not detectable in merozoites by western blotting, nor is it in the shed MSP-1 complex, suggesting that the cleavage of MSP-7_{33} into MSP-7_{22} occurs at or

just after merozoites are released by schizont rupture. The MSP-7_{22} cleavage site shows a significant similarity to both the MSP-1_{30} primary processing site, and the MSP-6_{36} cleavage site (Stafford 1996; Pachebat *et al.* 2001; Trucco *et al.* 2001). All three cleavages are predicted to occur around the time of merozoite release, and the products are non-covalently bound in a complex on the merozoite surface. Hence it is likely that the protease responsible for MSP-1 primary processing also mediates the MSP-6_{36} and MSP-7_{22} cleavages. The parasitophorous vacuole location of the cysteine protease, SERPH, would make this protease an ideal candidate for these processing reactions. MSP-6_{36} is predicted to bind to MSP-1 via a C-terminal coiled-coil region, which shows similarity to the C-terminus of MSP-3 (Trucco *et al.* 2001). The function and mechanism of: MSP-6 transport to the merozoite surface, cleavage to MSP-6_{36} and subsequent association with the primary processed MSP-1 polypeptides, is unknown and a potential avenue for future investigation.

The third MSP-7 processing step, that of MSP-7_{22} to MSP-7_{19} occurs on the merozoite surface before MSP-1 undergoes secondary processing. This third MSP-7 processing step is not inhibited by calcium chelators, or by serine protease inhibitors. Hence the calcium-dependent serine protease responsible for secondary processing of MSP-1_{42}, is not responsible for processing of MSP-7_{22} to MSP-7_{19} (Blackman and Holder 1992; Blackman *et al.* 1993). Antibodies to MSP-7 do not inhibit the processing of MSP-1_{42}. It is unknown what effect antibodies to either MSP-1 or MSP-7 would have on the processing of MSP-7_{22} to MSP-7_{19}, as processing of MSP-7_{22} had already occurred in the merozoite samples prior to analysis. As both MSP-7_{22} and MSP-7_{19} are present in the shed MSP-1 complex, and MSP-1 and MSP-7 are complexed together in roughly equal stoichiometric amounts, does the presence of MSP-7_{19} have any relevance to the processing of MSP-1_{42} and subsequent release of the shed MSP-1 complex, or is the

processing to MSP-7_{19} just an artifact due to an unrelated protease released during merozoite release? The MSP-7_{19} cleavage site shows similarity with a motif in MSP-2, but the relevance of this remains to be elucidated.

The interaction between the MSP-1 and MSP-7 precursors appears to be highly conserved, and raises several interesting questions. How does the binding of MSP-7 affect the structure of the MSP-1 precursor, and the structure of the subsequent primary and secondary processed MSP-1 complex? Is binding of the MSP-7 precursor an essential step in the transport of the MSP-1 precursor to the plasma membrane? If either the MSP-1 or MSP-7 genes were disrupted or the MSP-1 – MSP-7 binding site mutated, would the precursors remain in the ER, or would both precursors still undergo translocation to the merozoite surface? Additionally does formation of the MSP-1 - MSP-7 precursor complex, and any of the subsequent processing events, result in conformational changes to either MSP-1 or MSP-7, that present cleavage sites to the proteases responsible for the MSP-1 and MSP-7 processing events, or allow binding of MSP-6_{36} after primary processing of MSP-1?

MSP-7 probably has a specific function either in the developing or released merozoite, most probably in its interaction with MSP-1. Its close association with MSP-1 during translocation to the merozoite surface, the high level of conservation at the binding site of MSP-1 and MSP-7, and similarity in processing events, in particular with the primary processing event of MSP-1, suggests that MSP-7 has an essential role bound to MSP-1 in the merozoite. Hence MSP-7 warrants further study to define its importance as part of the structure of the MSP-1 complex, and the function of the three proteolytic cleavages it undergoes whilst complexed to MSP-1, since the proteases responsible are potential drug targets.

There are a great number of potential avenues down which the work on MSP-7 that I have started could be continued. The use of stable transfection in the erythrocytic life cycle would enable rapid determination of whether *msp-7* is an essential gene by performing a knockout of *msp-7*, whilst the introduction of subtle changes into the MSP-1, MSP-6 and MSP7 precursors would enable their functions and interactions to be studied further. Of particular interest would be the effect of mutations in the MSP-1 - MSP-7 binding site and in the MSP-7 processing sites on the formation of the MSP-1 - MSP-7 precursor complex, its translocation to the merozoite surface, processing of both MSP-1 and MSP-7, the attachment of MSP-6_{36}, and erythrocyte invasion.

The MSP-1 - MSP-7 binding site is highly conserved, and the MSP-1 and MSP-6_{36} binding site is predicted to be similarly highly conserved. This suggests that the interactions of MSP-1 with MSP-6 and MSP-7 are essential in the MSP-1 biosynthesis pathway, and hence would be ideal drug or vaccine targets. Cross-linking experiments could be used to confirm these sites of MSP-1 interaction with MSP-6 and MSP-7. In addition the location in the parasite of MSP-6 cleavage and interaction of the MSP-6_{36} product with the MSP-1 - MSP-7 complex should be identified. To do this, further pulse chase experiments could be carried out using antibodies specific to MSP-1, MSP-6 and MSP-7; and the *msp-1*, *msp-6* and *msp-7* genes tagged with green and blue fluorescent proteins in dual transfections, enabling the exact location in the parasite where MSP-1 and MSP-6 associate to be identified by Fluorescence Resonance Energy Transfer.

The MSP-7 processing reactions should be investigated further as they are potential antibody and drug targets. The MSP-7_{33} cleavage site needs to be identified, either by N-terminal sequencing of MSP-7_{33}, or by mass spectroscopy analysis of the MSP-7_{20} and MSP-7_{33} cleavage products. Antibodies specific to the MSP-7 cleavage sites and products should then be raised, and used in dual immunofluorescence,

immunoprecipitation, and pulse-chase experiments, to characterise the transport and cleavage of all the MSP-7 products in the schizont and merozoite. These antibodies could also be used in erythrocyte invasion, and MSP-1 and MSP-7 processing inhibition assays, to test for their ability to inhibit the processing events of the MSP-1 - MSP-7 complex and erythrocyte invasion.

The classes of proteases responsible for the MSP-7 cleavage events should be identified. Schizonts could be treated with a variety of protease inhibitors, and the subsequent effects on MSP-7 (and MSP-1 and MSP-6) processing determined by immunoprecipitation or western blot analysis. Alternatively the proteases could be purified directly, perhaps by a novel technique such as - irreversible active site capture - in which mutations introduced into MSP-7 cleavage sites result in irreversible binding of the active site of the protease to the substrate, allowing subsequent purification and identification of the protease by mass spectroscopy.

The proteases responsible for processing of MSP-7 may be located in the merozoite organelles. The rhoptries, dense granules, micronemes, and parasitophorous vacuole could be purified (Blackman and Bannister 2001), and their contents tested for processing activity using recombinant or purified MSP-7 as a substrate. Once identified a protease could be isolated from the contents of the appropriate organelle by fractionation and analysed by mass spectrometry.

Once the MSP-7 processing events have been fully characterised, and MSP-7 shown to be essential for parasite growth, further experiments could be performed to validate their potential as chemotherapy targets. Assuming that the proteases involved in cleavage of MSP-7 are unique to *Plasmodium* or to protozoans, drugs could be designed to inhibit the MSP-7 biosynthesis pathway. For example, peptidomimetics could be used to design to mimic the MSP-7 cleavage sites, with the aim of specifically and irreversibly

binding the active sites of these proteases, thereby inhibiting entry of the MSP-7 cleavage sequence into the protease's active site. This method could also be applied to the MSP-6_{36} cleavage site, and to the site of interaction between MSP-1 and MSP-6_{36}.

The MSP-7 sequence is highly conserved in *P. falciparum* lines, and its interaction with the highly conserved block three of MSP-1 suggests that it has an essential function in the MSP-1 – MSP-7 complex. This suggests that MSP-7 is an ideal vaccine candidate, as it is unlikely to exhibit much variation under immune pressure. To determine whether MSP-7 is immunogenic in natural infection and if antibodies to MSP-7 play a role in naturally acquired immunity, human immune sera should be tested for the presence of antibodies to MSP-7. If antibodies to MSP-7 are present, they should be purified and tested in assays for their effect on MSP-7 processing and erythrocyte invasion.

Homologues to MSP-7 have been identified in rodent malarias, and MSP-7 is predicted to have a conserved function in its association with MSP-1 throughout the *Plasmodium* genus. This implies that rodent malaria models could be used to test the efficacy of drugs targeted to the MSP-7 biosynthesis pathway, and the vaccine potential of MSP-7.

In summary, I have identified the gene coding for MSP-7, a novel protein, in a number of *Plasmodium* species. In *P. falciparum* MSP-7 is expressed in schizonts, during the latter stages of the erythrocytic cycle, and soon after translation forms a complex with the MSP-1 precursor. This MSP-1 – MSP-7 complex is translocated through the Golgi to the developing merozoite surface, whereupon both MSP-7 and MSP-1 undergo a number of proteolytic processing reactions. MSP-7 undergoes three N-terminal processing steps, the second of which is predicted to occur in conjunction with primary processing of MSP-1, and processing of MSP-6. The C-terminal region of MSP-7 remains associated with

MSP-1 on the surface of free merozoites, and on erythrocyte invasion is shed from the surface with the majority of the MSP-1. The highly conserved nature of the association between MSP-1 and MSP-7, suggests that MSP-7 plays an essential role whilst complexed to MSP-1. The protein-protein interactions and processing events of MSP-7 are potential chemotherapy and vaccine targets, and hence require further characterisation. The work I have described in this thesis is being continued by a number of researchers, with some promising results.

Figure 6.0 Processing Events in the MSP-1 - MSP-7 Complex

In schizonts the MSP-1 (195 kDa) and MSP-7 (48 kDa) precursors form a non-covalently bound complex in the TuRNER prior to the *trans*-Golgi. The C-terminal region of MSP-7 is predicted to bind to block 3 of MSP-1. During the processes of merogony, schizont rupture and erythrocyte invasion, whilst remaining bound in the MSP-1 - MSP-7 complex, MSP-7 undergoes three consecutive N-terminal cleavage events, whilst MSP-1 undergoes two proteolytic processing steps.

The MSP-1 - MSP-7 precursor complex is translocated to the nascent merozoite surface via the Golgi. During transport to or once at the surface of the developing merozoite, the MSP-7 precursor undergoes its first processing event to an N-terminal 20 kDa MSP-7_{20} fragment, and a C-terminal 33 kDa MSP-7_{33} fragment. MSP-7_{20} is lost from the MSP-1 - MSP-7 complex, whilst MSP-7_{33} remains bound to block 3 of the MSP-1 precursor. MSP-1 is bound to the merozoite membrane via a C-terminal GPI anchor.

During or just prior to schizont rupture, the MSP-1 precursor undergoes primary processing into 30 (MSP-1_{30}), 38 (MSP-1_{38}), 42 (MSP-1_{42}) and 83 (MSP-1_{83}) kDa polypeptides. At the same time that MSP-1 is processed, ~11 kDa is cleaved from the N-terminus of MSP-7_{33} to give the 22 kDa MSP-7_{22}; whilst the MSP-6 precursor undergoes N-terminal cleavage into the 36 kDa MSP-6_{36}. The primary processed MSP-1 polypeptides are on the merozoite surface, in the form of a non-covalently bound complex with MSP-6_{36} and MSP-7_{22}. It is predicted that the same protease, perhaps located in the parasitophorous vacuole, is responsible for these cleavages.

On the surface of released merozoites, MSP-7_{22} is partially cleaved to MSP-7_{19}. This appears to occur independently of, and prior to, secondary processing of MSP-1. Both MSP-7_{19} and MSP-7_{22} remain bound to the MSP-1 complex via MSP-1_{83}.

On erythrocyte invasion, secondary processing of MSP-1 occurs, cleaving MSP-1_{42} into a 19 kDa (MSP-1_{19}) C-terminal fragment that remains on the merozoite surface and is taken into the invaded red blood cell, and an N-terminal 33 kDa (MSP-1_{33}) fragment that is shed from the merozoite surface with the remainder of the MSP-1 complex. Both MSP-7_{19} and MSP-7_{22} are components of the shed MSP-1 complex.

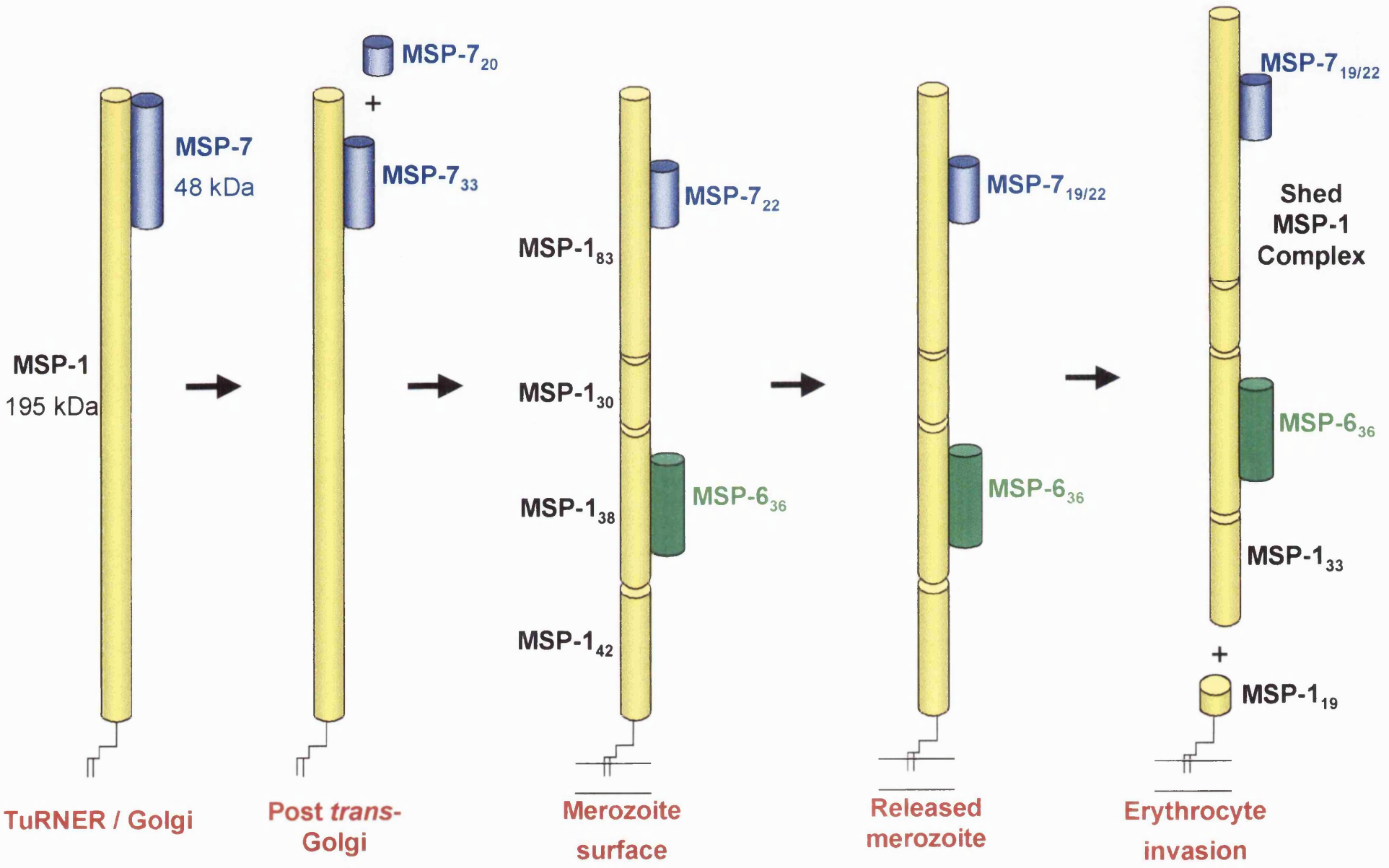
MSP-1
195 kDa
MSP-7
48 kDa
MSP-7 20
+
MSP-7 33
MSP-1 83
MSP-1 30
MSP-1 38
MSP-1 42
MSP-7 22
MSP-6 36
MSP-7 19/22
MSP-6 36
MSP-7 19/22
Shed
MSP-1
Complex
MSP-6 36
MSP-1 33
+
MSP-1 19
TuRNER / Golgi
Post trans-
Golgi
Merozoite
surface
Released
merozoite
Erythrocyte
invasion

APPENDIX

SECTION ONE : BUFFERS, EQUIPMENT AND REAGENTS

All buffers were made using sterile distilled water (SDW), autoclaved under standard conditions and stored at room temperature (RT) unless otherwise stated.

ABI PRISM™ δRhodamine Terminator Cycle Sequencing Ready Reaction Kit, Perkin Elmer Applied Biosystems #403044.

ABI PRISM 377 DNA Sequencer.

Acetic Acid Glacial, Fisher Scientific #A/0400/PB17.

Acetone ACS reagent, Sigma #A-4206.

Acetonitrile HPLC grade, Rathburns.

Acrylamide, Biorad #161-0158. 30% acrylamide / Bis solution, 37.5:1. Stored 4°C.

Agarose MP (multipurpose), Boehringer Mannheim #1444 964.

Ammonium Persulphate, Sigma #A-7460. Prepared as 10% stock in SDW. Stored -20°C.

Ampicillin, Sigma #A-9518. Prepared as 50mgml^{-1} stock in SDW, filter sterilised through 0.2μm filter. Stored -20°C.

Amplify™ (fluorographic reagent), Amersham #NAMP 100.

AmpliTaq Gold™, 5Uμl^{-1}, PE Applied Biosystems #N808-0240. Store -20°C.

Blue Dextran / EDTA, PE Applied Biosystems #402055. 25mM EDTA (pH8.0), 50mgml^{-1} Blue dextran.

β-ME (β-Mercaptoethanol), Sigma #M-3148.

Brefeldin A, Sigma, B-6542. Prepared as 1mgml^{-1} stock in methanol. Stored -20°C.

Brilliant Blue R 250, Sigma #B-7920.

Bromophenol Blue, Sigma #B-5525.

Bovine Serum Albumin, Sigma #A-3294. Stored 4°C.

Centrifuges

Beckman J-6B Centrifuge, swing bucket rotor.

Beckman TL-100 Ultracentrifuge, rotor TL-100.3.

Beckman L7 Ultracentrifuge, type 70 TI rotor.

Sigma 1K15 Laboratory Centrifuge.

Sigma 4K15 Laboratory Centrifuge.

Sorval RC-5B (refrigerated superspeed centrifuge), SS-34 rotor.

Centrifuge Tubes, Beckmann #355631. Polycarbonate, thick wall, 1 x 3½ inches.

Centrifuge Tubes, Beckmann #270-453122-A. Polycarbonate, ½ x 2 inches.

Centrifuge Tubes, Nalgene #3119-0030. Oak ridge Polypropylene Copolymer, 25.5 x 94.3 mm.

Chelex 100 Resin, Bio-Rad #143-2832.

Chloroform : Isoamyl Alcohol (ratio 24:1), Sigma #C-0549.

4-Chloro-1-napthol, Sigma #C-8890.

Citifluor AF1 (glycerol/PBS solution), Citifluor Ltd.

cØmplete™, Protease Inhibitor Cocktail Tablets, Boehringer Mannheim #1 697 498. Stored 4°C. Prepared as 25x stock by dissolving 1 tablet in 2ml SDW.

cØmplete™ EDTA-free, Protease Inhibitor Cocktail Tablets, Boehringer Mannheim #1 873 580. Stored 4°C. Prepared as 25x stock by dissolving 1 tablet in 2ml SDW.

Coomassie Blue Stain, 1g Brilliant blue R-250, 450ml methanol, 100ml acetic acid, SDW to 1L.

Coomassie Destain Solution, 7% Glacial acetic acid, 20% methanol, in SDW.

DAPI (4',6-Diamidino-2-phenylindole), Sigma #D-9542. 0.5μgml^{-1} in PBS A. Store wrapped in foil at RT.

DeltaVision Olympus Epifluorescent Microscope, SoftWorks Image Analysis Software.

Dimethylformamide (DMF), Sigma #D-4551.

Dithiothreitol (DTT), Sigma, D-9779. Prepared as 1.5M stock, 0.2μm filter sterilised. Stored -20°C.

DNA Electrophoresis Markers

100bp DNA ladder, Range 100 – 1500 bp, New England Biolabs #323-1S.

100bp DNA ladder, Range 100 – 2072 bp, Life Technologies #15628-019.

Supperladder-Mid2 200bp DNA Ladder, Range 200 – 5000 bp, Advanced Biotechnologies #SLM-200.

1kb DNA ladder, Range 500 – 10000 bp, New England Biolabs #323-2S.

1kb DNA ladder, Range 75 – 12216 bp, Life Technologies #15615-016.

DNase I, 10mgml^{-1}. Rnase free, Sigma #D-7291. Store -20°C.

Econo-Column® & Flow Adapter, Bio-Rad #738-0014

EDTA (ethylenediaminetetraacetic acid), Sigma E-5134. Prepared as 0.5M stock, pH adjusted to 8.0.

EGTA (Ethylene glycol-bis[β-aminoethylether]-N,N,N'N'-tetraacetic acid), Sigma E-3889. Prepared as 0.5M stock, pH adjusted to pH 8.0.

ENHANCE spray, NEN Life Science Products, #NEF970G.

Epicurian Coli® BL21-Gold Competent Cells, Stratagene #230130. Store -70°C.

Ethanol, 99.7-100% v/v (absolute) AnalaR, BDH #10107 7Y.

Ethidium Bromide (10mgml^{-1} aqueous solution), Sigma #E-1510. Store 4°C.

Evans Blue, Sigma E-2129.

Evans Blue Stain
0.01% Evans Blue in PBS A. Store wrapped in foil at RT.

Fetal Bovine Serum, Sigma #F-0643.

Formamide deionised 99.5%, Sigma #9037.

Freunds Adjuvant, incomplete, Sigma #F-5506.

Freunds Adjuvant, complete, Sigma #F-5881.

Geneclean *II*® Kit, Bio 101 Inc.

Glutamine (L-2-Aminoglutaramic acid), Sigma #G-5763.

Glutathione, reduced, Sigma #G-4251. Store 4°C.

Glutathione Agarose, Sigma #G-4510. Store –20°C.

Glutathione Sepharose 4B, Pharmacia Biotech #52-2303-00. 10ml surry in 20% ethanol. Store 4°C.

Glycerol, molecular biology grade, BDH #44448 2V.

GST-Fusion Protein Lysis & 1st Wash Buffer, 50mM Tris-HCl pH8, 1mM EDTA, 0.2% NP40, 1mM PMSF, 1x Complete Protease Inhibitors. Store 4°C.

GST-Fusion Protein 2nd Wash Buffer, 50mM Tris-HCl pH 8, 1mM EDTA, 1mM PMSF, 1 x Complete Protease Inhibitors

GST-Fusion Protein Elution Buffer, 50mM Tris-HCl pH8, 1mM EDTA, 5mM Reduced Glutathione.

Guanidine thiocyanate, Sigma #G-6639. Prepared fresh as 1M stock.

Hognes Freezing Buffer, x 10. 36mM $K_2HPO_4.3H_2O$, 13mM KH_2PO_4, 20mM Sodium Citrate (Tris), 10mM $MgSO_4.7H_2O$, 44% glycerol. Store -20°C.

Horse Radish Peroxidase Streptavidin, Vector Laboratories #SA-5004. Stored 4°C.

Hybond™ N+, positively charged nylon membrane, Amersham Life Science #RPN 203G.

Imidazole, Sigma #I-0250.

Immunoprecipitation Solubilisation Buffer DOC (0.5%), 0.5% w/v DOC, 50mM TrisHCl pH8.2, 5mM EDTA, 5mM EGTA.

Immunoprecipitation Solubilisation Buffer Nonident P40 (1%), 1% NP40, 5mM EDTA, 5mM EGTA, 1mM PMSF, 1 x Complete Protease Inhibitors, 1xPBS.

Immunoprecipitation Solubilisation Buffer SDS (1%), 1% w/v SDS, 50mM TrisHCl pH8, 5mM EDTA.

Immunoprecipitation Wash Buffer I, 50mM Tris-HCl pH 8, 5mM EDTA, 0,5% Triton X100, $1mgml^{-1}$ BSA, 0.5M NaCl, 1x cØmplete Protease Inhibitors without EDTA. Store 4°C.

Immunoprecipitation Wash Buffer II, 50mM Tris-HCl pH 8, 5mM EDTA, 0,5% Triton X100, 1x cØmplete Protease Inhibitors without EDTA. Store 4°C.

ImmunoType™ Mouse Monoclonal Antibody Isotyping Kit, Sigma #ISO-1. Store 4°C.

Iodoacetamide 'SigmaUltra', Sigma #I-1149. Prepared fresh as 1M stock in 0.2M Tris-HCl pH8.2.

IPTG (Isopropyl-β-D-thiogalactoside), Melford Laboratories #MB 1008. Prepared as 1M stock in SDW, 0.2μm filter sterilised. Stored -20°C.

Isopropanol (2-propanol), Sigma #I-9516.

Kodak Biomax MR-1 Autoradiography film.

L-Agar, 1.0%Tryptone, 0.5% Yeast Extract, 1.0% NaCl, (pH7.0). 1.5% L Agar.

L-Broth, 1.0%Tryptone, 0.5% Yeast Extract, 1.0% NaCl, (pH7.0).

Lysozyme, Sigma #L-6876. Prepared as 100mgml^{-1} stock in SDW. Stored -20°C.

$MgCl_2$ (Magnesium chloride), 25mM stock solution, Perkin Elmer #58002032-01.

Micro BCA Protein Assay Reagent, Pierce #0023235.

Mineral Oil, Sigma #400-5.

Multitest 15 well slides, ICN Biomedicals #6041505.

NICK^{TM} Column - Sephadex G-50 DNA grade**,** Pharmacia Biotech #52-2076-00.

Nonident P40 (NP40), BDH #56009.

Northern Blot Prehybridisation Buffer (Church & Gilberts), 0.2M $NaH_2PO_4.2H_2O$, 0.3M Na_2HPO_4, 0.5M EDTA, 7% SDS, in SDW.

Nucleic Acid Gel Electrophoresis Apparatus, Phamacia #GNA-100.

O-Phenylenediamine Dihydrochrloride – 10mg tablet, Sigma #P8287.

Optitran®BA-S85 Reinforced Nitrocellulose, Schleicher & Schuell #439-196.

Original TA Cloning® Kit, INVαF' *E. coli,* Invitrogen #K2000-01.

[^{32}P]-dATP, 9.25MBq, Amersham Pharmacia Biotech #AA0018.

PBS 'A' Dulbecco's, NaCl 10g, KCl 0.25g, Na_2HPO_4 1.437g, KH_2PO_4 0.25g, distilled water 1L.

PD-10 Column - Sephadex G-25M, amersham pharmacia biotech #17-0851-01

PCR Buffer II no $MgCl_2$ **(x10),** Perkin Elmer #58002026-01.

PEG_{8000} (polyethylene glycol, Mol. Wt : 8000), Sigma #p4463.

2D Peptide Mapping 1° Dimension Electrophoresis Buffer, 2% Pyridine, 4% acetic acid, 15% acetone, 79% SDW.

2D Peptide Mapping 2° Dimension Electrophoresis Buffer, 7.5% butanol, 25% pyridine, 37.5% butanol, 30% SDW.

2D Peptide Mapping Markers

0.2mgml^{-1} Xylene cyanol FF, 0.5mgml^{-1} DNP lysine.

Percoll, Prepare isotonic percoll by mixing 1 volume of 10x PBS with 9 volumes Percoll.

pGEX-3X, PharmaciaBiotech #27-4803. Store -20°C. (See appendix for map).

Phenol, 'Sigma Ultra', Sigma #P-5566.

PMSF (Phenylmethyl-Sulfonyl Fluoride), Sigma #P-7626. Prepared fresh as 100mM stock in isopropanol.

Potassium Acetate, 'Sigma Ultra', Sigma #P5708. Prepared as 3M stock.

Prime-It® II Random Primer Labeling Kit, Stratagene #300385. Store -20°C.

PRO-MIX™ L-[^{35}S] *in vitro* cell labeling Mix, Amersham Pharmacia Biotech #SJQ 0079. 70% L-[^{35}S] methionine and 30% L-[^{35}S] cysteine. 92.5MBq total activity.

Pronase E, Sigma #P-0652.

Propan-2-ol, (isopropyl alcohol) HPLC grade, Sigma #27,049-0.

Protein G Sepharose® 4 Fast Flow, Amersham Pharmacia Biotech #17-0618-01. 5ml slurry in 20% ethanol. Store 4°C.

PTC-100™ Programmable Thermal Cycler, MJ Research.

Pyridine, HPLC grade, Sigma #27,040-7.

QIAGEN Blood and Cell Culture DNA Kit, Qiagen #13323.

QIAquick PCR Purification kit, Qiagen #28104.

Recombinant RNasin® Ribonuclease Inhibitor, Promega #N2511. Store -20°C.

Restriction Endonuclease BamH1, 10 unitsμl^{-1}, Boehringer Mannheim #1175 084. Store -20°C.

Restriction Endonuclease EcoR1, 10 unitsμl^{-1}, Boehringer Mannheim #656 275. Store -20°C.

RNase Erase™, ICN #821682.

RNaseZAP™ Solution, Invitrogen #R600-01.

Rneasy Mini Kit, Qiagen #74103.

$RPMI_{1640}$ w/o glutamine, Sigma #R-7880. Store 4°C.

$RPMI_{com}$, Gibco #074-1800.

Sample Buffer (SB, x 5) (nucleic acid electrophoresis), 500µl glycerol, 500µl 10 x TBE, 0.05% bromophenol blue.

Saponin, Prepared as 1% stock.

SDS (Sodium Dodecyl Sulphate), Sigma #L-4390.

SDS-PAGE Apparatus, Mighty Small Electrophoresis Units, Hoefer #SE 250.

SDS-PAGE Mass Markers

Kaleidoscope Prestained Standards (7.5 – 215 kDa range), Bio-rad #161-0324.

MultiMark™ Multi-Coloured Standard, Invitrogen / Novex #LC5725.

Prestained Protein Molecular Weight Standards, Low Range, Life Technologies #16040-016.

Prestained Protein Molecular Weight Standards, High Range, Life Technologies #26041-020.

Prestained SDS-PAGE Standards, Broad Range, Bio-rad #161-0318.

Prestained SDS-PAGE Standards, Low Range, Bio-rad #161-0305.

Prestained SDS-PAGE Standards, High Range, Bio-rad #161-0309.

Rainbow™ coloured protein molecular weight markers, High molecular weight range (14.3–220kDa), Amersham LifeScience #RPN756.

SDS PAGE Gel (8%) Volumes given are for 5 x mini gel castor.

Separating Gel (8%), 8.1ml acrylamide, 11.2ml 1M Tris pH8.8, 10.6ml SDW, 300µl 10% SDS, 20µl Temed, 100µl 10% ammonium persulphate.

Overlay with water saturated butanol.

Stacking Gel (3%), 1.0ml acrylamide, 1.25ml 1M Tris pH6.8, 7.7ml SDW, 100µl 10% SDS, 10µl Temed, 50µl 10% ammonium persulphate.

SDS PAGE Gel (12.5%) Volumes given are for 5 x mini gel castor.

Separating Gel (12.5%), 12.5ml acrylamide, 11.2ml 1M Tris pH8.8, 6.2ml SDW, 300µl 10% SDS, 20µl Temed, 100µl 10% ammonium persulphate.

Overlay with water saturated butanol.

Stacking Gel (5%), 1.67ml acrylamide, 1.25ml 1M Tris pH6.8, 7.03ml SDW, 100µl 10% SDS, 10µl Temed, 50µl 10% ammonium persulphate.

SDS PAGE Running Buffer pH8.3 (x 10), 30.3g Tris, 144.2g Glycine, 10.0g SDS, made up to 1L with SDW.

SDS Sample Cocktail (SC, x 2), 150mM TrisHCl pH6.8, 4.6% SDS, 23% glycerol, 0.01% w/v Bromophenol Blue, SDW. Store 4°C.

Sigma Fast™ BCIP / NBT Buffered Substrate Tablets, Sigma #B-5655. Store -20°C. Prepare fresh by adding 1 tablet to 10ml SDW.

Sigma ImmunoType™ Mouse Monoclonal Antibody Isotyping Kit, Sigma #ISO-1.

S.N.A.P.™ MiniPrep Kit, Invitrogen #K1900-01.

SOC Medium, 2.0% Tryptone, 0.5% Yeast Extract, 10.0mM NaCl, 2.5mM KCl, 10.0mM $MgCl_2$-$6H_2O$, 20.0mM glucose.

Sorbitol, Sigma #S-7547.

SSC (Sodium Chloride/Sodium Citrate) **x 20,**

NaCl 175.2g, trisodium citrate 88.2g, SDW to 1L. pH 7.0-7.2.

Sodium Chloride (NaCl), Sigma S-3014. Prepared as 5M stock solution in SDW.

Subcloning Efficiency DH5α™ Competent Cells, Life Technologies #18265-017. Store -70°C.

Superscript II Reverse Transcriptase, GibcoBRL #18064-014. Store -20°C.

Supersignal® West Pico Chemiluminescent Substrates, Pierce #34080 Store 4°C.

T4 DNA Ligase, 3unitsμl^{-1}, Promega #M1801. Store -20°C.

TAE (Tris Acetate EDTA) **x 50,** Tris base 242g, Glacial acetic acid 57.1ml, EDTA 18.612g, SDW to 1L.

TBE (Tris Borate EDTA) **x 10,** Tris base 121.1g, Boric acid 61.83g, EDTA 18.6g, SDW to 1L.

TE (Tris EDTA), 10mM Tris-HCl, 1mM EDTA (pH 8.0).

Temed (N,N,N',N'-Tetramethylethylenediamine), Sigma #T-7024.

Terrific Broth, 17mM KH_2PO_4, 72mM K_2HPO_2, 1.2% Tryptone, 2.4% Yeast extract, 0.4% glycerol.

TLC Plates (Thin Layer Chromatogarphy), plastic backed cellulose 0.1mm thick, Merck #5577.

TOPO TA Cloning® Kit, TOP10F' *E. coli,* Invitrogen #K4500-01/40.

Tris (methhylamine), BDH #103156.

Tris-HCl Buffers were prepared as described in (Sambrook *et al.* 1989).

Triton X100 (t-Octylphenoxypoly (ethoxyethanol)), Sigma #X-100.

TRIzol Reagent, Gibco Life Technologies #15596-026.

Trypsin, DPCC-treated, Salt-free, Sigma #T-1005.

Tween 20 (Polyoxyethylenesorbitan), monolaurate, Sigma #P-7949.

Ultrafiltration Regenerated Cellulose Membranes (44.5mm), Amicon #YM10.

Ultrapure dNTP Set, Parmacia Biotech #27-2035-01. Each at 100mM, prepared as 2.5mM stock solution in SDW. Stored -20°C.

VectaSpin™ 3 Centrifuge Tube Filters, Whatman #6830 0206.

Vectorette II Primer (phosphorylated), Genosys #DN-16-320. Store -20°C.

Vectorette II T9-96 *P. falciparum AluI, DraI, RsaI, Sau3AI, XhoII* Libraries, (Gunaratne *et al.* 2000).

Western Blotting Apparatus, Hoefer TS Series.

Western Blot Buffer, 1.15% w/v glycine, 0.24% w/v Tris, 20% methanol, SDW.

Wizard™ PCR Preps DNA Purification System, Promega #A7170.

X-Gal (5-bromo-4-chloro-3-indolyl-β-galactoside), Sigma #B-9146. Prepared as 40mgml^{-1} stock in DMF. Stored -20°C in foil.

X-OMAT™ AR Film, 18 x 24cm, Kodak.

X509-sepharose, 5mg X509:1ml Sepharose.

Xpress™ System Protein Purification Kit, Invitrogen # 25-0006.

SECTION TWO : ANTIBODIES, CELL LINES, OLIGONUCLEOTIDES, PLASMIDS AND WEB SITES

ANTIBODIES

Primary Antibodies

Anti-Bip (PfGRP), rat polyclonal sera, J. Adams.

Anti-EBA-175, rat polyclonal sera, J. Adams.

Anti–GST, mouse polyclonal sera (Mα-GST), S. Ogun.

Anti–GST, purified from goat serum, cross-absorbed against *E. coli* proteins (Gt α-GST), Amersham Pharmacia Biotech, #27-4577.

Anti–GST-MSP-7A, mouse polyclonal sera (M α-GST-MSP-7A),section 2.7.

Anti–GST-MSP-7B, mouse polyclonal sera (M α-GST-MSP-7B), section 2.7.

Anti-MSP-1_{19}, (12.8) mouse monoclonal antibody.

Anti-MSP-1_{19}, (1E1) mouse monoclonal antibody.

Anti-MSP-1_{19} MAD-20 type (8A12), mouse monoclonal antibody, T.Scott-Finnigan.

Anti-MSP-1_{19} Wellcome type (2F10), mouse monoclonal antibody.

Anti-MSP-1_{33}, (X509) human monoclonal antibody.

Anti-MSP-1_{33}, (X509) human monoclonal antibody, biotinylated.

Anti-MSP-1_{33}, (G13) mouse monoclonal IgG2b antibody, S. Wilkins.

Anti-MSP-1_{83}, (89.1) mouse ascites.

Anti-MSP-7B, (JP-1) mouse IgA monoclonal antibody, section 2.8.

Anti-MSP-7_{22} N-terminal amino acid synthetic peptide (Mα22.1), mouse polyclonal serum, M. Blackman.

Anti–MSP-7_{22} purified from T9-96 shed MSP-1 complex, rabbit polyclonal serum, absorbed with *E. coli* proteins (Rb αMSP-7_{22}), (Stafford *et al.* 1996).

Anti-*Pf* subtilisin 1, (Rb α-*Pf*sub1) rabbit polyclonal serum, (Blackman *et al.* 1998).

Anti-Rhoptery proteins 110,140, 150kDa, mouse ascites (61.3), A.A. Holder, S Ogun, I Ling.

Anti-Xpress, mouse IgG_1 monoclonal antibody, Invitrogen, #R910-25.

Normal Mouse (BalbC) Sera (NMS), (section 2.7).

Normal Rabbit Serum (NRS), Sigma #R-4505.

Secondary Antibodies

Anti-Goat IgG (whole molecule), AP conjugate, Rabbit affinity isolated antigen specific antibody, Sigma #A-4187.

Anti-Goat IgG, Peroxidase conjugate, Rabbit antibody, Dako #P0160.

Anti-Human IgG (H+L chain), Peroxidase conjugate, Sheep affinity isolated antigen specific antibody, ICN #683931.

Anti-Human IgG, IgA, IgM (H+L chain), FITC conjugate, Rabbit antibodies, ICN #652081.

Anti-Human polyvalent Immunoglobulins, FITC conjugate, Goat antibodies, Sigma #F-6506.

Anti-Mouse IgA (α chain specific), FITC conjugate, Goat affinity isolated antigen specific antibody, Sigma #F-9384.

Anti-Mouse IgA (α chain specific), Peroxidase conjugate, Goat affinity isolated antigen specific antiserum, Sigma #A 4789.

Anti-Mouse IgG (whole molecule), AP conjugate, Sheep affinity isolated antigen specific antibody, adsorbed with human serum proteins, Sigma #A-5324.

Anti-Mouse IgG (whole molecule), FITC conjugate, Goat affinity isolated antigen specific antibody, adsorbed with human serum proteins, Sigma #F-0257.

Anti-Mouse IgG, Peroxidase conjugate, Goat antibody, Biorad #170-6101.

Anti-Mouse IgG, Texas Red conjugate, Mike Blackman.

Anti-Mouse IgG (H+L chain), Oregon Green conjugate, Goat antibody, Molecular Probes #O-6380.

Anti-Mouse IgG (H+L chain), Peroxidase conjugate, Sheep affinity isolated antigen specific antibody, ICN #683961.

Anti-Mouse IgG (γ-chain specific), FITC conjugate, Goat affinity isolated antigen specific antibody, Sigma #F-8264.

Anti-Rabbit IgG (whole molecule), AP conjugate, Goat affinity isolated antigen specific antibody, adsorbed with human serum proteins, Sigma #A-3812.

Anti-Rabbit IgG (whole molecule), AP conjugate, Goat affinity isolated antigen specific antibody, Sigma #A-3687.

Anti-Rabbit IgG (whole molecule), FITC conjugate, Goat affinity isolated antigen specific antibody, adsorbed with human IgG, Sigma #F-9887.

Anti-Rabbit IgG (whole molecule), TRITC conjugate, Goat antibody, adsorbed with human IgG, Sigma #T-6778.

Anti-Rabbit IgG (H+L chain), Peroxidase conjugate, Goat antibody, Biorad #170-6615.
Anti-Rat IgG (H+L chain), Oregon Green conjugate, Goat antibody, Molecular Probes #O-6382.

E.COLI GENOTYPES

BL21-Gold: F⁻ *ompT hsdS*(r_B^- m_B^-) *dcm*$^+$ Tet^r *gal endA* Hte.

DH5α: F ϕ80d*lacZ*ΔM15 Δ(*lacZYA-argF*)U169 *deoR recA1 endA1 hsdR17* (r_k^-, m_k^+) *phoA supE44* λ⁻ *thi-1 gyrA96 relA1*.

INVαF': F' *endA1 recA1 hsdR17* (r_k^-, m_k^+) *supE44 thi-1 gyrA96 relA1* ϕ80*lacZ*ΔM15 Δ(*lacZY A-argF*)U169 λ⁻.

TOP10F': F' {*lacI*^{q} Tn*10* (Tet^R) }*mcrA* Δ(*mrr-hsd*RMS-*mcr*BC) Φ80*lacZ*ΔM15 Δ*lacX74 recA1 deoR araD139* Δ(*ara-leu*)1797 *galU galK rpsL* (Str^R) *endA1 nupG*.

HYBRIDOMAS

JP-1 mouse hybrodoma (α-MSP-7 IgA), raised by J.A. Pachebat & T. Scott-Finnigan.

MYELOMA CELLS

SP2/0-AG14 myeloma cells

PLASMODIUM FALCIPARUM CLONED LINES

3D7 - supplied by D. Walliker, Institute of Animal Genetics, University of Edinburgh, Edinburgh, UK. (MSP-1 MAD-20 type) (Walliker *et al.* 1987).

T9/96 - supplied by D. Walliker, Institute of Animal Genetics, University of Edinburgh, Edinburgh, UK. (MSP-1 MAD-20 type) (Thaithong *et al.* 1984).

FCB-1-originally isolated by C. Espinal, Instituto Nacional de Salud, Bogota, Columbia (MSP-1 Wellcome type).

OLIGONUCLEOTIDES

All oligonucleotides were synthesed by Oswel DNA service, and supplied in sterile water unless otherwise stated. Primers were diluted in sterile dH_2O to a working concentration of $10pm\mu l^{-1}$ and stored at -20°C.

Primer	Tm (°C)	Position relative to *msp-7*	Nucleotide sequence (5' to 3')
p225prime	61.0	-588 - –564	CCTTTTTAATTTATCGACACACGC
Pfp22F	57.9	-570 - –547	CACACGCATGAATAGAAATTAGACATG
p22F1	46.8	-26 - –7	AATGTGTAATTTTTGTATCC
Pre22Fexp	56.3	66 – 87	GCCGGATCCAATCAACTCATAGTACACCAG
p22R2	62.5	115 – 83	AATTCTTCTTGATCTTCTTCATTATTTACTGG
p22F3	66.1	396 – 423	TTTGAAAATGTTGATGATGACGCAGTAG
p22F2	48.2	487 – 504	GATTATTCGGTAAAAACG
p22Fexp	55.7	525 – 555	GCCGGATCCAAAGTGAAACAGATACTCAATCTAAAAATG
Pre22Rexp	56.6	529 – 503	GCCGAATTCCTTTGTGCCTTTACCTTTGATAATACG
p22R1	52.7	538 – 521	TCTGTTTCACTTTGTGCC
p22F4	68.1	602 – 630	AGGAGGAGAATCGACATTTCAAAAAGACC
p22F5	64.6	811 – 842	TTGGTCAAGAAGATAATAAGAGTAAAAATGGC
p22F6	58.4	945 – 974	GTTTATAGTTATGCAAAACAAAATAGTCAC
p22Rexp	53.6	1053 – 1019	GCCGAATTCATTGTGTTTAGTAAATTAAATGAATATTCTAAG
Pfp22r	58.0	1175 – 1150	AAAGGTACACAATTTAACCGAATG
M-21	55.0	GTAAAACGACGGCCAGT	
M-13	55.0	CAGGAAACAGCTATGAC	
PGEXF	55.0	CCTTTGCAGGGCTGGCAAGCC	
PGEXR	55.0	TTTTCACCGTCATCACCG	
Vectorette II primer	71.9	GGAGAACCCCATGAAGCTTGAATTCGGATCCACGTTG	

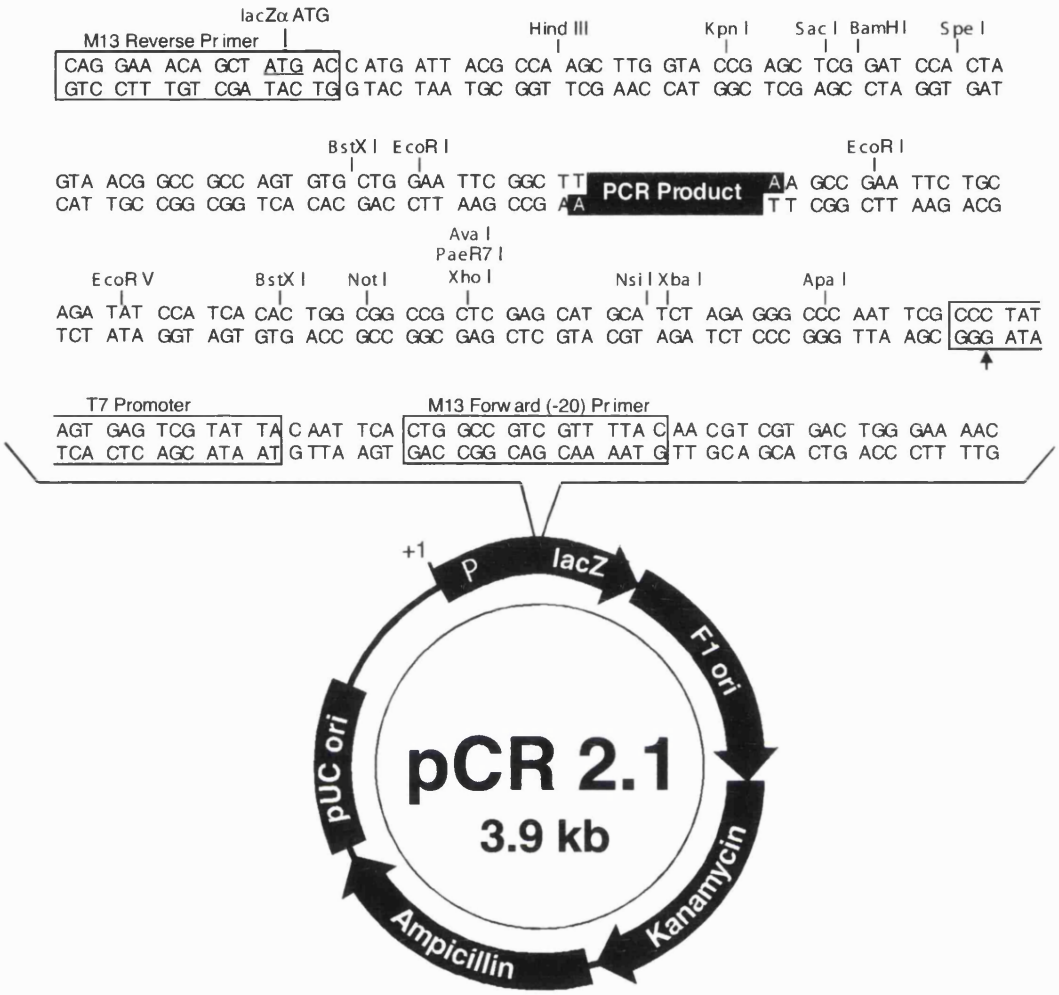

Comments for pCR2.1
3929 nucleotides

LacZα gene: bases 1-545
M13 Reverse priming site: bases 205-221
Multiple Cloning Site: bases 234-355
T7 promoter: bases 362-381
M13 (-20) Forward priming site: bases 389-404
f1 origin: bases 546-983
Kanamycin resistance ORF: bases 1317-21 11
Ampicillin resistance ORF: bases 2129-2989
pUC origin: bases 3134-3807

Invitrogen™
life technologies

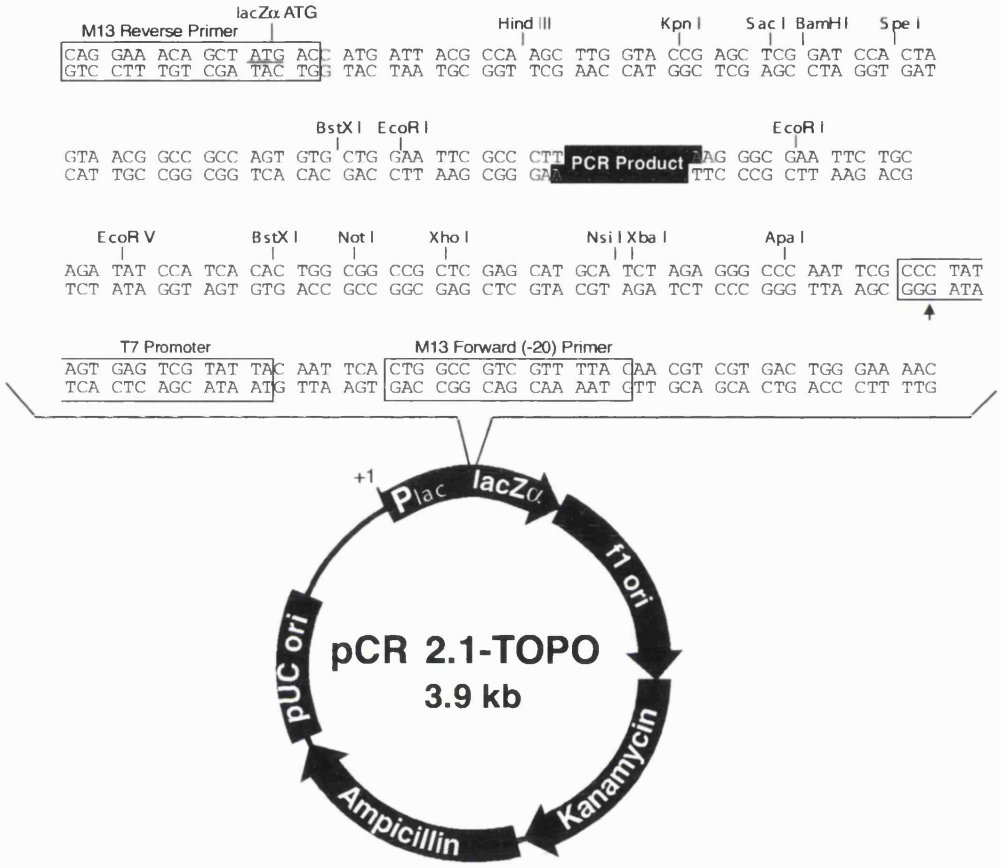

Comments for pCR 2.1-TOPO
3931 nucleotides

LacZα fragment: bases 1-547
M13 reverse priming site: bases 205-221
Multiple cloning site: bases 234-357
T7 promoter/priming site: bases 364-383
M13 Forward (-20) priming site: bases 391-406
f1 origin: bases 548-985
Kanamycin resistance ORF: bases 1319-2113
Ampicillin resistance ORF: bases 2131-2991
pUC origin: bases 3136-3809

Invitrogen™
life technologies

pGEX-3X

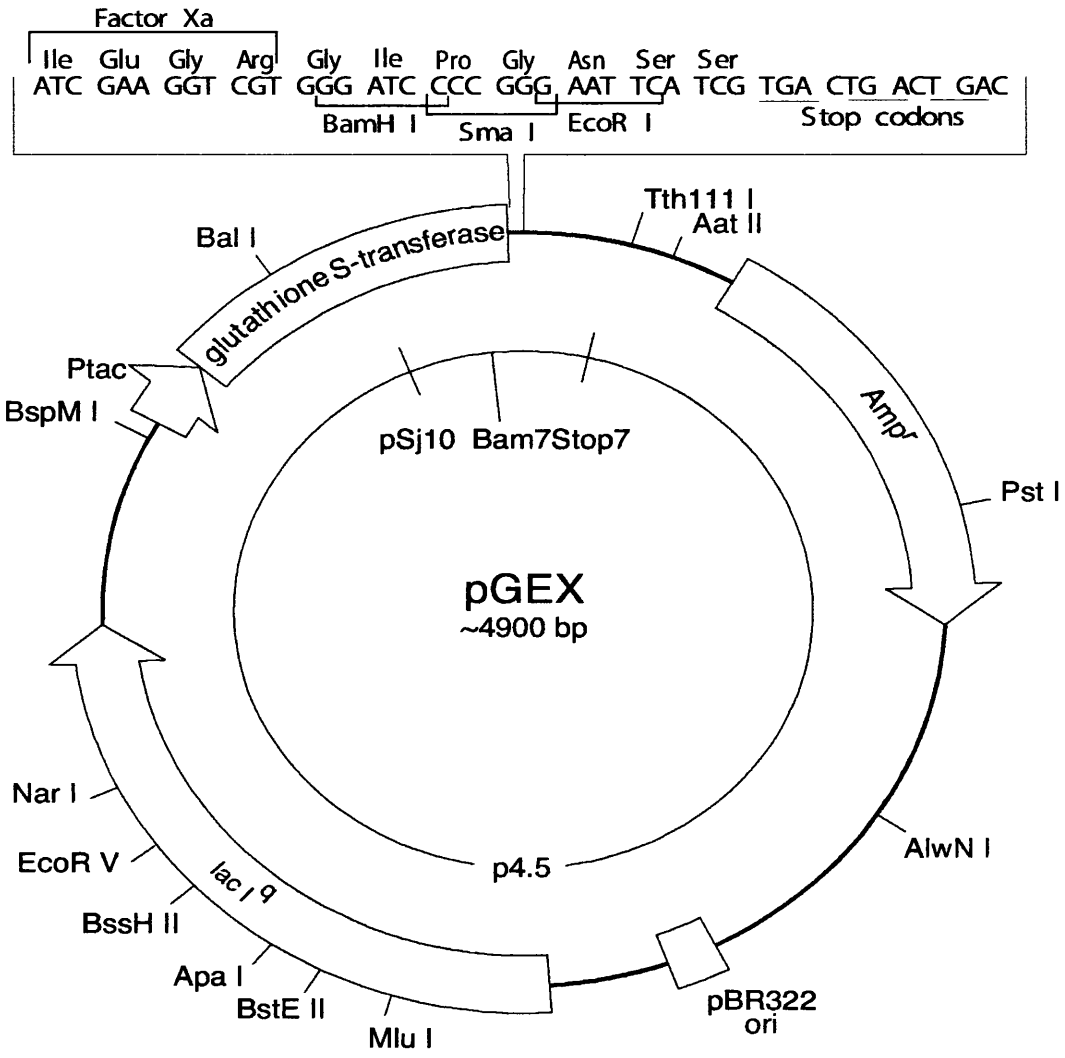

Amersham Pharmacia Biotech

pTrcHis C Multiple Cloning Site

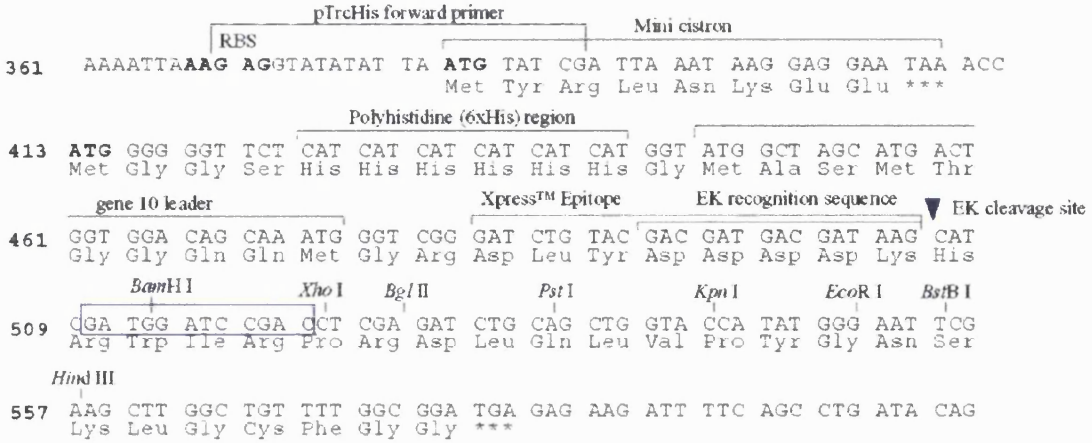

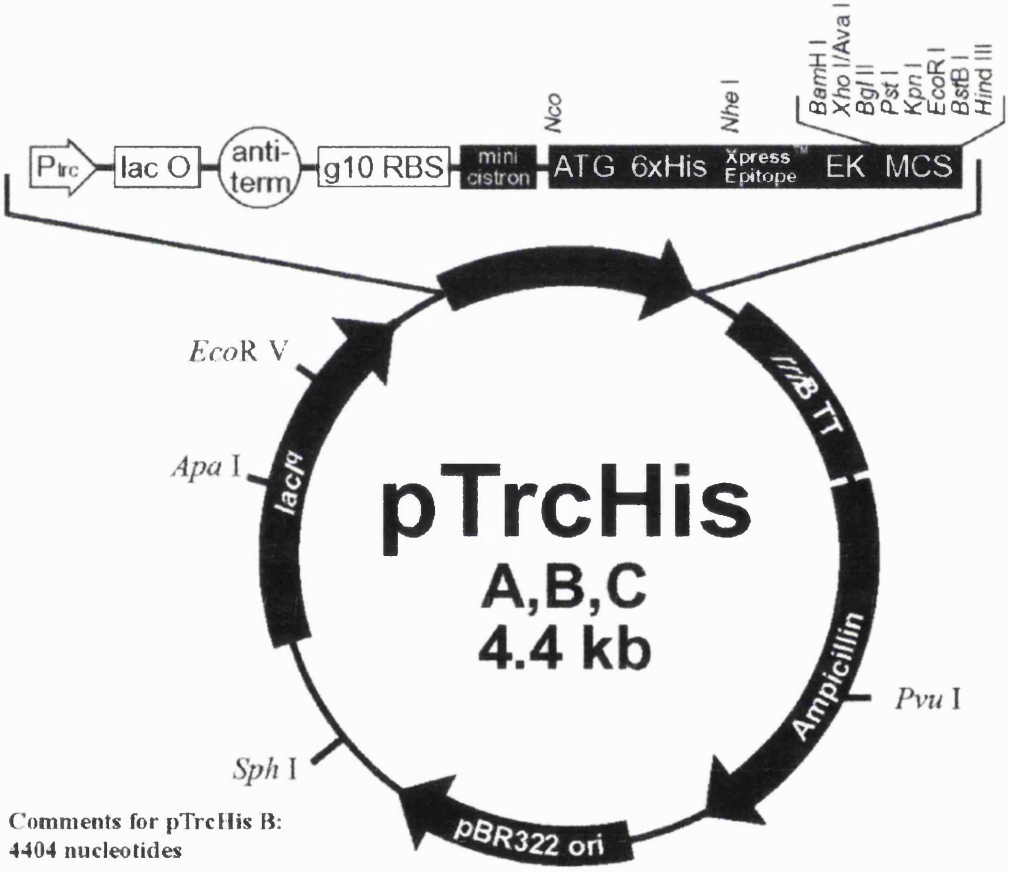

Comments for pTrcHis B:
4404 nucleotides

trc promoter: bases 191-221
lac operator: bases 228-248
*rrn*B anti-termination sequences: bases 264-333
T7 gene 10 translational enhancer: bases 346-354
Ribosome binding site: bases 370-374
Mini-cistron: bases 383-409
Polyhistidine and enterokinase cleavage site: bases 425-504
Xpress™ epitope: bases 482-505
Multiple cloning site: bases 515-554
*rrn*B transcriptional termination sequence: bases 637-794
Ampicillin resistance ORF: bases 1074-1934
pBR322 origin: bases 2079-2752
lac I^q ORF: bases 3281-4365

Invitrogen™
life technologies

SEQUENCE ANALYSIS PROGRAMS

AutoAssembler 3.1, ABI.

Fractura 1.2, ABI

Sequencing Analysis 2.1.1, ABI.

MacVector 6.5 Sequence Analysis Software, EastMan Kodak.

WEB SITES USED FOR SEQUENCE SEARCHES

http://www.tigr.org

http://www.sanger.ac.uk

http://www.stanford.edu

http://plasmodb.org

http://www.ncbi.nlm.nih.gov/BLAST/

WEB SITES USED FOR PROTEIN PREDICTION PROGRAMS

http://plasmodb.org **(For links to all malaria search engines)**

http://blocks.fhcrc.org (Blocks)

http://www.ch.embnet.org/cgi-bin/COILS (Coils)

http://www.biokemi.su.se/~server/DAS/tmdas.cgi (DAS TMpred)

http://www.sanger.ac.uk/Software/Pfam (Pfam)

phd@EMBL-Heidelberg.de (Predict Protein)

http://www.biochem.ucl.ac.uk/bsm/dbbrowser/PRINTS/PRINTS.html (PRINTS)

http://www2.ebi.ac.uk/servicestmp (PrintsScan)

http://protein.toulouse.inra.fr/prodom.html (ProDom)

http://psort.nibb.ac.jp (Psort)

http://www.expasy.ch/sprot/prosite.html (Scan Prosite)

http://www.cbs.dtu.dk/services/SignalP/ (Signal P)

http://smart.embl-heidelberg.de/smart (SMART)

http://www.ch.embnet.org/cgi-bin/TMPRED (TMPred)

References

Aikawa, M. (1988). "Morphological changes in erythrocytes induced by malarial parasites." Biology of the Cell **64**: 173-81.

Aikawa, M., M. Torii, A. Sjolander, K. Berzins, P. Perlmann and L. H. Miller (1990). "Pf155/RESA Antigen is Localised in Dense Granules of *Plasmodium falciparum* Merozoites." Experimental Parasitology **71**: 326-9.

Allen, M. J., A. Collick and A. J. Jeffreys (1994). "Use of vectorette and subvectorette PCR to isolate transgene flanking DNA." PCR Methods and Applications. **4**: 71-5.

Alles, H. K., K. N. Mendis and R. Carter (1998). "Malaria Mortality Rates in SouthAsia and in Africa: Implications for Malaria Control." Parasitology Today **14**: 369-75.

Altschul, S. F., T. L. Madden, A. A. Schaffer, J. Zhang, Z. Zhang, W. Miller and D. J. Lipman (1997). "Gapped BLAST and PSI-BLAST: a new generation of protein database search programs." Nucleic Acid Research **25**: 3389-402.

Anders, R. F. and A. Saul (2000). "Malaria Vaccines." Parasitology Today **16**: 444-7.

Baldi, D. L., K. T. Andrews, R. F. Waller, D. S. Roos, R. F. Howard, B. S. Crabb and A. F. Cowman (2000). "RAP1 controls rhoptry targetting of RAP2 in the malaria parasite *Plasmodium falciparum*." EMBO Journal **19**: 2435-43.

Bannister, L. H., G. A. Butcher, E. D. Dennis and G. H. Mitchell (1975). "Structure and invasive behaviour of *Plasmodium knowlesi* merozoites in vitro." Parasitology **71**: 483-91.

Bannister, L. H. and A. R. Dluzewski (1990). "The ultrastructure of red cell invasion in malaria infections: a review." Blood Cells **16**: 257-92.

Bannister, L. H., J. M. Hopkins, R. E. Fowler, S. Krishna and G. H. Mitchell (2000). "Ultrastructure of rhoptry development in *Plasmodium falciparum* erythrocytic schizonts." Parasitology **121**: 273-87.

Barale, J. C., T. Blisnick, H. Fujioka, P. M. Alzari, M. Aikawa, C. Braun-Breton and G. Langsley (1999). "*Plasmodium falciparum* subtilisin-like protease 2, a merozoite candidate for the merozoite surface protein 1-42 maturase." Proceedings of the National Academy of Sciences **96**: 6445-50.

Bell, A. (1998). "Microtubule Inhibitors as Potential Antimalarial Agents." Parasitology Today **14**: 234-40.

Black, C. G., W. Tieqiao, L. Wang, A. R. Hibbs and R. L. Coppel (2001). "Merozoite surface protein 8 of *Plasmodium falciparum* contains two epidermal growth factor-like domains." Molecular and Biochemical Parasitology. **114**: 217-26.

Blackman, M. J. (2000). "Proteases Involved in Erythrocyte Invasion by the Malaria Parasite: Function and Potential as Chemotherapeutic Targets." Current Drug Targets **1**: 59-83.

Blackman, M. J. and L. H. Bannister (2001). "Apical organelles of Apicomplexa: biology and isolation by subcellular fractionation." Molecular and Biochemical Parasitology **117**: 11-25.

Blackman, M. J., J. A. Chappel, S. Shai and A. A. Holder (1993). "A conserved parasite serine protease processes the *Plasmodium falciparum* merozoite surface protein-1." Molecular and Biochemical Parasitology **62**: 103-14.

Blackman, M. J., E. D. Dennis, E. M. Hirst, C. H. Kocken, T. J. Scott-Finnigan and A. W. Thomas (1996). "*Plasmodium knowlesi*: secondary processing of the malaria merozoite surface protein-1." Experimental Parasitology **83**: 229-39.

Blackman, M. J., H. Fujioka, W. H. Stafford, M. Sajid, B. Clough, S. L. Fleck, M. Aikawa, M. Grainger and F. Hackett (1998). "A subtilisin-like protein in

secretory organelles of *Plasmodium falciparum* merozoites." Journal of Biological Chemistry **273**: 23398-409.

Blackman, M. J., H. G. Heidrich, S. Donachie, J. S. McBride and A. A. Holder (1990). "A single fragment of a malaria merozoite surface protein remains on the parasite during red cell invasion and is the target of invasion- inhibiting antibodies." Journal of Experimental Medicine **172**: 379-82.

Blackman, M. J. and A. A. Holder (1992). "Secondary processing of the *Plasmodium falciparum* merozoite surface protein-1 (MSP1) by a calcium-dependent membrane-bound serine protease: shedding of MSP133 as a noncovalently associated complex with other fragments of the MSP1." Molecular and Biochemical Parasitology **50**: 307-15.

Blackman, M. J., I. T. Ling, S. C. Nicholls and A. A. Holder (1991a). "Proteolytic processing of the *Plasmodium falciparum* merozoite surface protein-1 produces a membrane-bound fragment containing two epidermal growth factor-like domains." Molecular and Biochemical Parasitology. **49**: 29-34.

Blackman, M. J., T. J. Scott-Finnigan, S. Shai and A. A. Holder (1994). "Antibodies inhibit the protease-mediated processing of a malaria merozoite surface protein." Journal of Experimental Medicine **180**: 389-93.

Blackman, M. J., H. Whittle and A. A. Holder (1991b). "Processing of the *Plasmodium falciparum* major merozoite surface protein-1; identification of a 33-kilodalton secondary processing product which is shed prior to erythrocyte invasion." Molecular and Biochemical Parasitology. **49**: 35-44.

Blanco, A. R. A., A. Paez, P. Gerold, A. L. Dearsly, G. Margos, R. T. Schwarz, G. Barker, M. C. Rodriguez and R. E. Sinden (1999). "The biosynthesis and post-translational modification of Pbs21 an ookinete-surface protein of *Plasmodium berghei*." Molecular and Biochemical Parasitology **98**: 163-73.

Bojang, K. A., P. J. M. Milligan, M. Pinder, L. Vigneron, A. Alloueche, K. Kester, W. R. Ballou, D. J. Conway, W. H. H. Reece, P. Gothard, L. Yamuah, M. Delchambre, G. Voss, B. M. Greenwood, A. Hill, K. P. W. J. McAdam, N. Tornieporth, J. D. Cohen and T. Doherty (2001). "Efficacy of RTS,S/AS02 malaria vaccine against *Plasmodium falciparum* infection in semi-immune adult men in the Gambia: a randomised trial." The Lancet **358**: 1927-34.

Bojang, K. A., S. K. Obaro, A. Leach, U. D'Alessandro, S. Bennett, W. Metzger, W. R. Ballou, G. A. T. Targett and B. M. Greenwood (1997). "Follow-up of Gambian children recruited to a pilot safety and immunogenicity study of the malaria vaccine SPf66." Parasite Immunology **19**: 579-81.

Carucci, D. J. (2000). "Malaria Research in the Post-genomic Era." Parasitology Today **16**: 434-8.

Carucci, D. J. and S. Hoffman (2000). "The malaria genome project: from sequence to functional." Nature Medicine **Special Focus: Malaria**: 6-8.

Chappel, J. A. and A. A. Holder (1993). "Monoclonal antibodies that inhibit *Plasmodium falciparum* invasion in vitro recognise the first growth factor-like domain of merozoite surface protein-1." Molecular and Biochemical Parasitology **60**: 303-11.

Cheng, Q., N. Cloonan, K. Fischer, J. Thompson, G. Waine, M. Lanzer and A. Saul (1998). "stevor and rif are *Plasmodium falciparum* multicopy gene families which potentially encode variant antigens." Molecular and Biochemical Parasitology **97**: 161-76.

Clyde, D. F., H. Most, V. C. McCarthy, J. P. Vanderberg (1973). "Immunization of man against sporozoite-induced *falciparum* malaria." American Journal of the Medical Sciences **266**(169-177).

Cohen, S., I. A. McGregor and S. Carrington (1961). "Gamma globulin and acquired immunity to human malaria." Nature **192**: 733-7.

Collins, F. H. and N. J. Besanky (1994). "Vector biology and the control of malaria in Africa." Science **264**: 1874-5.

Congpuong, K., J. Sirtichaisinthop, P. Tippawangkosol, K. Suprakrob, K. Na-Bangchang, P. Tan-ariya and J. Karbwang (1998). "Incidence of antimalarial pretreatment and drug sensitivity *in vitro* in multidrug-resistant *Plasmodium falciparum* infection in Thailand." Transactions of the Royal Society of Tropical Medicine and Hygiene **92**: 84-6.

Cowman, A. F. (2000). "Functional analysis of proteins involved in *Plasmodium falciparum* merozoite invasion of red blood cells." FEBS Letters **476**: 84-8.

Crabb, B. S., T. Triglia, J. G. Waterkeyn and A. F. Cowman (1997). "Stable transgene expression in *Plasmodium falciparum*." Molecular and Biochemical Parasitology. **90**: 131-44.

Craig, A. G., A. P. Waters and R. G. Ridley (1999). "Malaria Genome Project Task Force: A Post-genomic Agenda for Functional Analysis." Parasitology Today **15**: 211-4.

Crary, J. L. and K. Haldar (1992). "Brefeldin A inhibits protein secretion and parasite maturation in the ring stage of *Plasmodium falciparum*." Molecular and Biochemical Parasitology. **53**: 185-92.

Curtis, C. F. (1992). "Personal protection methods against vectors of disease." Review of Medical & Veterinary Entomology **80**: 543-53.

Das, A., H. G. Elemdorf, W. L. Li and K. Haldar (1994). "Biosynthesis, export and processing of a 45 kDa protein detected in membrane clefts of erythrocytes infected with *Plasmodium falciparum*." Biochemical Journal **302**: 487-96.

de Koning-Ward, T. F., C. J. Janse and A. P. Waters (2000). "The development of genetic tools for dissecting the biology of malaria parasites." Annual Review of Microbiology **54**: 157-85.

Debrabant, A. and P. Delplace (1989). "Leupeptin alters the proteolytic processing of P126, the major parasitophorous vacuole antigen of *Plasmodium falciparum*." Molecular and Biochemical Parasitology. **1989**: 151-8.

Dluzewski, A. R., I. T. Ling, K. Rangachari, P. A. Bates and R. J. M. Wilson (1984). "A simple method for isolating viable mature parasites of *Plasmodium falciparum* from cultures." Transactions of the Royal Society of Tropical Medicine and Hygiene **78**: 622-4.

Dooren, G. v., R. F. Waller, K. A. Joiner, D. S. Roos and G. I. McFadden (2000). "Traffic Jams: Protein transport in *Plasmodium falciparum*." Parasitology Today **16**: 421-7.

Druilhe, P. and J. L. Perignon (1999). "Malaria from Africa blows hot and cold." Nature Medicine **5**: 272-3.

Egan, A. F., P. A. Burghaus, P. Druilhe, A. A. Holder and E. M. Riley (1999). "Human antibodies to the 19kDa C-terminal fragment of *Plasmodium falciparum* merozoite surface protein 1 inhibit parasite growth *in vitro*." Parasite Immunology **21**: 133-9.

Engers, H. D. and T. Godal (1998). "Malaria vaccine development: current status." Parasitology Today. **14**: 56-64.

Fairlamb, A. (1996). "Pathways to drug discovery." The Biochemist **Feb/Mar**: 11-6.

Fowler, R. E., A. M. C. Smith, J. Whitehorn, I. T. Williams, L. H. Bannister and G. H. Mitchell (2001). "Microtubule associated motor proteins of *Plasmodium falciparum* merozoites." Molecular and Biochemical Parasitology. **117**: 187-200.

Freeman, R. R. and A. A. Holder (1983). "Surface antigens of malaria merozoites: A high molecular weight precursor is processed to an 83,000 mol wt form expressed on the surface of *Plasmodium falciparum* merozoites." Journal of Experimental Medicine **158**: 1647-53.

Gardner, M. J. (1999). "The genome of the malaria parasite." Current Opinion in Genetics & Development **9**: 704-8.

Gardner, M. J., H. Tettelin, D. J. Carucci, L. M. Cummings, L. Aravind, E. V. Koonin, S. Shallom, T. Mason, K. Yu, C. Fujii, J. Pederson, K. Shen, J. Jing, C. Aston, Z. Lai, D. C. Schwartz, M. Pertea, S. Salzberg, L. Zhou, G. C. Sutton, R. Clayton, O. White, H. O. Smith, C. M. Fraser, M. D. Adams, J. C. Venter and S. Hoffman (1998). "Chromosome 2 Sequence of the Human Malria Parasite *Plasmodium falciparum*." Science **282**: 1126-32.

Gerold, P., L. Schofield, M. J. Blackman, A. A. Holder and R. T. Schwarz (1996). "Structural analysis of the glycosyl-phosphatidylinositol membrane anchor of the merozoite surface proteins-1 and -2 of *Plasmodium falciparum*." Molecular and Biochemical Parasitology **75**: 131-43.

Goda, S. K. and N. P. Minton (1995). "A simple procedure for gel electrophoresis and Northern blotting of RNA." Nucleic Acids Research **23**: 3357-8.

Guevara Patino, J. A., A. A. Holder, J. S. McBride and M. J. Blackman (1997). "Antibodies that inhibit malaria merozoite surface protein-1 processing and erythrocyte invasion are blocked by naturally acquired human antibodies." Journal of Experimental Medicine **186**: 1689-99.

Gunaratne, R. S., M. Sajid, I. T. Ling, R. Tripathi, J. A. Pachebat and A. A. Holder (2000). "Characterisation of N-myristoyltransferase from *Plasmodium falciparum*." Biochemical Journal **348**: 459-63.

Gupta, S., R. W. Snow, C. A. Donnelly, K. Marsh and C. Newbold (1999). "Immunity to non-cerebral severe malaria is acquired after one or two infections." Nature Medicine **5**: 340-3.

Hackett, F., M. Sajid, C. Withers-Martinez, M. Grainger and M. J. Blackman (1999). "*Pf*SUB-2: a second subtilisin-like protein in *Plasmodium falciparum* merozoites." Molecular and Biochemical Parasitology **103**: 183-95.

Haldar, K. and A. A. Holder (1993). "Export of parasite proteins to the erythrocyte in *Plasmodium falciparum*-infected cells." Seminars in Cell Biology **4**: 345-53.

Harlow, E. and D. Lane (1988). Antibodies: A Laboratory Manual., Cold Spring Harbour Laboratory.

Hayashi, M., S. Taniguchi, Y. Ishizuka, H. S. Kim, Y. Wataya, A. Yamamoto and Y. Moriyama (2001). "A homologue of *N*-Ethylmaleimide-sensisitive Factor in the malaria parasite *Plasmodium falciparum* is exported and localized in vesicular structures in the cytoplasm of infected erythrocytes in the Brefeldin A-sensitive pathway." Journal of Biological Chemistry **276**: 15249-55.

Hengen, P. N. (1995). "Vectorette, splinkerette and boomerang DNA amplification." TIBS **20**: 372-3.

Hirunpetcharat, C., J. H. Tian, D. C. Kaslow, N. van Rooijen, S. Kumar, J. A. Berzofsky, L. H. Miller and M. F. Good (1997). "Complete protective immunity induced in mice by immunisation with the 19-kDa carboxyl-terminal fragment of the MSP-1 (MSP-119) of *Plasmodium yoelii* expressed in *Saccharomyces cerevisiae*." Journal of Immunology. **159**: 3400-11.

Hoffman, S., G. M. Subramanian, F. H. Collins and J. C. Venter (2002). "*Plasmodium,* human and *Anopheles* genomics and malaria." Nature **415**: 702-9.

Holder, A. A. (1988). "The precursor to major merozoite surface antigens: structure and role in immunity." Progress in Allergy **41**: 72-97.

Holder, A. A. (1994). "Proteins on the surface of the malaria parasite and cell invasion." Parasitology **108**(Suppl): S5-18.

Holder, A. A. (1996). "Malaria Vaccines." The Biochemist **Feb/Mar**: 17-20.

Holder, A. A. (1999). "Malaria Vaccines." Proceedings of the National Academy of Sciences **96**: 1167-69.

Holder, A. A. and M. J. Blackman (1994). "What is the function of MSP-1 on the malaria merozoite?" Parasitology Today **10**: 182-4.

Holder, A. A., M. J. Blackman, P. A. Burghaus, J. A. Chappel, I. T. Ling, N. McCallum-Deighton and S. Shai (1992). "A malaria merozoite surface protein (MSP1)-structure, processing and function." Memorias do Instituto Oswaldo Cruz **87**(Suppl 3): 37-42.

Holder, A. A. and R. R. Freeman (1981). "Immunisation against blood-stage rodent malaria using purified parasite antigens." Nature **294**: 361-4.

Holder, A. A., M. J. Lockyer, K. G. Odink, J. S. Sandhu, V. Riveros-Moreno, S. C. Nicholls, Y. Hillman, L. S. Davey, M. L. Tizard and R. T. Schwarz (1985). "Primary structure of the precursor to the three major surface antigens of *Plasmodium falciparum* merozoites." Nature **317**: 270-3.

Holder, A. A., J. S. Sandhu, Y. Hillman, L. S. Davey, S. C. Nicholls, H. Cooper and M. J. Lockyer (1987). "Processing of the precursor to the major merozoite surface antigens of *Plasmodium falciparum*." Parasitology **94**: 199-208.

Howard, R. F., D. L. Narum, M. J. Blackman and J. Thurman (1998). "Analysis of the processing of *Plasmodium falciparum* rhoptry-associated protein 1 and localization of Pr86 to schizont rhoptries and p67 to free merozoites." Molecular and Biochemical Parasitology. **92**: 111-22.

Howard, R. F. and R. T. Reese (1990). "*Plasmodium falciparum*: Hetero-oligomeric Complexes of Rhoptry Polypeptides." Experimental Parasitology **71**: 330-42.

Howard, R. F. and C. M. Schmidt (1995). "The secretory pathway of *Plasmodium falciparum* regulates transport of p82/RAP-1 to the rhoptries." Molecular and Biochemical Parasitology. **74**: 43-54.

Howell, S., C. Withers-Martinez, C. H. Kocken, A. W. Thomas and M. J. Blackman (2001). "Proteolytic Processing and Primary Structure of *Plasmodium falciparum* Apical Membrane Antigen-1." Journal of Biological Chemistry **276**: 31311-20.

Jaikaria, N., C. Rozario, R. G. Ridley and M. E. Perkins (1993). "Biogenesis of rhoptry organelles in *Plasmodium falciparum*." Molecular and Biochemical Parasitology **57**: 269-80.

Jakobsen, P. H., J. A. L. Kurtzhals, E. M. Riley, L. Hviid, T. G. Theander, S. Morris-Jones, J. B. Jensen, R. A. L. Bayoumi, R. G. Ridley and B. M. Greenwood (1997). "Antibody responses to Rhoptry-Associated Protein-1 (RAP-1) of *Plasmodium falciparum* parasites in humans from areas of different malaria endemicity." Parasite Immunology **19**: 387-93.

James, S. and L. H. Miller (2000). "Malaria vaccine development: Status report." Nature Medicine **Special Focus: Malaria**(Web Reprint).

Kappe, S. H. I., A. R. Noe, T. S. Fraser, B. P. L and J. H. Adams (1998). "A family of chimeric erythrocyte binding proteins of malaria parasites." Proceedings of the National Academy of Sciences **95**: 1230-5.

Khan, S., W. Jarra and P. Preiser (2001). "The 235 kDa rhoptry protein of *Plasmodium (yoelii) yoelii*: function at the junction." Molecular and Biochemical Parasitology. **117**: 1-10.

Knell, A. J. (ed) (1991). "Malaria." Oxford University Press.

Kyes, S. A., J. A. Rowe, N. Kriek and C. I. Newbold (1999). "Rifins: A second family of clonally variant proteins expressed on the surface of red cells infected with

Plasmodium falciparum." Proceedings of the National Academy of Sciences **96**: 9333-8.

Laemmli (1970). "Cleavage of structural proteins during the assembly of the head of bacteriophage T4." Nature **277**: 680-5.

Lambros, C. and J. P. Vanderberg (1979). "Synchronization of *Plasmodium falciparum* erythrocytic stages in culture." Journal of Parasitology **65**: 418-20.

Lyon, J. A., J. M. Carter, A. W. Thomas and J. D. Chulay (1997). "Merozoite surface protein-1 epitopes recognized by antibodies that inhibit *Plasmodium falciparum* merozoite dispersal." Molecular and Biochemical Parasitology. **90**: 223-34.

Macreadie, I., H. Ginsburg, W. Sirawaraporn and L. Tilley (2000). "Antimalarial Drug Development and New Targets." Parasitology Today **16**: 438-44.

Marshall, V. M., A. Silva, M. Foley, S. Cranmer, L. Wang, D. J. McColl, D. J. Kemp and R. L. Coppel (1997). "A second merozoite surface protein (MSP-4) of *Plasmodium falciparum* that contains an epidermal growth factor-like domain." Infection and Immunity **65**: 4460-7.

Marshall, V. M., W. Tieqiao and R. L. Coppel (1998). "Close linkage of three merozoite surface protein genes on chromosome 2 of *Plasmodium falciparum.*" Molecular and Biochemical Parasitology **94**: 13-25.

McBride, J. S. and H. G. Heidrich (1987). "Fragments of the polymorphic Mr 185,000 glycoprotein from the surface of isolated *Plasmodium falciparum* merozoites form an antigenic complex." Molecular and Biochemical Parasitology **23**: 71-84.

Miller, L. H., D. I. Baruch, K. Marsh and O. K. Doumbo (2002). "The pathogenic basis of malaria." Nature **2002**: 673-9.

Miller, L. H., M. F. Good and G. Milon (1994). "Malaria pathogenesis." Science **264**: 1873-83.

Miller, L. H. and S. Hoffman (1998). "Research towards vaccines against malaria." Nature Medicine Vaccine Supplement **4**: 520-4.

Morgan, W. D., B. Birdsall, T. A. Frienkiel, M. G. Gradwell, P. A. Burghaus, S. E. Syed, C. Uthaipibull, A. A. Holder and J. Feeny (1999). "Solution structure of an EGF module pair from the *Plasmodium falciparum* merozoite surface protein 1." Journal of Molecular Biology. **289**: 113-22.

Myler, P. J. (1990). Transcriptional Analysis of the Major Merozoite Surface Antigen Precursor (GP195) Gene of *Plasmodium falciparum.* Parasites:Molecular Biology, Drug and Vaccine Design, Wiley-Liss: 123-37.

Narum, D. L. and A. W. Thomas (1994). "Differential localisation of full-length and processed forms of PF83 / AMA-1 an apical membrane antigen of *Plasmodium falciparum* merozoites." Molecular and Biochemical Parasitology. **67**: 59-68.

Noe, A. R. and J. H. Adams (1998). "*Plasmodium yoelii* YM MAEBL protein is coexpressed and colocalizes with rhoptry proteins." Molecular and Biochemical Parasitology **96**: 27-35.

Noe, A. R., D. J. Fishkind and J. H. Adams (2000). "Spatial and temporal dynamics of the secretory pathway during differentiation of the *Plasmodium yoelii* schizont." Molecular and Biochemical Parasitology **108**: 169-85.

O'Donnell, R. A., T. F. de Koning-Ward, R. A. Burt, M. Bockarie, J. Reeder, A. F. Cowman and B. S. Crabb (2001). "Antibodies against merozoite surface protein (MSP)-1_{19} are a major component of the invasion-inhibitory response in individuals immune to malaria." Journal of Experimental Medicine **193**: 1403-12.

O'Donnell, R. A., A. Saul, A. F. Cowman and B. S. Crabb (2000). "Functional conservation of the malaria vaccine antigen MSP-1(19) across distantly related *Plasmodium* species." Nature Medicine **6**: 91-5.

Ogun, S. A. and A. A. Holder (1994). "*Plasmodium yoelii*: brefeldin A-sensitive processing of proteins targeted to the rhoptries." Experimental Parasitology **79**: 270-8.

Pachebat, J. A., I. T. Ling, M. Grainger, C. Trucco, S. Howell, D. Fernandez-Reyes, R. S. Gunaratne and A. A. Holder (2001). "The 22 kDa component of the protein complex on the surface of *Plasmodium falciparum* merozoites is derived from a larger precursor, merozoite surface protein 7." Molecular and Biochemical Parasitology. **117**: 83-9.

Pang, X. L., T. Mitamura and T. Horii (1999). "Antibodies reactive with the N-terminal domain of *Plasmodium falciparum* serine repeat antigen inhibit cell proliferation by agglutinating merozoites and schizonts." Infection and Immunity **67**: 1821-7.

Perkins, M. E. and L. J. Rocco (1988). "Sialic acid-dependent binding of *Plasmodium falciparum* merozoite surface antigen, Pf200, to human erythrocytes." Journal of Immunology. **141**: 3190-6.

Phillips, R. S., A. K. Raham, R. J. Wilson (1975). Proceedings: Invasion of human red cells by *Plasmodium falciparum in vitro.* Transactions of the Royal Society of Tropical Medicine and Hygiene **69**: 432.

Pinder, J. C., R. E. Fowler, L. H. Bannister, A. R. Dluzewski and G. H. Mitchell (2000). "Motile systems in malaria merozoites: how is the red blood cell invaded?" Parasitology Today **16**: 240 - 5.

Preiser, P., W. Jarra, T. Capoiod and G. Snounou (1999). "A rhoptry-protein-associated mechanism of clonal phenotypic variation in rodent malaria." Nature **398**: 618-22.

Preiser, P., M. Kaviratne, S. Khan, L. H. Bannister and W. Jarra (2000). "The apical organelles of malaria merozoites: host cell selection, invasion, host immunity and imune evasion." Microbes and Infection **2**: 1461-77.

Reed, M. B., S. R. Caruana, A. H. Batchelor, J. K. Thompson, B. S. Crabb and A. F. Cowman (2000). "Targeted disruption of an erythrocyte binding antigen in *Plasmodium falciparum* is associated with a switch toward a sialic acid-independent pathway of invasion." Proceedings of the National Academy of Sciences **97**: 7509-14.

Richie, T. L. and A. Saul (2002). "Progress and challenges for malaria vaccines." Nature **415**: 694-701.

Ridley, R. G., B. Takacs, H. Etlinger and J. G. Scaife (1990a). "A rhoptry antigen of *Plasmodium falciparum* is protective in Saimiri monkeys." Parasitology **101**: 187-92.

Sachs, J. and P. Malaney (2002). "The economic and social burden of malaria." Nature **415**: 680-5.

Sajid, M., C. Withers-Martinez and M. J. Blackman (2000). "Maturation and specificity of *Plasmodium falciparum* subtilisin-like protease-1, a malaria merozoite subtilisin-like serine protease." Journal of Biological Chemistry **275**: 631-41.

Salmon, B. L., A. Oksman and D. E. Goldberg (2001). "Malaria parasite exit from the host erythrocyte: A two step process requiring extraerthrocytic proteolysis." Proceedings of the National Academy of Sciences

Sambrook, J., E. F. Fritsch and T. Maniatis (1989). Molecular Cloning-A Laboratory Manual., Cold Spring Harbour Laboratory Press.

Shai, S., M. J. Blackman and A. A. Holder (1995). "Epitopes in the 19kDa fragment of the *Plasmodium falciparum* major merozoite surface protein-1 (PfMSP-1(19)) recognized by human antibodies." Parasite Immunology **17**: 269-75.

Snounou, G., W. Jarra and P. Preiser (2000). "Malaria Multigene Families: The Price of Chronicity." Parasitology Today **16**: 28-30.

Snow, R. W., J.-F. Trapre and K. Marsh (2001). "The past, present and future of childhood malaria mortality in Africa." Trends in Parasitology **117**: 593-7.

Stafford, W. H. (1996). Analysis of the MSP-1 complex and protein secretion in *P. falciparum*. Ph.D Thesis, UCL, London.

Stafford, W. H., M. J. Blackman, A. Harris, S. Shai, M. Grainger and A. A. Holder (1994). "N-terminal amino acid sequence of the *Plasmodium falciparum* merozoite surface protein-1 polypeptides." Molecular and Biochemical Parasitology **66**: 157-60.

Stafford, W. H., B. Gunder, A. Harris, H. G. Heidrich, A. A. Holder and M. J. Blackman (1996a). "A 22kDa protein associated with the *Plasmodium falciparum* merozoite surface protein-1 complex." Molecular and Biochemical Parasitology **80**: 159-69.

Stafford, W. H., R. W. Stockley, S. B. Ludbrook and A. A. Holder (1996b). "Isolation, expression and characterization of the gene for an ADP- ribosylation factor from the human malaria parasite, *Plasmodium falciparum*." European Journal of Biochemistry **242**: 104-13.

Stowers, A. W., V. Cioce, R. L. Shimp, M. Lawson, G. Hui, O. Muratova, D. C. Kaslow, R. Robinson, C. A. Long and L. H. Miller (2001). "Efficacy of two alternate vaccines based on *Plasmodium falciparum* merozoite surface protein 1 in an *Aotus* challenge trial." Infection and Immunity **69**: 1536-46.

Tanabe, K., M. Mackay, M. Goman and J. G. Scaife (1987). "Allelic dimorphism in a surface antigen gene of the malaria parasite *Plasmodium falciparum*." Journal of Molecular Biology. **195**: 272-87.

Targett, G. A. T. (1995). "Malaria -advances in vaccines." Current Opinion in Infectious Diseases **8**: 322-27.

Thaithong, S., G. H. Beale, M. Chutmongkonkul (1984). "Susceptibility of *Plasmodium falciparum* to five drugs: an *in vitro* study of isolates mainly from Thailand." Transactions of the Royal Society of Tropical Medicine and Hygiene 77: 228-31.

Thompson, J. K., T. Triglia, M. B. Reed and A. F. Cowman (2001). "A novel ligand from *Plasmodium falciparum* that binds to a sialic acid-containing receptor on the surface of human erythrocytes." Molecular Microbiology **41**: 47-58.

Tian, J. H., S. Kumar, D. C. Kaslow and L. H. Miller (1997). "Comparison of protection induced by immunisation with recombinant proteins from different regions of merozoite surface protein 1 of *Plasmodium yoelii*." Infection and Immunity **65**: 3032-6.

Tine, J. A., D. E. Lanar, D. M. Smith, B. T. Wellde, P. Schultheiss, L. A. Ware, E. B. Kauffman, R. A. Wirtz, C. Taisne, G. S. N. Hui, S. P. Chang, P. Church, M. R. Hollingdale, D. C. Kaslow, S. Hoffman, K. P. Guito, W. R. Ballou, J. C. Sadoff and E. Paoletti (1996). "NYVAC-Pf7: a poxvirus-vectored, multiantigen, multistage vaccine candidate for *Plasmodium falciparum* malaria." Infection and Immunity **64**: 3833-44.

Tomas, A. M., A. M. van der Wel, A. W. Thomas, C. J. Janse and A. P. Waters (1998). "Transfection systems for animal models of malaria." Parasitology Today **14**: 245-9.

Trucco, C., D. Fernandez-Reyes, S. Howell, W. Stafford, T. J. Scott-Finnigan, M. Grainger, S. A. Ogun, W. R. Taylor and A. A. Holder (2001). "The merozoite surface protein 6 codes for a 36 kDa protein associated with the *Plasmodium falciparum* merozoite surface protein 1 complex." Molecular and Biochemical Parasitology **112**: 91-101.

Tsuji, M. and F. Zavala (2001). "Peptide-based subunit vaccines against pre-erythrocytic stages of malaria parasites." Molecular Immunology **38**: 433-42.

Uthaipibull, C., B. Aufiero, S. E. Syed, B. Hansen, J. A. Guevara Patino, E. Angov, I. T. Ling, K. Fegeding, W. D. Morgan, C. Ockenhouse, B. Birdsall, J. Feeny, J. A.

Lyon and A. A. Holder (2001). "Inhibitory and blocking monoclonal antibody epitopes on merozoite surface protein 1 of the malaria parasite *Plasmodium falciparum*." Journal of Molecular Biology. **307**: 1381-94.

Waller, K. L., B. M. Cooke, W. Numomura, N. Mohandas and R. L. Coppel (1999). "Mapping the binding domains involved in the interaction between the *Plasmodium falciparum* knob-associated histidine-rich protein (KAHRP) and the cytoadherence ligand *P. falciparum* erythrocyte membrane protein 1 (PfEMP1)." Journal of Biological Chemistry **274**: 23808-13.

Walliker, D., I. A. Quakyi, T. E. Wellems, T. F. McCutchen, A. Szarfman, W. T. London, L. M. Corcoran, T. R. Burkot and R. Carter (1987). "Genetic analysis of the human malaria parasite *Plasmodium falciparum*." Science **236**: 1661-6.

Wang, L., C. G. Black, V. M. Marshall and R. L. Coppel (1999). "Structural and antigenic properties of merozoite surface protein 4 of *Plasmodium falciparum*." Infection and Immunity **67**: 2193-200.

Ward, G. E., L. H. Miller and J. A. Dvorak (1993). "The origin of parasitophorous vacuole membrane lipids in malaria-infected erythrocytes." Journal of Cell Science **106**: 237-48.

Waterkeyn, J. G., B. S. Crabb and A. F. Cowman (1999). "Transfection of the human malaria *Plasmodium falciparum*." International Journal for Parasitology **29**: 945-55.

WHO (1998). Executive Summary for Economics of Malaria, Center for International Development, Harvard University and the London School of Hygiene and Tropical Medicine.

WHO (1999a). Economics of Malaria, World Bank.

WHO (1999b). Malaria prevention and control-Burdens and Trends., Division of Control of Tropical Disease, WHO.

WHO (1999c). New Perspectives. Malaria Diagnosis. Geneva, World Health Organisation.

WHO (1999d). The World Health Report 1999 *Making a Difference*. Chapter 4. Rolling Back Malaria, Division of Control of Tropical Disease, WHO.

Wilson, R. J. (1990). Biochemistry of red cell invasion. Blood Cells. **16**: 237-52.

Wirth, D. (1998). "A 21st century solution for an ancient disease." Nature Medicine **4**: 1360-2.

Wiser, M. F., H. N. Lanners, R. A. Bafford and J. M. Favaloro (1997). "A novel alternative secretory pathway for the export of *Plasmodium* proteins into the host erythrocyte." Proceedings of the National Academy of Sciences **94**: 9108-113.

Wooden, J., E. E. Gould, A. T. Paull, C. H. Sibley (1992). "*Plasmodium falciparum*: a simple polymerase chain reaction method for differentiating strains." Experimental Parasitology **75**: 207-12.

ELSEVIER

Molecular & Biochemical Parasitology 117 (2001) 83–89

MOLECULAR & BIOCHEMICAL PARASITOLOGY

www.parasitology-online.com

The 22 kDa component of the protein complex on the surface of *Plasmodium falciparum* merozoites is derived from a larger precursor, merozoite surface protein 7☆

Justin A. Pachebat [a,1], Irene T. Ling [a], Munira Grainger [a], Carlotta Trucco [a], Steven Howell [b], Delmiro Fernandez-Reyes [a,c], Ruwani Gunaratne [a], Anthony A. Holder [a,*]

[a] *Division of Parasitology, National Institute for Medical Research, Mill Hill, London NW 7 1AA, UK*
[b] *Division of Protein Structure, National Institute for Medical Research, Mill Hill, London NW 7 1AA, UK*
[c] *Division of Mathematical Biology, National Institute for Medical Research, Mill Hill, London NW 7 1AA, UK*

Received 9 April 2001; received in revised form 20 June 2001; accepted 28 June 2001

Abstract

The gene coding for merozoite surface protein 7 has been identified and sequenced in three lines of *Plasmodium falciparum*. The gene encodes a 351 amino acid polypeptide that is the precursor of a 22-kDa protein ($MSP7_{22}$) on the merozoite surface and non-covalently associated with merozoite surface protein 1 (MSP1) complex shed from the surface at erythrocyte invasion. A second 19-kDa component of the complex ($MSP7_{19}$) was shown to be derived from $MSP7_{22}$ and the complete primary structure of this polypeptide was confirmed by mass spectrometry. The protein sequence contains several predicted helical and two beta elements, but has no similarity with sequences outside the Plasmodium databases. Four sites of sequence variation were identified in MSP7, all within the $MSP7_{22}$ region. The *MSP7* gene is expressed in mature schizonts, at the same time as other merozoite surface protein genes. It is proposed that $MSP7_{22}$ is the result of cleavage by a protease that may also cleave MSP1 and MSP6. A related gene was identified and cloned from the rodent malaria parasite, *Plasmodium yoelii* YM; at the amino acid level this sequence was 23% identical and 50% similar to that of *P. falciparum* MSP7. © 2001 Elsevier Science B.V. All rights reserved.

Keywords: Malaria; *Plasmodium falciparum*; *Plasmodium yoelii*; MSP7, MSP1; merozoite

1. Introduction

There is considerable interest in the identification and characterisation of proteins on the surface of malarial merozoites. At least four *Plasmodium falciparum* merozoite surface proteins (MSP1, -2, -4 and -5) are probably linked to the plasma membrane by glycosyl phosphatidyl inositol anchors [1–3]. Proteins such as apical membrane antigen 1 (AMA1) that are secreted onto the merozoite surface from apical organelles are class 1 membrane proteins with a transmembrane domain [4,5]. Some proteins that are soluble in the parasitophorous vacuole, such as MSP3 and S-antigen are in part associated with the merozoite surface [6–8]. One such protein (MSP6) that is predominantly soluble but is also associated with MSP1, was described recently [9]. MSP1 is a precursor to four non-covalently associated polypeptides on the surface of the merozoite ($MSP1_{83}$, $MSP1_{30}$, $MSP1_{38}$, and $MSP1_{42}$; reviewed in [10]). At the time of erythrocyte invasion the MSP1 complex is shed from the surface of the merozoite, as the result of a proteolytic cleavage of $MSP1_{42}$, which creates a new fragment that is part of the shed complex ($MSP1_{33}$) and leaves $MSP1_{19}$ on the parasite surface [11,12].

Abbreviations: MALDI-TOF, matrix-assisted laser desorption/ionisation time-of-flight; MSP, merozoite surface protein.

☆ *Note:* Nucleotide sequence data reported in this paper are available in the EMBL, GenBank™ and DDJB databases under the accession numbers AF390150 to AF390153.

* Corresponding author. Tel.: +44-208-959-3666x2175; fax: +44-208-913-8593.

E-mail address: aholder@nimr.mrc.ac.uk (A.A. Holder).

[1] Present address: PNAC, Laboratory of Molecular Biology, MRC Centre, Hills Road, Cambridge CB2 2QH, UK.

0166-6851/01/$ - see front matter © 2001 Elsevier Science B.V. All rights reserved.
PII: S0166-6851(01)00336-X

Previous studies have shown the presence of a 22-kDa protein (p22) on the surface of *P. falciparum* merozoites [13,14]. This protein is non-covalently associated with the complex of polypeptides derived by proteolytic processing of MSP1 [15]. It is bound to MSP-1 of both the Wellcome and MAD20 types, and is derived from a distinct gene, based on its N-terminal amino acid sequence [14]. p22 is exposed on the merozoite surface and can be labelled by surface radioiodination and detected by immunofluorescence. p22 is an integral component of the shed complex. A second 19-kDa component (p19) of the shed complex is closely related to p22, as assessed by antibody cross reactivity and peptide mapping, but the two proteins have distinct N-termini [15] [14]. It was proposed that p19 resulted from the cleavage of p22 at the same time as processing of $MSP1_{42}$ since p19 is in the shed MSP-1 complex, but not on the merozoite surface [14].

In this report, we describe the gene that codes for both p22 and p19, showing that they are both derived from a larger precursor that codes for a peripheral membrane protein we have designated merozoite surface protein 7 (MSP7), and p22 and p19 as $MSP7_{22}$ and $MSP7_{19}$, respectively.

2. Materials and methods

2.1. In vitro culture of P. falciparum; DNA and protein purification

P falciparum lines 3D7, T9-96 and FCB1 were maintained in culture as described previously [16]. Parasite growth was synchronised by the use of sorbitol and fractionation on percoll gradients. DNA was prepared from parasites lysed with cold 1% acetic acid and washed with phosphate buffered saline (PBS), as described [17], using a Qiagen Blood and Cell Culture DNA kit. The soluble MSP-1 complex was purified from the culture medium of T9-96 parasites by binding to and elution from a monoclonal antibody affinity column [12].

2.2. Identification and sequence analysis of the MSP7 gene

Preliminary sequence data were obtained from The Institute for Genomic Research website (www.tigr.org). The sequencing was part of the International Malaria Genome Sequencing Project and was supported by awards from the National Institute of Allergy and Infectious Diseases, National Institutes of Health, the Burroughs Wellcome Fund and the US Department of Defense. Malaria Genome databases were searched using the programme tblastn ([18] http://www.ncbi.nlm.nih.gov/BLAST/) and the N-terminal sequences of $MSP7_{22}$ and $MSP7_{19}$ (SETDTQSKNEQEPST and EVQKPAQGGESTFQK, respectively) [14]. Using the single gel read sequence (PNACJ17TF) obtained from the TIGR website (http://www.tigr.org) that matched the $MSP\text{-}7_{22}$ N-terminal amino acid sequence, oligonucleotide primers were designed and used with Vectorette libraries prepared from T9-96 genomic DNA [19] to PCR amplified additional sequence. Three rounds of vectorette-based amplification were carried out using the primers P22F3, P22F4 and P22F5 (Table 1), complementary to the 5′ strand of the retrieved sequence. PCR reactions contained 1 μl of the appropriate Vectorette library, 2.5 U AmpliTaq Gold, 25 pM gene specific primer, 25 pM Vectorette II primer, 3 mM $MgCl_2$, 10 μl of 10× PCR Buffer II, 10 μl of 2.5 mM dNTPs, made up to 100 μl with water. Thermocycling was carried out using a Programmable Thermal Controller (Genetic Research Instrumentation): start conditions, 94 °C for 12 min; then 40 cycles of 94 °C for 1 min, 55 or 60 °C for 2 min, 72 °C for 3 min; final conditions, 72 °C for 10 min. PCR products were examined by agarose-TBE gel electrophoresis, cloned into the pCR®2.1 or TOPO-TA vectors (Invitrogen) and the inserts sequenced using ABI

Table 1
Oligonucleotide primers used in the analysis of *P. falciparum MSP7*

Primer	Sequence location	Nucleotide sequence
Pfp22F	−571 to −545	CACACGCATGAATAGAAATTAGACATG
Prep22Fexp	66–88	GCCGGATCCAATCAACTCATAGTACACCAG
p22R2	116–85	AATTCTTCTTGATCTTCTTCATTATTTACTGG
p22F3	397–424	TTTGAAAATGTTGATGATGACGCAGTAG
Prep22Rexp	530–504	GCCGAATTCCTTTGTGCCTTTACCTTTGATAATACG
p22Fexp	526–556	GCCGGATCCAAAGTGAAACAGATACTCAATCTAAAAATG
p22F4	603–631	AGGAGGAGAATCGACATTTCAAAAAGACC
p22F5	812–843	TTGGTCAAGAAGATAATAAGAGTAAAAATGGC
p22Rexp	1056–1020	GCCGAATTCATTGTGTTTAGTAAATTAAATGAATATTCTAAG
pfp22R	1176–1153	AAAGGTACACAATTTTAACCGAATG

The sequence location is numbered starting from the ATG in the open reading frame. Primers in the 5′→3′ orientation with respect to the gene are designated with 'F' in their name, primers in the 3′→5′ orientation are designated with an 'R'.

PRISM™ δrhodamine dye terminator chemistry and an ABI 377 DNA sequencer. DNA sequence data were assembled and analysed using Autoassembler 3.1 (ABI) and MacVector 6.5 (Eastman Kodak). The new sequence obtained was used to search against the genome databases for additional nucleic acid sequences using blastn [18].

DNA sequences were obtained across the *MSP7* open reading frame from 3D7, T9-96 and FCB-1 genomic DNA by PCR amplification with a number of primers (Table 1). *MSP7* gene sequence was amplified by PCR from FCB-1 DNA first using the primer pairs pre22Fexp/pre22Rexp and p22Fexp/p22Rexp and then the primer pairs pfp22F/p22R2, and p22F3/pfp22R. The DNA was amplified using AmpliTaq Gold, ligated into TOPO-TA vector, transformed into *E. coli*, and selected recombinants sequenced. Reverse transcriptase polymerase chain reaction was carried out as described previously on total RNA from the 3D7 line [9].

The gene was amplified from *Plasmodium yoelii* YM genomic DNA using the primers: 5′AATATACATATATATACACACACATTTAGACAAAATG (forward) and 5′ ATTACAAACTGTTTTATATGTATTTTATGTGTACAT (reverse). The reaction contained 30 ng of genomic DNA, 75 pmol of each primer, 12.5 pmol of dNTP mix, and 1.25 U of Platinum Pfx DNA polymerase (Gibco-BRL) in 50 μl amplification buffer with 4 mM $MgSO_4$. Thermocycling conditions were: start, 94 °C for 5 min; 30 cycles of 94 °C for 30 s, 51 °C for 30 s, 68 °C for 90 s; final conditions 68 °C for 10 min. The PCR product was cloned and insert was sequenced, as described above.

Each sequence was obtained from the analysis of at least two independent PCR products; to exclude sequence changes introduced during PCR amplification.

2.3. Analysis of the *P. falciparum* $MSP7_{22}$ and $MSP7_{19}$ primary structure

The MSP1 complex was fractionated by SDS-PAGE [15], and the 22 and 19-kDa components were digested with trypsin and analysed by peptide mass fingerprinting using a Bruker Reflex-III matrix-assisted laser desorption/ionisation time-of-flight (MALDI-TOF) mass spectrometer (Bruker Daltonics, Bremen, Germany), essentially as described earlier [9].

A variety of similarity searches at the NCBI website (http://www.ncbi.nlm.nih.gov/Malaria/plasmodi-umbl.html), and several pattern and profile searches (ExPASy server, Swiss Institute of Bioinformatics website http://www.expasy.ch/), were performed, including PSI-BLAST [18] and PHI-BLAST [20]. Signal peptide analysis was performed with SignalP V1.1 [21]. Protein secondary structure prediction was performed using PHDsec [22] and solvent accessibility predicted with PHDacc [23].

2.4. Northern blot analysis of *P. falciparum MSP7* transcription

Total RNA was purified using TRIzol [24] from synchronised 3D7 parasites at 2 h intervals over a period of 48 h. Approximately equal amounts of RNA were loaded on a gel, fractionated by electrophoresis, and blotted onto nitrocellulose. The blot was hybridised in 0.5 M sodium phosphate, pH 7.2 containing 7% SDS [24] with a 528 bp DNA fragment derived from *MSP-7* and labelled with [α-^{32}P] dATP using the Prime-It® II Random Primer Labelling Kit (Stratagene). After prehybridisation and overnight incubation with the probe at 55 °C, the blot was washed in 2 × SSC, 0.1% SDS, at room temperature for 10 min, followed by a second wash in 2 × SSC, 0.1% SDS, at 55 °C for 15 min. The blot was exposed to autoradiographic film at −70 °C and then developed.

3. Results

3.1. Identification of the gene coding for the 22 kDa protein and structure of the MSP7 gene in the T9/96 and 3D7 *P. falciparum* parasite lines

The N-terminal amino acid sequences of $MSP7_{22}$ and $MSP7_{19}$ [14,15] were used to search the *P. falciparum* 3D7 genome databases and a single 627 nucleotide sequence (PNACJ17TF) in the TIGR database was identified. Nucleotides 586–627 of PNACJ17TF coded for a sequence identical to 13 of the 14 N-terminal amino acids of MSP-7_{22}. Nucleotides 58–585 coded for an open reading frame upstream of the MSP-7_{22} sequence. An additional sequence read (PNAAG29TR) was identified extending the sequence 571 bp upstream of the putative initiator methionine, but no sequence extending the ORF was identified. Two rounds of Vectorette PCR were used to extend the gene sequence beyond the in-frame stop codon. The first step using the primer p22F3 extended the sequence 295 bp, and the second round PCR using primers p22F4 and p22F5 extended the sequence an additional 203 bp. In total, a 1925 bp contig was assembled, using one additional sequence read (PNAJO60TF). Analysis of the known DNA sequence upstream and downstream of *MSP-7* did not identify any additional exons and the single exon structure was confirmed by RTPCR to amplify the 5′ and 3′ regions of the gene (data not shown). The open reading frame of 1053 nucleotides, without introns, was identical in both 3D7 and T9/96 lines of *P. falciparum*. We have named this gene *MSP7* because it codes for a merozoite surface protein.

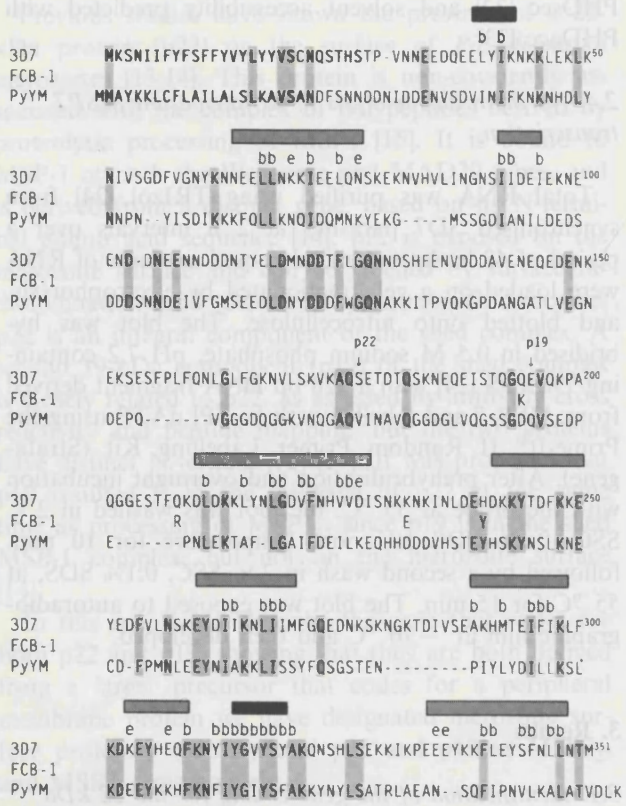

Fig. 1. The amino acid sequence of *P. falciparum* MSP7 and an orthologue from *P. yoelii*. The continuous 351 amino acid residue sequence shown is that derived from the parasite clones 3D7 and T9/96. Amino acid differences in the line FCB-1 are shown on the lines below, and only the sequence differences are indicated. The complete sequence from *P. yoelii* YM is also shown and the residues conserved between the *P. falciparum* and *P. yoelii* sequences are highlighted ( ). The putative signal peptides are shown in bold and the cleavage sites producing $MSP7_{22}$ and $MSP7_{19}$ are shown (↓). Predicted helical regions ( ) and beta sheet (■) are indicated above the sequence with an indication of the predicted surface accessibility of the residues within these structures (b, buried; e, exposed).

3.2. Primary structure of the protein

P. falciparum merozoite surface protein 7 consists of 351 amino acids (calculated mass 41 kDa, and pI 4.74; Fig. 1). A putative N-terminal signal sequence of 27 amino acids, precedes a 324 amino acid (38 kDa) polypeptide. The protein is mainly hydrophilic (33% charged residues) with a negative charge cluster from residue 94 to 148. The N-terminus of $MSP7_{22}$ and $MSP7_{19}$ were located at Ser177 and Glu195, respectively, suggesting that 38.5 kDa precursor undergoes cleavage between residues 176 (Gln) and 177 (Ser) into a N-terminal 17.2 kDa polypeptide and a C-terminal 20.7 kDa (20 738, $MSP7_{22}$) polypeptide. $MSP7_{22}$ is in the MSP-1 complex on the merozoite surface and undergoes further cleavage between residues 194 (Gln) and 195 (Glu), removing 18 amino acids from the N-terminus and producing $MSP7_{19}$ (18.7 kDa).

Analysis of $MSP7_{22}$ and $MSP7_{19}$ by tryptic digestion and MALDI-TOF mass spectrometry identified 83% of the expected $MSP7_{22}$ peptide products and all of the $MSP7_{19}$ sequence in peptide products (Fig. 2), confirming the DNA sequence analysis and that no post translational modification, such as glycosylation at the Asn-Lys-Ser sequence, was present.

A search of the Plasmodium data bases identified a similar sequence in the partial *P. yoelii* 17X database (contig 966; http://www.tigr.org). The corresponding gene was amplified from *P. yoelii* genomic DNA and the sequence (shown in Fig. 1) was identical to that in the *P. yoelii* 17X genome. At the amino acid level the sequence was 23% identical and 50% similar to that of *P. falciparum* MSP7. When *PfMSP7* was aligned to this putative *PyMSP7* and the alignment used to search protein databanks using the iterative search method PSIBLAST, no additional similar sequences were identified, other than in the partial *Plasmodium* databases.

The alignment was also used to predict the secondary structure and solvent accessibility of MSP7 sequences (Fig. 1). $MSP7_{22}$ is mostly helical, but two beta strand elements were also predicted in the MSP7 sequence. Interestingly the second beta sheet is near the C-terminus of the molecule and has sequence similarity to some other unique proteins found in the malaria databases (data not shown). The presence of these additional sequences suggests that *MSP7* may be part of a multigene family. A multiple alignment and pattern of this region (F-[KD]-[NK]-[YFV]-[IMV]-[YH]-G-[VIL]-[YN]-[SG]-[FY]-A-K-[QRK]-[HYN]-[SN]-[HY]-L) were used to refine the iterative protein databank searches and PHIBLAST searches, but no additional homologues outside of the malaria proteins were found.

3.3. MSP7 is conserved in different lines of P. falciparum

Since MSP-1 is found in two major sequence forms we were interested to determine whether or not the sequence of MSP7 is conserved. The sequence of the gene in the 3D7/T9-96 parasite clone was compared with that of a third parasite line, FCB-1. The entire *MSP7* gene was isolated from FCB-1 genomic DNA by amplification with four sets of primer pairs (covering 1747 bp) and the sequence compared with that of 3D7/T9-96. The comparison indicated that the gene is highly conserved in these parasite lines. Only four nucleotide differences were identified each of which resulted in a changed amino acid in the translated sequence: Gln194 to Lys, Gln208 to Arg, Lys232 to Glu, and His240 to Tyr. These amino acid differences are all in the $MSP7_{22}$ region of the protein (Fig. 1).

3.4. *P. falciparum MSP7 is expressed in mature asexual stage parasites*

Northern blotting analysis of RNA samples taken every 2 h throughout 48 h cycle indicated that *MSP7* was expressed in the asexual blood stages, predominantly in the schizont stages between 36 and 42 h post invasion (Fig. 3). The transcript size is approximately 2.5 kb.

4. Discussion

There is considerable interest in the identification of proteins on the surface of malarial merozoites, as potential targets of vaccine-induced antibodies to inhibit invasion of erythrocytes. The 22 kDa protein, $MSP7_{22}$, is on the merozoite surface and is intimately associated with the complex of MSP1 polypeptides shed from the surface of the merozoite at the time of erythrocyte invasion. The results of this study show that $MSP7_{22}$ and the subfragment $MSP7_{19}$ are derived from the C-terminus of a much larger precursor molecule, approximately twice the size of $MSP7_{22}$, which we have called MSP7. MSP7 is a polypeptide of 351 residues, starting with a putative signal peptide. The *MSP7* gene is transcribed by mature stages of the intracellular asexual blood stage parasite, and accumulates at a time coincident with *MSP1* message [17,24]. The cleavage of MSP7 to produce $MSP7_{22}$ probably occurs prior to merozoite release since the precursor is not detected on the merozoite surface with antibodies specific for $MSP7_{22}$ [14]. The analysis of $MSP7_{22}$ and $MSP7_{19}$ by mass spectrometry confirmed that these polypeptides correspond to the C-terminal region of the MSP7 sequence. Furthermore extensive modification, for example by *N*-glycosylation was ruled out. A single potential *N*-glycosylation site is present in $MSP7_{22}$, but clearly the site is not modified.

Some merozoite surface proteins sequences are highly polymorphic, whereas others appear to be conserved between parasite lines and isolates [9,25–27]. MSP7 is

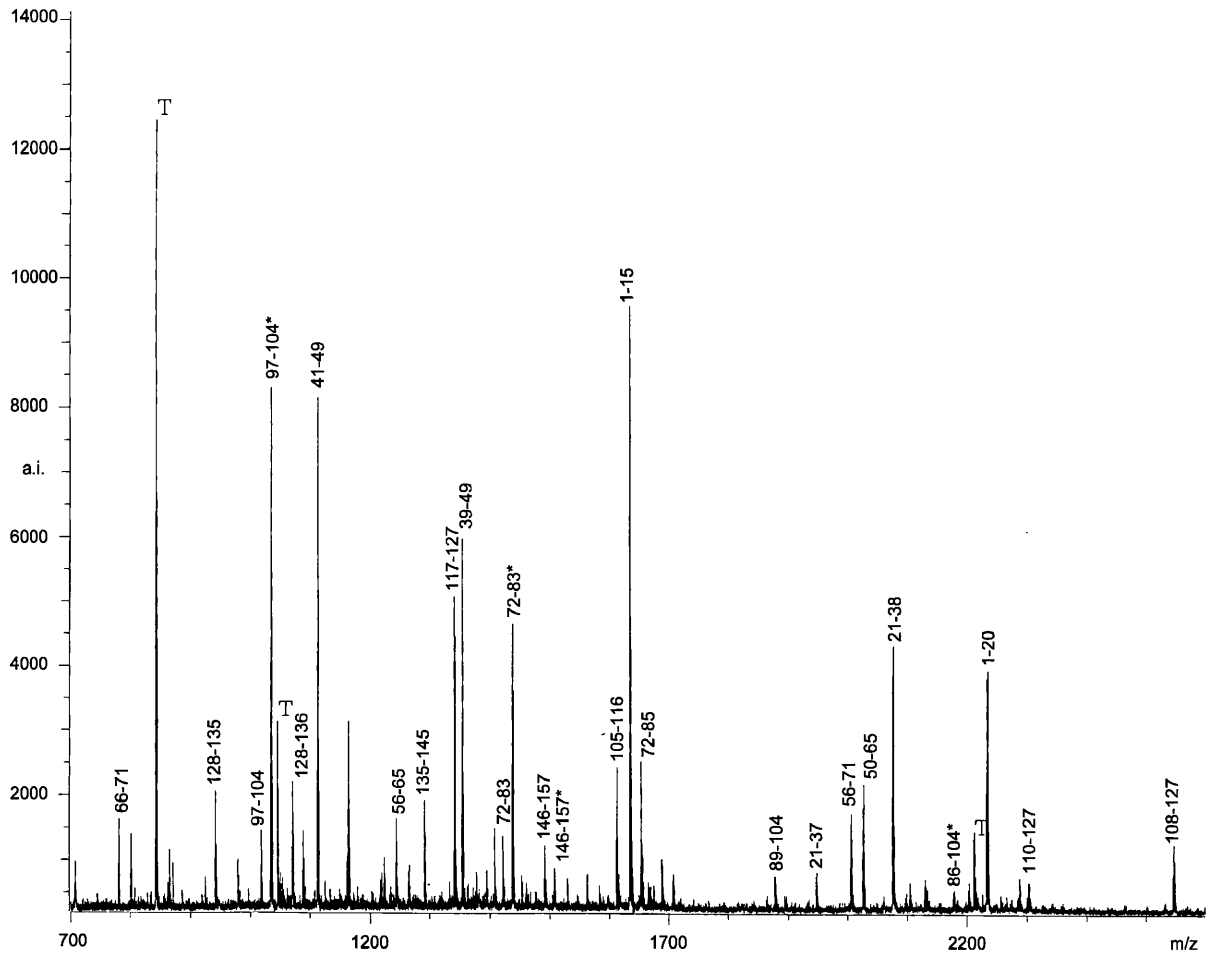

Fig. 2. Mass spectrum of tryptic peptides derived from *P. falciparum* $MSP7_{19}$. The MSP1 complex from T9-96 parasites was fractionated by SDS-PAGE, the 19-kDa band was digested with trypsin and the peptides analysed by mass spectrometry. The identity of peptides is by mass based on the amino acid sequence of $MSP7_{19}$, which begins at residue 194 in the MSP7 sequence. Peptides that contain oxidised methionine are indicated (*), as are those derived from trypsin (T).

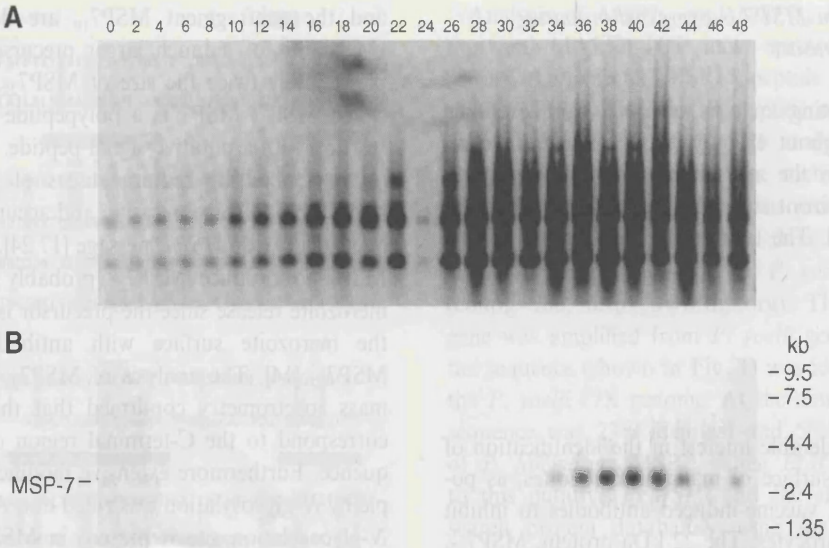

Fig. 3. Northern blot analysis of *MSP7* mRNA purified from samples collected every 2 h during a 48 h cycle of development of *P. falciparum* 3D7 asexual blood stage forms in vitro. The first time point (0 h) corresponds to the time of erythrocyte invasion. Total RNA was electrophoresed through agarose, stained with ethidium bromide (Panel A), transferred to nitrocellulose and hybridised with a radiolabelled DNA probe derived from *MSP7* (Panel B). The migration of molecular mass markers is shown.

conserved within the three *P. falciparum* lines examined, with only four amino acid substitutions identified in comparisons between FCB-1 and 3D7/T9-96 lines. All of these substitutions are within the C-terminal $MSP7_{22}$ part of MSP7, including one at the site where cleavage leading to the formation of $MSP7_{19}$ may occur. Whether or not this substitution (Gln to Lys) affects the formation of MSP-7_{19} is not known. The high degree of sequence similarity is in marked contrast to that described for some other merozoite surface proteins such as MSP2, but similar to that described for MSP3, MSP5 and MSP6.

The fact that the MSP7 gene is conserved in these parasite lines, may suggest that it is not under immune pressure, although sera from donors naturally exposed to malaria contain antibodies reacting with $MSP7_{22}$ (W.H. Stafford et al., unpublished observations). The sequence conservation may also reflect the fact that the protein binds to MSP1. MSP1 is found in two major forms [28] and it is likely that the complementary binding site on MSP1 is formed by sequences conserved in the two forms. A similar gene was identified and cloned from *P. yoelii* YM genomic DNA, and related sequences are present in the *P. vivax* and *P. berghei* databases (data not shown), but no similarities between MSP7 and other non-Plasmodium sequences were detected. The N-terminus of MSP7 is predicted to be largely loop or random coil, whereas the C-terminus which constitutes $MSP7_{22}$ and $MSP7_{19}$ is predicted to be of high helical content. The extreme C-terminus shares similarity with other open reading frames in the *Plasmodium* sequence databases, and the central conserved element corresponds to the hydrophobic beta sheet structure indicated as a buried structure on Fig. 1. It is possible that this sequence may be an essential structural core or may mediate the non-covalent binding of MSP7 to MSP1.

The MSP1 polypeptide complex consists of three gene products, and in each case the polypeptides are modified by proteolytic cleavage. In the case of MSP1, all the resulting polypeptides appear to be retained in the complex, whereas in the case of MSP6 and MSP7 only a C-terminal fragment of the protein is retained in the complex. Examination of the protease cleavage sites in MSP7 (NVLSKVKAQSETDTQS) and MSP6 (NITQVVQANSETNKNP), together with the one that gives rise to MSP-1_{30} (SITQPLVAASETTEDG) revealed a high degree of similarity, with the cleavage occurring immediately before the underlined SET residues. This sequence similarity suggests a similar protease specificity, so it is possible that these cleavages are carried out by a single enzyme. It is likely that the cleavages all occur at the same time in the development of the merozoite, which would be compatible with the action of a single enzyme.

Acknowledgements

We thank Sola Ogun, Helen Taylor, Chairat Upthaipibull and Mike Blackman for valuable criticisms throughout this work; Helen Taylor, Shahid Khan and Mallika Kaviratne for help with RNA preparation and Northern blotting; and José Saldahna for help with analysis of the sequence information. Justin Pachebat was the recipient of a Medical Re-

search Council studentship, Carlotta Trucco was supported by a Wellcome Trust Travelling Fellowship, and Ruwani Gunaratne was supported by the United States Agency for International Development. Preliminary sequence data were obtained from The Institute for Genomic Research website (www.tigr.org). The sequencing was part of the International Malaria Genome Sequencing Project and was supported by awards from the National Institute of Allergy and Infectious Diseases, National Institutes of Health, the Burroughs Wellcome Fund and the US Department of Defense.

References

[1] Gerold P, Schofield L, Blackman MJ, Holder AA, Schwarz RT. Structural analysis of the glycosyl-phosphatidylinositol membrane anchor of the merozoite surface proteins-1 and -2 of *Plasmodium falciparum*. Mol Biochem Parasitol 1996;75:131–43.

[2] Marshall VM, Silva A, Foley M, et al. A second merozoite surface protein (MSP-4) of *Plasmodium falciparum* that contains an epidermal growth factor-like domain. Infect Immun 1997;65:4460–7.

[3] Marshall VM, Tieqiao W, Coppel RL. Close linkage of three merozoite surface protein genes on chromosome 2 of *Plasmodium falciparum*. Mol Biochem Parasitol 1998;94:13–25.

[4] Peterson MG, Marshall VM, Smythe JA, et al. Integral membrane protein located in the apical complex of *Plasmodium falciparum*. Mol Cell Biol 1989;9:3151–4.

[5] Narum DL, Thomas AW. Differential localization of full-length and processed forms of PF83/AMA-1 an apical membrane antigen of *Plasmodium falciparum* merozoites. Mol Biochem Parasitol 1994;67:59–68.

[6] McColl DJ, Silva A, Foley M, et al. Molecular variation in a novel polymorphic antigen associated with *Plasmodium falciparum* merozoites. Mol Biochem Parasitol 1994;68:53–67.

[7] Oeuvray C, Bouharoun-Tayoun H, Gras-Masse H, et al. Merozoite surface protein-3: a malaria protein inducing antibodies that promote *Plasmodium falciparum* killing by cooperation with blood monocytes. Blood 1994;84:1594–602.

[8] Perkins ME, Rocco LJ. Chemical crosslinking of *Plasmodium falciparum* glycoprotein, Pf200 (190–205 kDa), to the S-antigen at the merozoite surface. Exp Parasitol 1990;70:207–16.

[9] Trucco C, Fernandez-Reyes D, Howell S, et al. The merozoite surface protein 6 gene codes for a 36 kDa protein associated with the *Plasmodium falciparum* merozoite surface protein 1 complex. Mol Biochem Parasitol 2001;112:91–101.

[10] Holder AA. Preventing merozoite invasion of erythrocytes. In: Hoffman SL, editor. Malaria Vaccine Development: a Multi-Immune Response and Multi-stage Perspective. Washington: ASM Press, 1996:77–104.

[11] Blackman MJ, Heidrich HG, Donachie S, McBride JS, Holder AA. A single fragment of a malaria merozoite surface protein remains on the parasite during red cell invasion and is the target of invasion-inhibiting antibodies. J Exp Med 1990;172:379–82.

[12] Blackman MJ, Holder AA. Secondary processing of the *Plasmodium falciparum* merozoite surface protein-1 (MSP1) by a calcium-dependent membrane-bound serine protease: shedding of MSP133 as a noncovalently associated complex with other fragments of the MSP1. Mol Biochem Parasitol 1992;50(2):307–15.

[13] McBride JS, Heidrich HG. Fragments of the polymorphic Mr 185,000 glycoprotein from the surface of isolated *Plasmodium falciparum* merozoites form an antigenic complex. Mol Biochem Parasitol 1987;23(1):71–84.

[14] Stafford WHL, Gunder B, Harris A, Heidrich HG, Holder AA, Blackman MJ. A 22 kDa Protein associated with the *Plasmodium falciparum* merozoite surface protein-1 complex. Mol Biochem Parasitol 1996;80:159–69.

[15] Stafford WHL, Blackman MJ, Harris A, Shai S, Grainger M, Holder AA. N-terminal amino-acid-sequence of the *Plasmodium falciparum* merozoite surface protein-1 polypeptides. Mol Biochem Parasitol 1994;66:157–60.

[16] Guevara Patino JA, Holder AA, McBride JS, Blackman MJ. Antibodies that inhibit malaria merozoite surface protein-1 processing and erythrocyte invasion are blocked by naturally acquired human antibodies. J Exp Med 1997;186(10):1689–99.

[17] Stafford WH, Stockley RW, Ludbrook SB, Holder AA. Isolation, expression and characterization of the gene for an ADP-ribosylation factor from the human malaria parasite, *Plasmodium falciparum*. Eur J Biochem 1996;242:104–13.

[18] Altschul SF, Madden TL, Schaffer AA, et al. Gapped BLAST and PSI-BLAST: a new generation of protein database search programs. Nucl Acids Res 1997;25:3389–402.

[19] Gunaratne RS, Sajid M, Ling IT, Tripathi R, Pachebat JA, Holder AA. Characterization of *N*-myristoyltransferase from *Plasmodium falciparum*. Biochem J 2000;348:459–63.

[20] Zhang Z, Schaffer AA, Miller W, et al. Protein sequence similarity searches using patterns as seeds. Nucl Acids Res 1998;26:3986–90.

[21] Nielsen H, Engelbrecht J, Brunak S, von Heijne G. Identification of prokaryotic and eukaryotic signal peptides and prediction of their cleavage sites. Prot Eng 1997;10:1–6.

[22] Rost B, Sander C. Prediction of protein secondary structure at better than 70% accuracy. J Mol Biol 1993;232:584–99.

[23] Rost B, Sander C. Conservation and prediction of solvent accessibility in protein families. Proteins 1994;20:216–26.

[24] Kyes S, Pinches R, Newbold C. A simple RNA analysis method shows var and rif multigene family expression patterns in *Plasmodium falciparum*. Mol Biochem Parasitol 2000;105:311–5.

[25] Wu T, Black CG, Wang L, Hibbs AR, Coppel RL. Lack of sequence diversity in the gene encoding merozoite surface protein 5 of *Plasmodium falciparum*. Mol Biochem Parasitol 1999;103:243–50.

[26] Miller LH, Roberts T, Shahabuddin M, McCutchan TF. Analysis of sequence diversity in the *Plasmodium falciparum* merozoite surface protein-1 (MSP-1). Mol Biochem Parasitol 1993;59:1–14.

[27] Felger I, Irion A, Steiger S, Beck HP. Genotypes of merozoite surface protein 2 of *Plasmodium falciparum* in Tanzania. Trans R Soc Trop Med Hyg 1999;93(Suppl. 1):3–9.

[28] Tanabe K, Mackay M, Goman M, Scaife JG. Allelic dimorphism in a surface antigen gene of the malaria parasite *Plasmodium falciparum*. J Mol Biol 1987;195:273–87.